FRAGMENTS OF MICROCIN B17 AS A SOURCE OF NEW TOPOISOMERASE INHIBITORS

Frédéric Collin

This thesis is submitted in partial fulfillment of the requirements of the degree of Doctor of Philosophy at the University of East Anglia.

Biological Chemistry Department

John Innes Centre

Norwich Research Park

Norwich NR4 7UH

December 2010

Statement

The research described in this thesis is my own work, except where due reference has been made, and has not been submitted to any university for any degree.

Frédéric Collin

Norwich, December 2010

Frédéric Collin   December 2010

Fragments of microcin B17 as a source of new topoisomerase inhibitors

Abstract:

     DNA topoisomerases are a broad class of enzymes responsible for topological changes in DNA. DNA gyrase is a prokaryotic topoisomerase with the essential function of negatively supercoiling closed-circular DNA at the expense of ATP hydrolysis. There are two main known families of gyrase inhibitors: quinolones and aminocoumarins. A few bacterial toxins are also known for their inhibitory properties on gyrase, among them CcdB and microcin B17. Microcin is a peptide produced by strains of *Escherichia coli* expressing the plasmid-borne *mccB17* operon, which is post-translationally modified to convert serine- and cysteine- containing sequences into oxazole, thiazole, and oxazole-thiazole fused rings. Previous work has shown that these heterocycles are critical, and alterations of these residues proved to be detrimental to MccB17's antibacterial activity. In spite of its attractive antibacterial properties, MccB17's physico-chemical properties prevent it from being a good drug candidate. In the pursuit of smaller inhibitors derived from MccB17, we describe here how modifications of the whole toxin led to a better understanding of the elements that are critical for its activity. We generated fragments of MccB17 by chemical and biochemical methods and we show that some of these fragments are topoisomerase inhibitors. The active fragments generated, in addition to highlighting features responsible for MccB17 activity, will be valuable starting points for the design of new inhibitors. Additionally, novel small molecules topoisomerase inhibitors sharing structural features with the heterocycles found in MccB17 were identified and characterized. This work had mainly focused on *E. coli* gyrase as a model target, but we have shown as well that MccB17 and its fragments had potential application on other topoisomerases.

List of contents

List of figures

List of tables

Acknowledgements

First and foremost, my deepest gratitude goes to my supervisor Prof Tony Maxwell, for his guidance through this work, his support in difficult times, and his ability to share his passion and research insight for topoisomerases.

I am very grateful to my co-supervisor Prof Chris Pickett and my advisor Dr Rebecca Goss for their thoughtful advice, particularly regarding the chemical aspects of this project and their unyielding encouragements.

My particular thanks go to Lesley Mitchenall, for her mentoring on the technical aspects of biochemistry, and for her friendship. Marcus Edwards has my gratitude for his support in these fields as well.

I greatly appreciate Will Parks and Olivier Pierrat help and advice in my first steps with microcin B17.

I wish to thank Martin Rejzek and Gerhard Saalbach for their constant assistance, particularly regarding the purification and analytical aspects of this work. I am thankful as well to Lionel Hill and Shirley Fairhurst for their help in these areas.

A special thanks to my colleagues and friends from the Biological Chemistry department at John Innes Centre and Chris Pickett's Lab in the University of East Anglia, that contributed to make these places not only places to do good science, but also amazingly enjoyable places to work in.

There is no word to express the extent of my love and gratitude to my Family.

To my friends from John Innes Centre, UEA, capoeira, and France who have shared these years with me, I am grateful for the warmth of your friendship.

CHAPTER I
Introduction

CHAPTER I Introduction

Overview

In the present health climate, where the occurrence of pathogenic bacteria resistant to most of the commonly used antibacterial drugs combined with the significant decrease in new antibiotics being brought to the market, threaten to bring us back to the dark ages of the pre-antibiotic area, there is an urgent need to discover new bactericidal agents (Norrby, Nord et al. 2005; Boucher, Talbot et al. 2009). The identification of new cellular targets through genomics has not lived up to its initial promises and so exploration of known targets with alternate ways to affect them is a safe strategy to overcome bacterial resistance. For this purpose a better understanding of the structure and mechanism of action of these enzymes as well as their interaction with known drugs is of major interest to develop new active entities. Present antibacterial agents interact with pathogens in various ways: they can interfere with the cell wall synthesis like penicillin (Waxman, Yocum et al. 1980), block protein synthesis via the ribosome similar to chloramphenicol (Vazquez 1966), inhibit essential metabolic pathways like sulfonamides with the tetrahydrofolic acid biosynthesis (Seydel 1968), or alter the nucleic acid synthesis as fluoroquinolones do (Wolfson and Hooper 1985). We have chosen to focus on this last cellular process and particularly on the family of enzymes targeted by fluoroquinolones: the topoisomerases. Topoisomerases are a broad class of ubiquitous enzymes controlling the topology of DNA in the cell, they deal with the interlinking and twisting of DNA molecules that are essential for DNA replication, transcription, recombination, as well as for chromosome compaction and segregation (Gellert 1981). This crucial role in the regulation of DNA topology has made them attractive and already successful targets, with DNA gyrase and topoisomerase IV for antimicrobial therapy and with human topoisomerase I and II for anticancer therapy. One of the most efficient ways to exploit these enzymes against their host is by stabilizing a covalent intermediate they form with the DNA during its topology modification this leading to the release of double-strand breaks that are lethal to the cell. This mechanism is often referred as topoisomerase poisoning. Examples of topoisomerase poisons are the drugs belonging to the fluoroquinolones family for gyrase and topo IV (Drlica and Zhao 1997), etoposide (Chen, Yang et al. 1984) and amsacrine (Nelson, Tewey et al. 1984) for topo II. Interestingly, two bacterial toxins are known to be gyrase poisons as well, namely CcdB (Bernard, Kezdy et al. 1993) and microcin B17 (MccB17) (Heddle, Blance et al. 2001). These two peptides are not exploitable *per se* as antibacterial drugs due to their large size (12 kDa for CcdB, and 3 kDa for MccB17) and physical properties, but they are useful tools to understand the mechanism of cleavage-complex stabilization as well as potential templates to develop molecules bearing the same properties. Recent insight into the mechanism of action of CcdB suggested that its potential as a template to generate new compounds is limited. In fact it appears that the

activity of CcdB relies mostly on the steric hindrance of a gyrase cavity by the whole protein (Dao-Thi, Van Melderen et al. 2005); unfortunately this mode of action cannot be easily mimicked by small molecules. The precise mechanism of action of MccB17 is still unknown and this compound has not being widely studied in the context of designing novel antibacterial molecules. Considering the need for new antibacterials, MccB17 seems a promising model to inspire new inhibitors. We decided to investigate further the mode of action of MccB17 and generate related compounds as potential topoisomerase inhibitors. The following chapters will describe how these two aspects have been addressed. But first we will give a brief overview of the two therapeutic fields where topoisomerases are involved: antibacterial and anticancer drugs. We will then focus on topoisomerases and their inhibitors. Finally the present state of knowledge on MccB17 will be covered.

1 Antibacterial mode of action and rise of resistance

The discovery and uses of antibacterial agents with a broad-spectrum of activity on a large scale had brought us in the comfort of the antibacterial golden age: an era where we have the tools to fight infectious diseases and avoid epidemics; where pneumonia, scarlet fever, and syphilis are not anymore common causes of death; where wounds or surgery have no chance of killing from septicemia. Unfortunately this state is threatened by the rise of drug-resistant species. Below are shown a few milestones of the history of antibacterials that led us to this golden age.

1.1 Milestones of antibacterials history

1670's: identification of bacteria by A. P. Van Leeuwenhoek with the help of his invention, the microscope.

1870's: connection between diseases and bacteria with the work of L. Pasteur and R. Koch.

1870's: concept of antiseptic surgery by Baron J. Lister.

1900's: first synthetic antibacterial compounds by P. Herlich, salvarsan (arsphenamine) against syphilis. Concept of chemotherapy.

1930's: synthesis (J. Klarer and F. Mietzsch) and antibacterial potential (P. Domagk) of prontosil from Bayer. The later identification by J. Trefouel and T. Trefouel of prontosil as a pro-drug of sulfanilamide lead to the discovery of the sulfonamide antibacterial drug class. Sulfonamide was the first antibacterials class available on a large scale.

1940's: after the early discovery of penicillin potential by A. Fleming in 1929, it is only in the 40's that penicillin through the work of H. Florey, N. Heatley, A. J. Moyer was brought to the mass production scale. The wide use of penicillin was followed a few years later by the occurrence of resistant strains.

1949: clinical use of first broad spectrum antibacterial: chloramphenicol, soon after its discovery by D. Gottlieb. Chloramphenicol was the first antibiotic to be produced synthetically on a large scale.

1953 E. Kornfeld isolates the first aminoglycoside antibacterial vancomycin from soil samples.

1964: first cephalosporin (resistance to β-lactamase).

1962: discovery of nalidixic acid, clinical use in 1967. This discovery led to the development and success of fluoroquinolones drugs.

2000's: declining new antibacterials, increasing bacterial resistances.

1.2 Bacteria structure and antibacterial targets

Antibacterials mainly affect three essential activities in bacteria: cell wall biosynthesis, protein synthesis and DNA synthesis. Other mechanisms of action include detergent-like destabilisation of cytoplasmic membrane, and activation of toxic species by the bacteria's metabolism. We will detail further these aspects, but first give a brief description of bacteria

structures. Figure 1 is a diagram of Gram-positive and Gram-negative bacteria and their cellular antibacterial targets. The genomic DNA of the bacteria, the ribosome responsible for the protein synthesis, and the various elements of the cell function like plasmids and enzymes are contained in the cytoplasm. The cytoplasm is enclosed in the cytoplasmic membrane, a phospholipid bilayer that separates the intracellular components of the cell from the outside. The cytoplasmic membrane is surrounded by the peptidoglycan, this is a mesh structure composed of a linear polymer of alternating of *N*-acetylglucosamine and *N*-acetylmuramic acid units crosslinked by peptide chains. The peptidoglycan is thicker in Gram-positive bacteria and forms the external layer, it is the target of colour staining that defined the Gram classification. In Gram-negative bacteria, the thinner peptidoglycan layer is enclosed in another phospholipid bilayer: the outer membrane, this second membrane differs from the cytoplasmic membrane by the fact that it contains lipopolysaccharides on its outer layer, lipoproteins that anchor it to the peptidoglycan and porins that are responsible for the passive transport of metabolites through the outer membrane. The outer membrane gives Gram-negative bacteria a potential extra advantage against antibacterial agents.
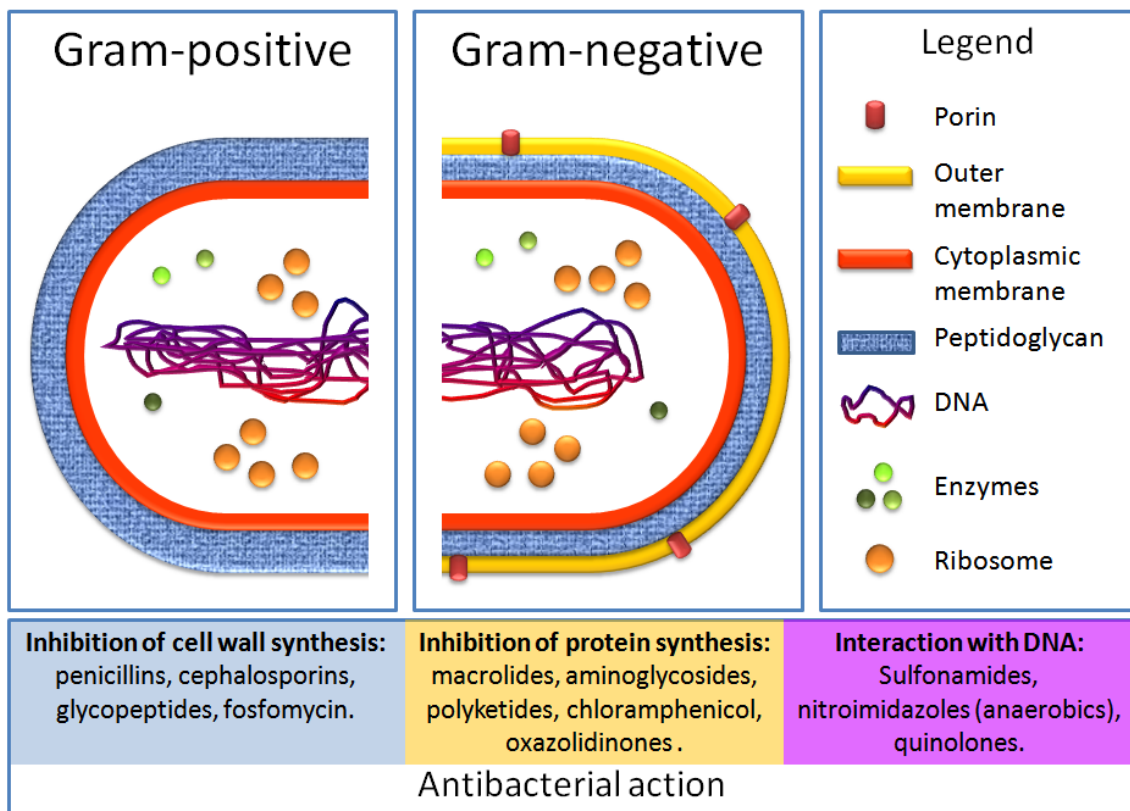
Figure 1 Schematic view of Gram-positive and Gram-negative bacteria and antibacterial action.
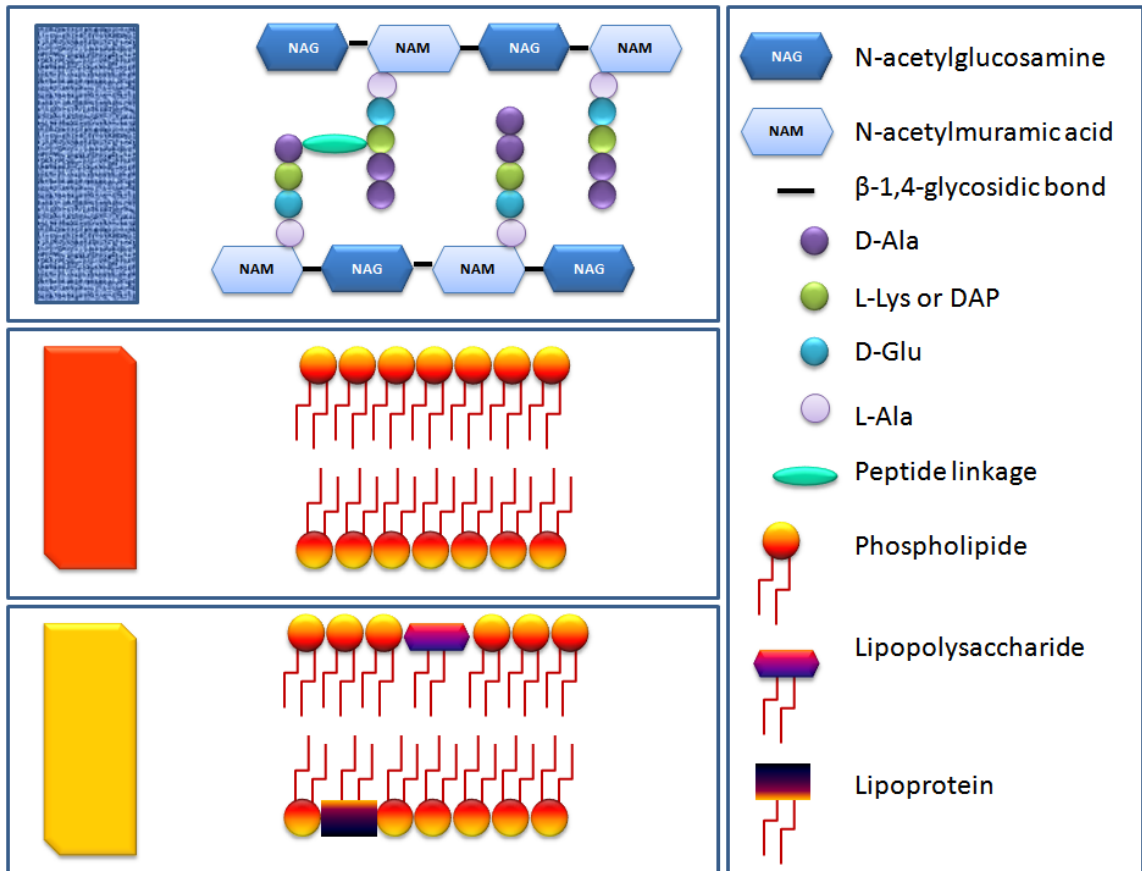
Figure 2 Details of cellular structure from Figure 1: top left, details of the peptidoglycan: glycan chains of β-1,4-linked N-acetylglucosamine and N-acetylmuramic acid, are crossed-linked by interconnected peptides, sequences are given for illustration purpose and can vary between organisms. Middle left, details of the cytoplasmic membrane, a bilayer of phospholipids. Bottom left, details of the outer membrane, a phospholipid bilayer containing lipopolysaccharide on the external surface and lipoprotein on the internal surface. Right side: legend.

1.3 General mechanism of bacterial resistance

Bacteria have different ways of protecting themselves against antibacterials: the most obvious method is by not letting the antibacterial get into the cell or not stay in long enough to be harmful; this is achieved by alteration of membrane permeability, by reduction of the number of porins (in Gram-negative bacteria) or mutations to make them "too small" to allow antibacterials through, or expression of efflux proteins that will pump out the harmful molecule faster that it gets in. The second possibility is to destroy or modify the noxious compound so it will lose its activity. A typical example is the beta-lactamase that renders penicillin inactive by hydrolysing the beta-lactam ring. Another strategy is to mutate the antibacterial target so it will be not or less susceptible to the antibacterial drug: as an example the modification of the cross linking system of peptidoglycan synthesis gives resistance to vancomycin: the peptide sequence changes from terminal -D-Ala-D-Ala motif to -D-Ala-D-Lac

(lactate); the resulting dipeptide has a significantly decreased affinity for vancomycin. These different mechanisms will be illustrated in the following part where the different antibacterials commonly used are classified by mode of action will be described. Occurrence of resistance specific to a specific mode of action will be included within this mode of action (Alekshun and Levy 2007).

1.4 Common multi-drug-resistant bacteria

Gram-positive: *Staphylococcus aureus*: meticillin-resistant *S. aureus* (MRSA), *Enterococcus faecium*: vancomycin resistant *Enterococcus* (VRE), *Clostridium difficile*, and *Streptococcus pneumonia* (Woodford and Livermore 2009).

Gram-negative: *Pseudomonas aeruginosa*, *Acinetobacter baumannii*, *Escherichia coli*, *Enterobacter* spp: ESBL producing *Enterobacter*, *Salmonella*, *Klebisella pneumoniae*, *Serratia marcescens*, *Neisseria gonorrhoeae*, *Stenotrophomonas maltophilia* (Slama 2008; Souli, Galani et al. 2008; Volles and Branan 2008)

Other: *Mycobacterium tuberculosis:* multidrug-resistant *M. tuberculosis* (MDR-TB), extensively drug-resistant *M. tuberculosis* (XDR-TB) (Chiang, Centis et al.).

1.5 Inhibitors of cell wall synthesis
The peptidoglycan is what gives bacteria structure, without it the bacteria is not able to deal with its internal osmotic pressure caused by the gradient of electrolyte concentration between the inside and the outside of the cell. The peptidoglycan biosynthetic pathway being specific to bacteria, compounds disrupting it are less likely to affect human enzymes. These characteristics make the enzymes involved in peptidoglycan biosynthetic pathway the perfect targets for antibacterial: lethal and specific.

1.5.1 Cell wall synthesis
(Vollmer, Blanot et al. 2008)

An overview of the constituents of peptidoglycan has been given with the description of the cell structure, we will describe here briefly how peptidoglycan is synthesized. Peptidoglycan is an assembly of long glycan chains cross-linked by peptides. The peptide gives flexibility to the structure whereas the glycan is the rigid part. The glycan chain is formed of an alternating sequence of β-1, 4-linked N-acetylglucosamine (GlcNAc) and N-acetylmuramic acid (MurNAC). The chemistry of the glycan is conserved among different bacteria. The peptide structure however varies among species. The peptide is bound to the carboxyl group of the muramic acid by its N-terminus, it is referred to as the peptide subunit. Peptide subunits can be connected by a peptide linker; this linker varies greatly through different species. The synthesis starts in the cytoplasm where UDP-GlcNAc and UDP-MurNAc-(peptide subunits) are formed. At the cytoplasmic membrane the lipid precursor is synthesized by the addition of phospho-MurNAc-(peptide subunit) to bactoprenol to form lipid I: MurNAc-(peptide subunit)-

pyrophosphoryl-undecaprenol. The formation of a 1, 4-β glycoside bond between GlcNAc from the UDP-GlcNAc and lipid I lead to lipid II. Lipid II: GlcNAc-β-1, 4-MurNAc-(peptide subunit)-phosphoryl-undecaprenol, is the substrate that will provide the building block used to assemble the final peptidoglycan, once it has crossed the cytoplasmic membrane. The mechanism of the cytoplasmic membrane crossing is not clearly identified yet. The assembly of the building blocks is carried out by the penicillin binding protein (PBP); this enzyme had two functions transglycosidase and transpeptidase. PBP with its transglycosidase activity will assemble the glycan chain, by link the precursor to an existing glycan strand, releasing the undecaprenylpyrophosphate that will dephosphorylate to bactoprenol and extending the glycan chain. PBP is involved as well with peptide cross-linking; PBP will replace the terminal a D-Ala in the D-Ala-D-Ala bond, thus activating the bond to react with another peptide subunit or a peptide bridge. These two events produce the mesh structure. The mechanism of formation of peptidoglycan shows how essential PBP is, and therefore a good antibacterial target. Figure 3 shows the peptidoglycan synthesis and its actors (Scheffers and Pinho 2005).
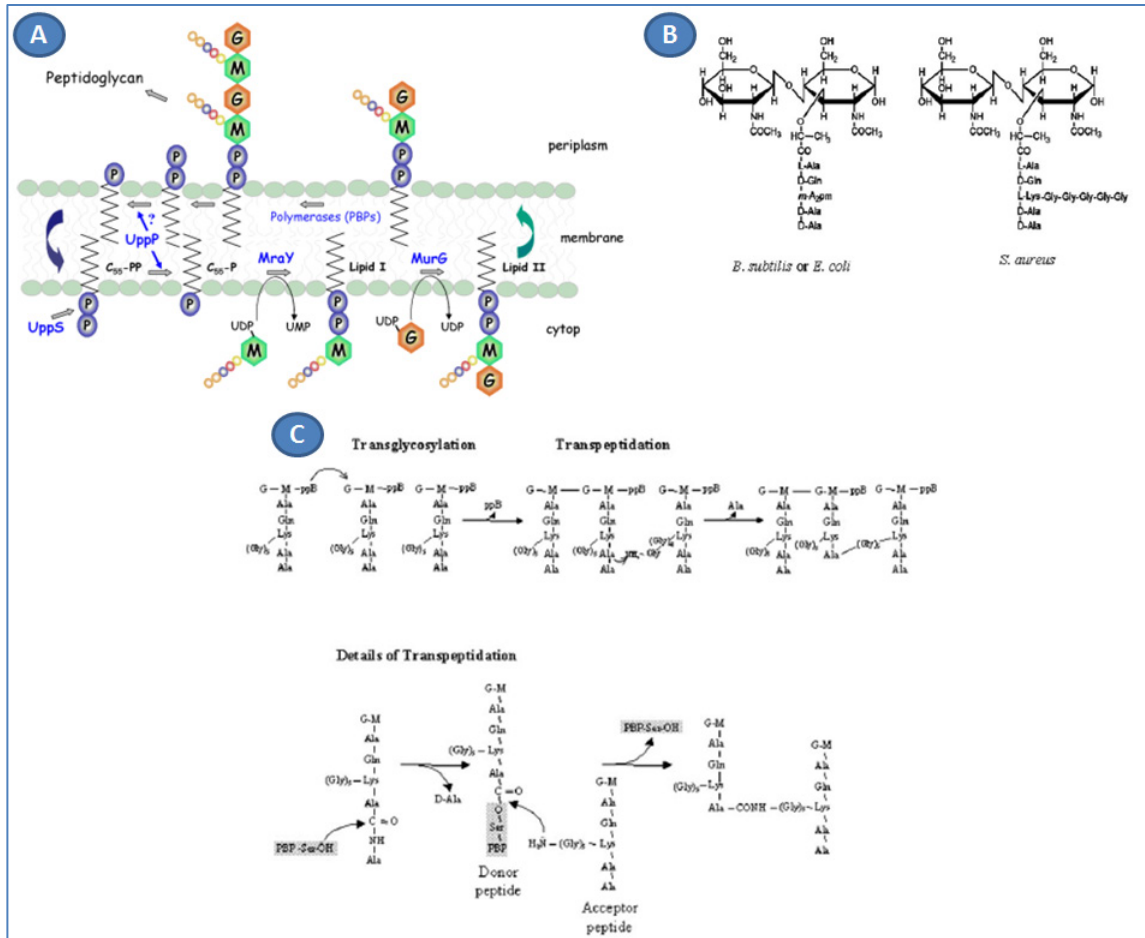
Figure 3 Peptidoglycan synthesis: A) membrane steps of peptidoglycan biosynthesis. M, G and the five coloured beads linked to M represent MurNAc, GlcNAc and the pentapeptide, respectively. C55-PP and C55-P are for undecaprenyl pyrophosphate and undecaprenyl phosphate, respectively. **B)** and **C)**, building blocks and synthesis reactions of the peptidoglycan. Reproduced from Bouhss *et al* (Bouhss, Trunkfield et al. 2008). **B)** The basic unit of the peptidoglycan is a disaccharide-pentapeptide composed of the amino sugars N-acetylglucosamine and *N*-acetylmuramic acid, which are linked together by -1,4 glycosidic bonds. The pentapeptide is covalently linked to the lactyl group of the muramic acid, and its composition can vary between different bacteria. In both *E. coli* and *B. subtilis*, the dibasic amino acid of the stem peptide, which allows the formation of the peptide cross bridge, is meso-diamoinopimelic acid (m-A2pm), while in *S. aureus* it is L-lysine (L-Lys), to which a pentaglycine cross bridge is bound. **C)** Peptidoglycan chains are synthesized by transglycosylation and transpeptidation reactions which lead to the formation of long glycan chains cross-linked by peptide bridges. In the transglycosylation reaction, the reducing end of the N-acetylmuramic acid (M) of the nascent lipid-linked peptidoglycan strand is likely transferred onto the C-4 carbon of the N-acetylglucosamine (G) residue of the lipid-linked PG precursor, with concomitant release of undecaprenylpyrophosphate (ppB). In the transpeptidation reaction, the D-Ala–D-Ala bond of one stem peptide (donor) is first cleaved by a PBP enzyme, and an enzyme-substrate intermediate is formed, with the concomitant release of the terminal D-Ala. The peptidyl moiety is then transferred to an acceptor, which is the last amino acid of the pentaglycine cross bridge in the depicted case of *S. aureus*, and the PBP enzyme is released. **B)** and **C)** are reproduced from Scheffer and Pinho (Scheffers and Pinho 2005).

1.5.2 β-lactam antibiotics

The beta-lactam antibacterials are the heirs of penicillin (G). They all share the same mechanism of action, but display various degrees of stability and spectra of antibacterial activity.

1.5.2.1 *Mode of action*

(Waxman and Strominger 1983)

The β-lactams are analogous to the terminal D-Ala-D-Ala of the peptidoglycan precursor. The serine residue of the penicillin-binding protein perform a nucleophilic attack of the amide bond of the β-lactam instead of the D-Ala-D-Ala peptide bond of the peptidoglycan. This reaction opens the β-lactam and forms a covalent bond with the antibacterial, rendering the enzyme inactive. The mechanism is illustrated in Figure 4.
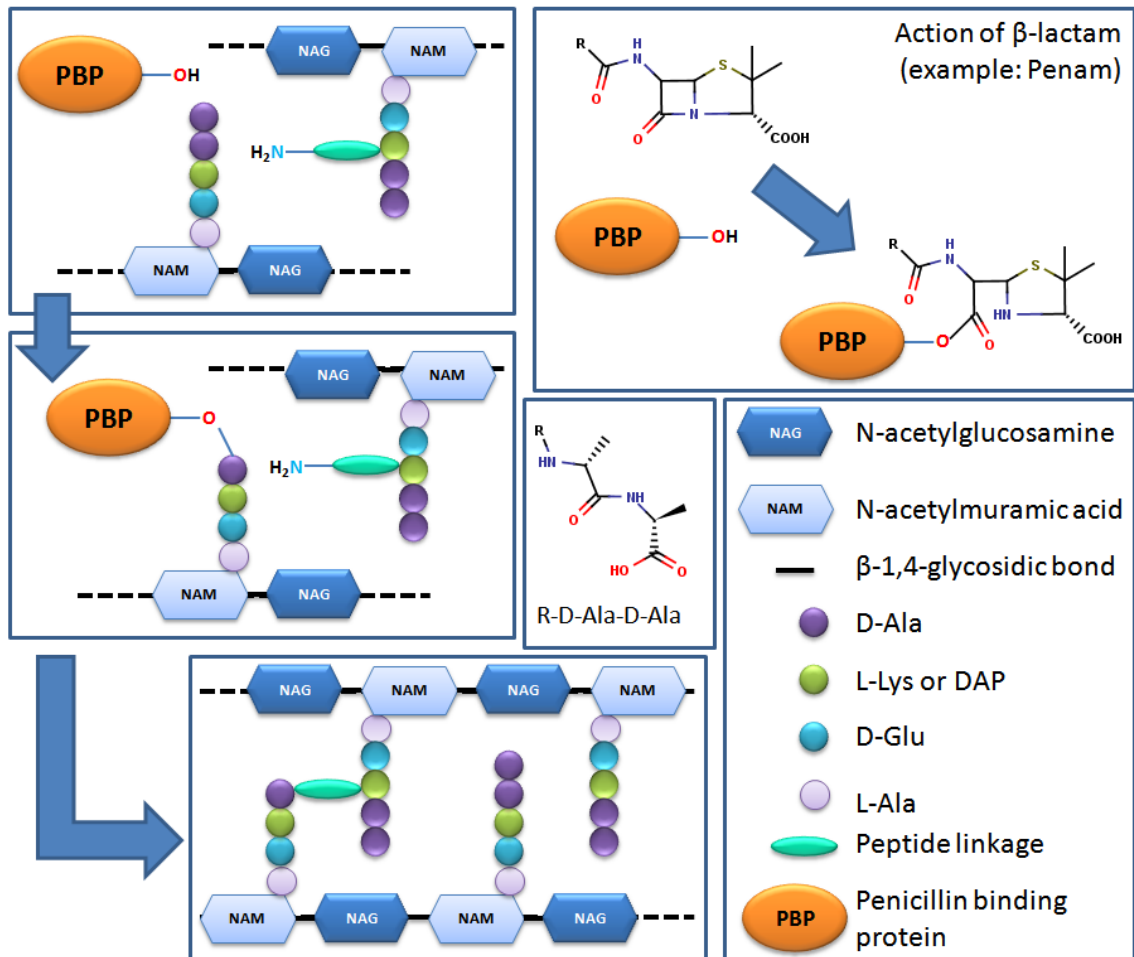
Figure 4 Mode of action of β-lactam antibacterials

Resistance to β-lactams is primarily achieved by the action of β-lactamases, enzymes that catalyze the hydrolysis of the β-lactam ring thus disarming the antibacterial warhead. The β-lactamases can be divided in two classes depending upon whether they have a serine active

site or a metal ion co-factor. Various substrate specificities to β-lactam and related antibacterial can be observed: penicillinase, cephalosporinase or carbapenamase; as well as different susceptibility to inhibitors like clavulanic acid (see below). Secondarily, resistance is achieved by mutation of the PBP reducing its affinity to the antibacterial like PBP2a for the infamous meticillin-resistant *S. aureus* (MRSA), or by modification of cellular permeability. A recent study reported an increase of *Enterobacteriaceae* carrying plasmids with multiple combinations of various extended spectrum β-lactamases and carbapenemases, thus conferring resistance to nearly all the β-lactam antibacterials, already worrying by itself, this kind of resistance can be easily transfered to other organism (Bush 2010).

1.5.2.2   Penams (penicillins)

The first representative that was widely used is the penicillin G, its only flaw was that it could not be orally administrated due to its instability at the stomach's pH; Penicillin V however is less potent but orally active. A wide range of hemi-synthetic penams have been developed from the (+)-6-aminopenicillanic acid. Penams are classified depending on their spectrum of action on Gram-positive and Gram-negative bacteria, and their stability toward β-lactamases. The initial appearance of resistance linked to penicillinase led to the development of meticillin, which is not anymore used clinically, and its substitutes oxacillin, cloxacillin and nafcillin. The need to broaden the types of bacteria affected by penams gave birth to the aminopenicillins: ampicillin and amoxicillin that are active on Gram-negative bacteria. Pro-drugs of ampicillin like pivampicillin and metampicillin have a better bioavailability and will release ampicillin upon hydrolysis in the body. Finally carboxypenicillin like carbenicillin, ticarcillin, temocillin have a Gram-negative spectrum including *Pseudomonas aeruginosa* and the ureidopenicillin piperacillin is a broad range covering *Pseudomonas aeruginosa* as well.

Name	R1
Cloxacillin	H
Dicloxacillin	Cl
Flucloxacillin	F
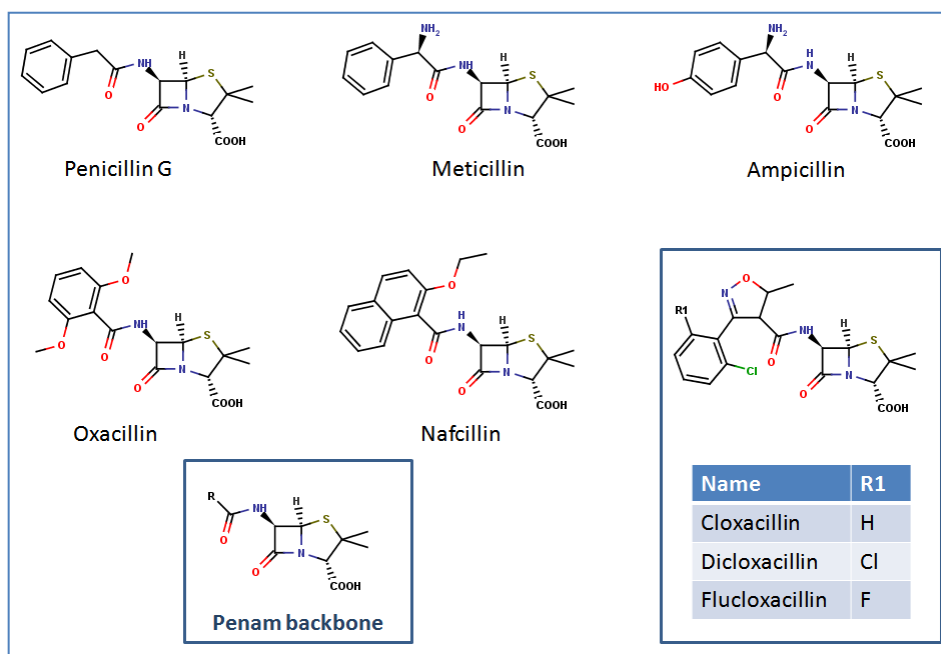
Figure 5 Penams: a few examples

29
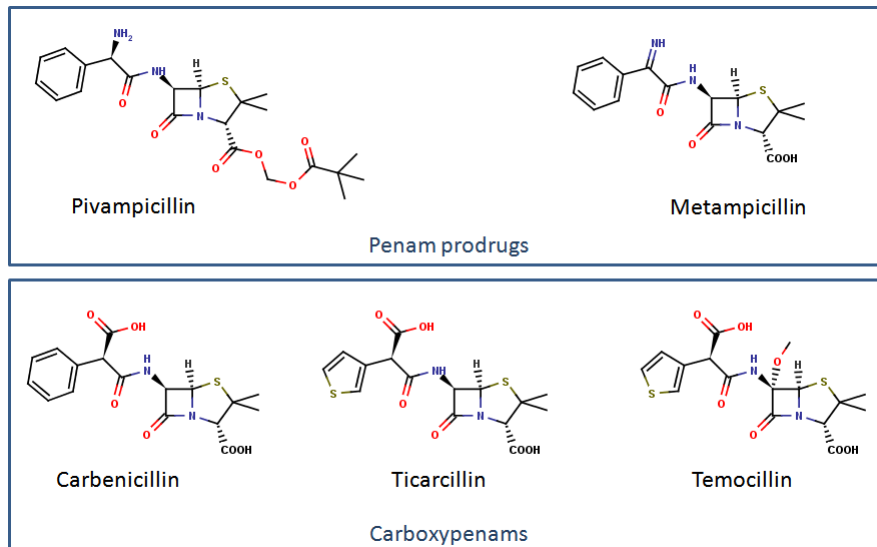
Figure 6 Penams: prodrugs and carboxypenams

1.5.2.3 Beta-lactamase inhibitors

(Payne, Cramp et al. 1994)

These compounds have no antibacterial properties but are directly involved with β-lactam antibacterials. They have a protective role: clavulanic acid, a substrate of β-lactamase will be hydrolysed in place of the active species, whereas sulbactam and tazobactam, irreversible inhibitors, will trap the enzyme.
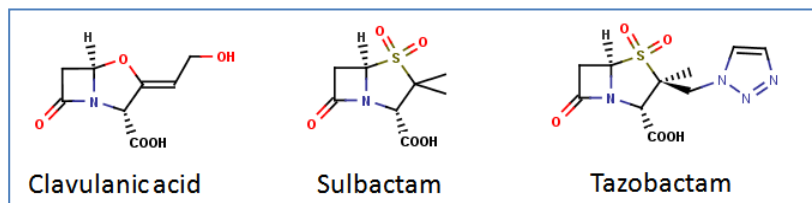
Figure 7 Beta-lactamase inhibitors

1.5.2.4 Penems

(Dalhoff, Janjic et al. 2006)

Thienamycin is an antibiotic active on Gram-positive and Gram-negative bacteria but unstable under physiological conditions, its derivative imipenem although is an injectable broad spectrum antibacterial resistant to β-lactamases. Imipenem is used in conjunction with cilastatin that prevent its degradation by dehydropeptidase. Meropenem, ertapenem and

doripenem are improvements of Imipenem, as they are not affected by dehydropeptidase. The use of penems is restricted to avoid development of bacterial resistance.
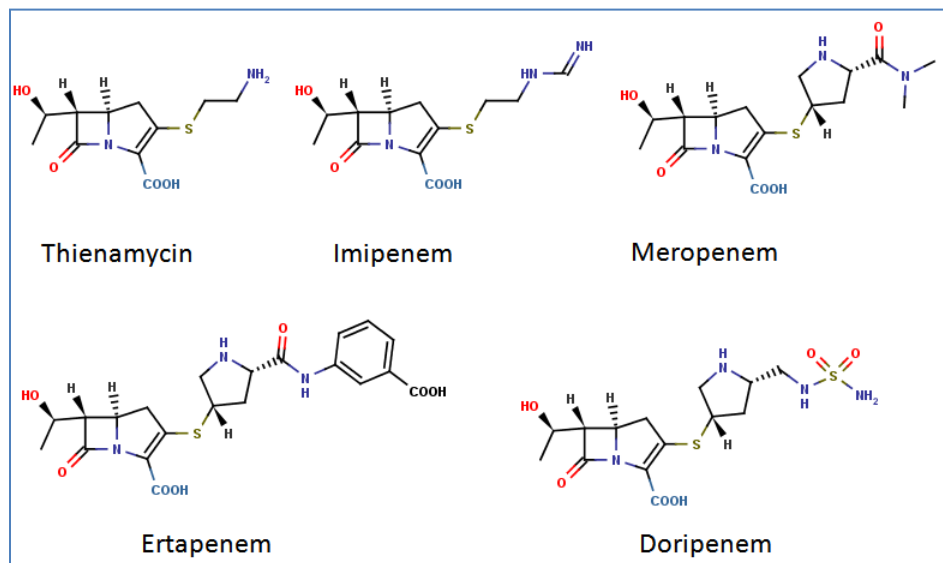
Figure 8 Penems

1.5.2.5 Cephems (cephalosporins)

The first cephalosporin, cephalosporin C, was isolated from *Cephalosporium acremonium*, the strain was collected from "self purifying" sea water next to a sewage outlet (Brotzu 1948). Cefalotin was the first cephalosporin to be clinically used, and is still in use nowadays (Griffith and Black 1964; Decroix, Chaumeil et al. 1984). The first generation cephems were active predominantly on Gram-positive bacteria (Nightingale, Greene et al. 1975). Similarly to penicillins extensive research has been carried out on cephalosporin and yielded a broad range of antibacterial, over what is often described as four (or more) generations, each generation bringing improvement. The classification can be described as follows: the 1st generation cephalosporins are only active on Gram-positive bacteria, whereas 2nd generation have a spectrum extended to some Gram-negative bacteria. The 3rd generation cephalosporins have a broad spectrum of activity, however some members have a diminished activity on Gram (+); ceftazimide, which belong to the 3rd generation, is active on *Pseudomonas aeruginosa.* The 4th generation cephalosporins have a broad spectrum of activity including *Pseudomonas aeruginosa,* and possess an increased resistance to β-lactamase; some are able to cross the blood-brain barrier, which allows them to be used against meningitis (El-Shaboury, Saleh et al. 2007). The last developed cephalosporins, ceftobiprole (Fritscher, Sader et al. 2008) and ceftaroline (Morrissey, Ge et al. 2009; Zhanel 2009) are active against MRSA and other drug-resistant strain. Cephalosporin is the largest class of antibacterial drug in term of sales (Hamad 2010).

31
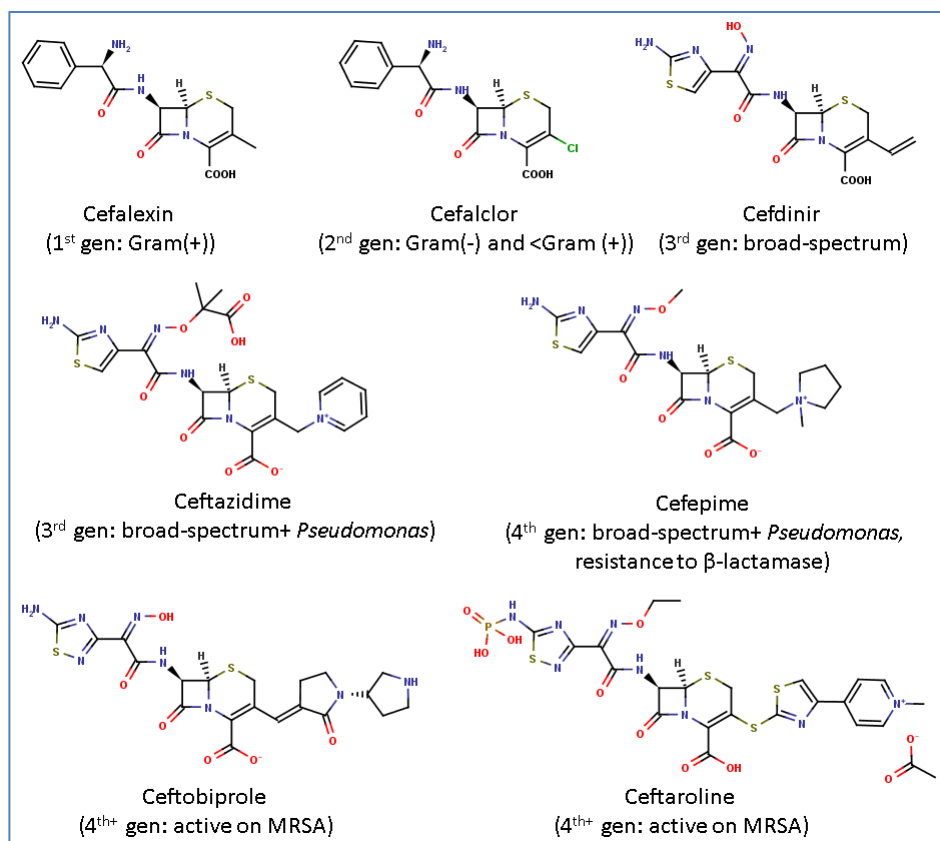
Figure 9 Cephalosporins: a few examples of cephalosporins from the various generations are shown with their spectrum of activity.

Below each structure:

Cefalexin
(1st gen: Gram(+))

Cefalclor
(2nd gen: Gram(-) and <Gram (+))

Cefdinir
(3rd gen: broad-spectrum)

Ceftazidime
(3rd gen: broad-spectrum+ *Pseudomonas*)

Cefepime
(4th gen: broad-spectrum+ *Pseudomonas*, resistance to β-lactamase)

Ceftobiprole
(4th+ gen: active on MRSA)

Ceftaroline
(4th+ gen: active on MRSA)

1.5.3 Glycopeptides

(Boger 2001)

The main representative of glycopeptides is vancomycin; teicoplanin and ramoplanin belong to this family as well. The glycopeptides are active against Gram-positive bacteria, and vancomycin is considered as a last resort drug. Even so, resistance to vancomycin and teicoplanin has started to appear and became of clinical importance; however ramoplanin is active against certain vancomycin-resistant strains (Collins, Eliopoulos et al. 1993; Bozdogan, Esel et al. 2003).
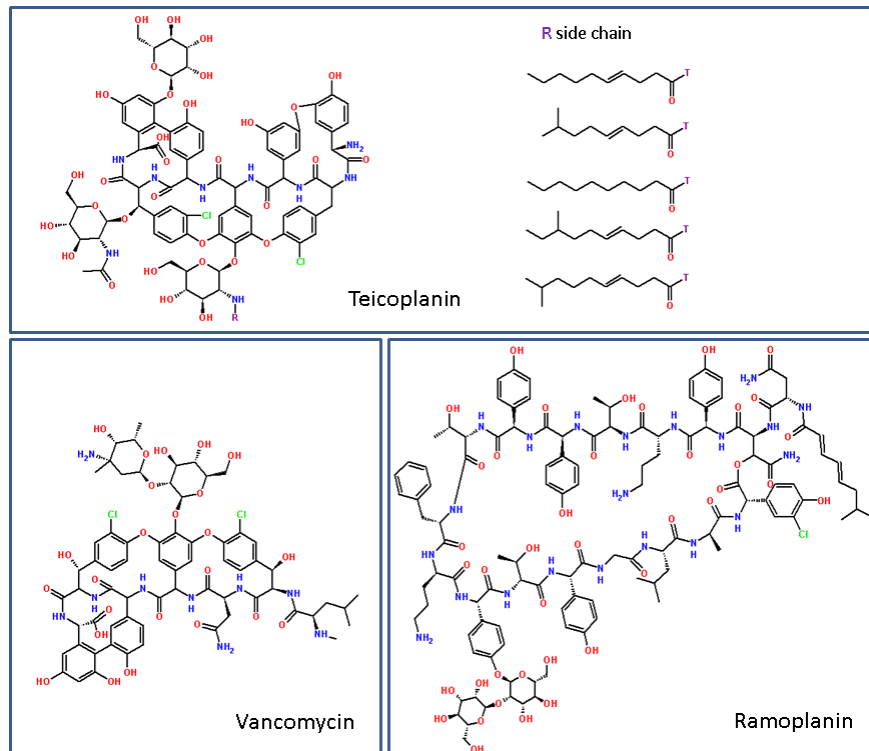
Figure 10 Glycopeptides

1.5.3.1 Mechanism of action
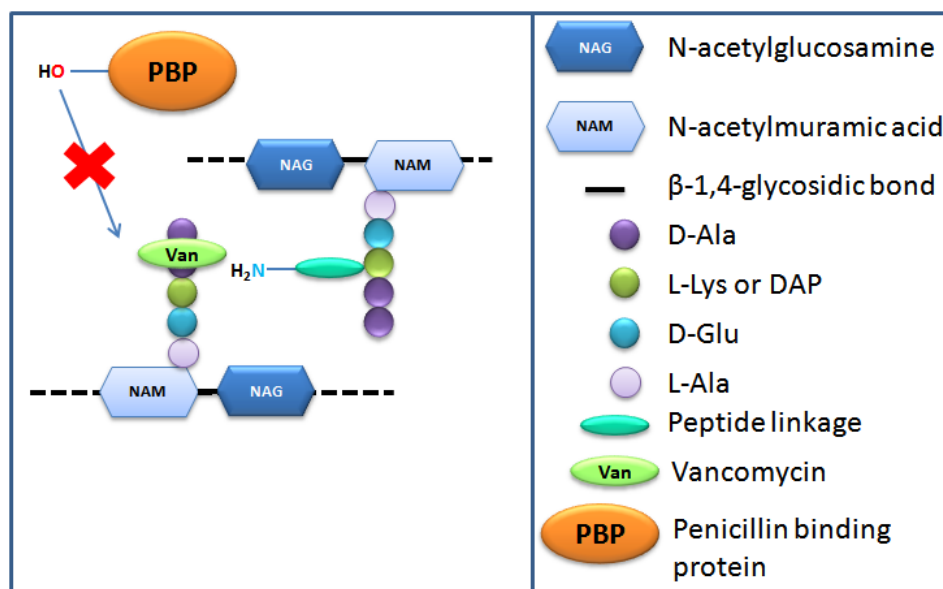
Figure 11 Inhibition of peptidoglycan synthesis by vancomycin

Vancomycin binds to the D-Ala-D-Ala motif of the peptide of the N-acetylglucosamin-N-acetylmuramic building block of the peptidoglycan (Reynolds 1989), blocking the cross-linking of the glycan polymers and thus weakening the peptidoglycan that can no longer contain osmotic pressure. The mechanism of other glycopeptides involve the same pathway, teicoplanin in the same way as vancomycin (Jung, Jeya et al. 2009), and ramoplanin but at different steps, the conversion of lipid I to lipid II (Walker, Chen et al. 2005).
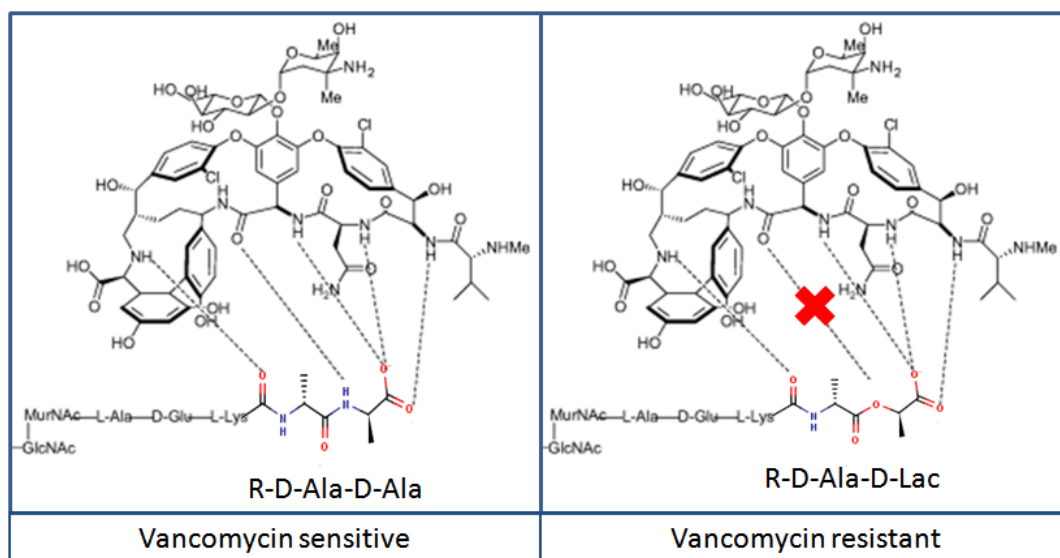
Figure 12 Illustration of vancomycin resistance mechanism

As mentioned before resistance to vancomycin has been achieved by a fundamental change in the peptidoglycan biosynthetic pathway: the terminal D-Ala-D-Ala vancomycin-binding motif has been either replaced by a D-Ala-D-Lac motif, that provides one less hydrogen bond donor as illustrated in Figure 12, or by a D-Ala-D-Ser where the bulky side chain prevent vancomycin binding (Reynolds and Courvalin 2005).

1.5.4 Fosfomycin

Fosfomycin is a broad-spectrum antibiotic isolated from *Streptomyces* that was initially relegated only to treat urinary tract infections, but in the light of the present problem of bacterial resistance it may have a second life where old antibacterials seems a good place to look to find a way around bacterial

Figure 13 Fosfomycin

34
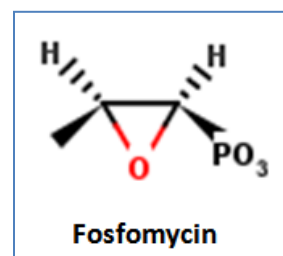
resistance (Samonis, Maraki et al. ; Falagas, Kastoris et al. 2009). Fosfomycin appears to produce a high rate of resistance, but can be used in conjunction with other antibacterials. Recent studies of combination with other antibacterials seems promising (Kastoris, Rafailidis et al. 2010).

1.5.4.1 Mechanism of action

Fosfomycin is an irreversible inhibitor of enolpyruvate transferase (MurA). MurA is involved in the synthesis of the N-acetylmuramic acid, one on the saccharide building block of the peptidoglycan (Figure 14) (Marquardt, Brown et al. 1994).
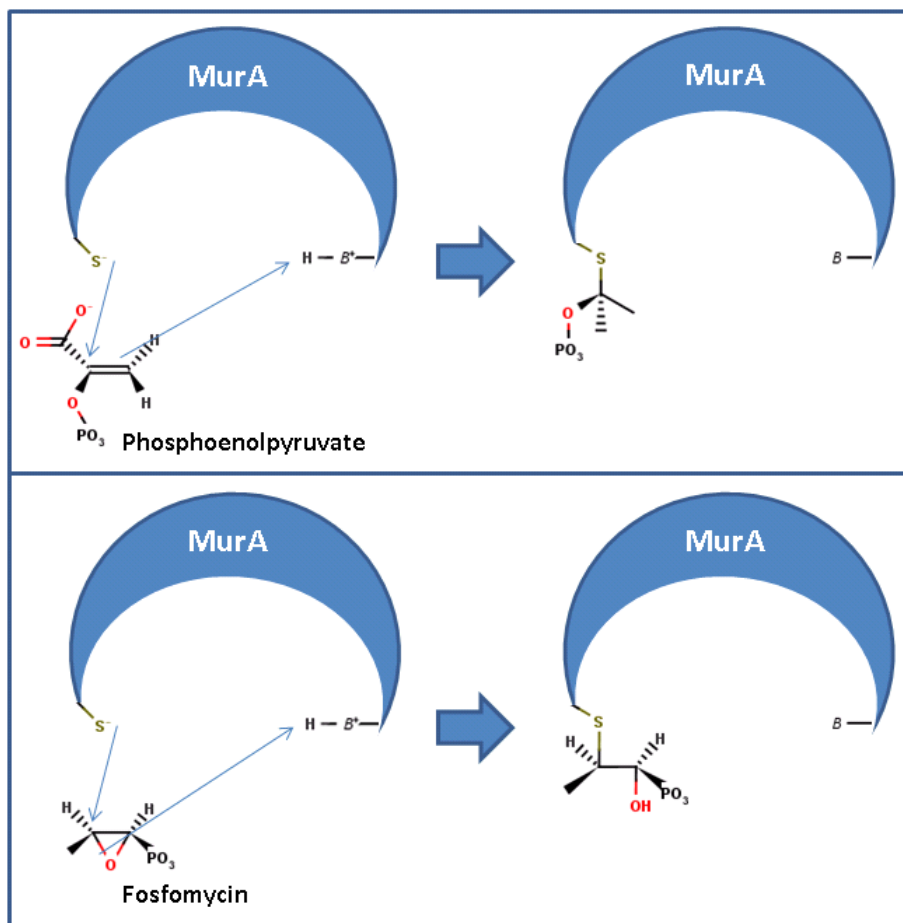
Figure 14 Mechanism of action of fosfomycin: the top figure shows the MurA reaction with its natural substrate. The bottom figure shows the irreversible reaction of MurA with fosfomycin.

1.5.5 Lipopeptides

Lipopeptides are an old class of antibacterial, but due to the recent addition of daptomycin and its activity against drug-resistant *S. aureus* in topic application, they have been put back in the front line. The mechanism of action of daptomycin is not clearly identified: it is a calcium-dependant process involving interaction of daptomycin with the membrane and oligomerisation leading to the destabilisation of the membrane in a way similar to detergents (Robbel and Marahiel ; Fowler, Boucher et al. 2006). Mutation in the chromosomal gene *mprF* coding for a lysylphosphatidylglycerol synthetase have be reported to give resistance to daptomycin (Baltz 2009).
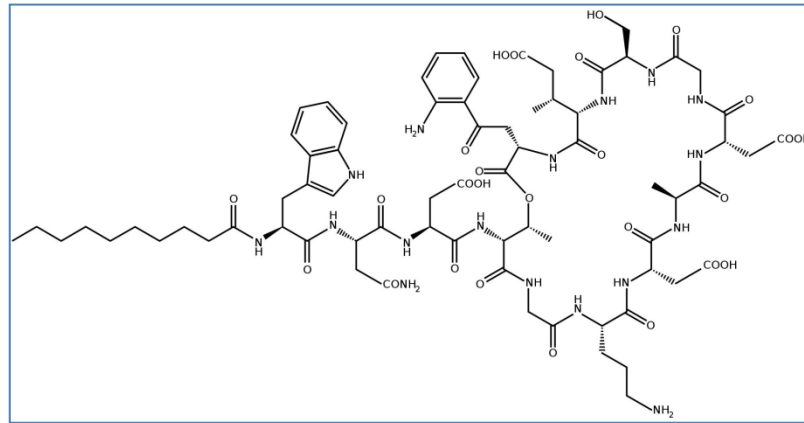
Figure 15 Daptomycin

1.5.6 Polymyxins

Polymyxins are cyclic peptides with a long hydrophobic tail that are produced by *Bacillus polymyxa* (Gram-positive) and are active against Gram-negative bacteria. They belong to the last resort antibacterials against *Pseudomonas aeruginosa* and *Acinetobacter* (Zavascki, Goldani et al. 2007).
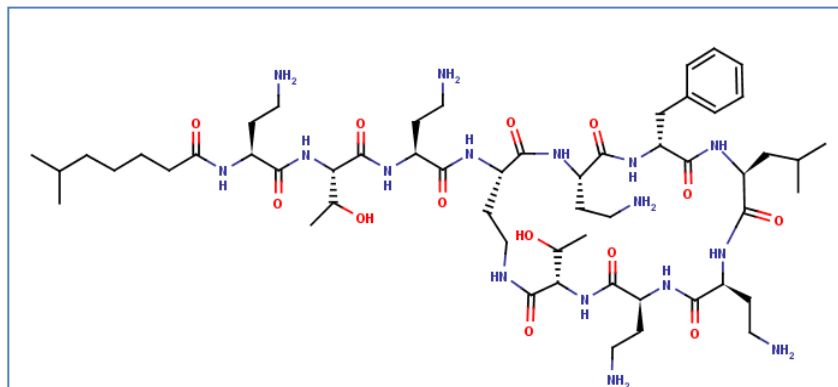
Figure 16 Polymyxin B

1.5.7 Isoniazid

Isoniazid is a pro-drug activated by an enzyme called KatG (catalase-peroxidase) and forms a covalent entity with NADH that disrupts the mycolic acid biosynthetic pathway. Mycolic acid is an essential element of the mycobacterial cell wall (Timmins, Master et al. 2004). Isoniazid is a front line drug for treatment of tuberculosis, resistance to isoniazid has been observed by loss of catalase and peroxydase activity, or by mutation of KatG leading to an enzyme unable to activate the prodrug (Somoskovi, Parsons et al. 2001).
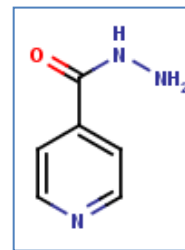
Figure 17 Isoniazid

1.6 Inhibitors of protein synthesis

1.6.1 Protein synthesis by the ribosome

The ribosome is a complex assembly of RNAs and proteins, divided into two main subunits, 30S and 50S, Figure 18 shows the two subunits and the important sites for protein synthesis. The ribosome translates the information encoded in DNA and transferred by mRNA into an amino acid sequence. The mRNA encodes a series of amino acids in the form of series of three bases called codons; start and stop signals are encoded the same way. Amino acids are brought to the ribosome by tRNAs, which are specific to a given amino acid and possess the corresponding anti-codon. The 30S unit is responsible for the "reading" of the mRNA. Protein synthesis is initiated when a start codon reaches the peptidyl (P) site and interacts with the initiator methionine-mRNA and the two subunits associate. A new tRNA is

Figure 18 Structure of the ribosome (Poehlsgaard and Douthwaite 2005)

accepted matching the next codon and after validation of the match in the 30S A site, the methionine is added to the tRNA amino acid in the 50S subunit. The ribosome moves to the next codon placing the dipeptide in the P site, and the methionine-tRNA in the exit (E) site. This is repeated until a stop codon reaches the A site, the peptide chain is then released (Poehlsgaard and Douthwaite 2005).

1.6.2 Mechanism of action

The main mechanism used by antibacterials to inhibit the protein synthesis is the disruption of the ribosome complex. Bacterial and human ribosomes are structurally different and that makes the bacterial ribosome an attractive target for antibacterial drugs. Figure 18 shows the ribosome subunits and their involvement in protein synthesis, whereas Figure 19

details the binding site on the different subunits of various antibacterial agents (Poehlsgaard and Douthwaite 2005).
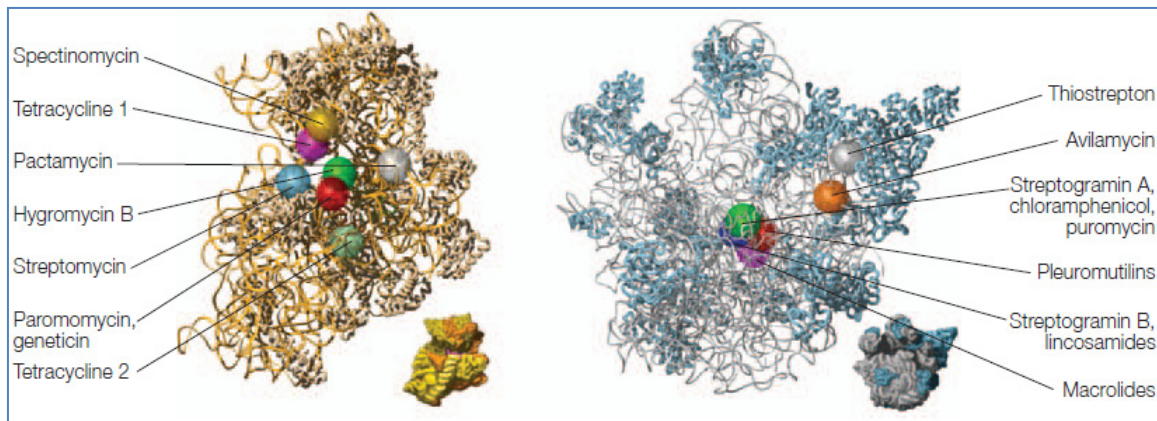
Figure 19 Binding sites of antibiotics on the bacterial ribosome: the 30S ribosomal subunit is shown on the left and the 50S ribosomal subunit is shown on the right. The antibiotic-binding sites were initially determined by biochemical and genetic techniques; subsequently, many sites were revealed in greater detail by X-ray crystallography. At the overlapping sites, antibiotic binding is usually mutually exclusive (for example, for macrolide, lincosamide and streptogramin B compounds), however, streptogramin A and B compounds bind synergistically at adjacent sites. Subunit models are based on the *Thermus thermophilus* 70S ribosome structure (Yusupov, Yusupova et al. 2001). In this figure, for clarity, part of the r-protein L9 has been omitted. Ribosomal RNAs are shown in yellow and grey and r-proteins in bronze and blue (reproduced from Poehlsgaard and Douthwaite (Poehlsgaard and Douthwaite 2005)).

1.6.3   Families

1.6.3.1   Chloramphenicol

Chloramphenicol inhibits protein synthesis by binding to the 50S subunit of the ribosome (Xaplanteri, Andreou et al. 2003), it is a broad-spectrum antibacterial. Due to the development of resistance and toxicity issues chloramphenicol is not a first line agent in developed countries, apart from brain infections, due to its very good penetration of the blood-brain barrier (Feder 1986). Chloramphenicol is a cheap drug which makes it an attractive drug for developing countries. Inactivation

Figure 20 Chloramphenicol

by acetyltransferase is the most common mechanism of resistance against chloramphenicol (Sands and Shaw 1973; Schwarz, Kehrenberg et al. 2004).

1.6.3.2   Aminoglycosides

The first aminoglycoside to be discovered was streptomycin, it was the first treatment used against tuberculosis. Most of the aminoglycosides bind to the 30S subunit and interfere with the initiation complex causing misreading of the mRNA, their exact mode of action is still

under investigation (Edson and Terrell 1999). Among other aminoglycosides that can be cited are amikacin, tobramycin, and gentamicin that are used against severe Gram-negative infection including *Pseudomonas aeruginosa,* and are of particular interest against multi-drug resistant strains (O'Neil 2006). The important side effects shared by this class of drug are: the ototoxicity that can lead to loss of hearing, and nephrotoxicity had restricted their use (Edson and Terrell 1999). Resistance to aminoglycosides has been observed by mutation in the 16S rRNA, and alteration of the small ribosome protein S12 (Jana and Deb 2006). Enzyme able to modify aminoglycosides by N-acetylation, phosphorylation, and adenylation are widespread among resistant bacteria (Jana and Deb 2006).
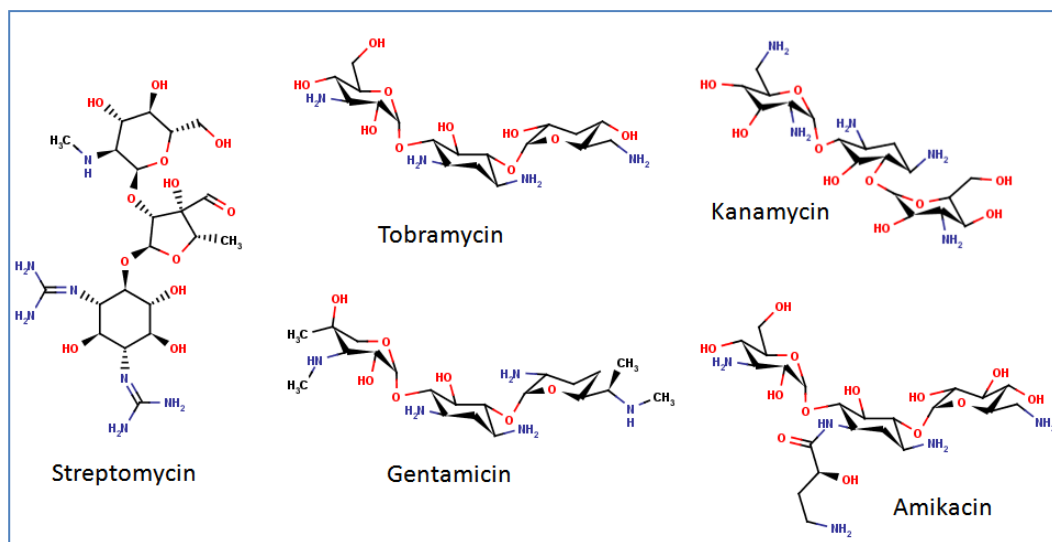
Figure 21 Aminoglycosides

1.6.3.3   Macrolides

Macrolides bind reversibly to the P site of the 50S subunit of the ribosome. Erythromycin has a spectrum of activity similar to penicillin. Azithromycin and clarithromycin have activity similar to erythromycin but with an activity extended to gram (-) bacteria, for azithromycin which made it a very successful antibacterial, and to *Mycobacterium* for clarithromycin. Erythromycin resistance takes place by mutation of the 23S rRNA (Zuckerman, Qamar et al. 2009).

Name	R
Erythromycin	H
Clarithromycin	CH$_3$
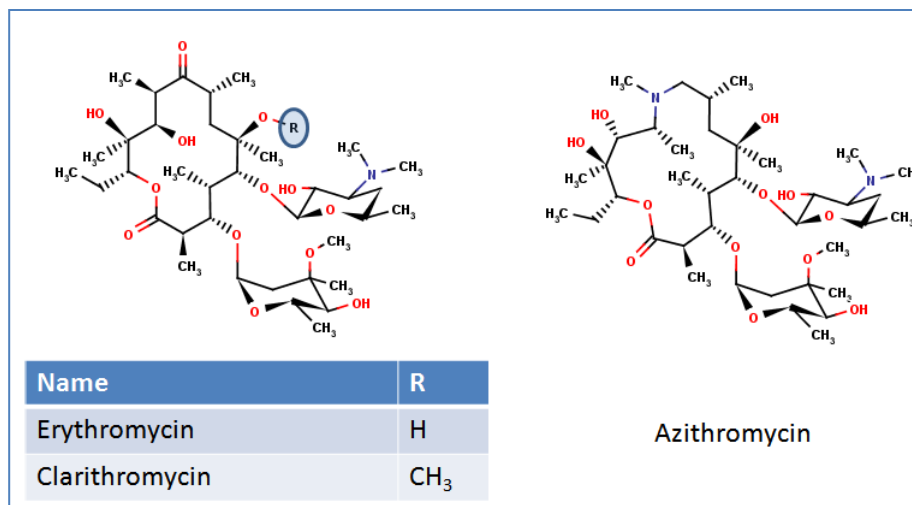
Figure 22 Macrolides

1.6.3.4 Lincosamides

Lincosamides are antibiotics binding to the 50S subunit of the ribosome, lincomycin and the more recent clindamycin are the two members of this class that are used clinically, they have bacteriostatic effect, and are active against Gram-positive bacteria (Spížek and Řezanka 2004).
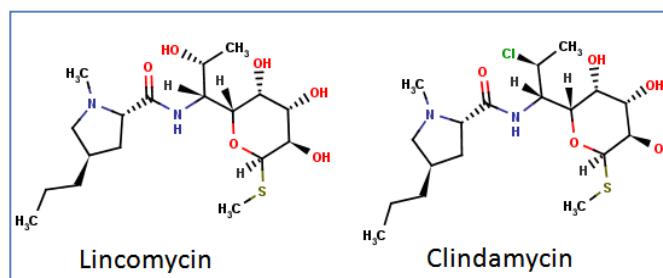
Figure 23 Lincosamides

1.6.3.5   Streptogramins

Quinupristin-dalfopristin is combination of two streptogramins with bacteriostatic activity that bind to the 50S subunit. Interestingly, used in conjunction they have bactericidal activity as quinupristin is an allosteric activator for dalfopristin. Pristinamycin belongs to this family as well. Streptogramins have found application against drug-resistant *Staphylococcus* and *Enterococcus*, they are delivered by injection (Johnston, Mukhtar et al. 2002). Mutations in the large ribosome protein L22 alter the activity of the quinupristin-dalfopristin combination.
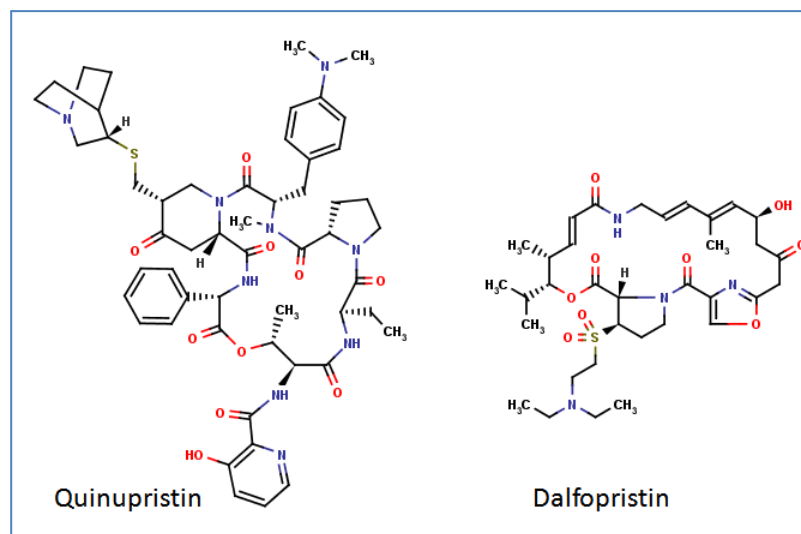
Figure 24 Streprogramins

1.6.3.6   *Note about macrolides, lincosamides, and streptogramins (MLS)*

These three families of compounds are often grouped together as MLS compounds, they share the same binding site, and mutation or methylation of this site confers resistance to all of them. It had been shown as well that mutation of the ribosome protein L4 and L22 alters susceptibility to MLS compounds. A secondary mechanism of resistance is the acquisition of a modifying enzyme: esterases and phosphotransferases for macrolides, nucleotidyltransferase for lincosamides, and hydrolase or acetyltransferase for streptogramin (Leclercq and Courvalin 1991; Roberts 2008).

1.6.3.7 Ketolides

Ketolides are newcomers, there is only one representative of this class of compounds used clinically since the 2000's: telithromycin, but other compounds of this class are under development. Telithromycin is related to macrolides, but displays a broader spectrum of activity, it possess two different binding sites on the 50S subunit (Zuckerman 2004). Mutation in the 23S rRNA, in the large ribosome protein protein L4, and the large ribosome protein L22 induce reduced susceptibility and give resistance to telithromycin (Roberts 2008).
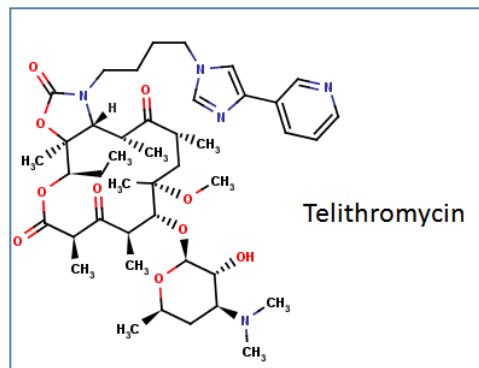
Figure 25 Ketolides: telithromycin

1.6.3.8 Tetracyclines

Tetracyclines are broad-spectrum polyketide antibiotic produces by *Streptomyces*. They bind to the 30S subunit. Minocycline and doxycycline are the tetracyclines currently used clinically. Resistance to tetracycline have been observed by point mutation in the 16S rRNA (Chopra and Roberts 2001). Evidence suggesting that resistance to tetracyclines is acquired through a monooxygenase that is regioselectively hydroxylating the antibacterial has been reported (Yang, Moore et al. 2004).
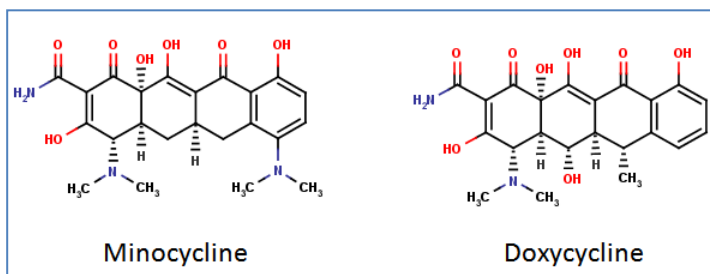
Figure 26 Tetracyclines

1.6.3.9 Tigecycline

Tigecycline is the first representative from a novel class of antibacterial related to tetracyclines developed to counter the resistances to tetracyclines. It is a broad spectrum antibacterial used against infection by drug-resistant *S. aureus* and *A. baumanni* (Livermore 2005).

1.6.3.10 Oxazolidinones: Linezolid

Linezolid is the sole representative of this class to be used clinically. It had become however a major player in the treatment of infection caused by resistant strains. Linezolid prevents the formation of the complex between the 30S and 50S subunits (Swaney, Aoki et al. 1998). Resistance to linezolid has been observed in the 23S rRNA (Kloss, Xiong et al. 1999).
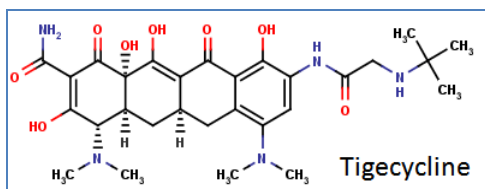
Figure 27 Tigecycline
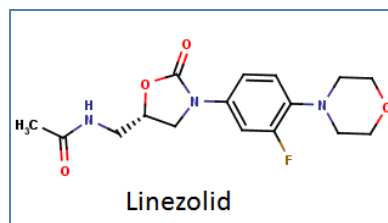
Figure 28 Oxazolidinone

1.7 Antibacterials affecting nucleic acids

1.7.1 Nitroimidazoles

Nitroimidazoles are antibacterial compounds specific to anaerobic Gram-negative and Gram-positive bacteria, and protozoa. Once inside the organism, the compounds react with the reduced form of ferredoxin, the product of this reduction reacts with DNA (Edwards 1993). Metronidazole and ornidazole are members of this drug family. They are the drug of choice to treat human infections caused by various anaerobic and microaerophilic bacteria: *Bacteroides*, *Clostridia*, *Helicobacter*; as well as parasites like *Trichomonas*, *Giardia, Entamoeba* (Edwards 1993).
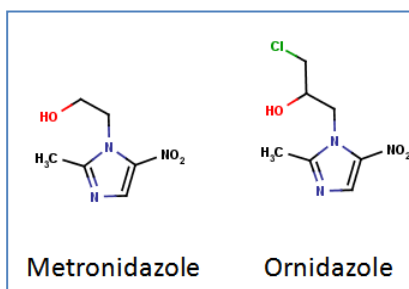
Figure 29 Nitroimidazoles

1.7.2   Sulfonamides (Sulfa drugs) and trimethoprim
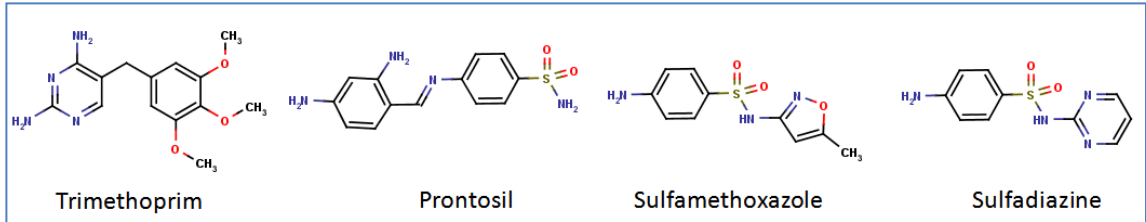
Figure 30 Trimethoprim & sulfa-drugs

Sulfonamide and trimethoprim do not interact directly with DNA but instead disrupt the nucleic acid biosynthetic pathway by blocking the formation of a precursor, folic acid. Sulfonamides mimic the folic acid precursor para-aminobenzoic acid and compete with dihydropteorate synthetase and dihydrofolate synthetase. Trimethoprim is inhibiting a later step in this pathway by interacting with dehydrofolate reductase. Among the sulfonamide drugs are: sulfanilamide (active principle of prontosil), sulfamethoxazole, and sulfadiazine. Occurrences of resistance results from mutations in the gene coding for the dihydropteroate synthetase for the sulfonamides or the dihydrofolate reductase for trimethoprim (Skold 2001).
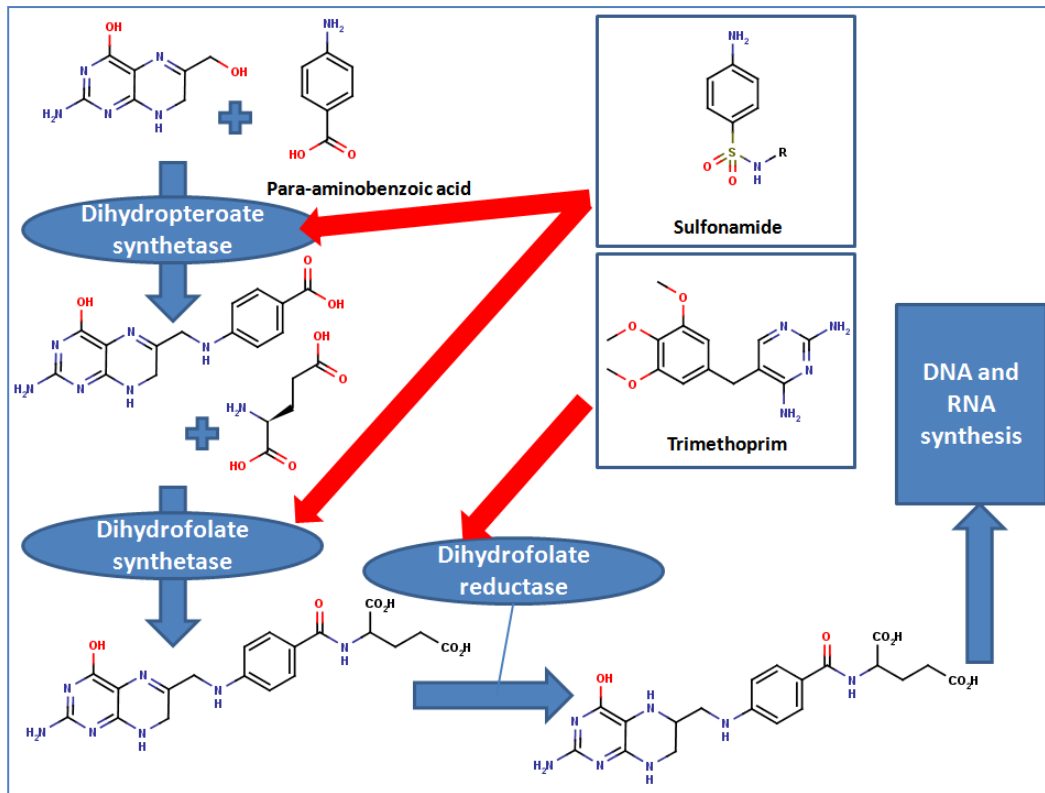
Figure 31 Inhibition of the folic acid synthesis by sulfonamides and trimethoprim

44

1.7.3 Rifamycins

Rifamycins are a class of antibacterials initially isolated from *Amycolatopsis mediterranei*, among them: rifampicin, rifapentine. These compounds inhibits bacterial RNA polymerase (Ho, Hudson et al. 2009). Rifampicin is a front line antituberculosis drug (van den Boogaard, Kibiki et al. 2009).
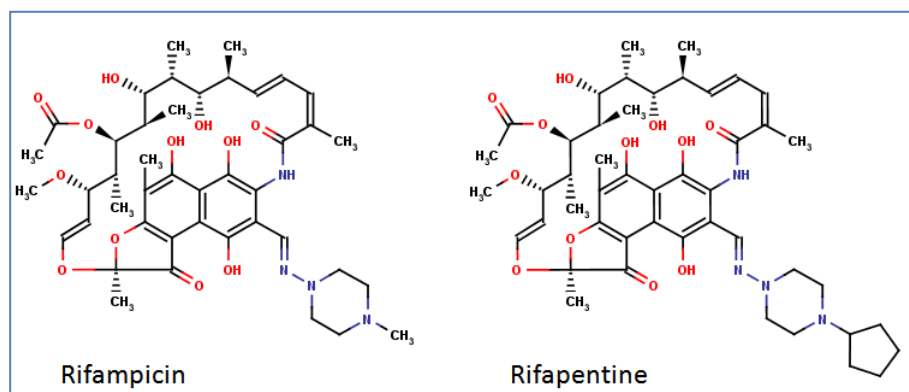
Figure 32 Rifamycins

1.8 Fluoroquinolones and aminocoumarins

Fluoroquinolones and aminocoumarins target type II topoisomerases: DNA gyrase and DNA topoisomerase IV. Aminocoumarins are catalytic inhibitors, preventing the binding of ATP, required for enzyme function (Gellert, O'Dea et al. 1976; Lewis, Singh et al. 1996); whereas fluoroquinolones are topoisomerase poisons, stabilizing an enzyme-cleaved DNA intermediate, thus generating toxic species (Drlica and Zhao 1997). Topoisomerases and their use as drug targets will be more extensively covered in the following section. Resistance to fluoroquinolones involves mutation mostly in the GyrA or ParC subunit in what is referred to the quinolone-resistance-determining region (QRDR), that prevent the interaction with the DNA-topo complex (Hopkins, Davies et al. 2005). Another mechanism of resistance involve the production of the pentapeptide repeat protein Qnr. Qnr is able to bind gyrase subunits in the absence of DNA, thus by interacting at an early stage of the gyrase cycle it can prevent the binding of fluoroquinolones (Hopkins, Davies et al. 2005). Another member of this family found in *M. tuberculosis* MfpA is mimicking B-form DNA, and interacts with gyrase disrupting fluoroquinolone activity (Hegde, Vetting et al. 2005). These mechanisms give low-level resistance to the organism but provide the bacteria just enough room to acquire more efficient mechanisms of resistance. It is interesting to note that McbG, the MccB17-producing strain self-immunity protein, belongs to this family as well (Bateman, Murzin et al. 1998).

2 General information about topoisomerases

The first topoisomerase was discovered in 1971 (Wang 1971), it was *E. coli* topo I (the *E. coli*-omega protein), it was characterized by its ability to remove negative superhelical twists from DNA. This finding was closely followed by a second in 1972, with the calf-thymus swivelase (Champoux and Dulbecco 1972), this protein was shown to relax both positively and negatively supercoiled DNA. Topoisomerases solve the topological problems occurring during DNA replication, transcription, recombination, and chromatin remodelling by introducing temporary single- or double-strand breaks in DNA. They regulate the steady-state level of DNA supercoiling in order to facilitate DNA-protein interaction and prevent the deleterious excess of supercoils. The initial classification of these enzymes relies on the mechanism used to change DNA topology: type I topoisomerases act via single-strand breaks, whereas type II topoisomerases work through a double-strand breaks (Wang 2002). Several families and subfamilies of these two types have been described in the three cellular domains of life (Archaea, Bacteria, Eukarya) as well as viruses infecting eukaryotes or bacteria (Forterre, Gribaldo et al. 2007). We will describe succinctly these different topoisomerases, their role and their pharmacological significance.

2.1 Classification of topoisomerases

(Forterre, Gribaldo et al. 2007)

Topoisomerases are first divided into type I topoisomerases, designated with odd numbers, and type II topoisomerases designated with even numbers; this classification derives from the mechanism used by the enzyme to handle DNA topology: cleaving a single strand of the DNA duplex for type I and a double strand for type II.

2.1.1 Type I DNA topoisomerases

(Champoux 2001)

Type I topoisomerases are enzymes that affect DNA topology by transiently cleaving one DNA strand at a time. All share the same chemistry to break the phosphodiester bond: the enzyme attacks a phosphodiester bond of the DNA with a tyrosyl group forming a covalent bond on one side of the break and releasing a free hydroxylated strand on the other side. The reverse reaction: the attack of the phosphotyrosine by the free hydroxylated strand restores the phosphodiester bond and releases the enzyme for next catalytic cycle. The cleavage-religation process does not require ATP hydrolysis as the final state of the phosphodiester bond is the same as the start. The subdivision of topo I into the A and B subfamilies is linked to the polarity of the strand cleavage. Topo IA forms a transient 5′-phospho-tyrosine covalent intermediate, releases a free 3′-OH strand and promotes passage of the intact strand through the broken strand; whereas topo IB forms a 3′-phospho-tyrosine covalent intermediate, releases a free 5′-OH strand and leaves the broken strand free to rotate around the intact strand. This subdivision is supported by the absence of sequence or structural similarities (Wang 2002). Almost all topo IA and topo IB are monomeric and formed by a single topoisomerase domain. The topo IA class includes bacterial topo I and topo III, eukaryotic topo

III, and the unique reverse gyrase which is able to introduce positive supercoils into DNA at the expense of ATP; this last enzyme is found uniquely in hyperthermophiles (Kikuchi and Asai 1984; Shibata, Nakasu et al. 1987). The topo IB class includes eukaryotic topo I and poxvirus topo I. Topoisomerase V has been initially included in the type IB family, but structural analysis argue toward the possibility that topo V is the first identified member defining a new class, the type IC topoisomerases (Taneja, Patel et al. 2006).

2.1.2 Type II DNA topoisomerases
(Champoux 2001)

Type II DNA topoisomerases introduce double-strand breaks in a DNA duplex and force the passage of another duplex through this break before resealing it. The cleavage-religation reaction is similar to those performed by type I topoisomerases with the formation of a covalent bond between a tyrosine from the enzyme and the DNA phosphate, but the transient link is exclusively formed with the 5' end of the DNA breaks. All type II topoisomerases are ATP-dependent multimeric enzymes with a dyad symmetry. Each unit of the enzyme is composed of an ATP-binding domain and a catalytic breakage-religation domain that contains the covalent bond-forming tyrosine residue. In eukaryotic and viral topo II these two domains form a single entity organised as a homodimer whereas in bacterial and archeal gyrase and topo IV they are two separate subunits A and B organised as a A_2B_2 tetramer, in both case the dyad symmetry is conserved. The enzymes proceed through what is referred as a "two-gate" mechanism as follows: A first segment of DNA duplex is bound by the breakage-religation domain and will be referred as the gate segment (or G segment), a second DNA duplex is bounded by the N-terminus domain of the enzyme or N-gate, it will be referred as the transported segment (or T segment) (Berger, Gamblin et al. 1996). The second DNA duplex belongs either to the same molecule in the case of supercoiling/relaxation and unknotting/knotting reactions, or to another in the case of decatenation/catenation reaction. The selectivity of the binding is driven by the topology of the substrate DNA. How the enzyme is able to sense this topology is still under investigation, hypotheses involving local geometry of cross-over and wrapping have been proposed (Liu, Mann et al. 2006; Schoeffler and Berger 2008). Upon binding of ATP, the two ATP-binding domains dimerise adopting a closed conformation of the N-gate and trapping the T-segment. At each catalytic cycle, the enzyme goes through a series of conformational changes allowing the cleaved duplex to be pulled apart, opening the G segment to the passage of the T-segment, this event is called strand passage. The link between ATP hydrolysis and strand passage is not clearly defined and may vary among the different type II topoisomerases. What is certain is that ATP hydrolysis and release of its products will induce the conformational changes that will reset the enzyme for the next catalytic cycle. Most of the type II topoisomerases belong to the type IIA family. Type IIB topoisomerases class consists of only one member: topo VI, it had been first discovered in *archaea* (Bergerat, Gadelle et al. 1994; Bergerat, de Massy et al. 1997), and other representatives were found later in plants (Hartung and Puchta 2001), *algae*, some bacteria (Malik, Ramesh et al. 2007), and in plasmodium (Aravind, Iyer et al. 2003). Topo VI possess the same mechanism of action as other type II topo

but differs by the absence an exit gate, there is no protein structure after the cleavage-religation domain (Bergerat, Gadelle et al. 1994).

2.2 The occurrence of DNA topoisomerases in different cell types
(Champoux 2001; Forterre, Gribaldo et al. 2007)

2.2.1 Eubacteria
Four DNA topoisomerases are found in *E. coli*; DNA topoisomerases I and III, which are type IA topoisomerases, and DNA gyrase and DNA topoisomerase IV which belong to the type IIA family. Each enzyme has evolved to carry out a specific set of topological alterations although some overlap of function can occur. There is some variation in other bacteria: some mesophilic bacteria lack a homologue of topo III but possess the three others topoisomerases, this is probably the result of the apparent redundancy of function between topo III and topo IV; others seems to possess the minimal requirement for cell to function, only two topoisomerases, one homologous to *E. coli* DNA gyrase, the second homologous to *E. coli* topo I. Hyperthermophiles possess a reverse gyrase, which introduces positive supercoiling probably to counteract the helix unwinding and strand separation effects of growth at high temperature. Finally a topoisomerase V has been identified in hyperthermophiles; it is the only known type IB topoisomerases in bacteria, its recently solved crystal structure shows that it possesses a unique structure among topoisomerases and might be the first representative of a new class (Taneja, Patel et al. 2006).

2.2.2 Archaebacteria
Known archaea seem to share a common ensemble of topoisomerases: a reverse gyrase, a type IA topo, and topoisomerase VI.

2.2.3 Yeasts
Saccharomyces cerevisiae and *Schizosaccharomyces pombe* encode the following topoisomerases: topo I (IB subfamilly), topo II (IIA subfamilly), and topo III (IA subfamily).

2.2.4 Higher eukaryotes
All higher eukaryotes contain a single topo I which plays a major role in cell functions. Most higher eukaryotes appear to possess two type IIA isoforms termed topo IIα and topo IIβ. They also have two isoforms of topisomerase III, termed topo IIIα and topo IIIβ.

3 Topoisomerases as drug targets
Among the topoisomerase family, some are of particular importance due to their relevance as drug targets in antimicrobial and anticancer therapy. The most efficient agents stabilise the topoisomerase-DNA covalent complex, so a special emphasis will be put on these. We will particularly focus on gyrase as it is the target of MccB17, but we will also cover topo IV the second prokaryotic topo II affected by fluoroquinolones and the eukaryotic topo I and topo II as they are prone to have their protein-DNA cleavage complex stabilized by inhibitors with some similarities to their bacterial counterparts. The various topoisomerases used as drug

target will be described with their inhibitors. A final part will deal with the different structures of topoisomerases in the presence of cleavage complex stabilizing agents observed by crystallography.

3.1 Eukaryotic Topoisomerase I
(Holden 2001)

Among the type I topoisomerases, only human topo I had found its use for therapeutics; the bacterial type I topoisomerases might be useful targets for antibacterial compounds but none have been identified so far (Tse-Dinh 2009). A drug called camptothecin was isolated from the Chinese tree *Camptotheca acuminata* and showed in early studies some interesting anticancer properties (Wall, Wani et al. 1966), but unfortunately unacceptable toxicity was observed during clinical trials. Camptothecin's molecular target was identified as being topo I and its mode of action was discovered to be the poisoning of the enzyme (Porter and Champoux 1989). Anti-cancer derivatives of camptothecin were successfully generated: topotecan and irinotecan are currently used in anti-cancer therapy and other derivatives are in clinical trials (Pommier 2009). The crystal structure of the topo I–DNA covalent complex in the presence of topotecan shows how the compound intercalates in the cleavage site between the (-1) and (+1) base-pairs and forms hydrogen bonds with topo I. In this position topotecan hinders the religation process and traps the complex in its open form (Staker, Hjerrild et al. 2002). Camptothecin suffers three flaws detrimental to its activity: first the lactone ring is easily hydrolyzed at physiological pH leading to an inactive carboxylate form, second camptothecin is fairly insoluble, and last camptothecin has important side-effects. Topotecan and irinotecan successfully addressed the problem of solubility and they are two orally administered anti-cancer drugs, however new compounds in the pipeline and clinical trials are awaited as stability and toxicity issues remained to be addressed.

3.2 Eukaryotic Topoisomerase II
(Holden 2001; Pommier, Leo et al. 2010)

Anticancer drugs targeting topo II are among the most widely used chemotherapeutic agents, including doxorubicin, etoposide and mitoxantrone. These drugs fall in two different groups: topoisomerase poisons that generate toxic species by increasing the steady-state levels of the transient DNA-topo II intermediate, or topoisomerase catalytic inhibitors that block enzyme function. Topo II poisons can be further divided into two classes depending on which stage of the cleavage-religation reaction they affect: the first comprise ellipticine (Stiborova, Rupertova et al. 2010), azatoxin (NSC640737) (Cline, Macdonald et al. 1997), genistein (Yamashita, Kawada et al. 1990) and cytotoxic quinolones, that increases the amount of cleaved intermediate by stimulating its formation, whereas the second include etoposide, teniposide, doxorubicin, daunorubicin, and amsacrine that inhibit the religation reaction (Pommier, Leo et al. 2010). Topo II catalytic inhibitors can act at different steps of the complex catalytic cycle. This cycle can be dissected in seven distinct events:

Event: inhibitor(s) acting during this event

1) Binding of the enzyme to the DNA: anthracyclines (aclarubicin (Larsen, Escargueil et al. 2003)), suramin (Larsen, Escargueil et al. 2003).

2) Production of the double-strand break DNA: quinolones (CP-115953 (Bromberg, Burgin et al. 2003), voreloxin (Hawtin, Stockett et al.)), merbarone (inhibition)(Fortune and Osheroff 1998).

3) Binding of ATP, dimerisation of the N-terminal domains: coumarins (novobiocin, coumermycin)(Larsen, Escargueil et al. 2003).

4) Strand passage.

5) Religation of the DNA break after strand passage: etoposide (VP16), teniposide (VM26), doxorubicin, daunorubicin, amasacrine (m-AMSA) (Pommier, Leo et al. 2010), TAS-103 (Fortune, Velea et al. 1999).

6) ATP hydrolysis: bisdioxopiperazine derivatives (ICRF-187, ICRF-193) (Andoh and Ishida 1998), staurosporine (Pommier, Leo et al. 2010).

7) Dissociation and release of the DNA from the topoisomerase.

Looking at this plethora of compounds and how they seem to cover every steps of the enzyme cycle, eukaryotic topo II can be regarded as a model of successful exploitation of a topoisomerase drug target.

3.3   Prokaryotic topoisomerase II:

In eubacteria, DNA gyrase and topoisomerase IV have been exploited by nature and the pharmaceutical industry as antibacterial targets. Two families of compounds have been successfully used on prokaryotic topo II, the fluoroquinolones (Drlica and Zhao 1997) and the aminocoumarins (Maxwell and Lawson 2003). The first has been extensively studied and had given a wide variety of antibacterial agents, the second possess only one member, novobiocin, that has been clinically used before being withdrawn from the market. These compounds display different level of activity on both gyrase and topo IV. These two targets and their inhibitors will be given an extensive treatment in the following part as they represent the primary enzymes we are studying.

4   DNA gyrase and topo IV (in *E. coli)*:

Gyrase and topo IV are very closely related enzymes both in structure and in their interaction with inhibitors, therefore they will be described in parallel in the following sections. We will mainly focus on the *E. coli* version of these enzymes to describe their structure.

4.1 Biological activity

DNA gyrase and topo IV are two highly homologous type II topoisomerases that have both been shown to be affected by quinolones (Drlica and Zhao 1997) and aminocoumarins (Maxwell and Lawson 2003). Gyrase is the only known topoisomerase that can introduce negative supercoils at the expense of ATP, by doing so it can relax positively supercoiled DNA or negatively supercoil relaxed DNA (Gellert, Mizuuchi et al. 1976). In the absence of ATP, gyrase can relax negatively supercoiled DNA by the reverse mechanism of negative supercoiling (Gellert, Mizuuchi et al. 1977). The major *in vivo* activity of gyrase is the introduction of negative supercoils into the chromosome. Topo IV is primarily specialised in decatenating (Ullsperger and Cozzarelli 1996) and unknotting DNA (Deibler, Rahmati et al. 2001); its ability to relax negatively and positively supercoiled DNA with a preference for the latter enable topo IV to remove the positive supercoils generated ahead of the replication fork (Crisona, Strick et al. 2000).
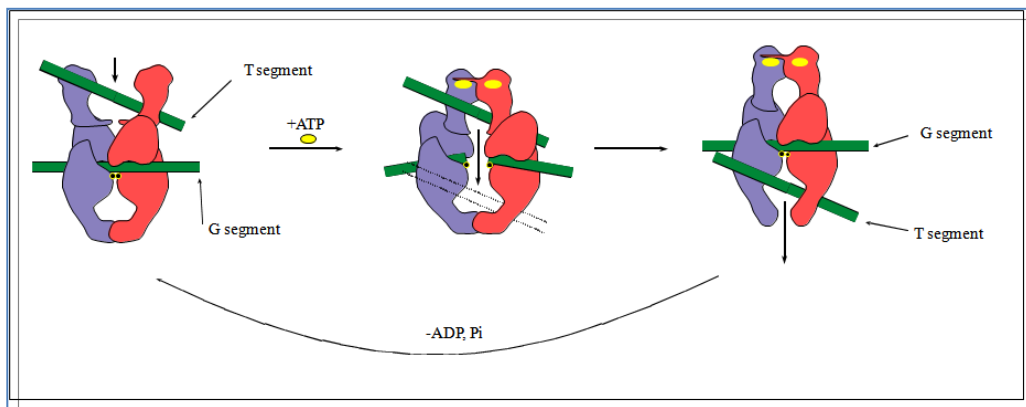
Figure 33 Illustration of type II topoisomerase mechanism (Bates 2001).

Before topo IV was discovered, gyrase was thought to be involved in unlinking the catenated chromosome at the end of replication to allow segregation of one copy to each of the daughter cells. However it has been discovered that topo IV is the major cellular decatenase for both replication- and recombination-generated catenanes. The superhelical density of the *E. coli* chromosome is regulated by the combined action of gyrase, topo I and topo IV, with the two latter balancing the activity of the first (Schvartzman and Stasiak 2004). This global supercoiling level is essential for the initiation of DNA replication, and general transcription, which requires the assistance of negative supercoiling to unwind origins and promoters. Another important issue with DNA gyrase is its participation in the elongation phase of DNA replication and transcription. Actually both of these processes necessitate unwinding of long stretches of the DNA duplex, the 4.6 megabases of DNA for replication of the *E. coli* chromosome. Unwinding the duplex produces positive supercoils that accumulate, they must be removed in order to withstand superhelical stress; it is done by gyrase, which introduces negative supercoils. Similarly, gyrase removes positives supercoils generated ahead of the advancing polymerase during transcription elongation (Hooper 1998; Nollmann, Crisona et al. 2007).

51

4.2 Structure

4.2.1 Gyrase
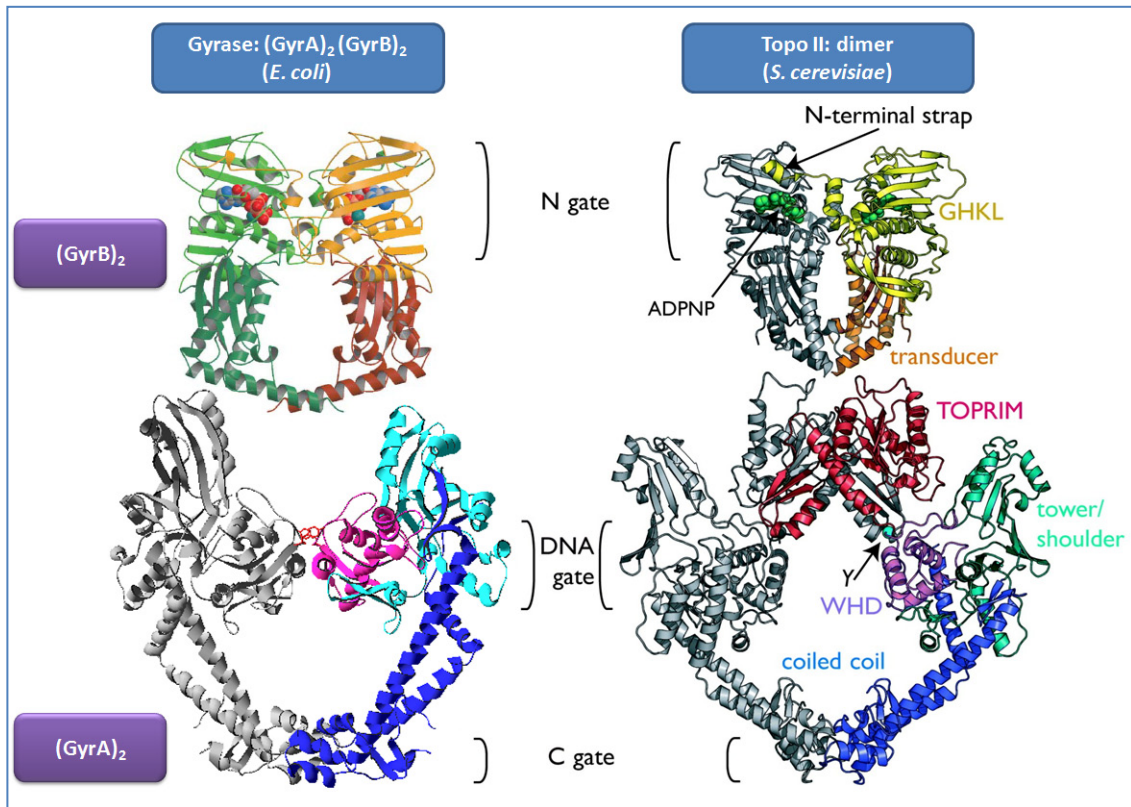
Figure 34 Structure of *E. coli* gyrase, comparison with *S. cerevisiae* topo II: left side, crystallographic structures related to *E. coli* gyrase; the top structure is the dimer of the N-terminal part of GyrB from Wigley *et al* (Wigley, Davies et al. 1991), the bottom structure is the GyrA N-terminal dimer from Edwards *et al* (2WL2) (Edwards, Flatman et al. 2009). Right side, *S. cerevisiae* topo II reproduced from Schoeffler and Berger (Schoeffler and Berger 2008) is displayed for comparison, the top structure is the topo II ATPase domain from Classen *et al* (1PVG), the bottom structure is the dimer of topo II (residues 410-1202) from Berger *et al* (1BGW). The different structures are colour coded according to their substructure: ADPNPs are shown as spheres, GHKL in light orange/yellow, transducer domain in orange, TOPRIM in red, WHD in pink, tower/shoulder in turquoise, and the coiled-coils in dark blue. No structure of *E. coli* gyrase TOPRIM domain is available. Catalytic tyrosines are show as red sticks (gyrase) or turquoise sphere (topo II). Note that the C-terminal domains are not present in the structures.

Gyrase is a type II-A topoisomerase composed of two subunits; GyrA with a molecular weight of 97 kDa (Swanberg and Wang 1987) and GyrB with a molecular weight of 90 kDa (Yamagishi, Yoshida et al. 1986), organized in a tetramer, A_2B_2. The main role of the GyrA is the cleavage-religation of DNA strands (Horowitz and Wang 1987); GyrB is responsible for the hydrolysis of ATP (Reece and Maxwell 1991). Limited proteolysis of GyrA and GyrB identified two domains for each subunit (Reece and Maxwell 1989; Kampranis and Maxwell 1998), these domains were later related to specific aspects of the enzyme activity: GyrA is divided into a 64

52

kDa N-terminal domain, which is the "breakage-reunion" domain and contains the quinolone-resistance-determining region (QRDR), and a 33 kDa C-terminal domain around which the DNA wrapped (Costenaro, Grossmann et al. 2005). GyrB is divided into a 43 kDa N-terminal domain, which is the ATPase domain (Wigley, Davies et al. 1991) and contains the aminocoumarin interaction site, and a 47 kDa C-terminal domain, which interacts with GyrA and DNA (Brown, Peebles et al. 1979). This last 47 kDa domain can be further divided into the TOPRIM and Tail domains according to their structure (Costenaro, Grossmann et al. 2007). Figure 34 shows the domains division in the type II topoisomerases gyrase and topo II. Recently a model has been constructed from small-angle X-ray scattering (SAXS) data from the full length gyrase in presence of DNA, it provides a picture of gyrase structure in solution of gyrase (Figure 35) (Baker, Weigand et al. 2010). A hypothesis, derived from the SAXS model, has been proposed for the wrapping of DNA around gyrase (Figure 35), however we want to arise some cautions, as the DNA appears to be in an unlikely conformation to accommodate the DNA bending observed at the DNA gate in other type II topoisomerase structures, like *S. cerevisiae* topo II for example as shown in Figure 36.
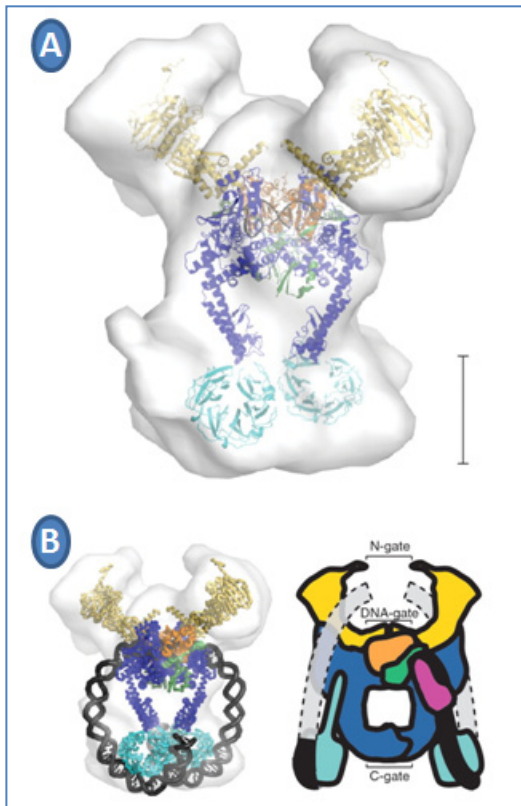
Figure 35 SAXS of full length *E. coli* gyrase with DNA: the top picture is the envelope extrapolated from SAXS data with the gyrase model fitted inside. The bottom picture shows the proposed model of DNA wrapping around gyrase (Baker, Weigand et al. 2010).
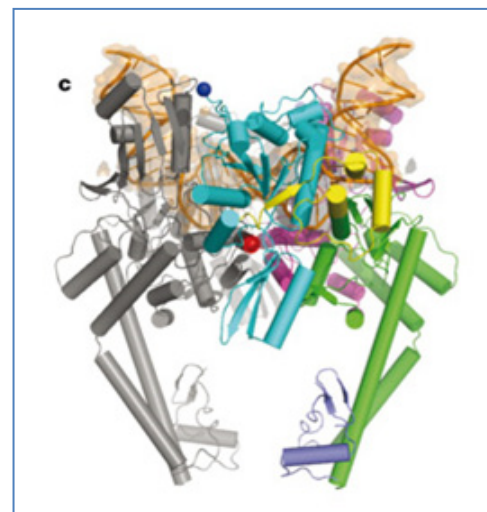
Figure 36 DNA bending by *S. cerevisiae* topo II (Dong and Berger 2007).

Structures of gyrases from organisms other than *E. coli* have been released recently: the TOPRIM and breakage reunion domain of *M. tuberculosis* (3M4I, 3IFZ)(Piton, Petrella et al.); the fusion protein of the C-terminus of GyrB (GyrB27) and GyrA N-terminus (GyrA56) of *S. aureus* in presence of DNA and cleavage complex stabilizing agents (2XCT and others)(Bax, Chan et al. 2010). These structures give insight on the general mechanism of gyrase, and additionally, if considered with the other elements available: the GyrA NTD (3ILW)(Tretter, Schoeffler et al.) and GyrB' CTD (2ZJT) (Fu, Wu et al. 2009) for *M. tuberculosis*, and the GyrB NTD for *S. aureus* (3G75)(Ronkin, Badia et al.), they are direct source of information to design inhibitors for these organisms.
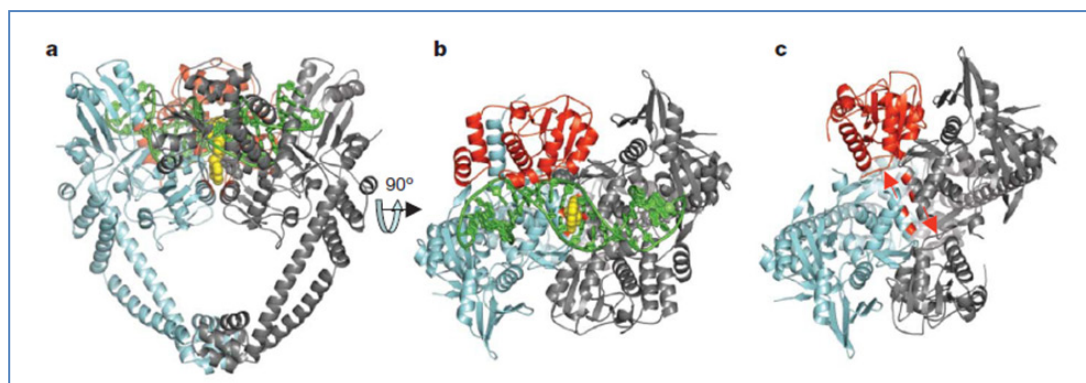
Figure 37 *S. aureus* gyrase (GyrB27–A56 fusion protein): a, b, Orthogonal views of 2.1 Å complex with GSK299423 (yellow, solid) and DNA (green). One fused GyrB27–A56(GKdel/Tyr123Phe) subunit is shown in grey, the other in red (GyrB) and blue (GyrA). c, 3 Å apo GyrB27–A56 structure. On formation of the complex the α3 helices slide approximately 6 Å past each other (indicated by red arrows) to align the red stripes (Ala68 and Gly72) underneath the compound (in b). Molecular figures generated with Pymol40. Reproduced from Bax *et al* (Bax, Chan et al. 2010).

The mechanism of supercoiling by gyrase has not been completely elucidated but a model, called the "two-gate mechanism", supported by biochemical evidence and structural information, has been formulated and should reflect what is happening. If we consider the gyrase structure, three interfaces can be in an open or closed conformation: the N-terminal domain of GyrB referred as the N-gate, the GyrA-GyrB-DNA interface where the DNA is cleaved, referred as the DNA gate, and the C-terminal area of coiled coils that are forming the C-gate. These three gates are involved as follows: the G-segment of DNA associates with the enzyme, at the interface of N-terminus of the GyrA dimer and the TOPRIM domain of GyrB (Morais Cabral, Jackson et al. 1997; Bax, Chan et al. 2010). DNA supercoiling by gyrase involves the wrapping of a segment of DNA around the enzyme in a right-handed supercoil of ~ 130 base pairs (Kampranis and Maxwell 1996). Wrapping of DNA on the gyrase C-terminal domains helps a second segment (transported or T-segment) belonging to the same DNA molecule to reach the N-gate. Upon binding of ATP the N-gate closes, trapping the T-segment (Wigley, Davies et al. 1991; Brino, Urzhumtsev et al. 2000). Two tyrosines from the GyrA dimer react

with the G-segments forming DNA-phosphotyrosyls 4 bp apart, and thus creating the double-strand break (Bax, Chan et al. 2010). This reaction requires the presence of Mg^{2+} (Noble and Maxwell 2002; Sissi, Chemello et al. 2008). The T-segment is pushed through the open DNA gate, the role of ATP hydrolysis and the involvement of the N-gate closing in the strand passage mechanism is still unclear. As the DNA gate closes and the DNA is resealed, the C-terminal gate opens to free the T-segment (Tingey and Maxwell 1996; Maxwell, Costenaro et al. 2005). The hydrolysis of ATP and release of ADP causes the N-gate to open and thus reinitializes the enzyme for the next cycle (Baird, Harkins et al. 1999; Baird, Gordon et al. 2001). One gyrase cycle introduces two supercoils in the DNA molecule at the expense of 2 ATPs. In the absence of ATP, gyrase can catalyse relaxation of negatively supercoiled DNA by the opposite mechanism (Gellert, Mizuuchi et al. 1977). The mechanism is illustrated in Figure 38.
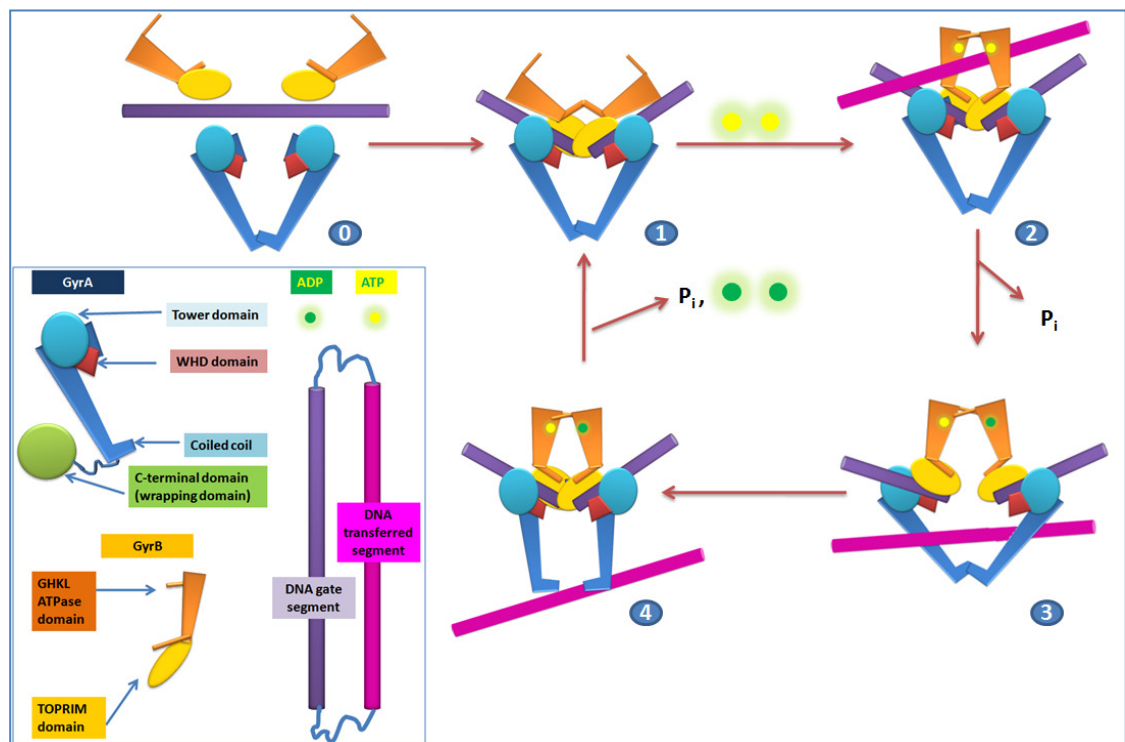
Figure 38 Gyrase supercoiling mechanism: The C-terminal domain of GyrA, responsible for wrapping DNA , has been omitted for two reasons: first it simplifies the scheme, and second it is a domain connected to GyrA N-terminal domain by a flexible arm, the exact position of C-terminal domain during gyrase cycle is still unknown. The supercoiling reaction proceeds as follows: the GyrA dimer, two GyrB monomers and DNA form the DNA-gyrase complex, the DNA segment (G-segment) becomes part of the DNA gate (1). Upon binding of ATP on each GyrB subunit they dimerise closing the N-gate around a second segment of DNA (the transferred or T-segment) (2). It had been proposed that hydrolysis of one ATP at this stage triggers conformational changes that push the T-segment through and opens the DNA gate. The DNA gate closes, and the GyrA C-gate formed by the coiled coils opens releasing the T-segment. Hydrolysis of the second ATP and release of the two ADPs reset the enzyme to step (1).

4.2.2 Topo IV

Topo IV has a structure very similar to gyrase; it possesses two subunits ParC (84 kDa) and ParE (70 kDa), the two proteins are respectively homologous to GyrA and GyrB, and like gyrase they are associated in a C_2E_2 tetramer (Kato, Nishimura et al. 1990). Two crystal structures of *E. coli* topo IV subunits are available: the full length ParC (1ZVU) (Corbett, Schoeffler et al. 2005), and the 43 KDa N-terminal fragment from ParE (1S16) (Bellon, Parsons et al. 2004). From these structures we can build a picture of the topo IV overall organisation, even if the domain of ParE that interacts with ParC and is involved in cleavage is missing.
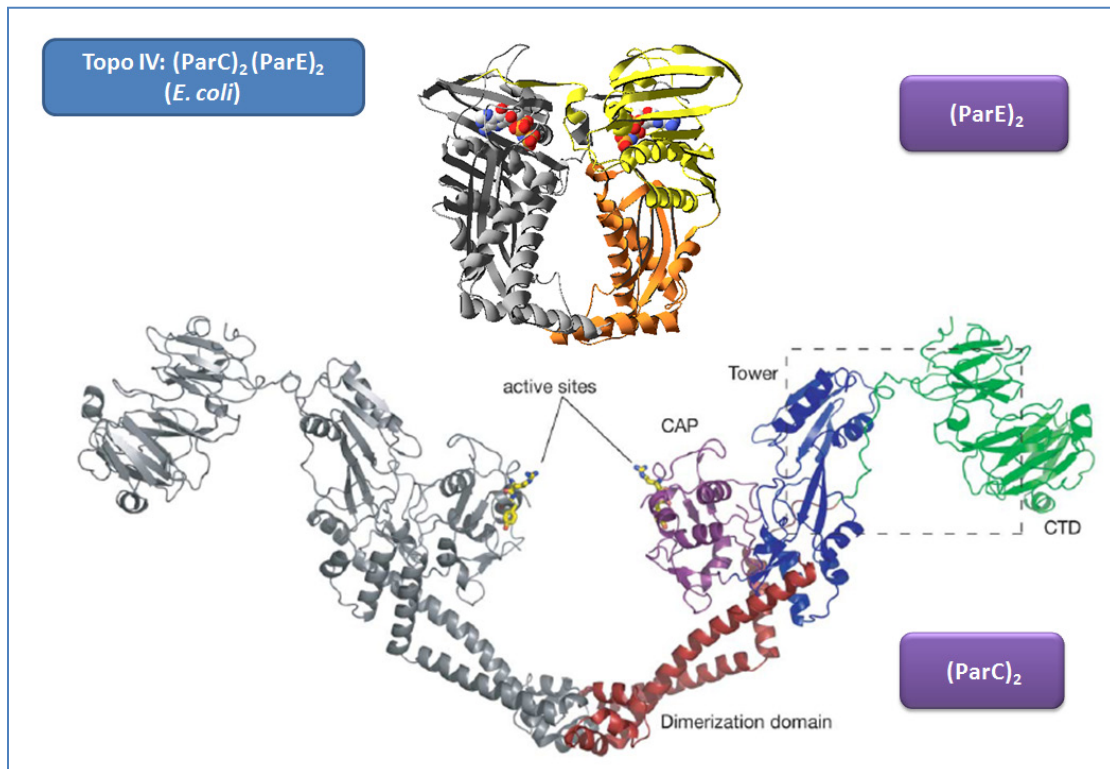
Figure 39 Topoisomerase IV structure: top structure is dimer of the N-terminal fragment of ParE from Bellon *et al (Bellon, Parsons et al. 2004)*, in yellow is the GHKL domain, in orange the transducer domain. The bottom structure is the full length ParC dimer from Corbett *et al (Corbett, Schoeffler et al. 2005)*. The various domains are colour-coded: CAP domain in purple, tower domain in blue, coiled-coil in red, C-terminal domain in green reproduced from Corbett *et al (Corbett, Schoeffler et al. 2005)*.

The general mechanism of topo IV is very similar to gyrase, but unlike gyrase, the enzyme does not wrap DNA around itself and shows a higher affinity for supercoiled DNA (Crisona, Strick et al. 2000) or DNA crossovers (Stone, Bryant et al. 2003), which account for topo IV relaxation, decatenation and unknotting activity. As for gyrase, topo IV crystal structures of other organism have been released recently: the fusion protein of ParE CTD and ParC NTD of *S. pneumoniae* (3LTN) (Laponogov, Sohi et al. 2009), and *A. baumannii* (2XKJ)

(Wohlkonig, Chan et al. 2010), they gave important information about the general mechanism of topo IV.
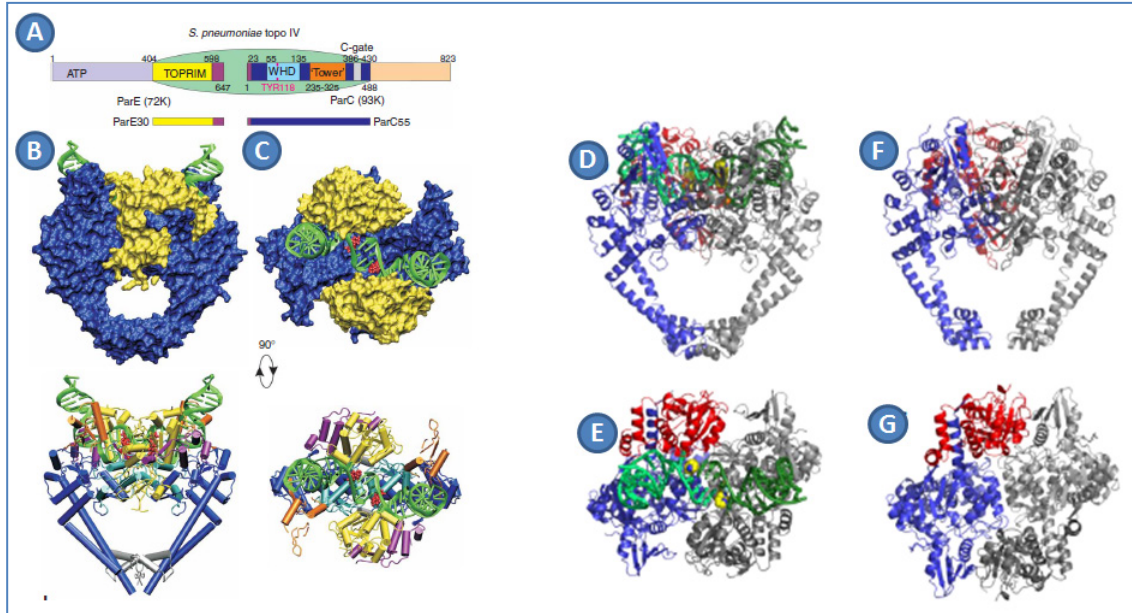
Figure 40 Organization and structure of the enzyme–quinolone–DNA cleavage complex of topo IV. (a) Domain organization of *S. pneumoniae* topo IV. (b,c) Front (b) and top (c) views of the topo IV ParC55 and ParE30 proteins complexed with the G-segment DNA and a quinolone drug (moxifloxacin), shown both in surface (above) and detailed cartoon (below) representations. DNA is in green, the TOPRIM domain (ParE30) is in yellow and the ParC55 is in blue. The drug molecules are shown in red. The WHD, 'tower' and C-gate are shown in cyan, orange and silver, respectively. The interface region between ParC and ParE subunits (involving the α1 helix) is in purple. Generated using VMD20 and POV-Ray (http://www.povray.org). Reproduced from Laponogov *et al* (Laponogov, Sohi et al. 2009). (d), (e), orthogonal views of the 3.27 Å *A. baumannii* topo IV ParE28-ParC58 complex with DNA (green) and moxifloxacin (yellow) and (f), (g) equivalent views of the 2.2 Å apoParE28-ParC58 structure. One covalently fused ParE28-ParC58 is shown in red (ParE) and blue (ParC), the other in grey. Reproduced from Wohlkonig *et al* (Wohlkonig, Chan et al. 2010) (Supplementary data).

4.2.3   A word about type II topoisomerases C-terminal domain (CTD)

As mentioned above, the selectivity of type II topoisomerases is dependent on their ability to wrap DNA and recognise crossovers, thus favouring inter- or intra-molecular DNA reactions and interaction with DNA of a particular topology. This selectivity has been shown to be related to the C-terminal domain of the enzyme. There is a significant difference between GyrA and ParC C-terminal domain (Figure 41); GyrA CTD is six bladed β-pinwheel, in comparison ParE CTD has only five blades and lacks the GyrA Box, an essential element for the gyrase supercoiling activity (Kramlinger and Hiasa 2006).
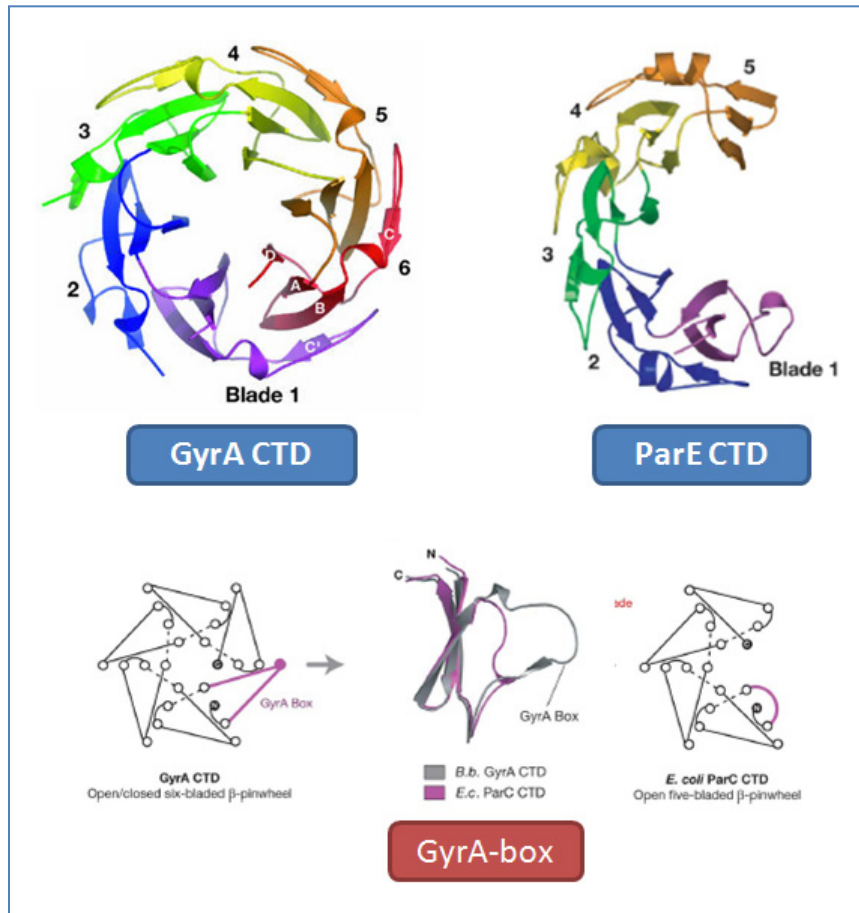
Figure 41 Comparison of GyrA and ParC CTD: top right, the crystal structure of *Borrelia burgdorferi* GyrA-CTD (Corbett, Shultzaberger et al. 2004), which is very similar to *E. coli*'s (Ruthenburg, Graybosch et al. 2005). Top left, the crystal structure of *E. coli* ParE CTD (Corbett, Schoeffler et al. 2005). GyrA CTD is a six bladed β-pinwheel, whereas ParE CTD has only five blades, and is lacking in particular the GyrA box which is essential for gyrase supercoiling activity (Maki, Takiguchi et al. 1992; Kramlinger and Hiasa 2006).

4.3   Gyrase and topo IV Inhibitors

DNA gyrase, is an essential enzyme for bacteria that is nearly only found in prokaryotes cells; in eukaryotes, it has been found in plants (Forterre, Gribaldo et al. 2007), and in plasmodium (Wilson 2002). This predominance in prokaryotes cells has made the gyrase a target of choice for antibacterial agents. The most used are the quinolones and the coumarins. These two families have different mechanism of action.

4.3.1   Coumarins

Aminocoumarins, also referred as coumarins, are natural compounds produced by *Streptomyces*; novobiocin, clorobiocin and coumermycin A1. belong to the family of coumarins. Known since the 1950s for their inhibitory properties on nucleic acid synthesis in bacteria, it

was found later, with the discovery of gyrase, that the coumarins inhibit gyrase-catalyzed supercoiling of DNA (Gellert, O'Dea et al. 1976).
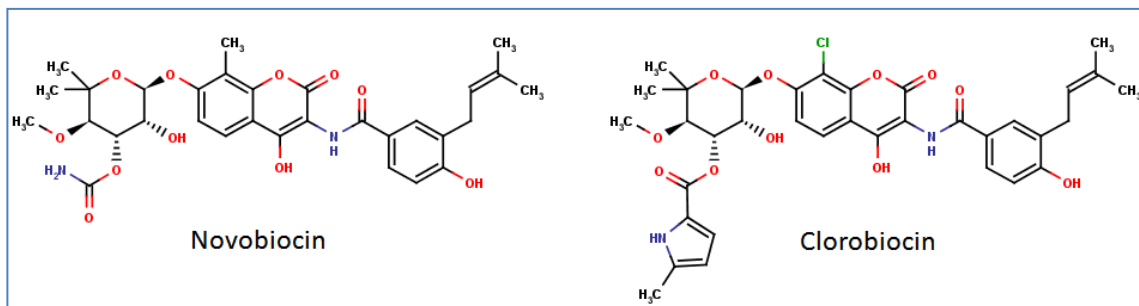
Figure 42 Aminocoumarins

The classical coumarins inhibit the ATPase reaction by competing with ATP for binding GyrB. Coumarins bind to the 24 kDa amino-terminal subdomain of GyrB, a domain that does not bind ATP by itself (Lewis, Singh et al. 1996), however when they bind to this domain, they overlap the ATP-binding site preventing ATP binding (Maxwell 1999). Resistance to novobiocin has been obtained by site-directed mutagenesis of the following five residues: R136, D73, G77, I78 and T165 (Gross, Parsons et al. 2003). Studies have shown that topo IV is a less sensitive secondary target for aminocoumarins; the mutation of R132, equivalent to gyrase R136 mutation, similarly confers some resistance.
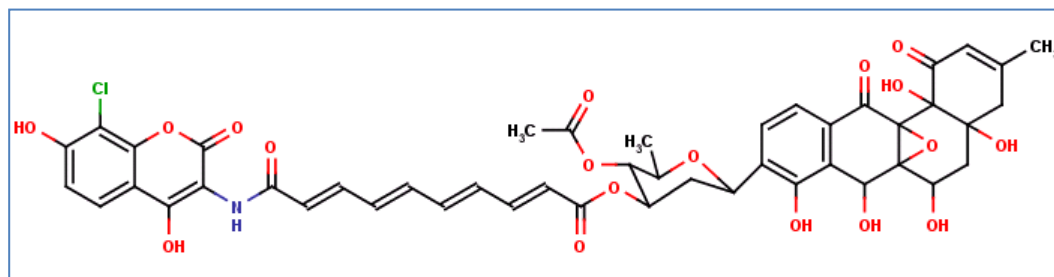
Figure 43 Simocyclinone D8

An antibiotic related to this family simocyclinone D8 (SimD8), a coumarin-polyketide hybrid, has been reported to have a different mechanism of action. Instead of inhibiting the ATPase, simocyclinone D8 (SimD8) prevents DNA binding by interacting with two different pockets on GyrA, one occupied by the polyketide, the other is interacting with the coumarin end. The crystal structure shows that four SimD8 molecules stabilise a tetramer of GyrA, with one simD8 bridging two GyrA molecules. A competing model is the occupation of the two sites

of a GyrA monomer by a single SimD8 molecule bend over the two sites. Both models will lead to the inactivation of GyrA (Edwards, Flatman et al. 2009). The two models are under investigation to prove which one is relevant *in vivo*. The novel mechanism of action and the identification of two binding sites are valuable information for future development of new antibacterials.

Coumarins are potent inhibitors of gyrase *in vitro* but their poor activity against Gram-negative bacteria, mammalian cytotoxicity, and poor solubility prevent them being successful drugs. Nevertheless, study of these compounds gives important information about gyrase-inhibition mechanisms and the molecular basis to develop new inhibitors. Moreover, their relative simocyclinone D8 highlights new binding sites that can be exploited in drug discovery.

4.3.2 Quinolones

Quinolones are totally synthetic drugs, with a lower affinity for gyrase than coumarins; but they are very potent antibacterial agents. The first generation quinolones, nalidixic acid (Goss, Deitz et al. 1965; Sugino, Peebles et al. 1977) and oxolinic acid (Staudenbauer 1976), have been surpassed by the fluoroquinolones, which have led to an explosion of new fluoroquinolones drugs such as ciprofloxacin and norfloxacin (2nd gen.) (Bauernfeind and Petermuller 1983), levofloxacin (3rd gen.) and the later moxifloxacin and gemifloxacin (Emmerson and Jones 2003).
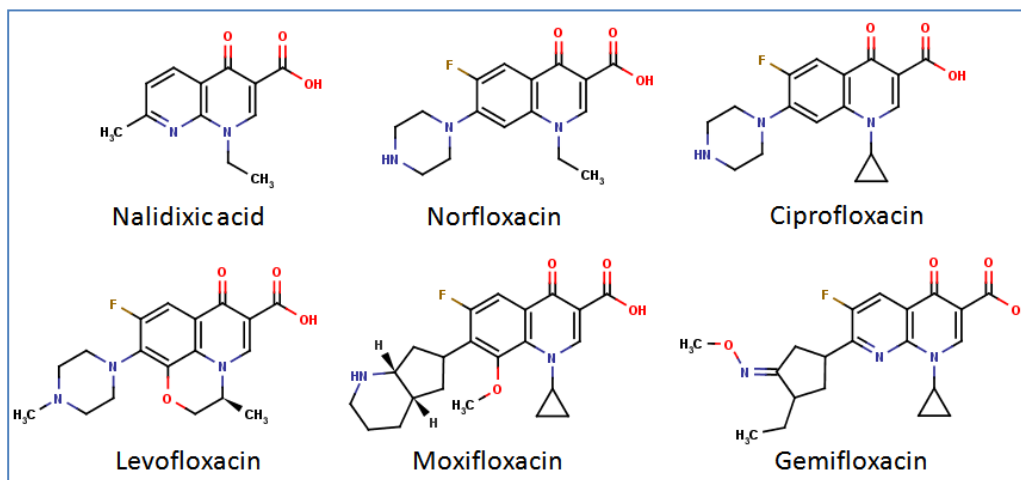
Figure 44 A few fluoroquinolones and their ancestor nalidixic acid.

After the discovery of gyrase it was shown that its supercoiling activity can be inhibited by oxolinic acid (Gellert, Mizuuchi et al. 1977); it has been shown later that topoisomerase IV, a similar enzyme is also affected by the compounds (Kato, Suzuki et al. 1992; Chen, Malik et al. 1996), and is likely to be the primary target in some Gram-positive bacteria (Drlica and Zhao 1997). Quinolones act by disrupting the DNA-breakage-reunion reaction, thus inhibiting DNA

supercoiling (Sugino, Peebles et al. 1977; Snyder and Drlica 1979). They stabilise the cleavage complex in which the enzyme is covalently linked to the 5′ end of the DNA, disrupt the enzyme cycle and can lead in vivo to cell death (Drlica and Zhao 1997). The exact quinolone-binding site on the A subunit is still under discussion, but amino acids Ala67-Gln106 in GyrA and Asp426-Lys447 in GyrB (in *E. coli*) are referred as the quinolone resistance–determining region (QRDR). Gyrase with changes in the polar residues S83 and D87, to hydrophobic residues exhibit high levels of resistance to quinolones, suggesting that these amino acids are involved in interaction with quinolones. Mutation at Ala67, Gly81, Ala84 and Gln106 confer lower level of resistance. Mutations out of the QRDR: Ala196Glu in clinical isolates, and Ala51Val *in vitro*, have been reported to confer resistance as well. Regarding GyrB, only the two positions delimiting its QRDR have been reported to confer resistance. If a reaction between gyrase, DNA, and a quinolone drug is terminated by the addition of sodium dodecyl sulphate, the DNA is broken in both strands and the GyrA subunits of the enzyme are attached to the 5′-phosphate at the break site via Tyr122, the active site tyrosine (Horowitz and Wang 1987).

This stabilisation of the cleavage complex is the essence of their antibacterial effect; this mechanism is similar to the effect of antitumour topo II inhibitors. Various crystal structures of quinolones in complex with gyrase or topo IV have been recently released: *A. baumannii topo* IV (2XKJ, 2XKK (with moxifloxacin)) (Wohlkonig, Chan et al. 2010); *S. pneumoniae* topo IV (3LTN (with PD0305970), 3FOF (with moxifloxacin)) (Laponogov, Sohi et al. 2009; Laponogov, Pan et al. 2010), *S. aureus* gyrase (2XCS (with GSK299423)) (Bax, Chan et al.). These structure shows that two quinolones molecules are interacting with the gyrase-DNA complex, each one is intercalated in the spaces opened by the formation of the covalent bond between the DNA strand and the catalytic tyrosine. The aromatic ring system of the drug is intercalated between the -1 and +1 bases at the break site, with the carbonyl of the quinolone pointing toward the WHD domain, whereas the C7 tail is pointing towards the toprim domain (Figure 45). An example of the interaction observed between DNA, gyrase and quinolones his reproduced below from Laponogov *et al* (Laponogov, Pan et al. 2010). Fluoroquinolones are among the most successful antibacterial drugs, they were a good alternative to overcome beta-lactamase-related resistance. Unfortunately, resistance to fluoroquinolones has appeared mainly through mutation in the QRDR region as mentioned above, but also by acquisition of plasmid coding for protein like Qnr, which can shield the topoisomerase from quinolone action (Hopkins, Davies et al. 2005; Tran, Jacoby et al. 2005).

61
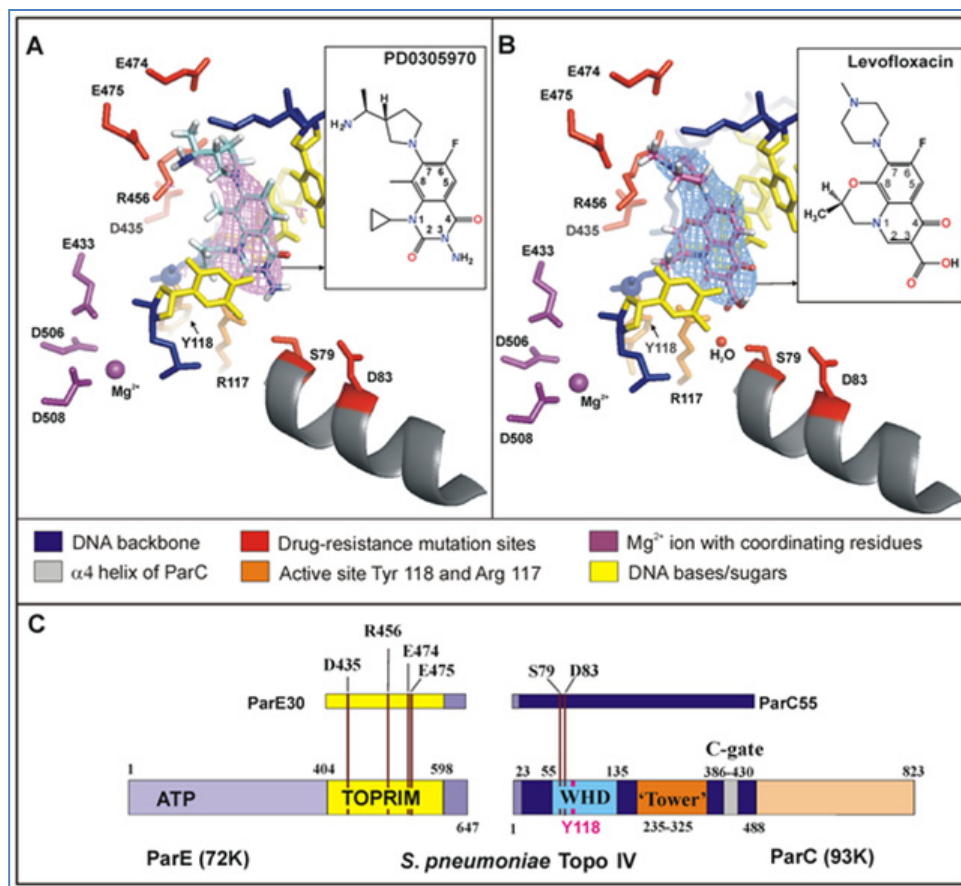
Figure 45 Example of stabilisation of the cleavage complex by quinolones: A and B, Cartoon/stick representations of the drug-binding pockets of topoisomerase IV-DNA in complex with PD 0305970 and levofloxacin, respectively. The σA-weighted $2F_{obs}-F_{calc}$ map is contoured around PD 0305970 (pink) and levofloxacin (light-blue) at 1.5σ. C, Domain organization of topo IV from *S. pneumoniae* with the individual sub-regions are highlighted by individual colours. Resistance mutation sites within the topoisomerase sequence are indicated by red lines. Reproduced from Laponogov *et al (Laponogov, Pan et al. 2010).*

4.3.3 Quinolone-like compounds
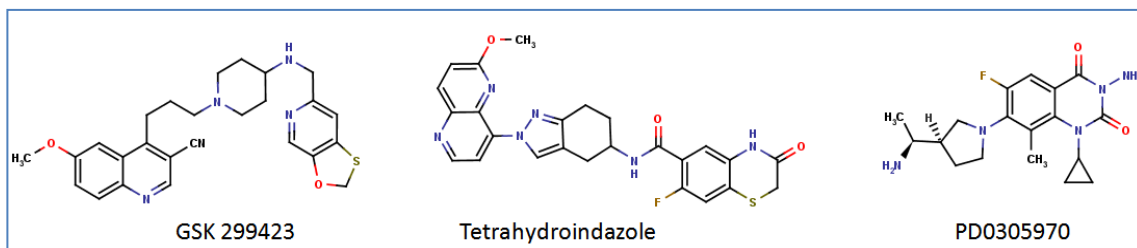
Figure 46 Prospective novel gyrase inhibitors

Sometime referred to by the catch-all term of NBTI (new bacterial topoisomerase inhibitor), these compounds are antibacterial molecules not belonging to the quinolone chemical family but acting in a similar manner, and not affected by quinolone-resistance mutations. Among them are GSK299423 (Bax, Chan et al. 2010), tetrahydroindazoles derivatives (Gomez, Hack et al. 2007; Wiener, Gomez et al. 2007), PD0305970 and PD0326448 two quinazoline-2,4-diones (Huband, Cohen et al. 2007). Some time will be required to evaluate the impact of these new compounds as antibacterials.

4.3.4   Other gyrase inhibitors

Other compounds targeting DNA gyrase exist outside the two previous categories, but even if generally they are not good candidates for antibacterial drugs they are good sources of information and inspiration.

4.3.4.1   Cyclothialidine

Cyclothialidine is a cyclic peptide isolated from *Streptomyces filipinensis*, its inhibitory activity *in vivo* is limited to eubacteria, probably due to uptake limitation (Nakada, Shimada et al. 1993), but it shows *in-vitro* inhibition of the supercoiling and ATPase activity of DNA gyrase (Nakada, Gmunder et al. 1994). Mutations observed in cyclothialidine-resistant mutants in *Staphylococcus aureus* and binding studies suggest that the cyclothialidine binding-site in GyrB overlaps the ATP- and coumarin-binding sites (Kampranis, Gormley et al. 1999). This biochemical evidence was supported by the crystallographic data of cyclothialidine bound with the 24-kDa GyrB amino-terminal subdomain (Lewis, Singh et al. 1996). In this structure the resorcinol ring of the drug has a similar position to the adenine ring of the non-hydrolysable ATP analogue ADPNP in the structure of the 43-kDa domain (Maxwell 1999). The total synthesis of cyclothialidine was performed by Goetshi *et al* (Goetschi, Angehrn et al. 1993), the various derivatives that were synthesized showed that the macrocyclic system can be a template to design new inhibitors. Further investigation of derivatives of cyclothialidine led to compounds that display activity on Gram-positive pathogens (Angehrn, Buchmann et al. 2004). Cyclothialidine is still used as a template for the discovery of new antibacterial agents (Oblak, Kotnik et al. 2007; Brvar, Perdih et al. 2010).
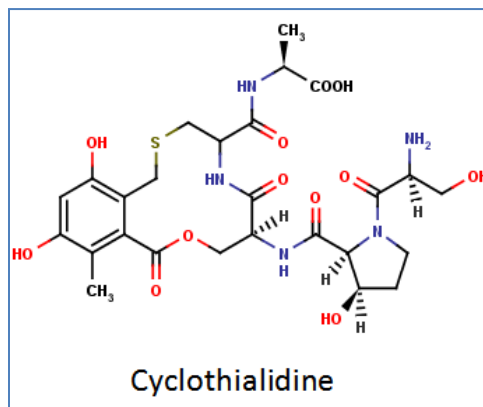
Figure 47 Cyclothialidine

4.3.4.2   Cinodine

Cinodine is a compound produced by *Nocardia* species that belongs to the glycocinnamoylspermidine antibiotic class (Martin, Kunstmann et al. 1978; Tresner, Korshalla

et al. 1978). It has been shown to bind to DNA (Greenstein, Speth et al. 1981) and inhibit DNA supercoiling by gyrase in *Micrococcus luteus in vitro* (Osburne, Maiese et al. 1990). Cinodine-resistant mutants with enhanced nalidixic acid-sensitivity have been isolated in *E. coli*, and *in vitro* experiments place the mutations on DNA gyrase. Three cinodine species have been identified, they share the same general structure but differs in their pentose moiety (Figure 48) (Osburne, Maiese et al. 1990; Maxwell 1999). No exploitation of cinodine has been reported recently.
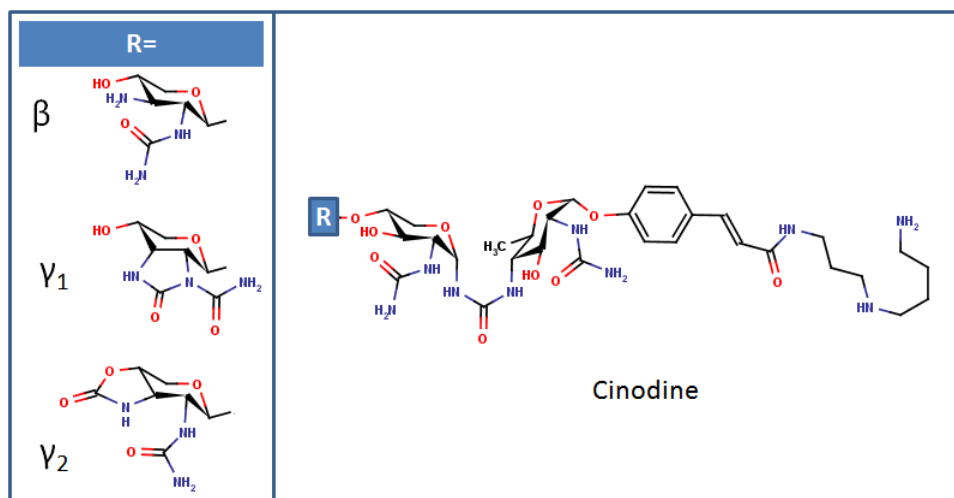
Figure 48 Cinodine variants structure

4.3.4.3   Clerocidin

The diterpenoid clerocidin was isolated from *Fusidium viridiae,* it is known as a cytotoxic and antibacterial agent (Andersen and Rasmussen 1984) that stimulates *in vitro* DNA cleavage, mediated by eukaryotic DNA topo II (Kawada, Yamashita et al. 1991) and gyrase (McCullough, Muller et al. 1993). Clerocidin promote *in vitro* cleavage by the *Streptococcus pneumoniae* topo IV (Richter, Leo et al. 2006) and gyrase (Pan, Dias et al. 2008). Clerocidin acts differently from other topoisomerase poisons, it creates a break at the guanine immediately preceding the topoisomerase DNA-cleavage site. The break created cannot be resealed by heating or salt

Figure 49 Clerocidin

treatment. In the absence of topoisomerase, clerocidin is able to form adduct with the guanines of short unpaired oligos. This reaction was shown to involve the attack by clerocidin epoxide group of the guanine nitrogen at position 7, leading to strand scission at the modified site (Gatto, Richter et al. 2001; Richter, Gatto et al. 2003). The reactivity of clerocidin towards
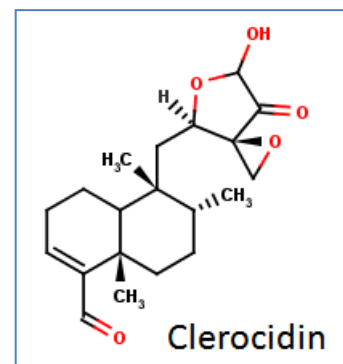
the other bases has been evaluated as well. No reaction was observed with thymine, but a two-site reaction of clerocidin with adenine or cytosine was reported, both for the bases in solution or in the context of small oligos. The mechanism involved the reaction of the base amino group with the clerocidin carbonyl, followed by the attack of the nitrogen at position 3 for cytosine, or 1 for adenine, by the epoxide group (Richter, Menegazzo et al. 2004; Richter, Menegazzo et al. 2009). Among the different bases, it is noteworthy that only the reaction of clerocidin with guanine led to the cleavage of the glycosyl bond. It had been confirmed *in vivo* that topoisomerase II is the target of clerocidin in HeLa cells, and that it binds to the enzyme before the formation of the cleavage complex (Jamora, Theodoraki et al. 2001). Concerning clerocidin structure, additionally to the reactive epoxide function the carbonyl group (Richter, Gatto et al. 2003) and oxirane ring have been shown to be essential for its activity (Richter, Gatto et al. 2003). The replacement of the diterpenoid moiety by a naphthalene ring system was reported to have no effect on the reaction with the bases in absence of topoisomerase (Richter, Gatto et al. 2003), however it causes a loss of the clerocidin cleavage activity in presence of topo IV (*S. pneumoniae*)(Richter, Leo et al. 2006). With *S. pneumoniae* Topo IV, clerocidin was still able to create strand breaks with the quinolone resistant ParC(S79F), but not with cleavage-deficient ParC(Y118F) mutant, and a clear preference for the attack of guanine at position -1 from the cleavage site was confirmed. The same preference for guanine at position -1 was shown in presence of murine topo II, but additionally reversible cleavage at cytosine at -1 position has been reported (Binaschi, Zagotto et al. 1997). This profile of reaction was further confirmed with *S. pneumoniae* gyrase (Pan, Dias et al. 2008). This evidence suggests that during the formation of the DNA-topoisomerase cleavage complex, the DNA adopt a conformation favourable for the reaction of clerocidin with a guanidine occupying the -1 and/or +5 position of the cleavage site; alternatively reversible cleavage will be favoured if a cytosine is present at one of these positions. The complete elucidation of clerocidin mechanism will require crystallographic structure (Pan, Dias et al. 2008). Clerocidin possess an unusual mode of action, the compound itself is too toxic to be used as a drug, but less toxic molecule able to mimic clerocidin activity will be of major interest.

4.3.4.4   CcdB

CcdB is of particular interest to us, its size of 11.7 kDa and the fact that it is a peptide structure able to poison gyrase give it a family likeness with MccB17 (Bernard and Couturier 1992). CcdB is the killer protein of the F plasmid, it is produced as a part of a two-component system maintaining plasmid copy (Miki, Park et al. 1992). CcdB is the toxin and CcdA is the antidote. CcdB kills bacteria by a mechanism similar to quinolones, although there is evidence showing that interaction between CcdB and gyrase takes place in a different domain and is ATP-dependent (Bernard, Kezdy et al. 1993). The mutation of Arg462 to Cys, which confers gyrase resistance to CcdB, is located in the central cavity of GyrA dimer, close to the primary dimer interface far from the QRDR (Tyr122)(Bernard and Couturier 1992), and no cross-resistance between CcdB and quinolones has been observed (Bernard and Couturier 1992). Biochemical evidence on the mode of action of CcdB pinpoints these differences: CcdB-induced cleavage of DNA by gyrase requires nucleotides (ATP for linear DNA and non-hydrolysable

nucleotide for negatively supercoiled DNA), and DNA templates of a minimum of 160 kb, whereas quinolone-induced cleavage does not require ATP and only 20 bp DNA template to proceed (Critchlow, O'Dea et al. 1997). In contrast to quinolones, CcdB is unable to mediate DNA cleavage with GyrA59 or GyrA64 associated with GyrB (Bahassi, O'Dea et al. 1999). Two types of activity have been observed with CcdB: the first requires several cycles of ATP hydrolysis and poisons gyrase, the second is a catalytic inhibition of gyrase.
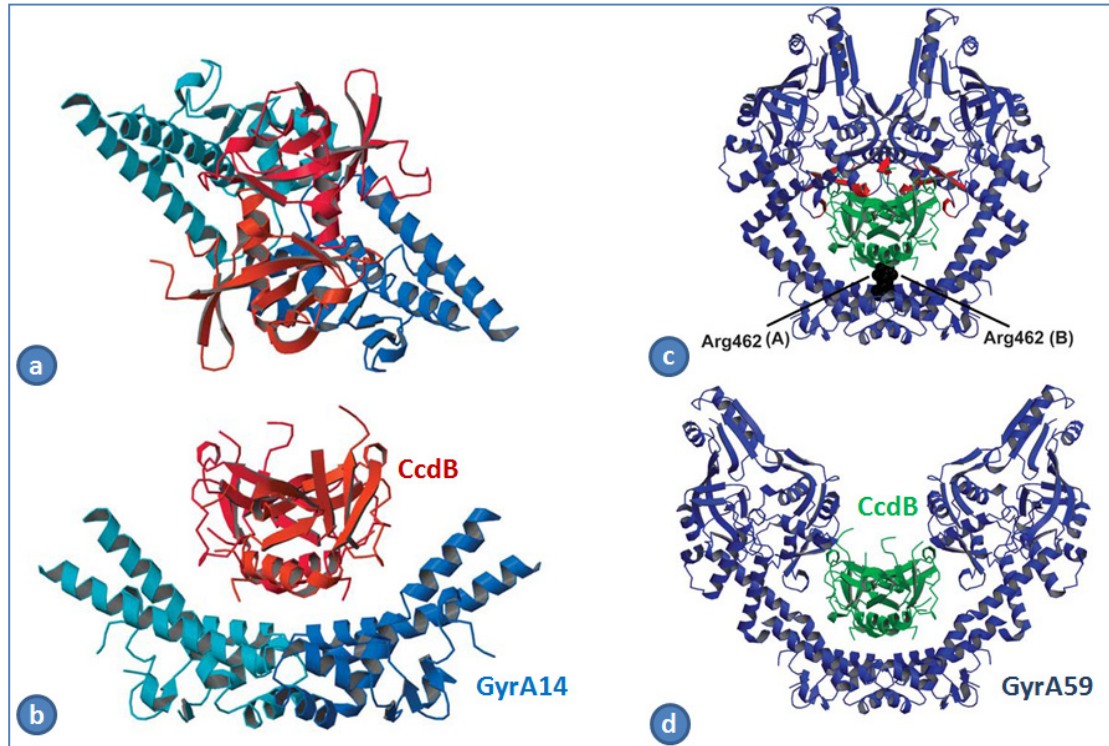
Figure 50 Complex of CcdB and GyrA14 and models: (a) Gyr-A14: CcdB complex viewed along its 2-fold axis. The two CcdB monomers are drawn in orange and red and the two GyrA14 monomers in two shades of blue. (b) Same as (a), but rotated 90°. (c) Model of closed GyrA59 (blue) with CcdB (green) docked onto it by superposition of the GyrA14:CcdB complex on the crystal structure of GyrA59 (Morais Cabral, Jackson et al. 1997). Residues Arg462 of both monomers of GyrA59 are highlighted. Strong steric overlaps (red) with the CAP domains are observed. (d) Model of the GyrA59: CcdB complex with GyrA59 in its open conformation. The open conformation of GyrA59 was modelled according to the corresponding yeast topoisomerase II structure (PDB entry 1BGW (Berger, Gamblin et al. 1996)). In this model, there is no steric overlap between CcdB and GyrA59. Reproduced from Dhao Thi & Van Melderen (Dao-Thi, Van Melderen et al. 2005).

Recent crystallographic data of CcdB co-crystallized with an N-terminal fragment of GyrA (GyrA14) (Dao-Thi, Van Melderen et al. 2004) suggests that the toxin is binding the GyrA dimer in a cavity between the two subunits. The structure confirms the role of Arg462 in CcdB binding to GyrA, as the two residues form a network of interactions with Trp99, Asn92, and Asn95, and shows that Ile101 is interacting with a hydrophobic cleft comprising Ile379, Leu383,

Leu461 and Ala457. Modelling from the CcdB-GyrA14 and GyrA59 crystal structures shows that such interaction will block the GyrA59 dimer in an open conformation, preventing its association with GyrB or DNA, and thus explaining the catalytic inhibition of gyrase by CcdB (Dao-Thi, Van Melderen et al. 2005). This interaction can account for gyrase poisoning as well: during the supercoiling reaction of DNA by gyrase, CcdB can squeeze in a similar GyrA dimer cavity during a transition state of the strand passage as demonstrated by biochemical evidences (Smith and Maxwell 2006). The short period of existence of this transition state will explain the requirement of several cycle of ATP hydrolysis for the poisoning to happen.
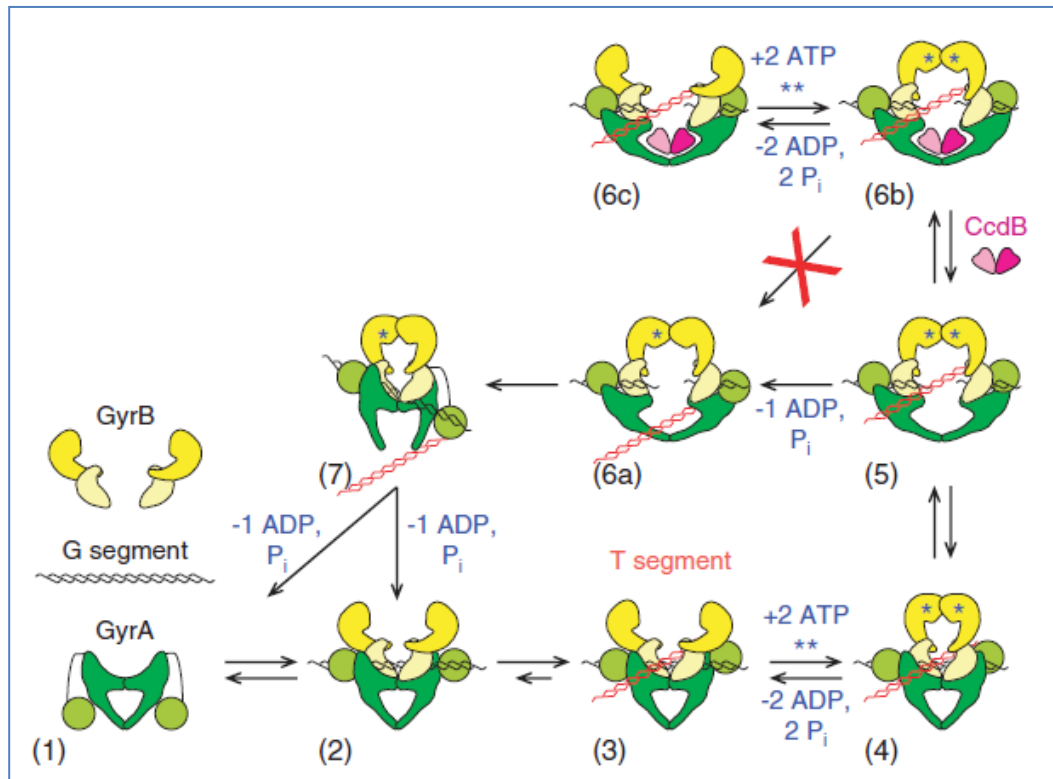
Figure 51 Model of gyrase inhibition by CcdB: The individual components (1) free in solution (Chatterji, Unniraman et al. 2000) come together (2) to form the holoenzyme with the G segment binding across the DNA gate (Heddle, Mitelheiser et al. 2004). (3) The DNA is wrapped by the GyrA-CTD to present the T segment over the G segment and a positive node is formed. (4) Upon ATP binding, the GyrB monomers dimerise and (5) the G segment is cleaved and the DNA gate opens. Either (6a) 'top-down' passage of the T segment occurs upon hydrolysis of a single ATP or (6b) CcdB accesses its binding site to stabilize the cleavage complex. (7) The DNA gate closes, the G segment is religated and the T segment passes out through the bottom gate, with hydrolysis of the second ATP resetting the enzyme. (6c) A futile ATP hydrolysis/ATP binding cycle can occur as per Kampranis et al. (Kampranis, Howells et al. 1999). Several cycles of (5) to (6a) transition may occur prior to CcdB binding in a (5) to (6b) transition. Reproduced

CcdB derivatives, about half the size of the native protein, comprising fragments of CcdB sequence connected by a 6-aminohexanoic acid flexible linker have been reported to have inhibitory activity on gyrase supercoiling and topo IV relaxation, this tend to suggest that

substructure of CcdB might be of interest (Trovatti, Cotrim et al. 2008). The crystal structure of CcdB/CcdA complex, the CcdB dimer with two CcdA (3G7Z) had been recently released, it shows how the CcdA antitoxin interact with the CcdB, and can dissociate the CcdB-gyrase complex , a process called rejuvenation (De Jonge, Garcia-Pino et al. 2009). A similar toxin from *Vibrio fischery*, CcdB$_{Vfi}$, has been characterized by X-ray crystallography and NMR, it provides an additional tool to understand the mechanism of interaction with gyrase (De Jonge, Buts et al. 2007).

84SHRENDIKNAINLMFWGI101   (*CcdBET1*)

1MQFKVYTYK9-Z-40RLLSDKVSREL50-Z-84SHRENDIKNAINLMFWGI101   (*CcdBET2*)

1MQFKVYTYK9-Z-84SHRENDIKNAINLMFWGI101   (*CcdBET3*)

68MASVPVSVIGEEVADLSHRENDIKNAINLMFWGI101   (*CcdBET4*)

The primary structures of the synthesized CcdB analogues (Z = ε-amino hexanoic acid).
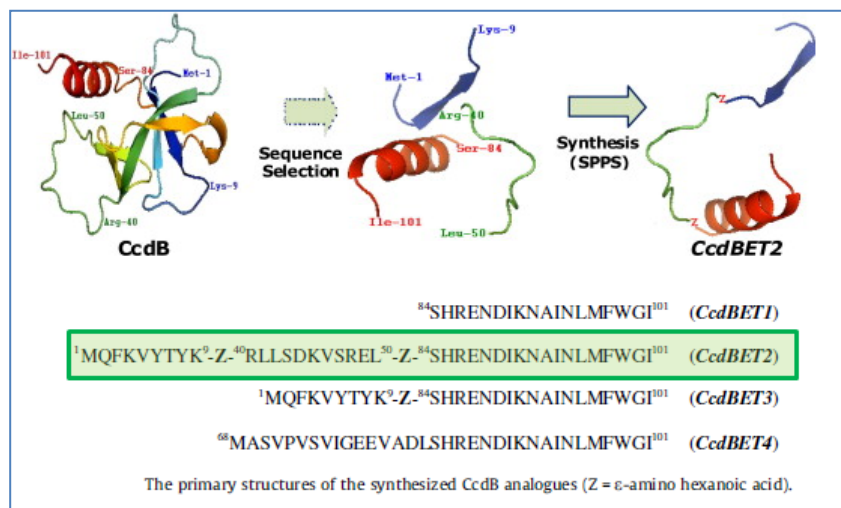
Figure 52 CcdB and derived peptides: the various peptides evaluated by Trovatti *et al*, the green box highlight the peptide that shows a complete inhibition of on gyrase at 10 μM and of topo IV at 5 μM (Trovatti, Cotrim et al. 2008).

4.3.4.5   Par E toxin

ParE toxin is produced by the RK2 plasmid as part of a ParE/ParD toxin/anti-toxin addiction system (Johnson, Strom et al. 1996). The toxin has been shown inhibit DNA synthesis and to stabilize the gyrase-DNA cleavage complex (Jiang, Pogliano et al. 2002). The X-ray structure of the ParE dimer and ParD dimers co-crystallized has been released recently (Dalton and Crosson 2010). There is enough significant similarities between CcdB and ParE to justify the investigation of ParE in a way similar to CcdB. ParD possess features that look similar to the exit gate of GyrA, it would be interesting to make some modelling on these two fragments.

Figure 53 Structure of the ParE toxin: on the left the ParE dimer (turquoise and violet) in complex with ParD dimer (red and yellow) (Dalton and Crosson 2010), on the right the gyrA59 dimer for comparison (Edwards, Flatman et al. 2009). The orientation of the two structures had been chosen by the author to highlight visual similarities between GyrA and ParD, but is not representative of any published evidence. The reader should note that the CcdB orientation while interacting with GyrA is opposite of the shown ParE if we consider its helix/β-sheet structure organization.

4.3.4.6   Microcin B17

Microcin B17 is a 3.1 kDa glycine-rich peptide produced by enterobacteria carrying the pMccB17 plasmid (Davagnino, Herrero et al. 1986). MccB17 is active against many enterobacteria (Asensio and Perez-Diaz 1976) and has been shown to inhibit DNA replication, leading to rapid arrest of DNA synthesis, induction of SOS response, DNA degradation and cell death (Herrero and Moreno 1986). MccB17 is inappropriate to be used as a drug as it shows poor physico-chemical properties, although it had been chosen in this study to be the base for designing novel drugs based on its particular heterocyclic structure and mechanism of action. Microcin B17 will be described more extensively below.

Figure 54 Microcin B17

69

5 Microcin B17

Figure 55 Microcin B17

5.1 The microcins

The microcins are bacterial toxins with a molecular weight below 10 kDa that have been isolated from strains of *E. coli* in 1976 (Asensio and Perez-Diaz 1976) and shown to inhibit the growth of a wide spectrum of microorganisms. Five types of microcins have been identified by cross-immunity. They have been initially classified depending on their mode of action: Type A, inhibition of metabolic enzymes, type B, inhibition of DNA replication, type D, impairment of the cell energy-generating system (Baquero and Moreno 1984). Microcins were proposed later to be classified depending on the presence or not of post-translational modifications (Pons, Lanneluc et al. 2002), this idea was further refined to take into account the nature of the modification and lead to the following classification of microcins of known structure (Duquesne, Destoumieux-Garzon et al. 2007):

- Class I: MW < 5 kDa, major peptide backbone modifications: MccB17, MccC7/C51, MccJ25.
- Class II : 5 < MW < 10 kDa:
  - IIa: contains only disulfide bonds as modification: MccL, MccV, Mcc24.
  - IIb: linear peptide, possibly contain a C-terminal modification: MccE492, MccM, MccH47, MccI47.

Other microcins are not included in this classification, as their structure have only been predicted by genetic studies, like MccH47, MccI47 and Mcc24; or is not known as they have been only characterized by biochemical studies like MccD13, Mcc140, Mcc15m, Mcc15n. Microcin B17 is one of the most studied microcin, we will not develop further the other microcins as they relate to MccB17 neither in structure nor in mode of action.

5.2 Activity of MccB17

The primary physiological effect of the MccB17 is the inhibition of semi-conservative DNA replication which triggers the SOS response, and finally induces DNA degradation and cell death (Herrero and Moreno 1986). Genetic and biochemical approaches have shown that the effect of MccB17 is linked to its ability to induce *E. coli* gyrase-mediated double-strand cleavage of DNA (Vizan, Hernandez-Chico et al. 1991). The uptake mechanism of MccB17 has

been linked with two proteins: the porin Ompf in the outer membrane, and SbmA an ABC transporter of the inner membrane (Lavina, Pugsley et al. 1986) that have been linked as well to the transport of MccJ25 (Salomon and Farias 1995) and bleomycin (Yorgey, Lee et al. 1994).

5.3   Interaction with gyrase

Microcin B17 is a weak inhibitor of gyrase compared to quinolones. Some evidence of the gyrase-DNA-MccB17 interaction had been reported. MccB17 works through a different mechanism compared to quinolones and coumarins. The inhibition of supercoiling and relaxation induced by the toxin can only be seen when these reactions are run over an extended period. Kinetic simulation of the cleavage-religation reaction suggests that MccB17 only enhances the cleavage of the second strand of DNA (Pierrat and Maxwell 2003): the conversion of open circular DNA to linear DNA. The effect of MccB17 on the DNA cleavage reaction is topology-dependent: in supercoiling conditions, with a relaxed DNA as substrate, the microcin can only weakly stabilize the cleavage complex in the absence of ATP, but more efficiently in its presence. Under relaxation conditions, with a negatively supercoiled DNA as substrate, microcin can more efficiently stabilize the cleavage complex in the absence of ATP (Pierrat and Maxwell 2003). It has been shown that MccB17 does not require the DNA-wrapping domain of GyrA or the ATPase domain of GyrB. This evidence, added to the fact that the only known MccB17-resistant mutation is at amino acid 751 of GyrB (W751R), led to the hypothesis that the action of the toxin involves binding to the C-terminal domain of GyrB preventing strand passage by trapping a transient enzyme intermediate (Pierrat and Maxwell 2005). Quinolone-resistance mutations GyrB (K447E) and GyrA (S83W) provide resistance to MccB17 as well; the CcdB-resistant mutant GyrA (R462C) was sensitive to MccB17. Limited proteolysis performed on GyrB in the presence of MccB17 showed that the C-terminal domain can be protected in the presence of GyrA and DNA, in comparison quinolones protected GyrB C-terminus alone, no protection was observed with the MccB17-resistant GyrB (W751R) (Pierrat and Maxwell 2005). This various information argue for MccB17 interacting with a transition state of the gyrase-DNA complex generated after ATP binding.

5.4   Resistance to MccB17

(Lavina, Pugsley et al. 1986),(del Castillo, del Castillo et al. 2001)

Spontaneous resistance to MccB17 appears with a frequency about 1×10^6. Two different mechanisms of resistance to MccB17 have been observed, the most prominent involves spontaneous mutation in the MccB17 uptake system, whereas the other involving mutation of the target has been artificially induced in strains where the uptake-related resistances have been disabled. Transport of MccB17 through the outer membrane is prevented by mutation of the genes *ompF*, the structural gene for OmpF, and *ompR* an OmpF positive regulator gene. These mutations give resistance to a wide range of compounds like other microcins or colicins. A second mediator of resistance linked with uptake is SbmA, mutation in the *sbmA* gene coding for this ABC transporter gives specific resistance to MccB17, bleomycin (Yorgey, Lee et al. 1994), and MccJ25 (Salomon and Farias 1995). When the putative

target of MccB17 was investigated, MccB17-resistant mutant strains were isolated through strategies that avoid uptake-related resistance. Two methods were used, the first uses a MccB17-producing strain lacking the *mcbG* gene coding for the immunity protein. This way the toxin is produced directly inside a sensitive strain, no uptake is involved, and the *mcbEF* genes responsible for MccB17 efflux, rescue partially the cells and allow them to grow slowly in favourable conditions. The second strategy involved a strain carrying a plasmid with multiple copies of the *sbmA* gene, so making sure that the protein will be expressed. As expected *ompR* and *ompF* mutants were isolated but a different type of mutation was isolated as well. Both strategies led to the same mutation: in *gyrB* an AT -> GC transition at position 2251, gives a GyrB with the Trp751 substituted by an Arg (W751R). *In vivo*, strains carrying this mutation are insensitive to MccB17, and *in vitro*, MccB17 is not able to stabilise the cleavage complex of gyrase carrying this mutation. Further investigation has been carried out by site-directed mutagenesis of GyrB W751: simple deletion led to an inactive GyrB; W751K, W751E, or W751G led to a resistance to MccB17 similar to W751R; W751F and W751H led to a low-level resistance to MccB17, in most of the cases the gyrase activity was altered. The substitutions that are not giving resistance to MccB17 are the ones with aromatic residues, suggesting that an essential aromatic or hydrophobic interaction is taking place between GyrB and MccB17 at this site.

5.5   Biosynthesis and structure

Microcin B17 is a 3.1 kDa post-translationally modified glycine-rich peptide (Davagnino, Herrero et al. 1986) produced by *E. coli* strains carrying the pMccB17 plasmid (formerly pRYC170) (Baquero, Bouanchaud et al. 1978; Baquero and Moreno 1984). This plasmid contains a 5.1 kb operon composed of the seven genes *mcbABCDEFG: mcbA* coding for MccB17 precursor sequence, *mcbBCD* coding for the multi-component enzyme responsible for MccB17 maturation (Genilloud, Moreno et al. 1989; Li, Milne et al. 1996; Videnov, Kaiser et al. 1996), and *mcbEFG* coding for export and immunity proteins (Garrido, Herrero et al. 1988). The first gene *mcbA* encodes a 69 amino acid peptide precursor of MccB17: preMccB17. This peptide is post-translationally modified to proMccB17 by the microcin synthetase, a multi-enzyme complex encoded by *mcbBCD* that converts specific sequences of residues from preMccB17 to five-membered heterocycles (Yorgey, Lee et al. 1994; Videnov, Kaiser et al. 1996).

The leader peptide, composed of the first 26 residues of the proMccB17, is an amphipatic α-helix involved in the recognition of the preMccB17 by the synthetase (Madison, Vivas et al. 1997). It undergoes a proteolytic cleavage to lead to mature MccB17 (Yorgey, Davagnino et al. 1993).The post-translational modification are the following: letters A to F will designate the modified sites, site A, Gly39-Ser40-Cys41 to 2-[2'-aminomethyloxazole-4'-yl]thiazole-4-carboxylic acid (oztz); Sites B and C, Gly47-Cys48 and Gly50-Cys51 to 2-aminomethylthiazole carboxylic acid (tz); site D, Gly54-Cys55-Ser56 to 2-[2'-aminomethylthiazole-4'-yl]oxazole-4-carboxylic acid (tzoz); sites E and F, Gly61-Ser62 and Gly64-Ser65 to 2-aminomethyloxazole-4-carboxylic acid (oz).

Figure 56 Microcin B17 and site reference

MccB17 synthetase has been intensively studied: McbB is a zinc-containing protein that probably catalyses the initial cyclisation by dehydration; McbC is a flavin protein that is likely to be involved in the dehydrogenation, and McbD is an ATP/GTPase that can act as a conformational switch (Milne, Roy et al. 1999). Tolerance of McbBCD to various substrates has been studied as well. The amino acids 39, 40, 41 corresponding to site A, and G42 were modified to evaluate the cyclisation product. Considering the wild type sequence being GSCG, GSC**A** gave the expected bisheterocyclic product, GSC**N** and GSC**V** only a monocyclic product, and **A**SCG, **D**SCG, **K**SCG, GSC**D**, GS**T**G, G**T**CG were not processed. This tends to show that the synthetase activity is very sensitive to steric hindrance both on the glycine and on the hydroxyl group involved in cyclisation; the downstream glycine seems slightly less sensitive (Sinha Roy, Belshaw et al. 1998). Kinetic studies of substrate sequences have been performed as well, using a maltose-binding protein linked to the first 46 amino acids of McbA with altered G39-S40-Cys41 to produce all possible bisheterocycles combinations led to the following preference: GSC > GCC> GCS >GSS (Belshaw, Roy et al. 1998). Additionally the role of the N-terminal polyglycine in MccB17 processing was evaluated by changing the number of glycines of the same MBP-McbA$_{1-46}$ from 10 to 3, 5, 7, 9 or 11 and monitoring the rate of conversion of GSC to oztz (Sinha Roy, Belshaw et al. 1998). Shortening the polyglycine cause a significant decrease of the processing of the GSC sequence, this favours the polyglycine being a spacer between the leader sequence and the processed sequences (Belshaw, Roy et al. 1998; Sinha Roy, Belshaw et al. 1998). Finally, McbE and McbF form an ABC transporter responsible for exporting the toxin and conferring partial immunity; *mcbG* encodes a pentapeptide repeat protein that prevents the binding of MccB17 to the gyrase of the producing organism (Garrido, Herrero et al. 1988).

The primary structure of MccB17 has been completely elucidated by mass spectrometry (MS), Gas Chromatography/MS coupling, NMR with [13]C- and [15]N- labelled MccB17 (Bayer, Freund et al. 1993; Bayer, Freund et al. 1995) and total synthesis of MccB17 (Yorgey, Lee et al. 1994; Videnov, Kaiser et al. 1996; Videnov, Kaiser et al. 1996). The total synthesis of MccB17 will be described below, as it is the starting point for synthesis of the compound we are interested in.

5.6 Structure-activity relationships in MccB17

Features influencing microcin B17 activity have been studied on various derivatives of the native toxin mainly focussing on its heterocyclic residues. Modification of MccB17's bisheterocyclic moieties of site A and D by *in vivo* processing has been reported. It shows that modification of the 4,2-fused oxazole-thiazole (oztz) in site A to oxazole-oxazole (ozoz) or

73

thiazole-thiazole (tztz) show respectively 25% and 5% decrease of inhibitory activity on cell lawn of ZK4 *E. coli* strain compared to the wild type MccB17. Alteration of site B causes at least a 66% drop in activity on the same test. Further modification of site D led to compounds with marginal activity for the monoheterocyclic species, or no activity for the compounds where the tzoz has been completely deleted. An interesting variant of MccB17 containing one extra oxazole moiety has been isolated, it resulted from the conversion of the thiazole (50-51)-Ser52 to Thia-Oxa. This mutant MccB17 shows a 50% increase in activity compared to MccB17, and can partially rescue the loss of activity caused by moderate site D modification. The various mutants and their activity are described in Table 1, based on the data reported by Sinha Roy *et al* (Sinha Roy, Kelleher et al. 1999) and Zamble *et al* (Zamble, Miller et al. 2001).

Table 1 Effect of heterocycle alteration on microcin B17 inhibitory activity: on the left, inhibition of altered MccB17, values are given in comparison with the native MccB17, they correspond to the maximum growth inhibition on lawn of ZK4 *E. coli* strain, bioefficacy is normalized to the native MccB17. On the right, schematic representation of the sequence of the altered MccB17. The brown line represents the peptide sequence with the oxazole ring in red and the thiazole ring in yellow.

Ref	Bioefficacy						
MccB17Δ[+1]	150						
MccB17	100						
A-GCC	95						
A-GSS5	75						
D-GSCΔ[+1]	50						
D-GCC	33						
D-GSS	33						
D-GGSΔ[+1]	13						
D-GSC	8						
D-GCG	5						
D-GGS	5						
D-GGGΔ[+1]	0						
D-GGG	0						

Microcin B17 features two asparagines residues at position 53 and 59; deamination by mild alkaline hydrolysis of these residues has shown a complete loss of ability to stabilise the cleavage complex (Parks, Bottrill et al. 2007). Finally alkaline hydrolysis of microcin, for 168 h in refluxed DMSO, has been conducted and led to a mixture of heterocycle-containing fragments

that still shows inhibition of gyrase (Coquin 2005). Liquid chromatography coupled with mass spectrometry (LC-MS) has been used to characterize the following fragments.

Figure 57 Fragments found in microcin B17 alkaline hydrolysate (Coquin 2005).

These fragments will be the starting point for our investigation for new topoisomerase inhibitors. In order to investigate the activity of different fragments, we aimed to synthesize the basic oxazole and thiazole heterocyclic and bis-heterocyclic amino acids. The activity on gyrase of these compounds will be evaluated. These heterocyclic amino acids will be used as building blocks to construct topoisomerase inhibitor peptides and investigate the main features responsible for the activity. We will describe now the strategy chosen to obtain these different heterocyclic amino-acids.

5.7 Total synthesis of MccB17

The total synthesis of Microcin B17 has been described (Videnov, Kaiser et al. 1996), part of that work is the production of the various heterocyclic moieties of MccB17.

5.7.1 Synthesis of thiazole and oxazole amino acids

i: (Boc)₂O, NEt₃ in THF/water (4/1).
ii: Lawesson's reagent in DME.
iii: 3-bromo-2-oxo-propanoic acid, CaCO₃ in dry EtOH.
iv: triethyloxoniumhexafluorophosphate in CH₂Cl₂.
v: H-Ser-OMe.HCl in CH₂Cl₂.
vi: DBU, CCl₄, pyridine in CH₃CN.
vii: NaOH in dioxane/water (1/4).
viii: TFA in CH₂Cl₂ (1/1)
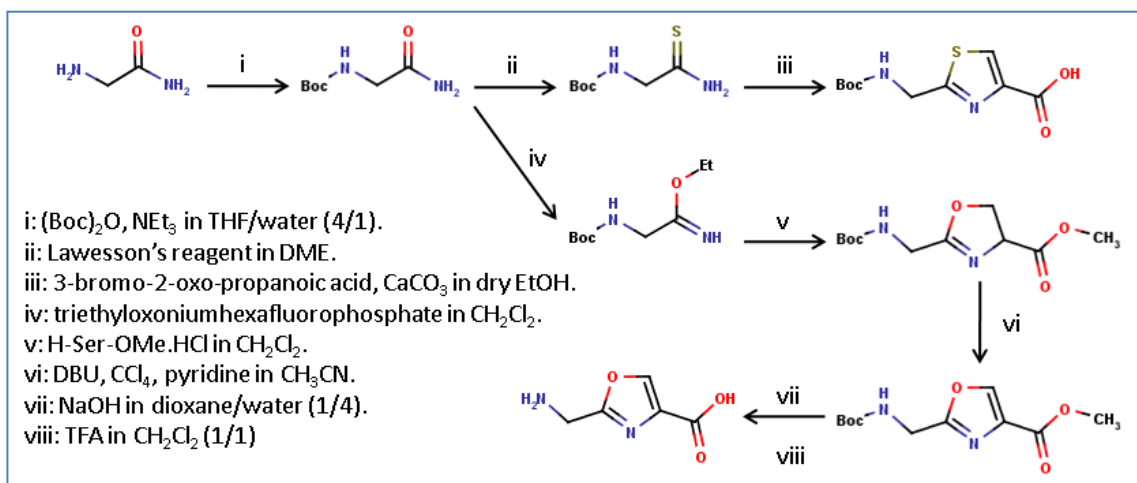
Figure 58 Synthetic route to thiazole and oxazole amino acids (tz, oz) (Videnov, Kaiser et al. 1996)

75

The synthetic route leading to these residues is derived from the Cornforth reaction for generation of the oxazole part (Cornforth and Cornforth 1947) and from the Hantzsch reaction for the thiazole part (Metzger 1979). Figure 58, Figure 59, and Figure 60 reproduced from Videnov *et al* (Videnov, Kaiser et al. 1996) describe respectively: the synthesis of thiazole and oxazole amino acids; the thiazole-oxazole amino acid; and the oxazole-thiazole amino acid.
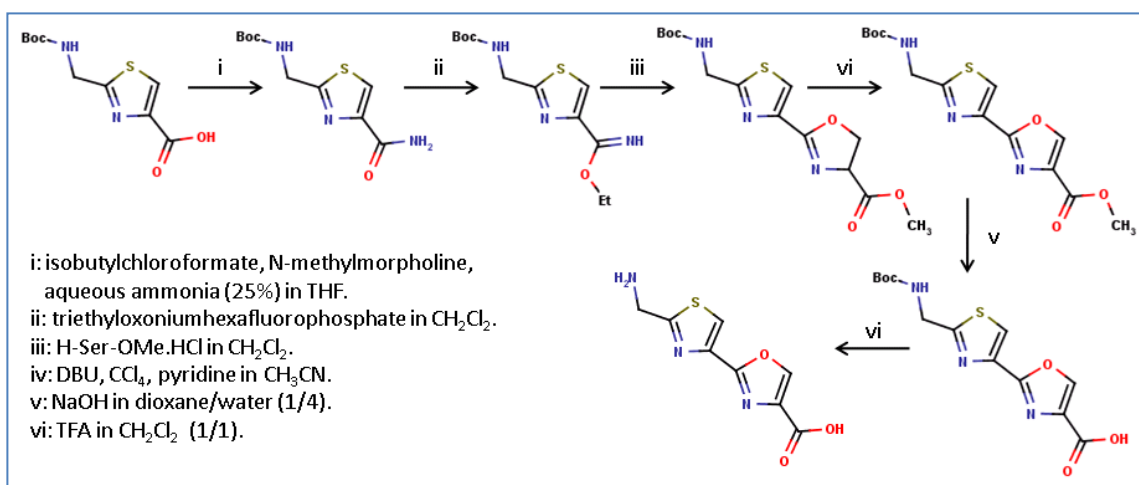
Figure 59 Synthetic route to oxazole-thiazole amino acid (oztz) (Videnov, Kaiser et al. 1996)
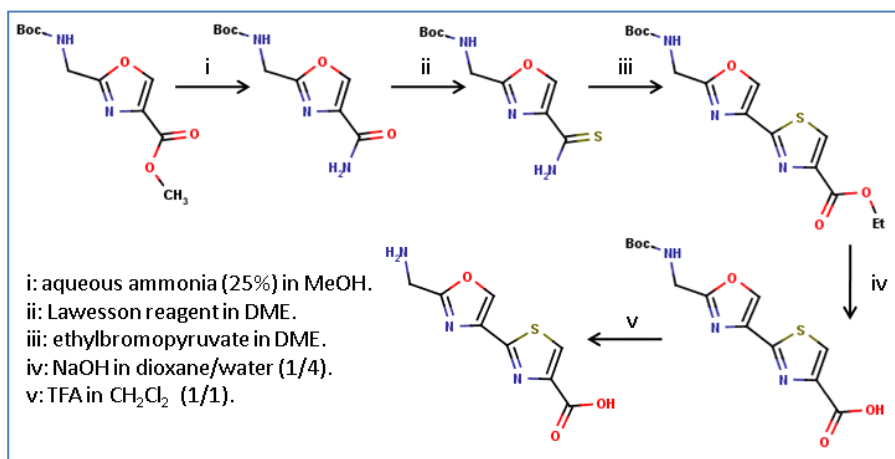
Figure 60 Synthetic route to thiazole-oxazole amino acid (tzoz) (Videnov, Kaiser et al. 1996)

5.7.2   Synthesis of MccB17

The different amino acids, natural and heterocyclic were assembled using an Fmoc solid phase strategy with a Wang resin. Starting from a Fmoc-Ile-Wang resin, Fmoc protected amino acids were coupled using 2-(1 H-benzotriazol-1-yl)-1, 1, 3, 3-tetramethyluronium tetrafluoroborate (TBTU), N-hydroxybenzotriazole (HOBt), and diisopropylethylamine (DIEA). Intermediate peptides were used to solve the problems cause by the synthesis of the polyglycine: in order of introduction, Fmoc-Gly-Gly-OH, Fmoc-Gly-Gly-Gly-OH, Fmoc-Ile-Gly-OH, and the final Boc-Val-Gly-OH. The final peptide was cleaved from the resin with a mixture of 3:3:3:91 dimethylsulfide, meta-cresol, ethanediol, and trifluoroacetic acid.

5.8   A synthetic approach to MccB17 chemistry

The previous paragraph described how MccB17 has been initially synthesized, it involved basically creating five-membered, or bis-five-membered heterocyclic amino acids. We will develop further this aspect, in order to include the progress in related synthetic methods and to give an insight on the variation that can be introduced in MccB17 through that kind of strategy.

5.8.1   Generating five-membered ring heterocyclic residues

Our intention here, is not to give an extensive analysis of the reactions leading to 5-membered heterocyclic rings, but a few alternative relevant routes to generate compounds similar to MccB17's heterocycles. We will cover here various methods to generate oxazole and thiazole, and the related isostere imidazole.

5.8.1.1   Thiazole synthesis

5.8.1.1.1   From a protected Cysteine

(You, Razavi et al. 2003):
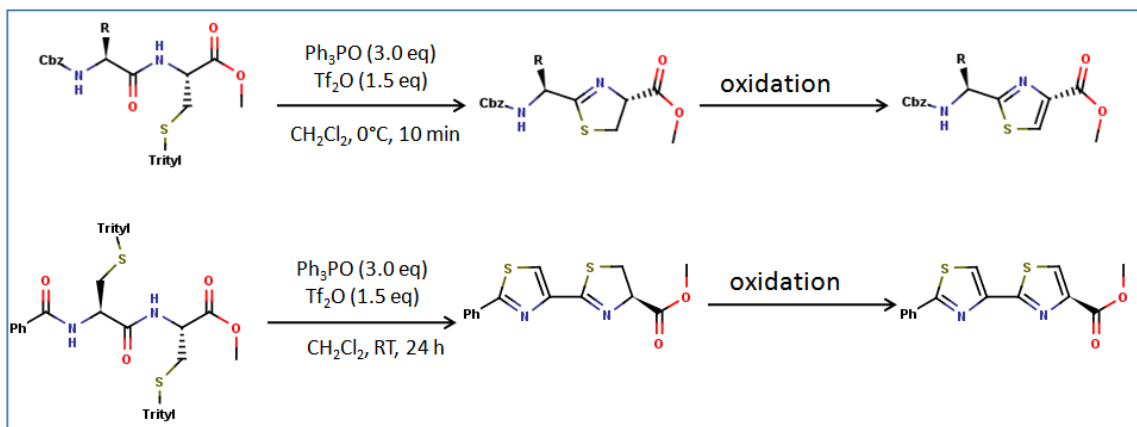
Figure 61 Alternative route to synthesize a thiazole ring using a cysteine

A dipeptide with a protected C-terminal cysteine can be converted into a thiazoline by cyclodehydration mediated by hexaphenyloxodiphosphonium trifluoromethanesulfonate. Further oxidation as described above will lead to the corresponding thiazole.

Method: 1.5 eq trifluoromethanesulfonic acid are added slowly to 3 eq triphenylphosphane oxide in dichloromethane at 0°C. The fully protected X-Cys, 1 eq is added, and the mixture is stirred 10 min at 0°C. The reaction mixture is quenched with 10% aqueous $NaHCO_3$, extracted with CH_2Cl_2, dried filtered and concentrated.

5.8.1.1.2 From a β-hydroxythioamide
(Khapli, Dey et al. 2003):
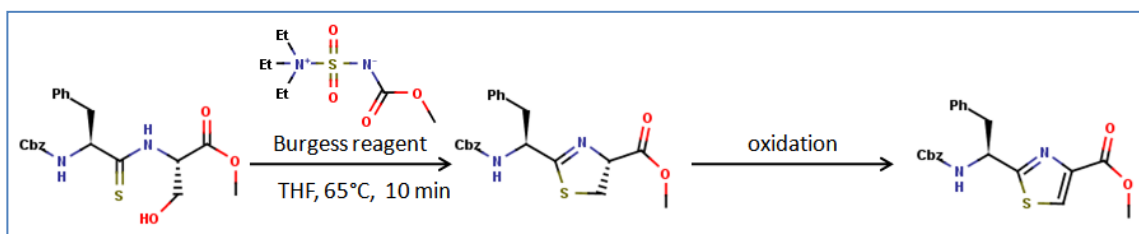
Figure 62 Alternative route to synthesize a thiazole ring from a β-hydroxythioamide.

This method uses the Burgess reagent dehydrating properties to induce the cyclisation of a serine with an N-thioamide bond.

Method: A solution of the thiamide in THF is treated with 1.1 eq of Burgess reagent and heated 10 min at 65°C. The reaction is cooled to RT, concentrated, and purified by chromatography.

5.8.1.2 Oxazole synthesis
(Wipf and Miller 1993; Phillips, Uto et al. 2000)

Methods to convert a dipeptide with a C-terminal serine into an oxazoline have been reported, two different conditions can lead to this result: the use of Burgess reagent as above, or the use of fluorinating agents like DAST and deoxo-fluor®. An oxidation step can be integrated in the last method without any other treatment to lead to the oxazole in a one-pot method.
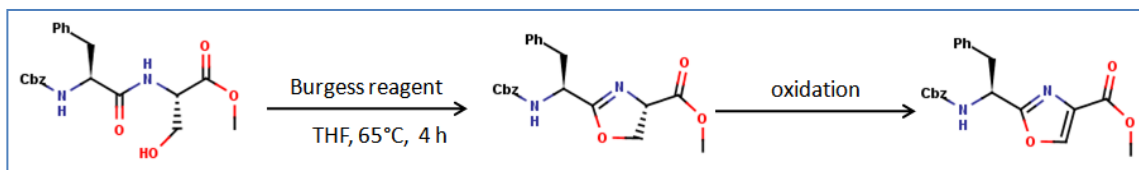
Figure 63 Alternative route to synthesize an oxazole from a beta-hydroxylamide with the Burgess reagent

Method with Burgess reagent: A solution of the β-hydroxyamides in THF is treated with 1.1 eq of Burgess reagent and heated 10 min at 65°C. The reaction is cooled to RT, concentrated, and purified by chromatography.
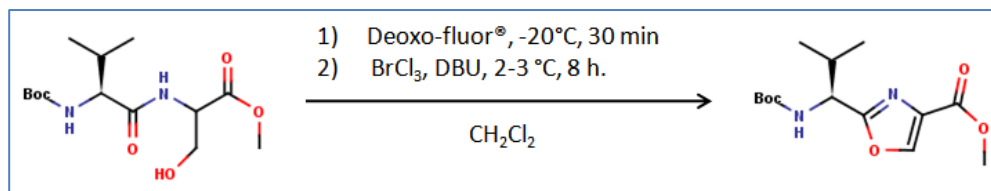
Figure 64 Alternative route to synthesize an oxazole ring from a beta-hydroxylamide using a fluoronating agent

Method with Deoxofluor®: 1.2 eq deoxo-fluor is added to 1 eq of Cbz-Val-Ser-OMe in dichloromethane, cooled at -20 °C. After 30 min 4 eq bromotrichloromethane, and 4 eq DBU are added. The reaction mixture is stirred for 8 h at 2-3°C. The mixture is then quenched with a saturated sodium bicarbonate solution. The mixture is extracted with ethyl acetate, dried, and concentrated.

5.8.1.3 Imidazole synthesis

There is two interesting routes to produce imidazole amino acids, one similar to the oxazole synthesis used by Videnov *et al* (Stankova, Videnov et al. 1999), the other uses a peptide with a C-terminal 2,3-diaminopropanoic acid (Biron, Chatterjee et al. 2006).
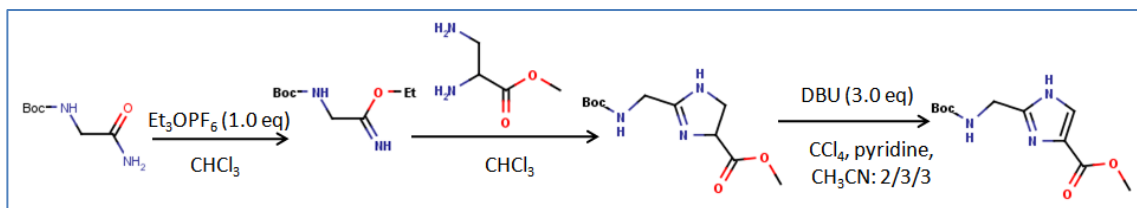
Figure 65 Synthesis of imidazole amino acid

Method: the triethyloxonium hexafluorophosphate was added to a solution of Boc-glycinamide in chloroform at 0°C, and stirred for 20 h. After treatment the product is mixed with 0.9 eq of L-2,3-diaminopropionic acid methyl ester hydrochloride in chloroform to lead to the imidazoline. The imidazoline can be oxidized using standard method.
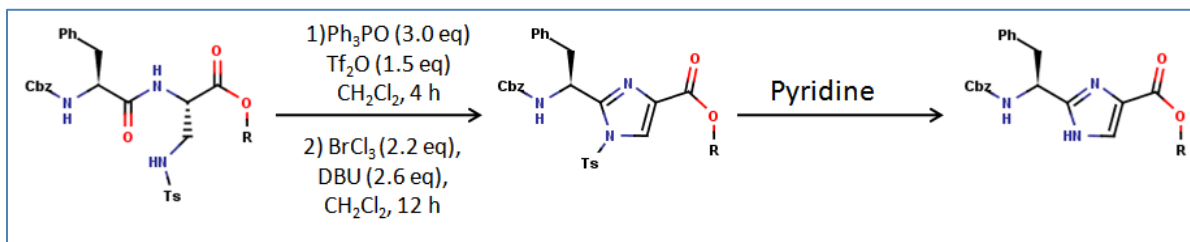
Figure 66 Synthesis of imidazole from a C-terminal (2, 3-diaminopropanoic acid)-containing peptide

Method: 1.5 eq of trifluoromethanesulfonic anhydride is added to 3 eq triphenylphosphine oxide in anhydrous dichloromethane at 0°C. The reaction mixture is stirred for 10 min at 0°C and the dipeptide is added. The mixture is stirred for 4 h at RT. After being isolated, the imidazoline can be oxidized to form the imidazole. The tosyl group on the imidazoline/imidazole can be removed by treatment in 20% pyridine in NMP.

6   Context and aims of this work

This chapter initially stated the desperate need in present days for new antibacterials, as underestimation of the resilience and adaptability of bacteria, added to the misuse of the panel of antibacterial at our disposition, has led to the loss of the advantage we had initially over pathogens. The various ways antibacterial molecules use to kill bacteria have been described with the different chemical families they belong to and their mode of action. Focus had been put on topoisomerases as major therapeutic targets, both for the present success with the fluoroquinolones and for the antibacterial efficiency represented by the topoisomerase poisoning mechanism. A glimpse of the application for topoisomerases in the context of anti-cancer therapy had been given as well. Antibacterial inhibitors of topoisomerases are targeting only two members of the type II family: gyrase and topo IV, and we stated that they will be our central interest in the present work. Inhibitors for these two enzymes have been described and a special emphasis had been put on MccB17. We have stated that MccB17's activity as a topoisomerase poison, different from quinolones, make it a particularly attractive molecule in the context of new drug development, and so more information on MccB17 was provided covering its bioactivity, biosynthesis, and related chemistry.

We have described a wide variety of antibacterial compounds that are working by very different mechanism on a set of essential bacterial targets. This panel was what produced the antibacterial golden age, unfortunately bacteria have their own set of tools to adapt to and resist such threats if they are given the chance, as demonstrated by the occurrence of resistance described in this chapter. As there is a need for novel antibacterials, our aim was to provide novel inhibitors or gather evidence that will lead to such discovery. We decided to use MccB17 for this purpose, because it is a molecule with a mode of action that involves the

already clinically validated target gyrase, and thus by a mechanism reminiscent of the very successful fluoroquinolone drugs, but different. It is not possible to use MccB17 itself as a drug, mainly because of its size and bad solubility, however the design of smaller molecules with better physico-chemical properties mimicking this mode of action, is likely to provide new antibacterials. To achieve this goal, one first must have a better understanding of the mechanism of MccB17, its interaction with gyrase and particularly how it stabilises the cleavage complex. Information concerning gyrase-MccB17 is scarce: the cleavage-complex stabilisation by MccB17 is ATP-dependent and so the toxin probably requires a specific conformation during the enzyme cycle to bind to the complex. MccB17-resistant mutants map to GyrB and some cross resistance is observed with the fluoroquinolones, this tends to prove that MccB17 binding site involves GyrB, and maybe the GyrA QRDR. Concerning the MccB17 molecule, its primary structure is known, it has been proven that the bisheterocycles play an important role in its activity, and that some of the amide residues are necessary to maintain the ability to stabilise the cleavage complex. There are a lot of gaps to fill before a clear picture of MccB17's mode of action can be drawn. Essential questions we want to address in the present work are: what are the elements in the MccB17 molecules that are required for its activity, and is it possible that fragments from the toxin able to retain some of its activity? Previous work on the heterocycles contained in MccB17 suggested that small peptide inhibitors can be built up from these structures, we wonder to what extent such derivatives can be used as inhibitors by improving their activity, and if stabilisation of the cleavage complex can be achieved with that kind of structure. To address these different questions, our study of MccB17 has taken on three main aspects that will be covered in separate chapters. An initial focus has been placed on improving our understanding of MccB17's mode of action, the significance of its different features, and particularly what is responsible for its ability to stabilise the cleavage-complex; this will be covered in Chapter II. Our second interest involved the production of inhibitors, two convergent approaches have been carried out for this purpose: the first one used MccB17 has a starting material, and generated fragments as potential topoisomerase inhibitors and information about the whole toxin; this aspect will be covered in Chapter III. The second approach starts from the unique amino acids found in MccB17 or related molecule to evaluate their potency and build from them to generate new compounds, this part will be explained in Chapter IV. The outcome from these different chapters will be summarized and discussed in Chapter V. A final chapter VI will cover the technical aspects and describe the experimental details of the methods used through the different chapters.

CHAPTER II
Microcin B17 properties and characterisation

CHAPTER II Microcin B17 properties and characterisation

This chapter will focus on the native microcin B17 molecule itself and derivatives retaining the overall structure. The first part of this chapter will describe the techniques commonly used to produce microcin B17 and characterise its activity on gyrase. These techniques are directly inspired from the literature with few variations but are described here as they are the core tools available to generate and evaluate MccB17 derivatives. Having considered MccB17 activity on *E. coli* gyrase we will widen the scope of targets and describe our investigation on other topoisomerases. The second part of this chapter will describe how analytical methods have been used to study Microcin B17 and its interaction with *E. coli* gyrase. Finally the effect of alteration of the ends of MccB17 as well as amide residues will be described.

1 Nomenclature:

MccB17 amino acids will be numbered accordingly to their counterparts in preMccB17, the peptide product of the *mcbA* gene. Concerning the heterocyclic amino acids, they will be numbered and referred to as follow: N-terminus; oztz; tz1; tz2, tzoz; oz1; oz2; C-terminus. This numbering has been chosen because it is the most commonly used in the literature and so it will be easier to link information from this work and the literature. MccB17 species lacking amino acids will be noted as follow: MccB17 minus Val27= Mcc\V27 or Mcc\V as there is only one V in MccB17. Microcin B17 species with extra or less heterocycles will be noted as follow: extra heterocycle MccB17Δ^{+1}, with two less heterocycles MccB17Δ^{-2}.
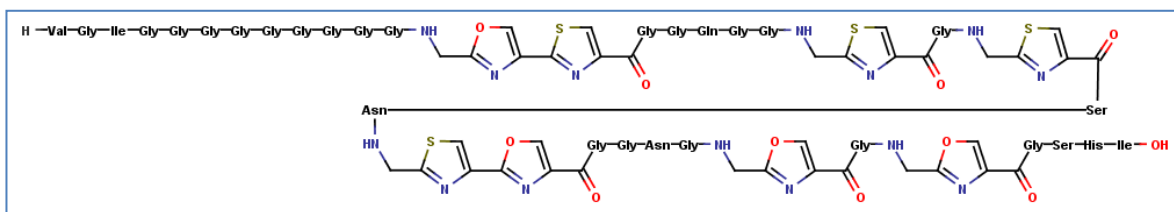
Figure 67 Microcin B17

N	1	2	3	4	5	6	7	8	9	10	11	12
MccB17	V	G	I	G	G	G	G	G	G	G	G	G
n	27	28	29	30	31	32	33	34	35	36	37	38
preMccB17												
n												

N	13	14	15	16	17	18	19	20	21	22	23	24
MccB17	oztz	G	G	Q	G	G	tz	G	tz	S	N	tzoz
n	NA	42	43	44	45	46	tz1	49	tz2	52	53	NA
preMccB17	GSC						GC		GC			GCS
n	39,40,41						47,48		50,51			54,55,56

N	25	26	27	28	29	30	31	32	33	34	35
MccB17	G	G	N	G	oz	G	oz	G	S	H	I
n	57	58	59	60	oz1	63	oz2	66	67	68	69
preMccB17					GS		GS				
n					61, 62		64, 65				

Figure 68 Microcin sequence numbering: the first row is the direct numbering of MccB17 residues, considering each amino acid including the post-translation modified products; the second row is the sequence of MccB17; the third row is the numbering associated with the *mcbA* protein product preMccB17; fourth and fifth rows shows residues and preMccB17 numbering of post-translationally modified residues.

2   Production of microcin B17

We produced the antibacterial peptide using a protocol inspired by Roy et al (Sinha Roy, Kelleher et al. 1999), for more details refer to Materials and Methods. The toxin was expressed in *E. coli* DH5α carrying the plasmid pUC19-mccb17: a pUC19 carrying the full biosynthetic operon mcbABCDEFG. Overnight cultures of DH5α-mccb17 in 12 X 5 ml LB media were used to inoculate 12 X 1 L of M63 glucose-Ampicillin media. After incubation for 48 h at 37°C the cells were pelleted by centrifugation at 4250 g. The pellets were disrupted by adding them to 500 ml of a boiling solution of 1 mM EDTA and 100 mM acetic acid, and allow the stirred mixture to boil for 10 min. The cellular debris was removed by centrifugating the solution at 4600 rpm for 15 min. The supernatant was loaded on 4 X 35 cc (10 g) Sep-Pak® C18 reverse phase cartridge each equilibrated with 250 ml acetonitrile and 250 ml water. Contaminants were removed by successive elution of 300 ml water and 300 ml 12% acetonitrile in water. The fraction containing MccB17 was collected by elution with 300 ml of 50% acetonitrile in water. The solution was concentrated under vacuum before being freeze dried, which led to solid crude MccB17. The crude microcin was solubilised in DMSO at ~3mM concentration and purified by HPLC using a preparative reverse phase column with a gradient of 13 to 23% acetonitrile in water with 0.1 %TFA over 40 min. The various fractions collected were concentrated under vacuum before being freeze dried.

3   Development of a methanol-water HPLC method

Due to the global shortage of acetonitrile in 2008-2009 the HPLC purification of microcin B17, which consumes a lot of solvents had to be rethought to accommodate a substitute for acetonitrile. We developed the method with methanol, which is a solvent with a higher polarity than acetonitrile (relative polarity $H_2O=1$; MeOH=0.762; $CH_3CN=0.460$)

(Reichardt 2003) but is known to be a good solvent for microcin. Following directions from HPLC suppliers concerning equivalence between acetonitrile/water and methanol/water system we started from the rough assumption that 10% CH_3CN was equivalent to 15% MeOH and 30% CH_3CN was equivalent to 40% MeOH. The microcin B17 was eluted with a gradient from 20% to 85% methanol in water with 0.1% TFA. The microcin peak is collected between RT=25 min to 28 min.

4   Isolation of microcin B17 by-products

During the purification of MccB17, our attention was drawn by series of small peaks ahead of the various MccB17 species. These peaks were isolated as they might be related to MccB17 and retain some of its properties.
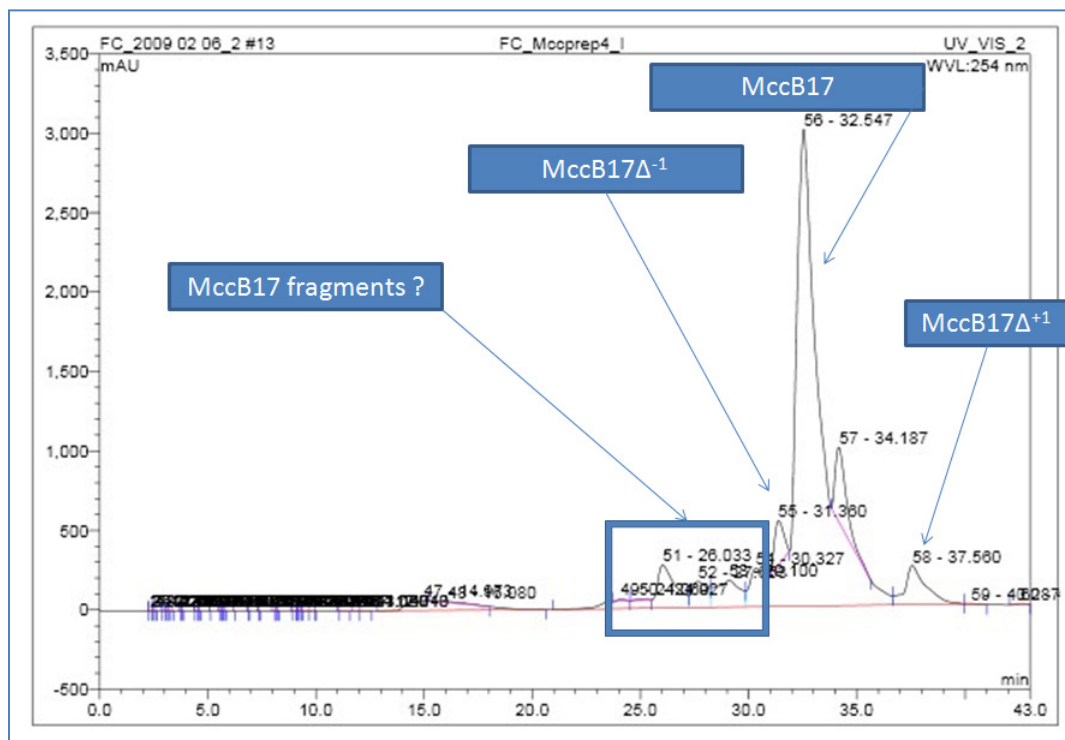
Figure 69 MccB17 HPLC purification trace.

Maldi-ToF MS analysis and study of fragmentation confirmed that indeed these isolates contain compounds related to MccB17. The main compounds observed had MWs of 1700.6, 1393.5, and 857.4 Da. The MS fragmentation spectra of the main peaks found in this isolated fraction are shown below:

85

4.1 MW = 1700.6

A very clear fragmentation spectrum by MALDI-ToF of this molecule has been obtained. We can clearly see the sequential removal of amino acids from the N-terminus with the typical polyglycines. This coupled with the fragment observed with m/z = 469.9 Da which correspond to GGtzGtz (MW = 469.07 Da) allowed us to conclude with confidence that this molecule corresponded to the 21 N-terminal residues of MccB17.
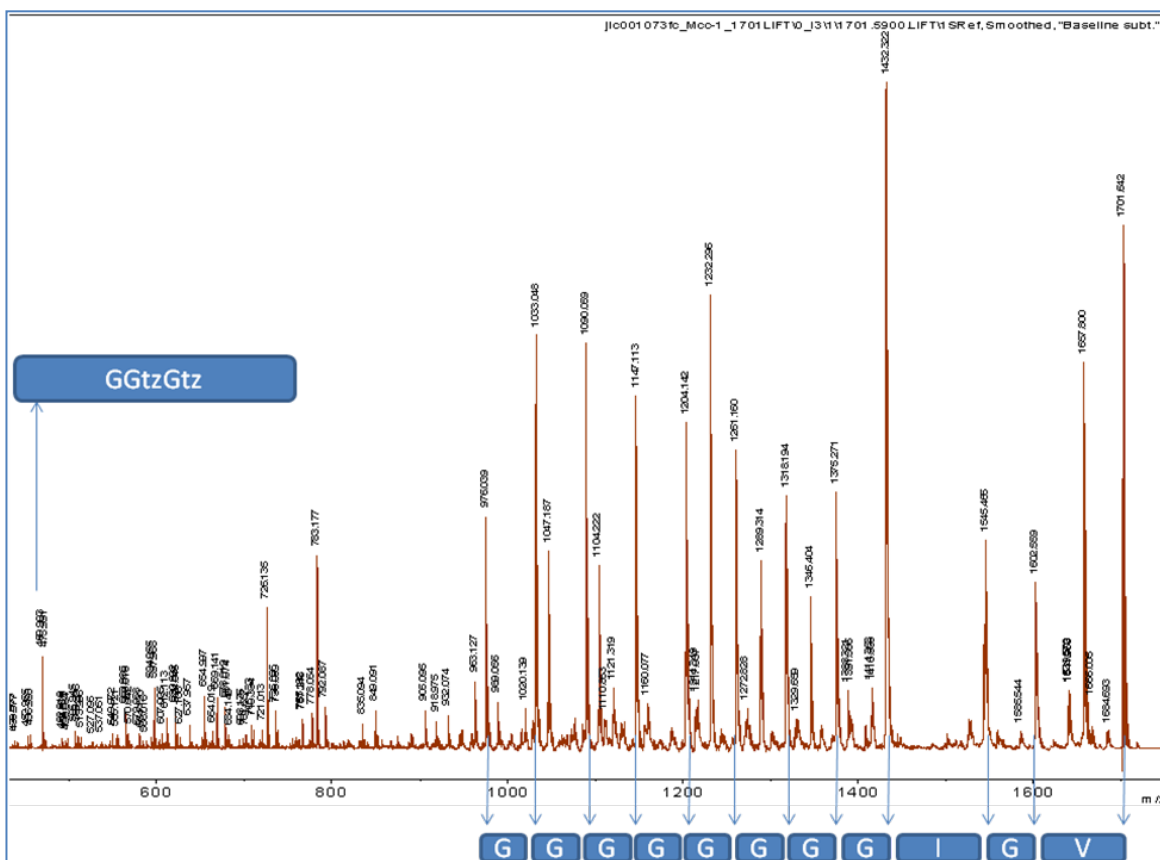
Figure 70 MALDI-Tof spectra of MW = 1700.6 fragmentation

4.2 MW = 1393.4

Analysis of this fragment was less straightforward, but low molecular weight fragments corresponding to HI (MW = 268.09 Da) and SHI (MW = 355.12 Da) which are the last 3 amino acids of MccB17 gave hints that this fragment was related to the C-terminal part of MccB17. Using this starting point, fragmentation can be traced backwards showing the expected *m/z* values as shown on Figure 71 below thus validating our assumption. This molecules contains the 13 C-terminal residues (residues Asn53 to Ile69) of MccB17, which correspond to a MW of 1323.37 Da (*m/z* = 1324.43 Da observed), addition of the next amino acid, Ser52 will lead to a MW of 1410.4 Da which was higher than what we observed. The molecular weight of the fragment isolated was between a 13- and a 14-residue long N-terminal fragment. Our assumption was that this fragment is a 17 Da lighter derivative of the 14 residue-long fragment. This molecule is likely to result from the elimination of an ammonia molecule.
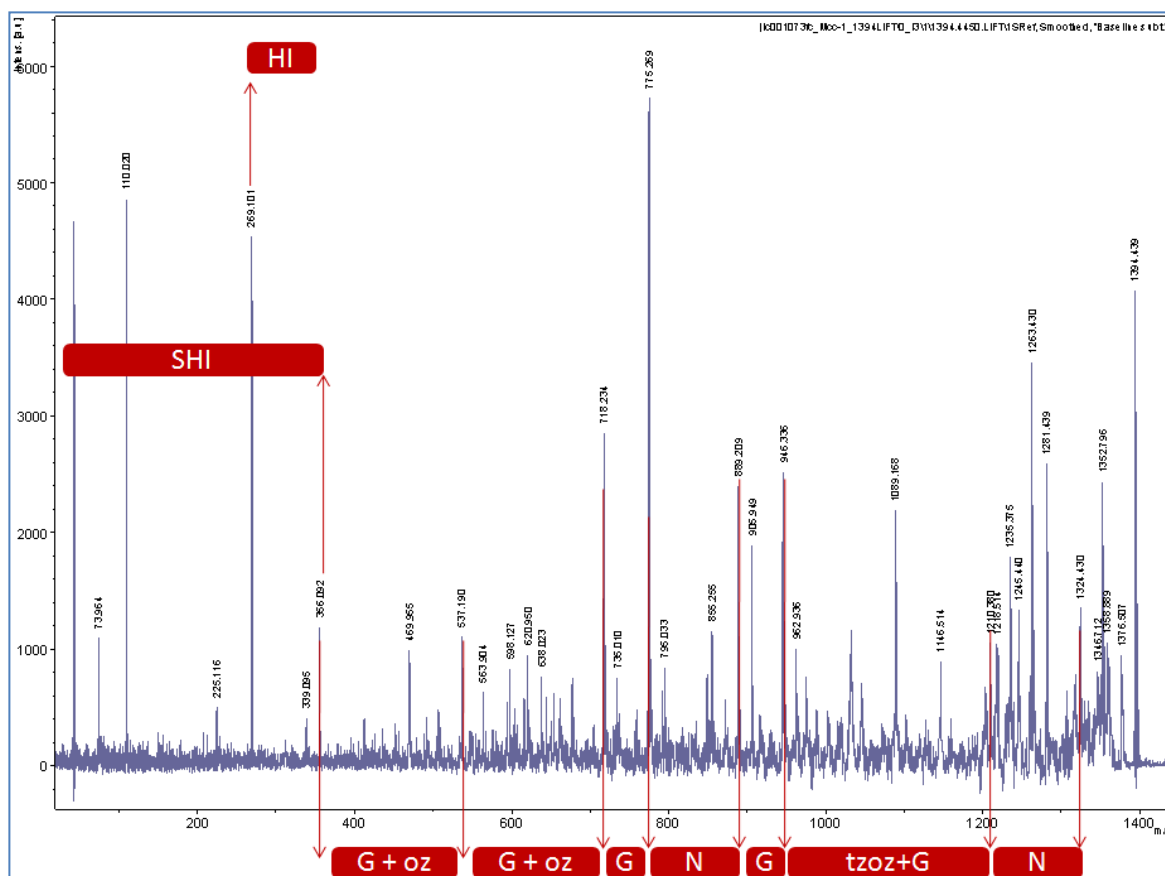
Figure 71 MALDI-Tof spectra of MW=1393.4 fragmentation

4.3 MW = 857.4

Spectra of MW = 857.4 Da were not as clear but the molecule was definitely a fragment containing the N-terminal VGIG residues and a cascade of glycine typical of the N-terminus of MccB17. The oztz ring that follows the polyglycine was not observed and would give a higher MW fragment of 1007.37 Da. If we forgot the strict MccB17 sequence, the MW would match the following formula VGI $(G)_{10}$, which corresponds to the whole N-term fragment of MccB17 preceding the oztz heterocycle but with an extra G. Our hypothesis is that this compound was not related to the mature MccB17 but to a MccB17 precursor which carries the GSC sequence instead of oztz ring. However MW = 857.4 was present as well in the digest of MccB17 by a carboxypeptidase, as a weak signal. It should have been degraded if the C-terminus residue is a Gly, this suggest that the C-terminus was likely to be a fragment of oztz.
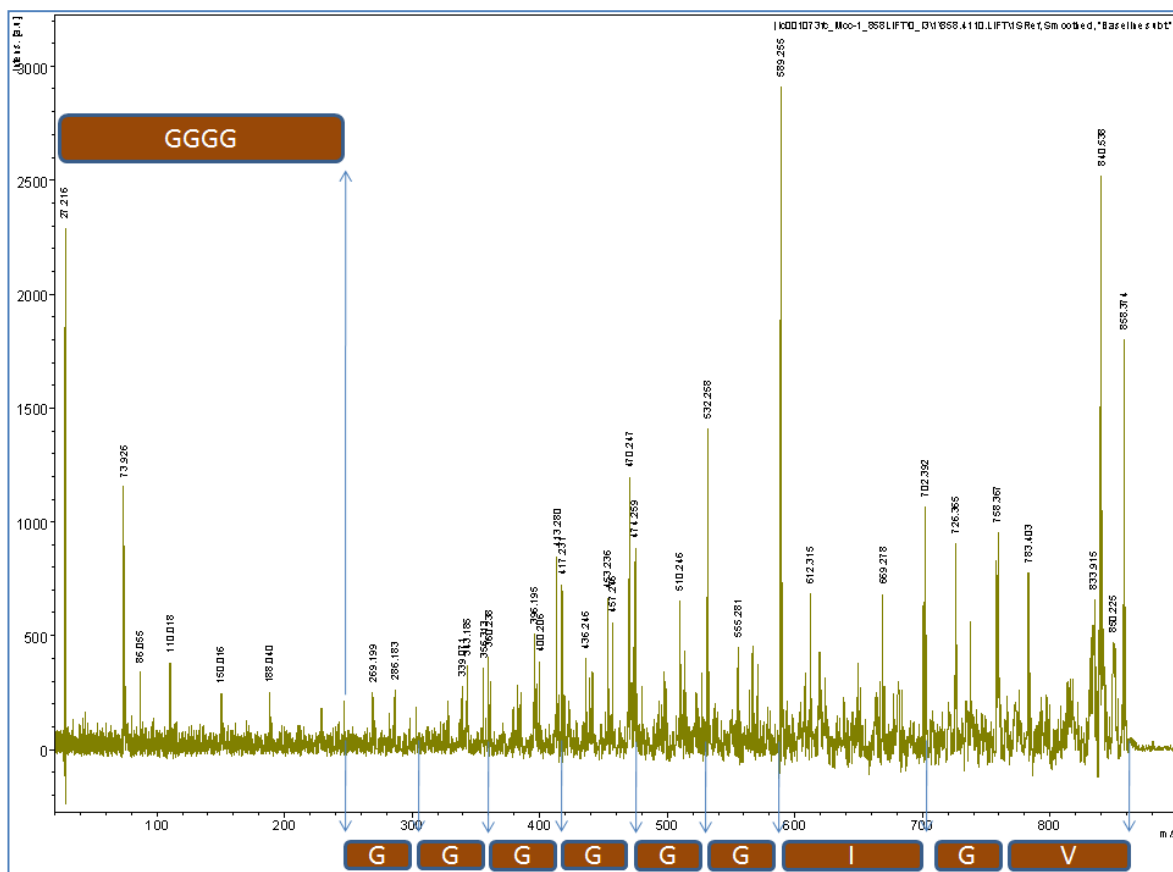
Figure 72 MALDI-Tof spectra of MW = 857.4 fragmentation

4.4 Comments

These molecules probably result from spontaneous cleavage occurring in the experimental conditions related to MccB17 preparation. Fragments MW = 1393 Da and 1700 Da appear to both result from a single cleavage of the peptide bond between tz2 and Ser52, and MW = 857 is probably a by-product of a MccB17 precursor. These structures are summarized in Figure 73 below. These compounds where added to our pool of MccB17 fragments even if they are unlikely to retain inhibitory activity, and therefore will be described further in Chapter 3.

Fragments from mccB17 preparation																												
Sequence																												
V	G	I	G	7xG	G	oztz	G	G	Q	G	G	tz	G	tz	S	N	tzoz	G	G	N	G	oz	G	oz	G	S	H	I
1700.57															1410.48													
857.41					G										?	1393.46												
																	1323.370											

Figure 73 Fragments of MccB17 isolated from MccB17 preparation: the sequence of MccB17 is shown in orange, the coloured boxes correspond to MccB17 fragments with their corresponding MW, in bold are the fragments isolated, in italic are related fragments for information.

5 *In vitro* activity on *E. coli* gyrase:

The activity of microcin B17 on *E. coli* gyrase has been characterized *in vitro* by its ability to stabilise the gyrase-DNA cleavage complex in presence of ATP by Heddle *et al* (Heddle, Blance *et al.* 2001) and its ability to slow down the supercoiling and relaxation reactions by Pierrat *et al* (Pierrat and Maxwell 2003). We will describe here the methods inspired by these sources that have been used to characterize produced MccB17 and other inhibitors of interest.
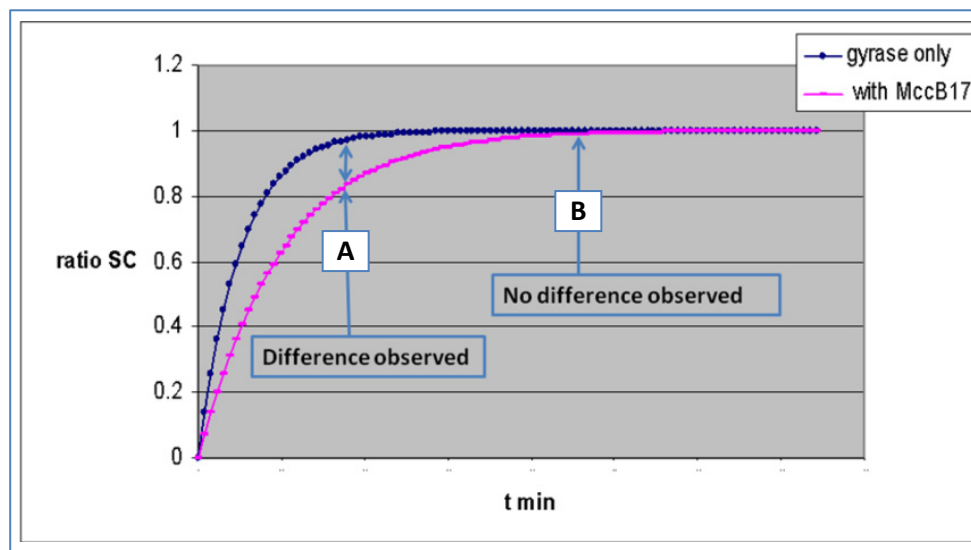
Figure 74 Effect of MccB17 on the supercoiling reaction over time: the ratio of supercoiled dna species to all dna species (ratio SC) is shown as a function of time. At time-point A the slowing down effect of MccB17 can be observed as opposed to time-point B where the MccB17-containing reaction had caught up with the control reaction.

Inhibition of supercoiling and relaxation by MccB17 is not straightforward to characterize as the toxin is only slowing down these processes. Experimental conditions require a precise tuning so that the reaction advancement will be at a point where this inhibitory activity can be observed, as illustrated by Figure 74.

5.1 Supercoiling

We have mentioned in the previous chapter how gyrase removes stress caused by accumulation of positive supercoils in the cells by introducing negative supercoils at the expense of ATP. We will describe here how this event can be reproduced *in vitro* and its alteration by MccB17 studied.

Time course: MccB17 is only slowing down the supercoiling reaction of gyrase so it is necessary to stop the reaction before it reaches its plateau as illustrated by Figure 75.

In order to stop the reaction at the optimum time, the supercoiling reaction was tracked over time as follows: a mixture containing 50 µM MccB17, 5.4 nM relaxed pBR322 DNA, 2.7 nM gyrase and 1 mM ATP was incubated at 25°C, samples were collected at t = 0.25, 0.5, 1, 1.5, 2, 3, 4 h. Samples were treated with one volume chloroform/isoamyl alcohol (24:1) and one volume STEB just after collection. Samples were analyzed on a 1% agarose gel. The same experiment but with no drug or with 8.5 µM ciprofloxacin were used as controls.

This experiment shows that the reaction should be stopped after 2 h incubation at 25°C as most of the DNA is supercoiled but not completely in the absence of MccB17, and MccB17 inhibition is clearly shown. Following this study, our standard supercoiling conditions are the following: 50 µM MccB17, 5.4 nM relaxed pBR322 DNA, 2.7 nM gyrase and 1 mM ATP are incubated at 25°C, after two hours samples are treated with one volume chloroform/isoamyl alcohol (24:1) and one volume STEB. Samples are analyzed on a 1% agarose gel. The same experiment but with no drug or with 8.5 µM ciprofloxacin were used as a controls.
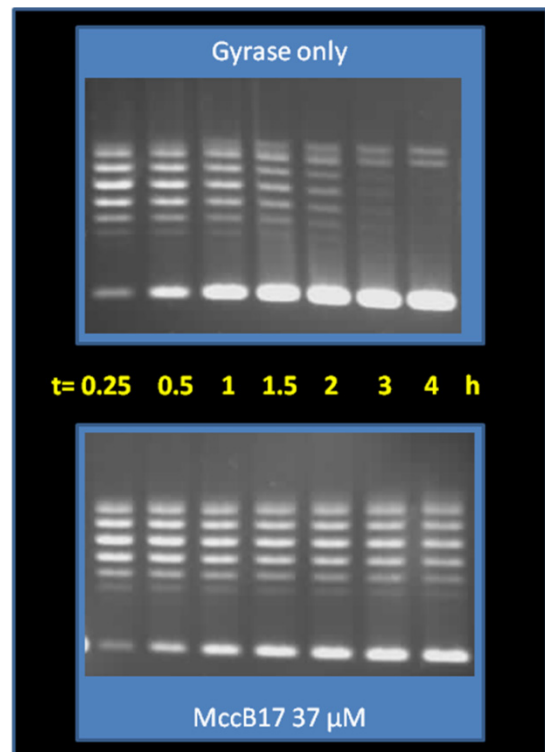
Figure 75 Time courses of gyrase supercoiling: the top gel shows the gyrase alone, the bottom gel the same reaction in presence of 37 µM MccB17. For all gels: the top ladder corresponding to relaxed DNA is converted over time into the bottom band corresponding to supercoiled DNA.

Example of final assay
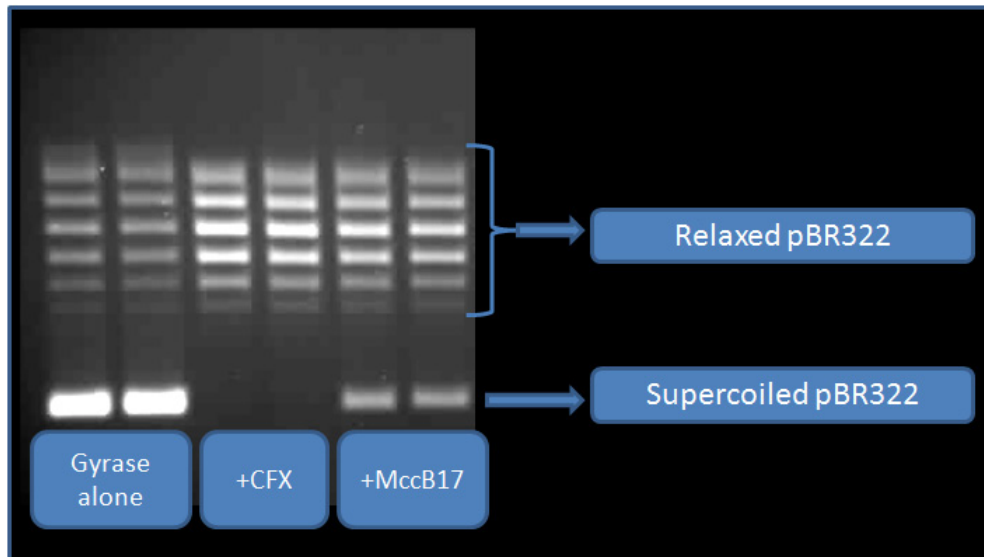
Figure 76 Example of gyrase supercoiling assays with the optimised conditions: the first two lanes are the enzyme alone, the next two are gyrase in presence of 8.5 µM ciprofloxacin, and the final two lanes in presence of 50 µM Mcc17. The top ladder corresponding to relaxed DNA is converted by gyrase into the bottom band corresponding to supercoiled DNA. CFX completely inhibits this reaction, whereas the reaction is partially inhibited by MccB17 in the conditions of the assay.

5.2 Relaxation

Relaxation is the opposite of the supercoiling reaction, it is driven by the gain of entropy of the DNA going from the supercoiled topological state to relaxed. The reaction does not require ATP to occur but is a less favourable reaction kinetically than supercoiling, so a larger amount of enzyme is used in order to stay in the same time frame. As gyrase is not a very good relaxing enzyme the effect of MccB17 is easier to observe than for the supercoiling reaction. As for the supercoiling assay the length of the reaction time was optimised using a time course. The relaxation reaction was conducted by incubating a mixture containing 50 µM MccB17, 5.4 nM supercoiled pBR322 DNA and 20 nM gyrase at 37°C, samples were collected at t= 0.5, 1, 2, 3h. Samples were treated with chloroform/isoamyl alcohol (24:1) and STEB just after collection. Samples aqueous phase was loaded on a 1% agarose gel. As before, reactions with no drug or 8.5 µM ciprofloxacin instead of MccB17 were used as controls.
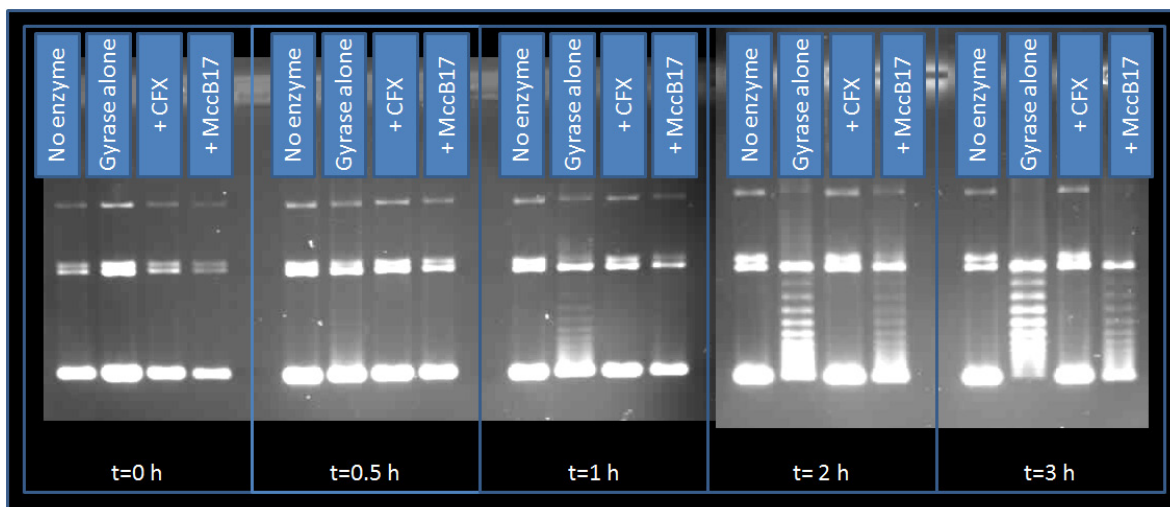
Figure 77 Time course of gyrase relaxation: for each time, lane one is without enzyme, lane two gyrase alone, lane three gyrase plus 8.5 μM ciprofloxacin, lane four gyrase plus 50 μM of MccB17. The supercoiled DNA band at the bottom of the gel is converted by gyrase to a ladder of band corresponding to relaxed DNA species. Ciprofloxacin completely blocks the reaction, whereas MccB17 slows it down.

Following further tests, the final conditions retained for relaxation are the following: 5.4 nM of supercoiled pBR322 DNA and 80 nM of gyrase were incubated in presence of no inhibitor, 50 μM MccB17 or 8 μM CFX for 2 h at 37°C. Samples were treated with chloroform/isoamyl alcohol (24:1) and STEB before being loaded on a 1% agarose gel.
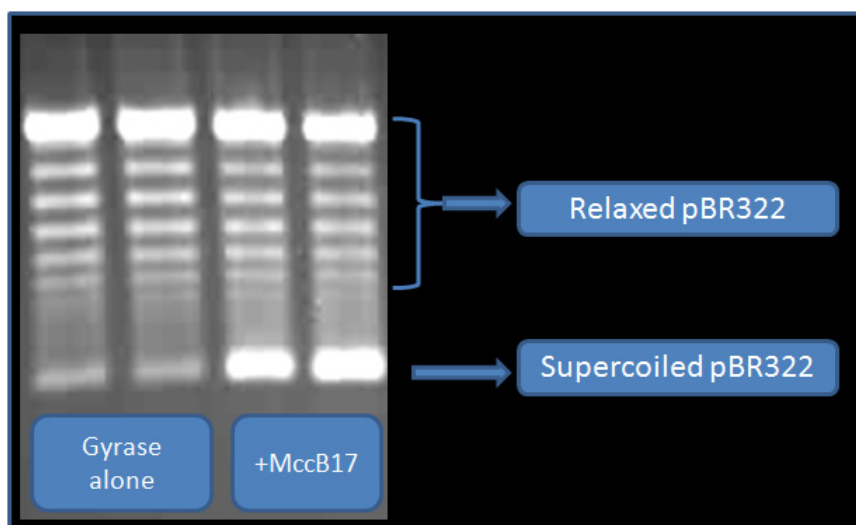
Figure 78 Example of gyrase relaxation assays with the optimised conditions: the first two lanes are the enzyme alone, and the next two lanes are gyrase in presence of 50 μM Mcc17. The bottom band, corresponding to supercoiled DNA, is converted by gyrase into the ladder at the top of the gel that correspond to relaxed DNA. The inhibitory effect of MccB17 is particularly clear: the ratio of intensity of supercoiled DNA (lower band) compared to the sum of all DNA species in the lane is significantly higher than what is observed with gyrase alone.

92

5.3 Cleavage

The great strength of the fluoroquinolone antibacterials is their ability to stabilise a DNA-gyrase cleavage complex that leads to the generation of species that are very toxic for the cell. The cleavage assay allows us to study *in vitro* the influence of compounds on the formation of DNA-gyrase cleavage complex. To do so, the same conditions as supercoiling are used but with a fifteen-fold increase in gyrase concentration, to increase the amount of cleavage complex formed. In the presence of compounds that are stabilising this cleavage complex there will be a significant enrichment of the population of linear DNA. Microcin B17 can only efficiently stabilise the cleavage complex in the presence of ATP; this ATP-dependence can be shown by running the experiment with versus without ATP. On Figure 79, lane 5 and 6, linear DNA is generated in the presence of MccB17 for both conditions, but the amount in the absence of ATP is very low. The reactions are run with no drug or 8.5 µM ciprofloxacin as a control, ciprofloxacin is able to stabilise the cleavage complex independently of the presence of ATP. The assay is conducted as follow: a mixture containing 50 µM MccB17, 5.4 nM relaxed pBR322 DNA, 80 nM gyrase and 1 mM ATP is incubated at 37°C for one hour, then 0.2% of SDS and 2 µg/µl of proteinase K are added and the reaction is incubated for 30 min at 37°C. The sample is treated with one volume of chloroform/isoamyl alcohol (24:1) and one volume of STEB before being analysed on a 1% agarose gel. The gel can contain ethidium bromide in order to have a better resolution between relaxed DNA topoisomers and linear DNA.
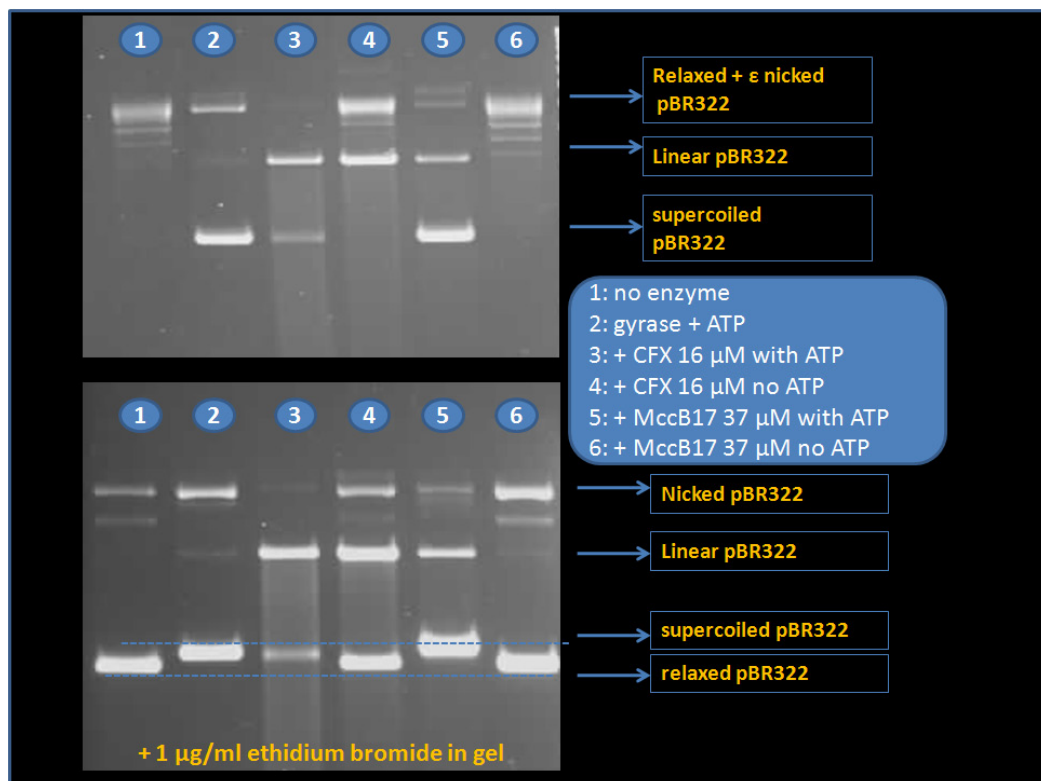
Figure 79 Gyrase cleavage assays: The top gel corresponds to the cleavage assay run on a standard agarose gel; the bottom gel correspond to the same cleavage assay but run on a 1 µg/ml ethidium bromide agarose gel. Lanes 5 and 6 highlight the ATP dependence of MccB17 stabilisation of cleavage complex.

It is important to note the difference between the lanes 5 and 6 in Figure 79, as it highlights the ATP-dependence of MccB17 stabilisation of cleavage complex.

5.4 Comments

Evidence gathered from supercoiling, relaxation and cleavage assays together give a good overview of the potency of an inhibitor and some insight on its mechanism of action. By comparing supercoiling and relaxation activity one can infer if ATP hydrolysis is involved in the inhibitory mechanism. If a compound inhibits supercoiling but not relaxation, complementary evaluation of its influence on ATPase activity should be carried out. Obviously stabilisation of cleavage complex and ATP dependence of this event reveal the type of mechanism involved.

5.5 Resistance to microcin B17 in *E. coli* gyrase

The mutation tryptophan 751 to arginine in the GyrB subunit (Y751R) confers gyrase immunity to MccB17 (Vizan, Hernandez-Chico et al. 1991). The assays with the mutant gyrase are conducted as described above for the wild type in order to determine whether compounds related to MccB17 are affected by this mutation, which is the only one conferring resistance to MccB17 that has been identified so far; we will describe in the next part our attempt to discover others.

6 *In vitro* activity on other topoisomerases

The activity of microcin B17 on gyrase is well documented, but surprisingly the field of investigation has not been extended to other topoisomerases. Three topoisomerases have been considered here: *E. coli* topoisomerase IV, which is closely related of gyrase and a well known secondary (or sometime primary) target for fluoroquinolones antibacterial drugs, and the gyrase from *Staphylococcus aureus,* which is an important health-threatening bacteria, and finally human topo II for its relevance to anti-cancer therapy.

6.1 *Staphylococcus aureus* gyrase

The activity of MccB17 on *Staphylococcus aureus* gyrase was studied in collaboration with Terence Chung. The assays were conducted in the following condition: 200 µM of MccB17 were added to 2.4 nM SaGyrA, 23 nM SaGyrB, 5.4 nM relaxed pBR322, 2 mM ATP and 3% DMSO. Samples were treated with chloroform/isoamyl alcohol (24:1) and STEB before being loaded on a 1% agarose gel. No inhibitory activity was observed at this concentration.

6.2 *E. coli* topoisomerase IV

The activity of MccB17 on *E. coli* topo IV relaxation was assayed using the following conditions: 11 nM supercoiled pBR322 DNA and 22 nM topo IV and 1 mM ATP were incubated in presence of no inhibitor, 37 µM MccB17 or 17 µM CFX for 30 min at 37°C. Samples were treated with chloroform/isoamyl alcohol (24:1) and STEB before being loaded onto a 1% agarose gel.
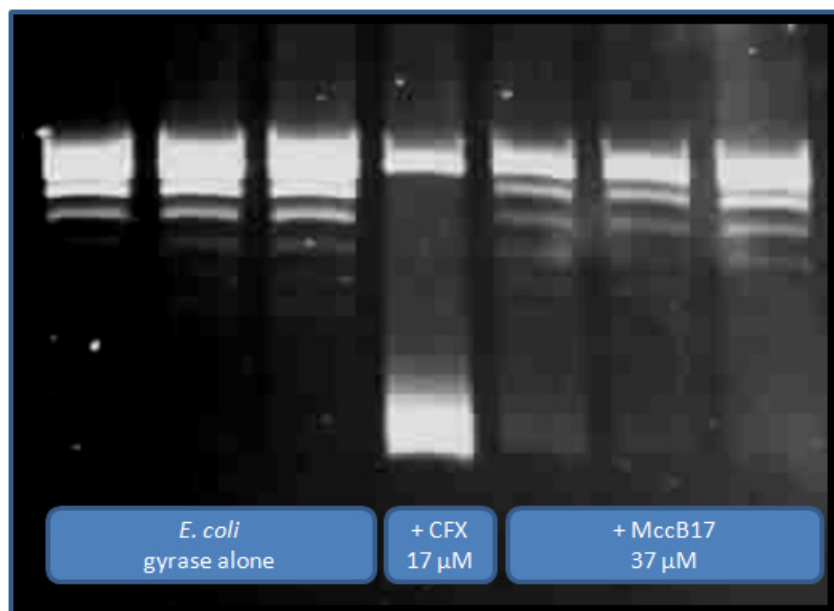
Figure 80 Effect of MccB17 on topo IV relaxation reaction: topo IV converts supercoiled DNA (bottom band) into relaxed DNA (top ladder of bands). In the presence of 17 μM ciprofloxacin an intense bottom band is visible due to its inhibitory activity. In the presence of 37 μM, a faint bottom band is visible, accounting for some inhibition by MccB17 of topo IV.

There is probably a weak inhibition of the reaction at 40 μM, visible as a shade at the level of the supercoiled species, and weaker relaxed bands. Unfortunately, due to time constraints we haven't been able to further validate this preliminary result and determine an IC$_{50}$, but this is an encouraging result to pursue investigation of the inhibition of topo IV by MccB17 and particularly evaluating if stabilisation of the cleavage complex can be achieved in the presence of MccB17.

6.3 Human topoisomerase II

The evaluation of the activity of MccB17 on human topo II relaxation was conducted as follow: to a mixture 5.4 nM of supercoiled pBR322, 1 U of human topo II, and 1 mM ATP, no drug, 100 μM etoposide or 200 μM MccB17 were added. Samples were treated with chloroform/isoamyl alcohol (24:1) and STEB before being loaded on a 1% agarose gel.
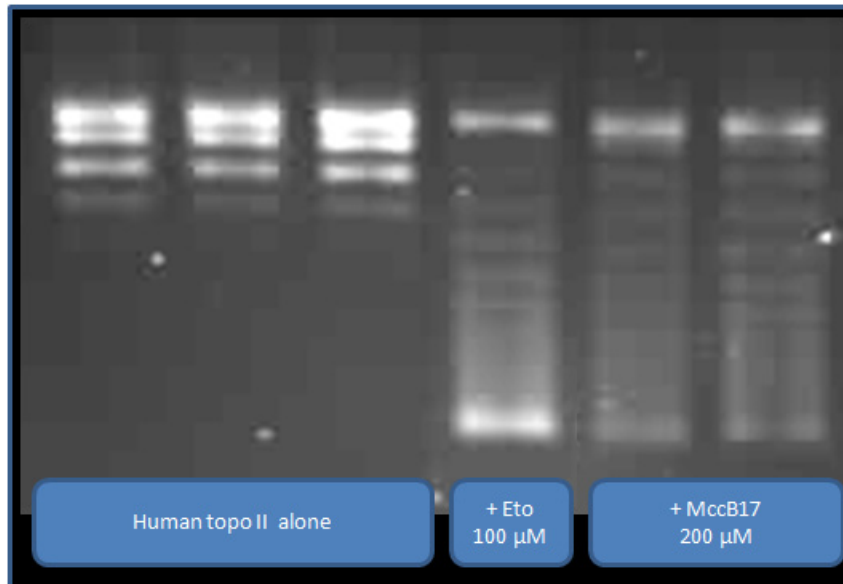
Figure 81 Evaluation of the inhibitory activity of MccB17 on human topo II: relaxation assays with human topo II, the lower band, corresponding to supercoiled DNA, is converted by the enzyme into the top ladder of bands, the relaxed DNA species. In the presence of an inhibitor such as etoposide, the intensity of the lower band is increased and the top ladder decreased. We can observe that MccB17 has an effect very similar to etoposide.

MccB17 inhibitory activity on topo II relaxation has been observed at 200 µM, which can be considered as a high concentration, but this is only twice the concentration of the etoposide control we are using. This suggests that MccB17 has some potential as a topo II inhibitor. For anti-cancer application, we are less interested in the stabilisation of the cleavage complex, however on a mechanistic point of view, and for a better understanding of MccB17 It would be useful to ascertain if it is a topo II poison.

7 Selection of new mutants resistant to microcin B17

We have mentioned in the first chapter that replacement of tryptophan 751 by arginine was the only gyrase spontaneous mutation identified that confers resistance to MccB17 (Vizan, Hernandez-Chico et al. 1991). Identifying mutated residues that are responsible for resistance to the toxin is a good way to have a better understanding of the interaction between the enzyme and its inhibitors. Resistance to microcin B17 occurs at an elevated rate (10^{-6}) (Lavina, Pugsley et al. 1986); the main resistance mechanism observed is linked with the alteration of the uptake system: OmpF in the outer membrane and SbmA in the inner membrane (Lavina, Pugsley et al. 1986), this reduces significantly the chance of isolating a

resistant strain carrying mutations that map to gyrase, as the toxin is not reaching its target. By using a permeable strain we aimed to overcome this problem by improving the chances of selecting resistance related to this cellular target.
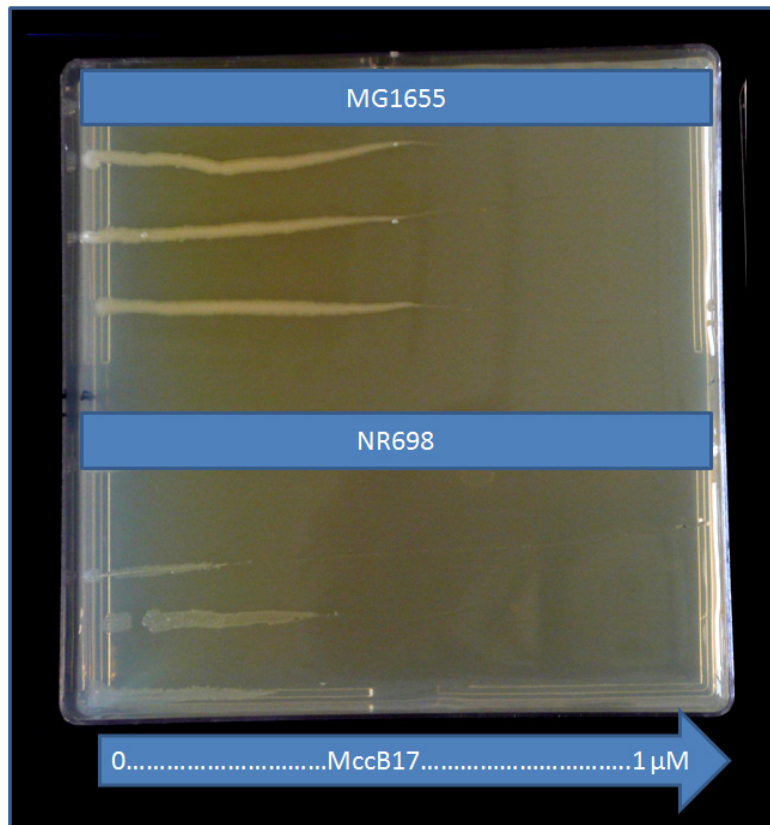
Figure 82 Comparison of MccB17 on the permeable strain vs standard *E. coli* strain: this is an LB-agar slop plate with a gradient of MccB17 from zero (right) to 1 μM (left). The top part is streaked with the standard MG1655 *E. coli* strain, the bottom part with NR698 *E. coli* permeable strain.

7.1 NR698 permeable strain

The permeable train *E. coli* NR698 was used is this study, it is an MC4100 strain with an in frame deletion of 23 amino acids (D330 to D352) in the *imp* (increased membrane permeability) gene (*imp4213*). *Imp* encodes for an essential protein involved in the outer membrane assembly. This deletion has been reported to increase permeability to drugs like Vancomycin (Braun and Silhavy 2002; Ruiz, Falcone et al. 2005).

7.2 Preliminary study

During standard halo assays with MG1655 involving MccB17, a few resistant colonies inside the inhibition halo were noticed. Following this observation we performed halo assays using MccB17 on plates inoculated with MG1655 (wild type) and NR698 (permeable strain), in order to evaluate the susceptibility of the permeable strain and the occurrence of resistant

colonies. Resistant colonies appeared with NR698 as for MG1655 and 4 of them were collected and stored as glycerol stocks. The resistance to MccB17 was confirmed by halo assays with MccB17 on LB-amp agar plates inoculated with the collected colonies.

7.3   Evaluation of microcin B17 MIC on NR698

MccB17 MIC on NR698 was estimated using an LB-agar slope plates with a gradient of MccB17. Slope plates at 5, 2, 1 µM MccB17 where used and lead to the estimated MIC MccB17$_{NR698}$= 0.33 µM and MccB17$_{MG1655}$= 0.6 µM. These results confirmed the greater sensitivity of the permeable strain compared to the wild type and allow us to proceed further with the isolation of resistant mutants.

7.4   Selection of resistant colonies

Resistant colonies were gathered from an LB-agar plate containing MccB17 inoculated with 2 X 10^9 cells grown overnight in LB. Concentrations up to 2.5 µM of MccB17 (MIC X7.5) were used in order to obtain an appropriate number of resistant colonies Around 5000 colonies were present out of 2X10^9 cells introduced on the plate initially, giving a frequency of one resistant colonies per 4X10^5 cells. 16 colonies were collected across the plate. Their resistance was validated on a "slope plate" containing 0 to 1 µM MccB17.

7.5   Sequencing of gyrA and gyrB genes of resistant colonies

To determine if mutations mapped to the *gyrA* or *gyrB* genes, a "colony PCR" of the resistant colonies was performed. The size of the amplicons was verified by running samples on 1% agarose gel before submission to sequencing. The resistance to MccB17 could not be related to any mutation of the *gyrA* or *gyrB* genes.

7.6   Investigation of resistance mechanism

As none of the 20 mutants isolated had shown mutation on gyrase we decided to investigate further the source of this resistance.

7.6.1   Loss of permeability

One of the possibilities that arose to explain these resistances is that the strain had reverted to a non-permeable type. In order to discard this eventuality, the sensitivity of the resistant strains to bile salts and to vancomycin was evaluated. NR698 have been reported to be sensitive to both compounds whereas wild type strain is not. Each mutant was streaked on two types of agar plates: MacConkey (bile salts) and LB-Vancomycin (2 µg/ml) and compared with MG1655. No mutant colonies grew on either plate during overnight incubation at 37°C whereas MG1655 did. This confirms that the resistant strains isolated are still permeable as they are still susceptible to these two environments.

7.6.2 SbmA alteration

SbmA impairment has been reported to be the most common source of resistance to MccB17. Our strategy that is improving the intake of MccB17 through the outer membrane still leaves the possibility for this inner membrane transporter to affect resistance to MccB17. SbmA is also involved in the uptake of bleomycin (Yorgey, Lee et al. 1994); in order to check if the transporter activity had been modified the sensitivity of the MccB17-resistant mutants to bleomycin was assessed. The various mutants were streaked on an LB-plate containing 1 µg/ml bleomycin. Unfortunately all the mutants were resistant to bleomycin, this strongly suggest that SbmA inactivation is the source of resistance in our isolated resistant strains. Sequencing of the *sbmA* gene should provide evidence for this hypothesis.
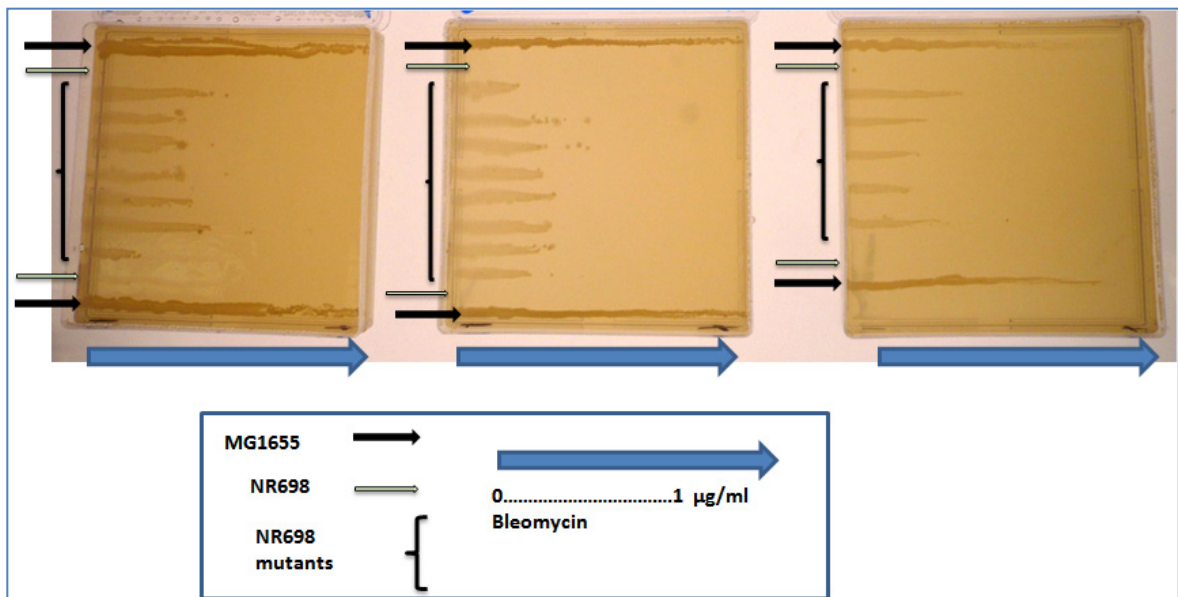
Figure 83 Resistance to bleomycin of MccB17-resistant NR698 mutants: slope plate with a gradient of 0 to 1 µg/ml of bleomycin (blue arrows). The black arrows represent the non-permeable strain (MG1655), the green arrows represent the wild type permeable strain (NR698), and the others are the isolated MccB17-resistant NR698. Wild type NR698 did not grow whereas the MccB17-resistant mutant did grow at a concentration of bleomycin ~0.3 µg/ml.

7.7 Conclusion

Isolation of strains that gain resistance to MccB17 through mutation in gyrase has proved unsuccessful, mainly because of the underestimation of SbmA alteration occurrence and its influence on resistance in our strategy. Enlightened by this fact we can now define a new process to address this issue. In this study bleomycin was used to implicate SbmA involvement in resistance to MccB17; following this idea, resistance to bleomycin can be used as a criterion to discard mutants unlikely to carry a mutation on gyrase. Basically if a mutant is resistant to MccB17 because of impairment in *SbmA* it should be also resistant to bleomycin, by using replica plating it will be possible to select only the strains that are resistant to MccB17 and still

sensitive to bleomycin thus improving the chance of isolating a gyrase mutant. Another possibility is to make sure that SbmA will be expressed in the strain by adding a high-copy plasmid carrying the wild type *SbmA* gene; this is an approach similar to what was done to isolate the W751K mutant (Vizan, Hernandez-Chico et al. 1991), but it will be applied on the permeable strain cumulating the advantage of an increased intake both through the outer and inner membranes.

8 Structural studies: crystallography trial

The primary structure of MccB17 is well known, but no information has been reported about its secondary structure. A way to address a better understanding of MccB17 spatial structure is through X-ray crystallography.

A solution of 1 mg/ml of MccB17 in water with 3% DMSO was used in three common crystallisation trials: Classics, JCSG and PACT. Pictures were taken every day for seven days and once a week for two more weeks. No positive results were obtained but some small crystal like structures were observed. The table below describes the results of these trials.

Table 2 crystallography screening

Screen	Hit	Type	Conditions
Classic	**C4**	Crystal-like structure	5 M lithium sulphate; 0.1 M NaHEPES; pH=7.5
JCSG	D5	Crystal-like structure	10% w/v PEG 1000; 10% PEG 8000.
	D7	Crystal-like structure	0.2 M lithium sulphate; 0.1 M Tris pH=8.5; 1.260 M ammonium sulphate
	G7	Heavy precipitate	0.2 M zinc acetate; 0.1 M sodium cacodylate; pH=6.5; 10% w/v 2-propanol
PACT	**D7**	Needles	0.2 M potassium thiocyanate; 20% w/v PEG 3350

A round of optimisation was carried out using the C4 and D7 conditions: C4 optimisation trial was performed using concentration of lithium sulphate ranging from 1.3 M to 1.8 Min 100 mM HEPES pH = 7.5. D7 optimisation involved varying the KSCN or the PEG concentrations: variation of KSCN ranging from 100 µM to 300 µM, with 50% PEG 3350 were used for the first optimisation. The second conditions involved variation of PEG 3350 from 30% to 55%, with 200 µM lithium sulphate. None of the optimisation condition tested yielded crystals.

9   Modified Microcin B17.

9.1   Chemical conversion of Asn/Gln to Asp/Glu

Incubation at mild alkaline pH converts MccB17 amide residues to acids residue, as reported by Parks *et al* (Parks, Bottrill et al. 2007); only the two asparagines, Asn53 and Asn59, out of three potential residues were modified during the process leaving Gln44 unchanged. One of the aims of this study is to evaluate if smaller fragments of MccB17 can be topoisomerase inhibitors so this modified MccB17 appeared to be a good template to use with endoprotease like endo. Glu-C. This protease will cut specifically after the Asp site potentially allowing us to generate fragment in a controlled manner. It was an opportunity as well to investigate further the properties of this modified MccB17: it has been reported to be unable to stabilize cleavage complex (Parks, Bottrill et al. 2007), but the effect of this compound on gyrase supercoiling and relaxation reactions have not been probed.

9.1.1   Production of the modified MccB17: MccB17(N23D,N27D)

The modified MccB17 was produced by incubating 12 mg of MccB17 in 500 ml of 100 mM sodium carbonate buffer pH=10 containing 1% DMSO at 37°C for 24 h. 1 mg of MccB17 in 100 ml MQ left for 24 h at 37°C was used as a control (Parks, Bottrill *et al*. 2007). The conversion of the two Asn residues was validated by MALDI-ToF MS, the main peak observed was *m/z* = 3096.17 which is an increase of two Da compared to WT MccB17, this corroborates the conversion of two amide residues. Fragmentation of the main peak with MALDI-ToF was in agreement with the conversion of the two Asn residues to Asp as described by Parks *et al* (Parks, Bottrill *et al*. 2007*)*. The mixture was purified further by HPLC with the same conditions used with MccB17.

9.1.2   Evaluation of inhibitory activity:

Our first aim was to evaluate if the change of the asparagine residues to aspartic acid was not only removing the capacity to stabilize cleavage complex, but the inhibitory activity on supercoiling and relaxation. The MccB17(N53D,N59D) was compared to MccB17 on supercoiling and relaxation assays as described above. As MccB17(N53D,N59D) seems to had lost only the cleavage complex stabilizer feature of the native MccB17 we decided to incorporate it in the assays performed on other topoisomerases. No inhibitory activity was observed with *Staphylococcus aureus* gyrase at 100 µM, however the modified MccB17 was able to inhibit human topo II relaxation at this concentration. All assays are summarized in Figure 84.

9.1.3   Proteolysis

The cleavage of MccB17(N53D,N59D) by endoprotease will be developed in Chapter III as this chapter will describe extensively the evaluation of MccB17 fragments.
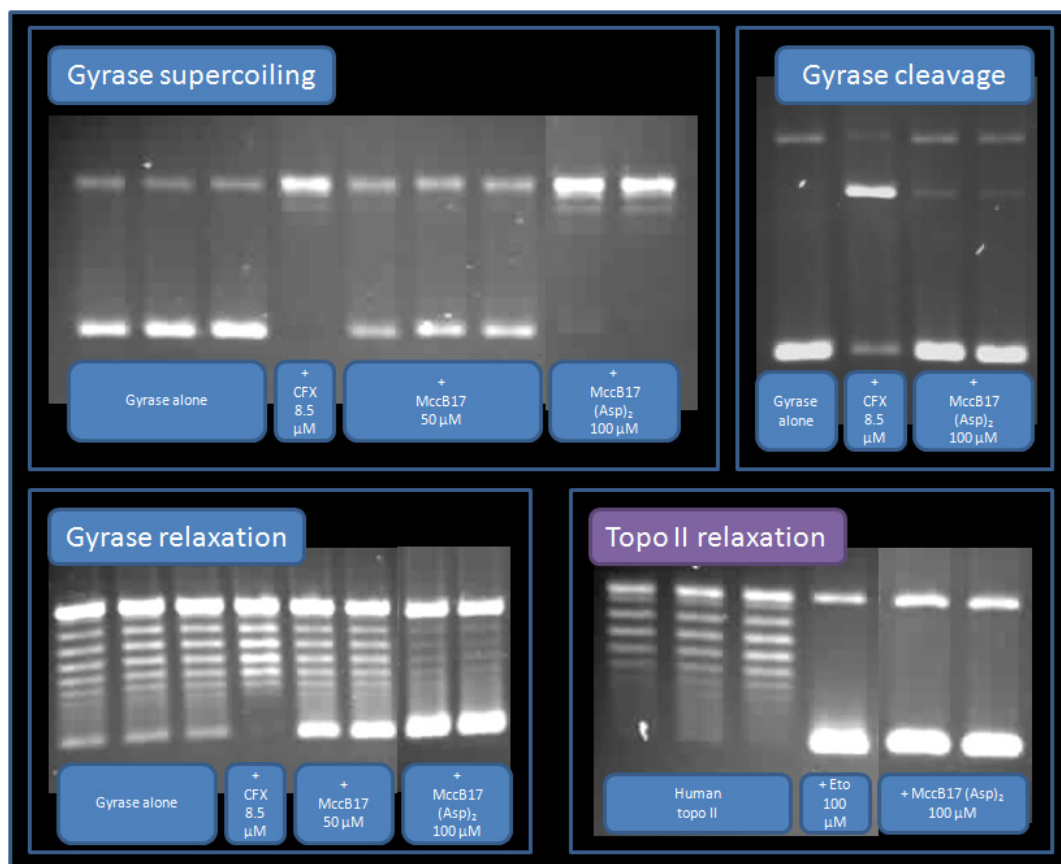
Figure 84 Evaluation of MccB17(N53D,N59D): top left; supercoiling assay of MccB17(N53D,N59D) noted as MccB17(Asp)$_2$, that display a complete inhibition of the reaction at 100 µM. Top right, cleavage assay with gyrase, a very weak cleavage band is present (in the middle). Bottom left, relaxation assay, MccB17(N53D,N59D) shows an inhibition of relaxation similar to MccB17. Bottom right, relaxation assays with human topo II, MccB17(N53D,N59D) shows an inhibitory activity similar to the etoposide control at the same concentration.

9.2 Evaluation of the importance of C and N terminal residues of MccB17

From previous studies it has been shown that the heterocycles in MccB17 are key features for its activity and that their structure is optimised for their purpose. Less is known about the other amino acids surrounding them. Alteration of the polyglycine chain in the C-terminal part of MccB17 has been shown to affect maturation of MccB17. The polyglycine appears to be a spacer necessary for MccB17 synthetase to mature MccB17 (Roy, Belshaw et al. 1998). Considering that fact, it is legitimate to wonder: from the residues upstream to the first heterocycle, which are required for MccB17 activity and which are only present for MccB17 maturation? From there it is straightforward to consider the other end of the molecule: are the N-terminal residues important for activity or are they there for other reasons linked to MccB17 production or transport? We will describe here how we have addressed these questions, at first by using exoproteases that allow us to generate mixtures of species

lacking a few terminal residues that can be screened for inhibitory activity and second using mutagenesis to generate several single mutants lacking a precise number of residues.

9.2.1 Enzymatic digestion by exoprotease

9.2.1.1 N-terminal digest: MccNexo

The digestion of the N-terminal end of MccB17 was carried out by using leucine aminopeptidase in the following conditions: to 300 µM of MccB17 in a 50 mM sodium phosphate buffer with 10% DMSO solution was added 0.1 unit of Leu-aminopeptidase, the mixture was incubated for 6 h 30 min at 37°C. The mixture was loaded on an Oasis™ (Waters) reverse-phase cartridge equilibrated with acetonitrile and water, eluted subsequently with H_2O and 50% CH_3CN/H_2O. The last fraction was collected, freeze-dried and redissolved at 1 mM concentration in 33% DMSO/H_2O solution for further analysis.

9.2.1.2 C-terminal digest: MccCexo

Carboxypeptidase A was used to digest the C-terminal end of MccB17: 3.5 units of carboxypeptidase A were added to a solution containing 300 µM MccB17, 25 mM Tris.HCl buffer pH = 7.5, 10% DMSO. The solution was then incubated for 6 h 30 at 25°C. The mixture was then loaded onto an Oasis™ (Waters) reverse-phase cartridge equilibrated with acetonitrile and water, eluted subsequently with H_2O and 50% CH_3CN/H_2O.The last fraction was collected, freeze dried and redissolved at 1 mM in 33% DMSO/H_2O solution for further analysis.

9.2.1.3 MS analysis:

9.2.1.3.1 MccNexo:

At first glance the spectra show that the proteolysis reaction had not worked, the main peaks are m/z = 3094.1, the starting material and m/z = 1394, a degradation product of MccB17, and none of the species corresponding to MccB17\(n)N-terminal residues are to be seen. In section 3) of this chapter we have described how some fragments of MccB17 are generated in experimental conditions including MW=1393. We described as well that usually this fragment comes with its complementary sequence with MW=1701. An interesting observation is that this fragment is not present at all, even as a trace. It is likely that this fragment had been degraded by the Leu-aminopeptidase to generate the following fragments than can be observed on the spectra: m/z = 1432 (1701\VGI), m/z = 1376 (1701\VGIG), and particularly m/z = 919 which correspond to the fragment 1701 minus all the residues preceding the oztz. This experiment didn't allow us to isolate MccB17 lacking amino acids on the C-terminal end that we expected. It appears that the enzyme was not able to digest native MccB17, although it was active in the conditions used, as fragments of MccB17 seem to have been processed. This puts a highlight again on the MccB17 spatial structure: was the enzyme not able to access the N-terminal end of the toxin due to its folding, or had the enzyme a better affinity for MccB17 fragments? If the second hypothesis is true, we should be able to access the products we seek by digesting MccB17 for a longer time in conditions limiting its

degradation. If the first hypothesis is true it will prove difficult to change the conditions in order to alter the structure of MccB17 while keeping the enzyme active. This investigation was not pushed forward as we got some of the answers we were seeking by other approaches that will be described in the next chapter.

Figure 85 MALDI-ToF spectra of MccNexo:

9.2.1.3.2 MccCexo:

The spectra shows beyond any doubt that the digest had been successful, the main product observed is MccB17\Ile, other species MccB17\HI (~30% intensity of main peak), MccB17\GHI and some residual native MccB17 (~15% int.) are also present.

Figure 86 MALDI-ToF spectra of MccCexo

9.2.1.4   Evaluation of the inhibitory activity of the exoprotease digests

Both mixtures were evaluated for inhibitory activity before their content was known. MccNexo and MccCexo were assayed at 100 µM final concentration in the standard supercoiling reaction conditions. We can see a weak inhibition by MccNexo which was probably due to the MccB17 present in this mixture. MccCexo didn't show any inhibitory activity. This is very interesting because the main component of this mixture was the MccB17 lacking only one amino acid: the C-terminal Isoleucine. This was strong evidence that modification of the C-terminal end of the molecule is very detrimental to MccB17. The possibility remains that the conditions we have used to produce this modified MccB17 have altered it folding thus disrupting its activity. In order to validate our assertion that MccB17 C-terminal amino acids are key to its inhibitory activity, we decided to produce this shortened MccB17 by mutating the *mcbA* gene and using the standard MccB17 production method described earlier in this chapter. We will describe now the method used to produce shortened MccB17 by mutagenesis.

9.2.2 Mutagenesis of MccB17

Using carboxypeptidase was a quick way to screen the effect of C-terminal amino acid removal on MccB17 inhibitory activity, but it carries inherent limitations: first only mixtures of shortened MccB17 can be obtained and second, if the toxin needs to be folded during its production to be active, there is no certainty that in the proteolysis conditions used this folding was not altered. These limitations can be circumvented by using a mutagenesis approach: by replacing the codon of a given amino acid in *mcbA* by a stop codon and expressing the toxin in *E. coli* as for the WT we should be able to harvest a MccB17 where the modified and all subsequent amino acids are missing. The modifications introduced, as they are taking place at the end of the peptide, should not alter the processing and export of the toxin.

Species lacking N-terminal residues can be obtained by a slightly different strategy: a lysine residue can be introduced by replacing the codon of one amino acid in the N-terminal region by the Lys codon. The mutated toxin can be produced and isolated as usual leading to a MccB17 carrying a Lys. A tryptic digest should cleave the peptide after the Lys residue leading to a MccB17 where all amino acids preceding the Lys have been removed. This strategy is more uncertain, we know that the polyglycine is important for the processing of the enzyme (Roy, Belshaw et al. 1998) and the modification is likely to hinder the processing of the heterocycles, and this will probably be more true the farther from the N-terminal end the Lys residue will be. Additionally, the consequences on MccB17 conformation and export, or on the immunity of the host cell, of this Lys introduction, are unknown.

9.2.2.1 *Extraction of pmccb17*

The template pUC19-*mccB17* was prepared from the DH5α strain used for MccB17 production described at the beginning of this chapter. The plasmid was extracted from a 5 ml overnight culture of DH5α-pUC19-*mccB17* in LB-Amp (1 mg/ml) with a QIAprep® Miniprep kit (Qiagen) following the supplier's protocol. The size of the plasmid was checked by running a sample digested by EcoRI on a 1% agarose gel.

9.2.2.2 *Mutagenesis of the mcbA gene*

The *mcbA* gene was mutated by PCR using primers carrying the desired modification. The PCR was carried out in a 50 µl reaction mixture containing 200 µM dNTP, 60 ng of pUC19-*mccB17*, 10 µM "forward" primer, 10 µM "reverse" primer, 2.5 U of Pfu Turbo® DNA polymerase in 1X Pfu supplier buffer. The PCR program and primers are described in the Table 1. The amplified mixtures were digested by Dpn1 in order to remove the wild type pUC19-*mccB17* template as follows: to 25 µl of the previous PCR reaction, 5 µl of NEBuffer nº4 (10X), 1 µl DpnI (20U) and 18 µl water were added, the mixture was incubated for 3 h at 37°C, then 1 µl DpnI (20U) was added and the mixture incubated overnight at 37°C. The resulting solution was used for the transformation.

Table 3 Primers used for site-directed mutagenesis of MccB17: two types of primers are described, the G(x)toK series correspond to the modification of the glycine(x) from the N-terminus of MccB17 to a Lysine, the G-, S-, H-, ItoStop correspond to the introduction of a STOP codon instead of the designed residue from the C-terminus of MccB17. The numbers in green squares are the primers that have lead to the expected mutant.

Serie i		n	Serie ii		n
G30toKF	tgttggcattaaaggtggtgg	1	G30toKF2	tgttggcattaaaggtggtggcg	17
G30toKR	ccaccacctttaatgccaaca	2	G30toKR2	cgccaccacctttaatgccaaca	18
G32toKF	attggtggtaaaggcggcg	3	G32toKF2	cattggtggtaaaggcggcggcg	19
G32toKR	cgccgcctttaccaccaat	4	G32toKR2	cgccgccgcctttaccaccaatg	20
G34toKF	attggtggtggtggcaaaggc	5	G34toKF2	tggtggtggcaaaggcggcggcg	21
G34toKR	gcctttgccaccaccaccaat	6	G34toKR2	cgccgccgcctttgccaccacca	22
G36toKF	ggcaaaggcggcggtag	7	G36toKF2	tggcggcggcaaaggcggcggta	23
G36toKR	ctaccgccgcctttgcc	8	G36toKR2	taccgccgcctttgccgccgcca	24
GtoStopF	cggaagttaatcacatatctgata	9	GtoStopF2	cggcggaagttaatcacatatct	25
GtoStopR	tatcagatatgtgattaacttccg	10	GtoStopR2	agatatgtgattaacttccgccg	26
StoStopF	aagtggttaacatatctgatacgtt	11	StoStopF2	cggaagtggttaacatatctgata	27
StoStopR	aacgtatcagatatgttaaccactt	12	StoStopR2	tatcagatatgttaaccacttccg	28
HtoStopF	aagtggttcataaatctgata	13	HtoStopF2	aagtggttcataaatctgatacg	29
HtoStopR	tatcagatttatgaaccactt	14	HtoStopR2	cgtatcagatttatgaaccactt	30
ItoStopF	ttcacattaatgatacgttgaattaa	15	ItoStopF2	tggttcacattaatgatacgttg	31
ItoStopR	ttaattcaacgtatcattaatgtgaa	16	ItoStopR2	caacgtatcattaatgtgaacca	32

9.2.2.3 Transformation of DH5α cells

MAX efficiency DH5α competent cells were used for the transformation, 2.3 µl of the DpnI-treated PCR solution were added to 50 µl of competent cell commercial suspension, the mixture was left 20 min on ice before being heat shocked for 2 min at 42°C. 500 µl of LB was added to the mixture back on ice, and the cells were allowed to grow for 1 h at 37°C before being centrifuged at 3000 rpm for 1 min. The supernatant was tipped off and the cells carefully resuspended in the remaining supernatant (~20 µl) and used to inoculate an LB-Amp-agar plate (0.1 mg/ml). The agar plate was incubated overnight at 37°C. Up to 3 surviving colonies were gathered and grown overnight in 10 ml LB-Amp (0.1 mg/ml), the suspension was used for further sequencing and storage of a glycerol stock.

9.2.2.4 Sequencing of the mcbA gene in transformed colonies

The pUC19 plasmid was extracted from 5 ml overnight culture of the transformed colonies with a QIAprep® Miniprep kit (Qiagen). Standard 17mer M13 forward primer was used to sequence the *mcbA* gene as a M13 site is present upstream of the *mcbA* gene. Four mutants were successfully isolated G30K, S67Stop, H68Stop, I69Stop.

9.2.2.5 Production of modified MccB17

All the mutant MccB17 were produced following the same protocol as for WT MccB17 leading to the following yields per litre of M63 glucose media: MccB17(G30K) = 0.075 mg/l, MccB17(S67Stop) = 2.6 mg/l, MccB17(H68Stop) = 4.2 mg/ml, MccB17(I69Stop) = 2.4 mg/l. As expected the yield for the Lys mutant is very low, but the other mutants are in the range of usual wild type yield ~6 mg/L.

9.2.2.6 Tryptic digest of MccB17(G30K)

Cleavage of the Lys-Gly bond was performed by incubating a mixture containing 6 µM of MccB17(G30K), 20 µg/ml trypsin, 1% DMSO in supplied trypsin buffer for 2 h at 37°C. The mixture was left for 5 min at 100°C to inactivate the trypsin. The sample was submitted to MALDI-ToF analysis and the successful cleavage was confirmed by the presence of the main peak *m/z* = 2767.83 Da corresponding to the hydrogen adduct of the expected MccB17 minus the N-term VGIG. The very weak peak of *m/z* = 3164.99 Da corresponding to the starting material MccB17(G30K) shows that the reaction was virtually complete.
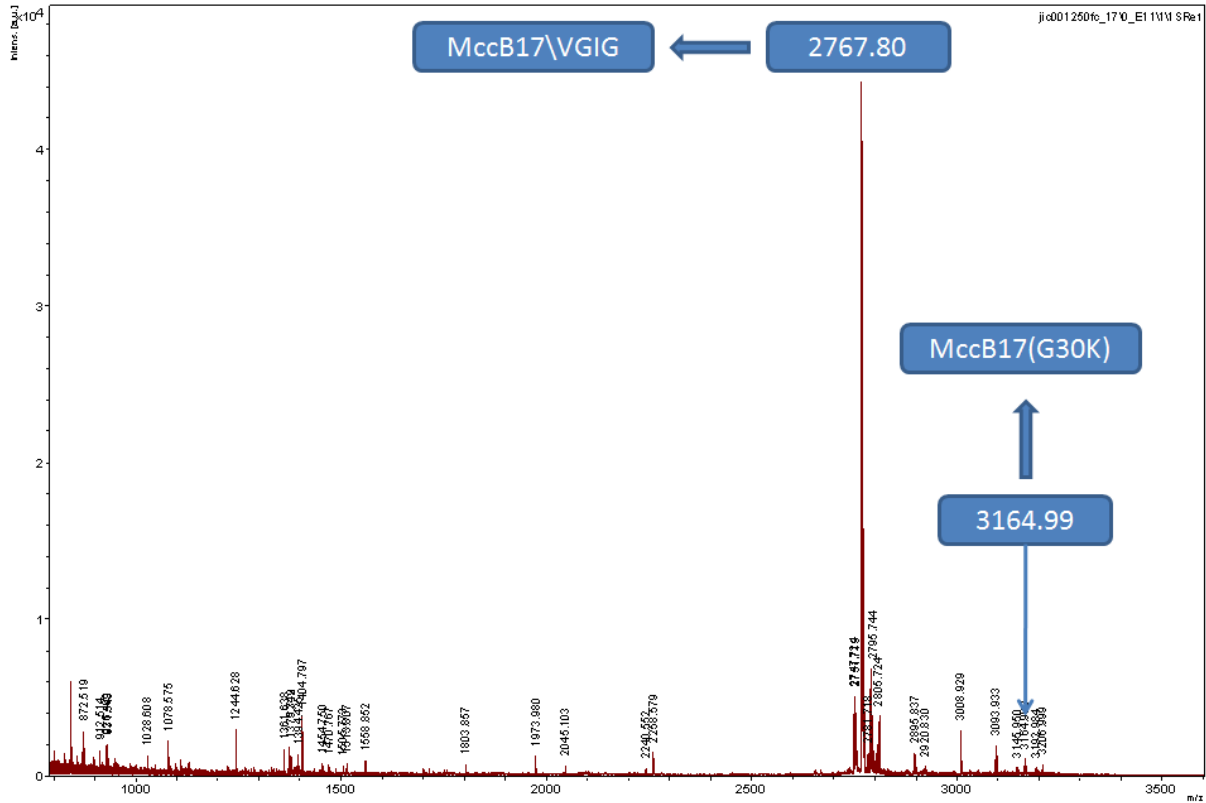
Figure 87 MALDI-ToF spectra of MccB17(G30K) tryptic digest product.

9.2.2.7 Shortened-MccB17 activity on gyrase

The four mutants were evaluated for activity on gyrase. Both inhibition of supercoiling and stabilisation of cleavage complex were evaluated using the standard assays. A moderate inhibition of the supercoiling reaction had been observed at 200 µM (4 X MccB17 IC in our assays) for the MccB17 derivatives with C-terminal modifications. By comparison the MccB17 derivative lacking VGIG from the N-terminus completely inhibits the reaction at 50 µM. MccB17 derivatives with C-terminal alterations show a definite loss of their ability to stabilize cleavage complex: at 100 µM, a moderate cleavage band appears with Mcc\I69, and none is visible for the two others; whereas for Mcc\VGIG at 50 µM, a cleavage band slightly weaker

108

than the MccB17 control is observed. The assays show that the Mcc\VGIG is able to inhibit gyrase supercoiling and stabilise cleavage complex efficiently in the same range as MccB17.
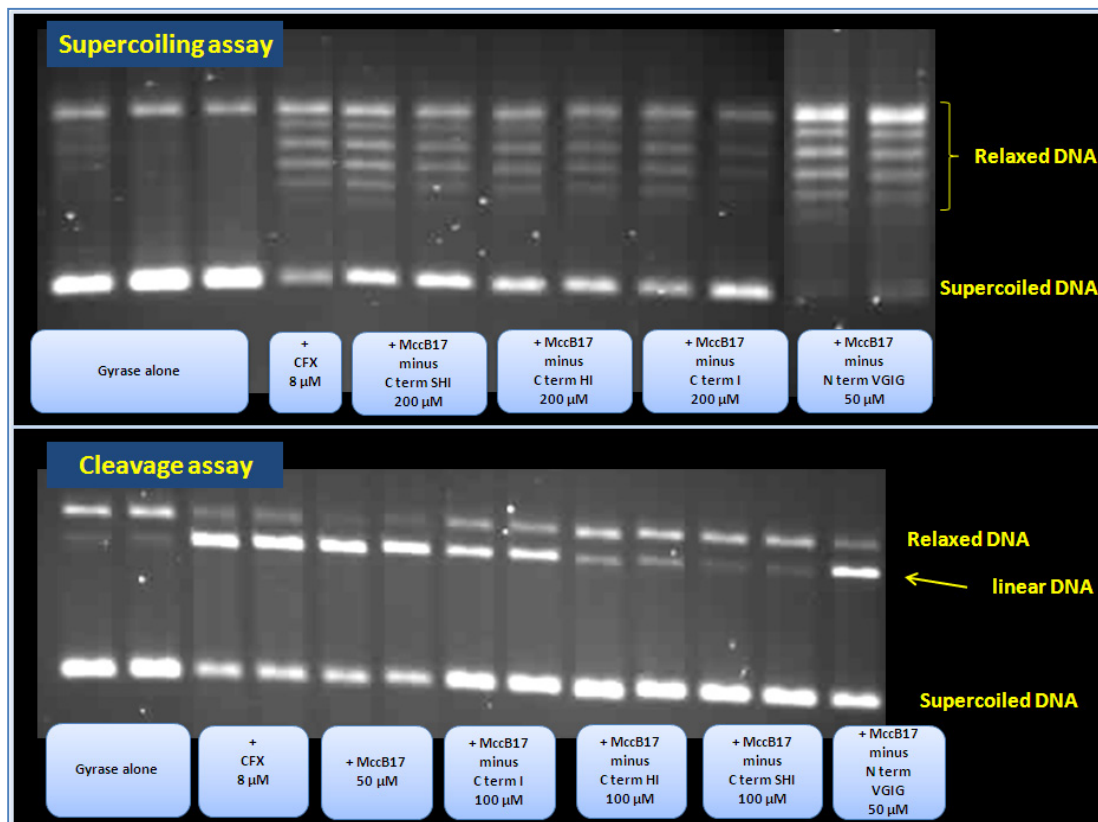
Figure 88 Evaluation of shortened version of MccB17: top gel, gyrase supercoiling assays of MccB17 derivatives lacking 3, 2, or 1 residue from the C-terminus, or 4 residues on the N-terminus Mcc\VGIG. A weak inhibitory activity is observed at 200 μM for the C-terminus-modified MccB17, whereas Mcc\VGIG had the same activity as what is expected from native MccB17 (strong activity at 50 μM). Bottom gel, gyrase cleavage assays of the MccB17 derivative lacking 3, 2, or 1 residue from the C-terminus, the band in the middle correspond to the linear DNA, a clear decrease of this band visible as amino acids are removed from the C-terminus, showing the loss of stabilisation of cleavage complex ability by these compounds. For Mcc\VGIG the activity is similar to native MccB17.

9.2.2.8   Comments

The assays show that the N-terminus-modified MccB17 is able to inhibit gyrase supercoiling and stabilise cleavage complex efficiently in the same range as MccB17, whereas any alteration on the other end of the molecule significantly reduces the activity. This evidence leads toward a polar model of the toxin where the C-terminal part of the molecule is critical for activity on gyrase when the N-terminal part is more involved in the biosynthetic process. The main question remaining is how many amino acids can be removed from the N-terminus without losing the toxic properties? Considering the C-terminus, we know that removing the

end Ile is detrimental to the activity, but what about replacing it by other amino acids? Following the same strategy it will be valuable to generate mutation of this residue with non-polar amino acids like Leucine or Valine.

10 Conclusion

This chapter began with the covering a range of experimental tools that are used to obtain and characterize MccB17. From this starting point we have shown how these tools could be exploited to generate new species, compared them to MccB17 and finally understand more about the toxin itself. Improving our understanding of MccB17 mechanism through the generation of resistant mutants has proved unsuccessful, but a better insight in the development of resistance to MccB17 has led us to develop strategies more likely to bring this approach forward. By altering the N- and C-terminal amino acids of MccB17 we have learned that the toxin has a "polar" nature: an N-terminal domain involved in its biosynthesis, and a C-terminal domain critical for its activity on gyrase. Modification of this N-terminal domain should be the starting point to generate lower molecular weight gyrase inhibitors derived from MccB17. The best approach will be to remove step by step amino acids from the N-terminus until activity is lost, we will have then reached the core of the MccB17 activity. The C-terminal isoleucine is another aspect that should be investigated, is this specific amino acid required or can it be replaced by any lipophilic residue without altering the activity? The inhibitory activity observed with MccB17 on human topo II opens the possibility of generating derivatives of MccB17 for this purpose. The fact that the toxin is inhibiting targets other than *E. coli* gyrase confirms the relevance of extending the study of MccB17 and derived compounds to other topoisomerases. We have described here that we can shorten the MccB17 molecule while keeping the inhibitory activity on gyrase and ability to stabilise the cleavage complex, in the next chapter we will bring this approach a step further by assaying the possibility that smaller fragments of MccB17 can still retain these characteristics.

CHAPTER III
Generation and evaluation of microcin B17 fragments

CHAPTER III Generation and evaluation of microcin B17 fragments

Despite its formidable antibacterial mechanism as one of the few non-quinolone stabilisers of the gyrase-DNA cleavage complex, MccB17 by itself is a poor drug. When considering the whole molecule it is important to remember that this structure is not only shaped by its antibacterial properties but also by the various enzymatic processes leading to its maturation, the necessity of its export, and evolutionary limitations. In order to identify the molecular features responsible for the antibacterial properties of MccB17, fragments of the toxin were generated and their activity assayed. The following paragraphs will describe two different approaches: chemical and enzymatic, that have been used to generate such fragments. Finally fragments spontaneously generated during MccB17 preparation will be discussed as they are kin to the fragments we are aiming to generate and isolate.

1 Alkaline hydrolysis

Preliminary results from previous work have shown that alkaline hydrolysis of MccB17 leads to a mixture of compounds that shows inhibitory activity on gyrase (Coquin 2005). Further investigation of the chemical cleavage of MccB17 will be described here as well as the various treatments used to separate the products generated.

1.1 Reported preliminary results

(Coquin 2005)

Hydrolysis carried out over seven days at 110°C with two different concentration of sodium hydroxide has been reported previously, respectively using two equivalents and ten equivalents of sodium hydroxide per peptide bond.

The use of a small excess of alkaline agent led to partial hydrolysis, the remaining fragment of MccB17 observed corresponds to the final degradation of the polyglycine from **G$_6$oztzGGQGGGtzGtz** to **oztzGGQGtzGtz,** a small amount of MW= 1700 can still be observed. The fact that the MW= 1701 fragment was the last large fragment to disappear, and that the main remaining fragments are the core fragment **oztzGGQGtzGtz** and its derivatives with various number of extra glycine, tend to prove that **oztzGGQGtzGtz** is the most stable part of MccB17, at least in alkaline conditions. This interesting observation makes one wonder if this resilience to alkaline condition is due to the chemical stability of the fragment or due to secondary structure. It would have been valuable to have information about the inhibitory activity of these fragments, but unfortunately none have been reported.

A higher excess of sodium hydroxide leads to complete destruction of MccB17 where only low molecular weight compounds can be observed, they correspond to **tz**, **oz**, **tzoz** or **oztz**, **tzozG** or **oztz+G**, and **Dtzoz**. Inhibition of supercoiling was observed with this hydrolysis mixture at 33 µM. The formulated hypothesis was that small molecules related to the heterocycles contained in MccB17 were responsible for the activity observed. As these results were preliminary and study of single MccB17 heterocyclic amino acids described in Chapter IV did not show strong inhibitory activity, the hydrolysis experiment was repeated with the purpose of first validating these observations and possibly identifying the novel compound(s) responsible for the activity in the mixture.

1.2 Validation of preliminary results

1.2.1 Hydrolysis reaction

The cleavage of the toxin was achieved by the action of ten equivalent/peptide bond of sodium hydroxide in water with 50% DMSO on 0.45 mM MccB17. The mixture was stirred at 120°C for seven days, afterwards the reaction mixture was neutralized with a hydrochloride solution 1 M before being freeze fried. The solid residue was triturated with a mixture of 10% methanol in ethyl acetate, the solution was filtered, evaporated and the residue was solubilised in DMSO in order to evaluate its effect on the *E. coli* gyrase supercoiling reaction.

1.2.2 Evaluation of inhibitory activity on gyrase

The solution used for this assay results from 7 mg of initial MccB17 that have been hydrolysed and gathered by trituration of the dry reaction mixture with 1 ml DMSO. As the real content of the mixture is unknown, the concentration will be given in equivalents of initial MccB17. The influence of the mixture on the three different reactions involving gyrase has been tested: supercoiling, relaxation and cleavage. The inhibitory activity on the supercoiling reaction of the gyrase resistant to MccB17 was tested as well.

The mixture of compounds resulting from the alkaline hydrolysis shows a strong inhibitory activity on supercoiling and relaxation by gyrase. No stabilisation of the cleavage complex could be observed and the gyrase $A_2B(W751R)_2$ is susceptible to inhibition by the hydrolysate. This suggests that the active compound of this mixture is acting by a different mechanism than MccB17. Having validated the potency of the alkaline digest, the next step was to identify the active component of this mixture.
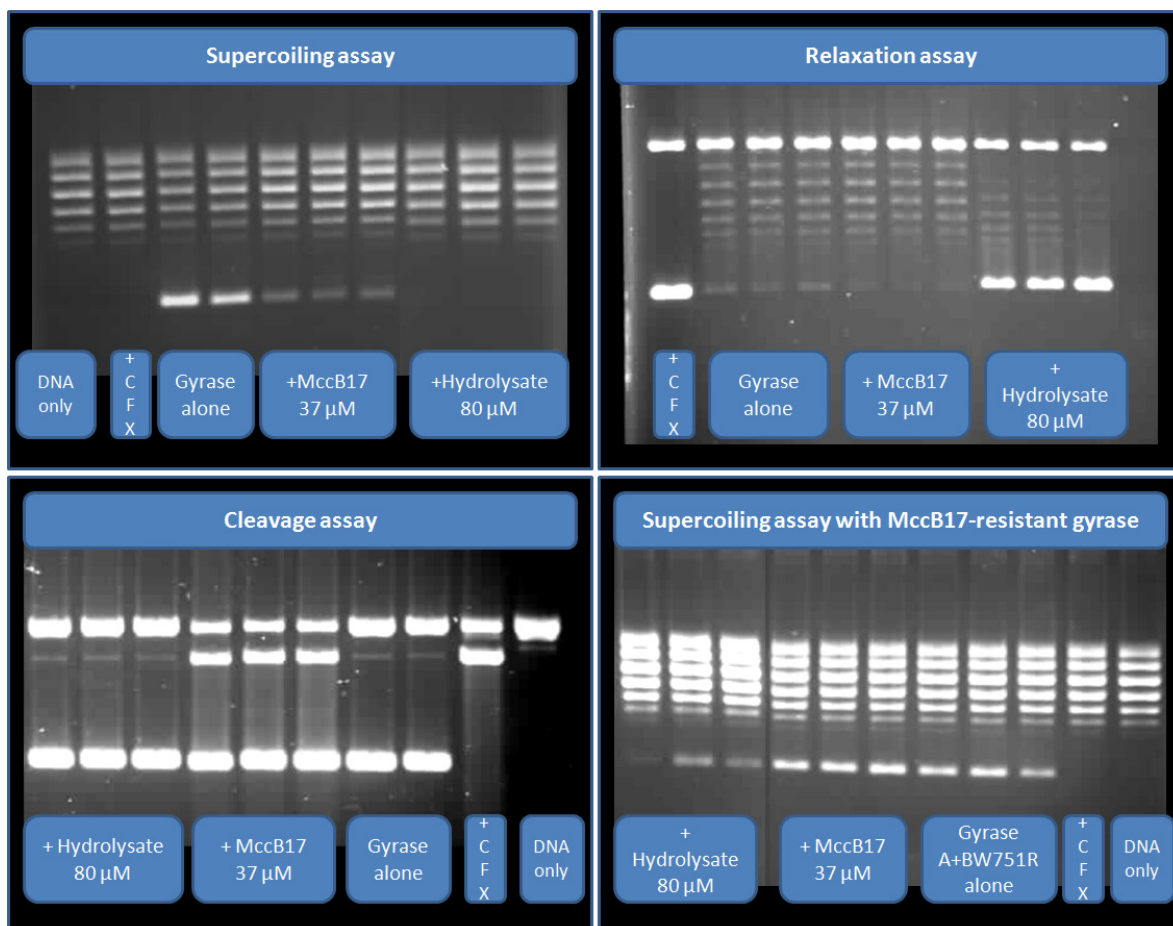
Figure 89 Evaluation of MccB17 alkaline hydrolysate activity on *E. coli* gyrase: the strong inhibitory effect of the MccB17 alkaline hydrolysate mixture on gyrase supercoiling (top left) and relaxation (top right); as well as on MccB17-resistant gyrase supercoiling (bottom right) is shown. The inability of the mixture to stabilise gyrase-DNA cleavage complex (bottom left) is also displayed. The ciprofloxacin control (CFX) is at 15 µM concentration.

1.3 Identification of active fragments

1.3.1 HPLC-MS analysis of hydrolysis mixture

The mixture was analysed on a 250x2 mm, 4 µ Polar RP column (reverse phase, pi-pi aromatic specificity) with a methanol gradient in water from 2 to 80%. Unfortunately the results showed mainly signals corresponding to very hydrophobic compounds that are very unlikely to be related to MccB17 and only a weak signal corresponding to **oz+G**, **tzozG** or **oztz+G**, and to the single heterocyclic amino acid could be observed. It is possible that the compounds we were looking for were present in too low amounts to be identified, as the trituration of the solid residue is probably not a very efficient extraction method considering the large amount of sodium chloride present. The hydrolysis was repeated in an increased scale in order to introduce liquid phase separation steps.

114

1.3.2 Separation methods

The treatment of MccB17 alkaline hydrolysis product has been improved over several experiments. We had to take in account that the species we are looking for can spread over a wide range of lipophilicity. Preparation of MccB17 described in Chapter II involved a preliminary purification step with a Sep-Pak® reverse phase column eluted with acetonitrile and water, first with 12% CH_3CN/H_2O to remove contaminants, then with 50% CH_3CN/H_2O to collect the MccB17 species. We considered using a similar method to fractionate the hydrolysis mixture; this way the sample will be desalted in the process and the fraction generated will be a less complex mixture, these two improvements should facilitate subsequent analysis. The logical next improvement was to use a gradient of acetonitrile to fractionate the mixture and identify which ones display inhibitory activity, and finally the refinement of this approach was to use a gradient of acetonitrile in water but on a preparative HPLC column. Each method was developed on a different batch of hydrolysate. The different purification methods will be described below, as well as the assays performed on the isolates from each methods, which consist of standard gyrase supercoiling assays as described in Materials & Methods. The results of the mass spectrometry analysis for all the techniques will be summarized in the final section.

1.3.2.1 *MccB17 purification method*

The dry hydrolysate residue was extracted with AcOEt/MeOH 9/1 as before. The organic extract was concentrated under vacuum and redissolved in DMSO for assays. The remaining solid was triturated with ethanol before being resuspended in water with 10% DMSO and filtered. The ethanol extract, after being concentrated, and the filtrate were kept for further analysis. The filtrate was purified on a Sep-pak® column following the standard MccB17 purification protocol described in Chapter II: both 12% and 50% fractions were collected, named respectively hyd2_12% and hyd2_50%, concentrated under vacuum, freeze dried, and redissolved in DMSO for the assays.
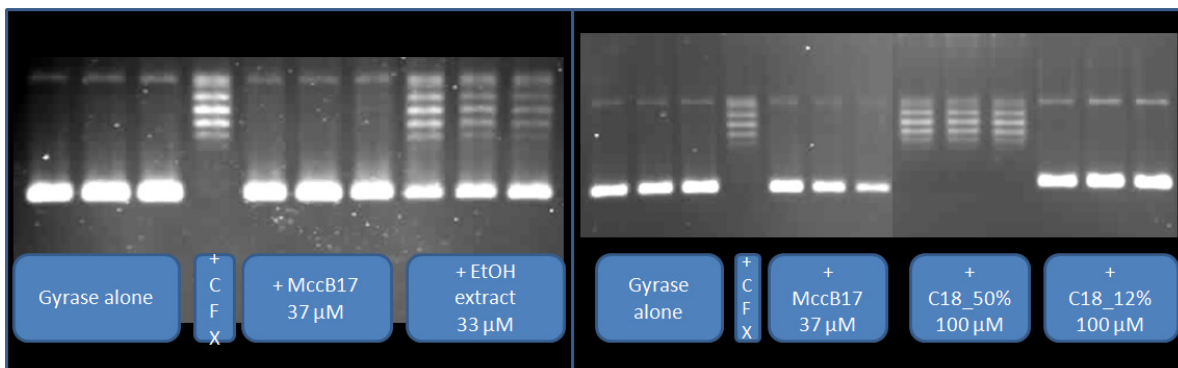
Figure 90 Supercoiling assays of the fractions from MccB17 alkaline hydrolysate: the activity of the fractions obtained from MccB17 alkaline hydrolysis is shown here, the extract from the initial solid residue with EtOH (EtOH extract), and the fraction separated on a sep-pak® with 12% or 50% CH₃CN in H₂O. The 50% CH₃CN fraction has a strong inhibitory activity, and the ethanol extract has a moderate inhibitory activity.

Two fractions having inhibitory properties with gyrase supercoiling, were isolated: the first was the ethanol extract from the dried reaction mixture, the second the 50% acetonitrile/water elution fraction from the sep-pak® column purification. Analysis of this last fraction shows that it contains species with MW around 1000 Da, this led us to further investigate separation on the reverse phase column as a method to isolate medium sized fragment of MccB17 with inhibitory activity.

1.3.2.2 Reverse phase column eluted with a gradient of acetonitrile in water

The hydrolysate after neutralization was directly loaded onto a Sep-Pak® column equilibrated with acetonitrile and water. The column was eluted with steps of 10% acetonitrile in water with 0.1% TFA from 0 to 90%, each fraction was collected, concentrated under vacuum and freeze dried. The solid residues were redissolved in DMSO in order to assay the activity on gyrase.
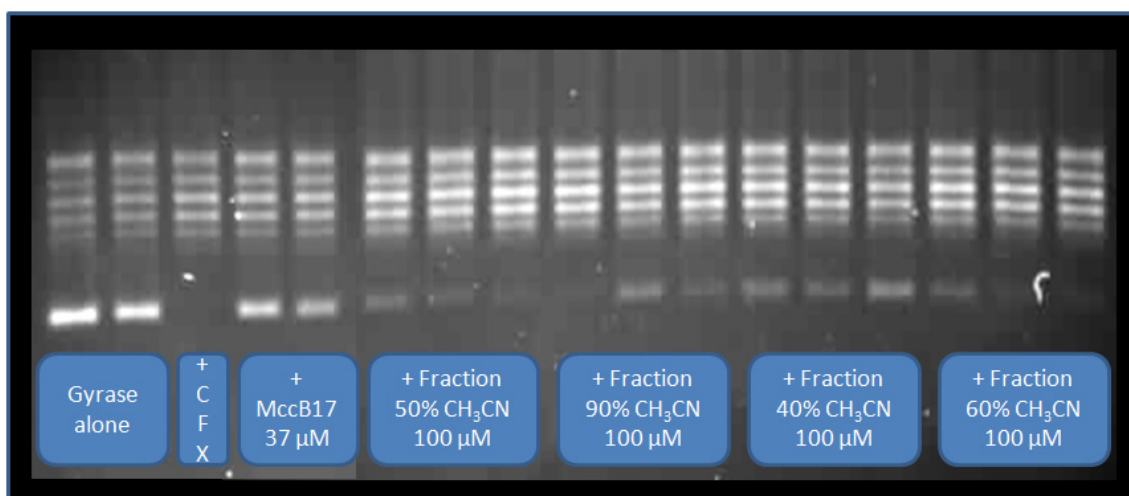
Figure 91 Activity of MccB17 alkaline hydrolysis fraction isolated from an acetonitrile gradient on a reverse phase column: this is the validation assay of the active fraction isolated from the separation by an acetonitrile gradient on a Sep-Pak® column. Only weak inhibition by MccB17 can be observed, however, ciprofloxacin (17 µM) show a strong inhibition as well as the hydrolysate fractions.

The separation was not very efficient as compounds were found in multiple fractions, but inhibitory activity was observed in the fractions 40, 50, 60, and 90%. The resort to an HPLC approach was a way of improving the separation while keeping track of what was eluting through the column.

1.3.2.3 HPLC with a gradient of acetonitrile in water

As the Sep-pak® column purification did not prove sufficient to isolate the active components of the mixture, we relied on the HPLC method to achieve this. HPLC has two advantages over the Sep-Pak® column: the resolution of HPLC column is far better, and the UV

absorbance can be followed during the elution. Following the UV absorbance is particularly advantageous as the active compounds are likely to carry heterocyclic moieties that are absorbing, specifically at 254 nm. The purification was performed on a Dionex Ultimate 3000 HPLC system with a preparative reverse phase column ACE 5 C18-300 250x21.2mm (ACE-221-2520). The elution system was acetonitrile in water with 0.1% TFA with a 4.5 ml/min flow. A gradient of 2% CH_3CN/min from 0 to 80% allows a rough separation of different fractions that would have been followed by a second run specifically adapted to the acetonitrile gradient elution window of each fraction. Unfortunately for technical reasons this experiment was not completed, and as other approaches gave promising results, this strategy was abandoned.

1.3.2.4   Results

Over the several experiments that have been conducted inhibitory activity has been consistently observed in the hydrolysis mixtures, and in some fractions, confirming that in alkaline conditions molecules with inhibitory properties on gyrase can be generated. Table 4 summarize the different the species observed with the various separation methods.

Table 4 Summary of the species observed in the various active fractions isolated from MccB17 alkaline hydrolysate

Experiment	Fraction	Mw observed	structure hypothesis
Preliminary hydrolysis	raw mixture	141.6	oz
		158.8	tz
		282.2	tzoz+G or oztz+G
"MccB17 type" purification	extract EtOH	129.0	contains sulphure, might be derived from tz
		299.2	
		356.1	previous Mw=299+Gly
	elution from sep-pack 50% CH_3CN	856.4	possibly amide form of VGIG$_{10}$
		857.4	possibly VGIG$_{10}$
		1700.4	Fragment of MccB17, V to tz2
		1156.8	
		1744.0	
Gradient of acetonitrile	40%	157.8	tz
		225.0	tzoz; oztz
		847.0	molecule contains the sequence GQGGtzGtz (Mw=654.2)
		856.3	
		857.4	
		885.2	probably related to G$_7$oztzGGQ (mw=865)
	50%	158.0	
		226.0	
		857.4	
		1028.4	possibly G$_5$oztzGGQGGtz (1006.3)+Na
	60%	856.4	
		857.4	
		1028.4	possibly G$_5$oztzGGQGGtz (1006.3)+Na
		1393.5	
		1700.6	
		3094.1	remaining MccB17
	90%	304.3	
		332.4	

Over the different experiments the heterocyclic amino acids contained in MccB17 have been consistently observed as single molecules or linked with a glycine residue; the evaluation of the heterocyclic amino acids is described in Chapter IV which will cover MccB17-related small molecules. Another set of species that was always present was the fragments with MW =

856 and MW = 857 Da, but they correspond probably to respectively $VGIG_9NHCH_2CONH_2$ and $VGIG_9NHCH_2COOH$, molecules that have been found as inactive MccB17 by-products. Unfortunately the data gathered did not lead to the identification of the active compound as no specific species were consistently observed in the active fractions. Part of the difficulty came from the fact that, in the harsh conditions being used, a wide variety of reactions can occur thus producing a very complex and variable system. Another issue was that molecules with molecular weights comprised between 75 and 3093 Da are potentially generated so we had to cross ESI and MALDI-ToF mass spectrometry analysis to cover this range. The compounds studied, similar to MccB17, showed different ionisation behaviour depending on the MS technique used for the analysis and led to different results for the same sample depending on the technique. Finally, technical issues with our HPLC column prevented us from completing our study on HPLC separation of the hydrolysis products. This strategy was not pushed forward for two reasons: first the MccB17 heterocyclic amino acids that are described in Chapter IV, have all displayed levels of activity around 400 µM apart from oxazole that shows none. This level of activity can't explain the strong inhibition observed, however it is possible that an additional glycine to one or multiple heterocyclic amino acids, increases the overall activity, but this seems unlikely to us. Therefore these derivatives have not been evaluated further, even if they might worth further studying. The second point was that the mixture generated, contrary to what had been reported in the preliminary study, did not stabilise the DNA-gyrase cleavage complex, which is the major feature of MccB17 we are interested in. Taking this into account, this strategy was abandoned in favour of a more selective way of cleaving MccB17 that gave promising preliminary results. This approach, involving enzymatic digestion, will be described in the following section.

2 Cleavage with endoprotease:

A good way to selectively cleave a peptide is to use an endoprotease that will cut the peptide bond specifically before or after a particular residue defined by the enzyme type. MccB17 aside from its specific heterocyclic moieties, does not possess a large diversity of amino acids, it is composed of 20 glycines and 9 other amino acids. With a closer look at the sequence of the toxin we can notice that amide residues are nicely distributed in the middle part of the molecule and are therefore sites of choice for selective cleavage. Two different possibilities have been considered: first the modification of asparagine and glutamine residues in MccB17 into their acid counterpart and the subsequent cleavage using endoproteinase Glu-C which is able to cut at the carboxyl of aspartic or glutamic acids residues. The second approach considered is the digestion of the native MccB17 by subtilisin, a less selective enzyme that will cut at the carboxyl of asparagine and glutamine residues but also at lipophilic residues such as isoleucine and valine thus generating more fragments in the process. Actually the difference of selectivity of the enzymes can be turned to our advantage, making it possible to compare activities of closely related fragment from the two enzyme digests. The fragments that can be theoretically generated with their respective molecular weight are described in Figure 92.
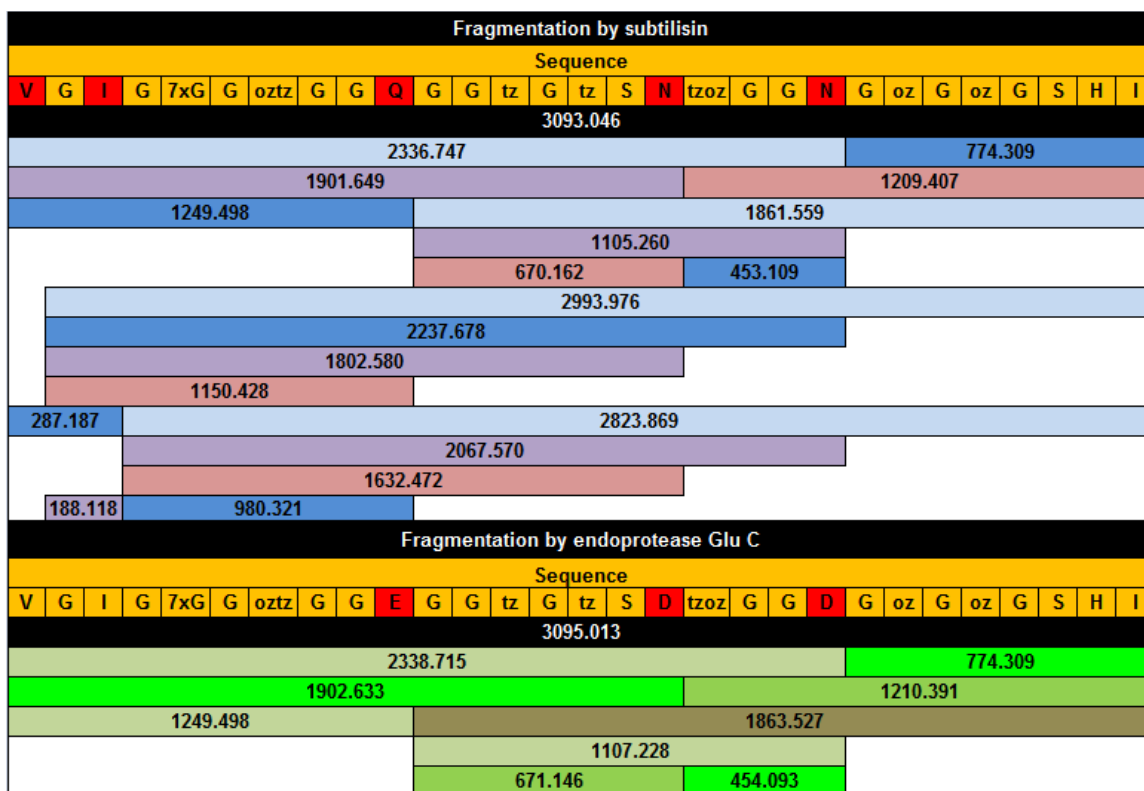
Figure 92 Potential cleavage products from MccB17 endoproteolytic digest: the top part of the figure shows the sequence of MccB17 with the cleavage site residues in red, predicted fragments from the proteolysis by subtilisin are show as coloured boxes with the corresponding MW displayed inside. Colouring is for readability only. The bottom part corresponds to the predicted fragment from endoprotease Glu-C proteolysis, using the same display.

2.1 Proteolysis reactions

2.1.1 Digestion of MccB17(N53D;N59D) by endoproteinase Glu-C

The production of MccB17(N53D; N59D) has been described in Chapter II and is available in more detail in the Materials & Methods chapter. One equivalent (w/w) of endoproteinase Glu-C was added to MccB17(N53D; N59D) in a 100 mM ammonium bicarbonate buffer (pH = 7, 10 % DMSO). The mixture was stirred at 37°C for 48 h. The solution was loaded on a Strata C18-EC QSPE reverse-phase column equilibrated with acetonitrile/water, the column was eluted respectively with water and with 50% CH_3CN in water, this second fraction was collected, concentrated under vacuum and freeze dried. The residue dissolved in DMSO was submitted to MALDI-ToF MS analysis.

2.1.2 Digestion of native MccB17 by subtilisin

Subtilisin was added to a solution containing 20 eq. of MccB17 in a 10 mM sodium acetate, 5 mM calcium acetate buffer pH = 7.5 with 10% DMSO. The mixture was incubated for 48 h at 37°C with stirring. The reaction mixture was loaded on a Strata C18-EC QSPE reverse phase column equilibrated with acetonitrile/water, the column was eluted first with water and

with 50% CH$_3$CN in water, the last fraction being collected, concentrated under vacuum and freeze dried. The residue dissolved in DMSO was and submitted to MS analysis.

2.2 Analysis of endoproteolytic mixtures

2.2.1 Endo Glu-C

The mass spectrometry spectra below (Figure 93) shows that MccB17 has not been completely digested by Endo Glu-C; there is still a significant starting material remaining (MW = 3093). Some expected fragments are present but in a very low proportion as shown in Figure 93. Fragmentations of the most intense peaks that are observed have shown that they are not related to MccB17, they are probably degradation products from the protease.
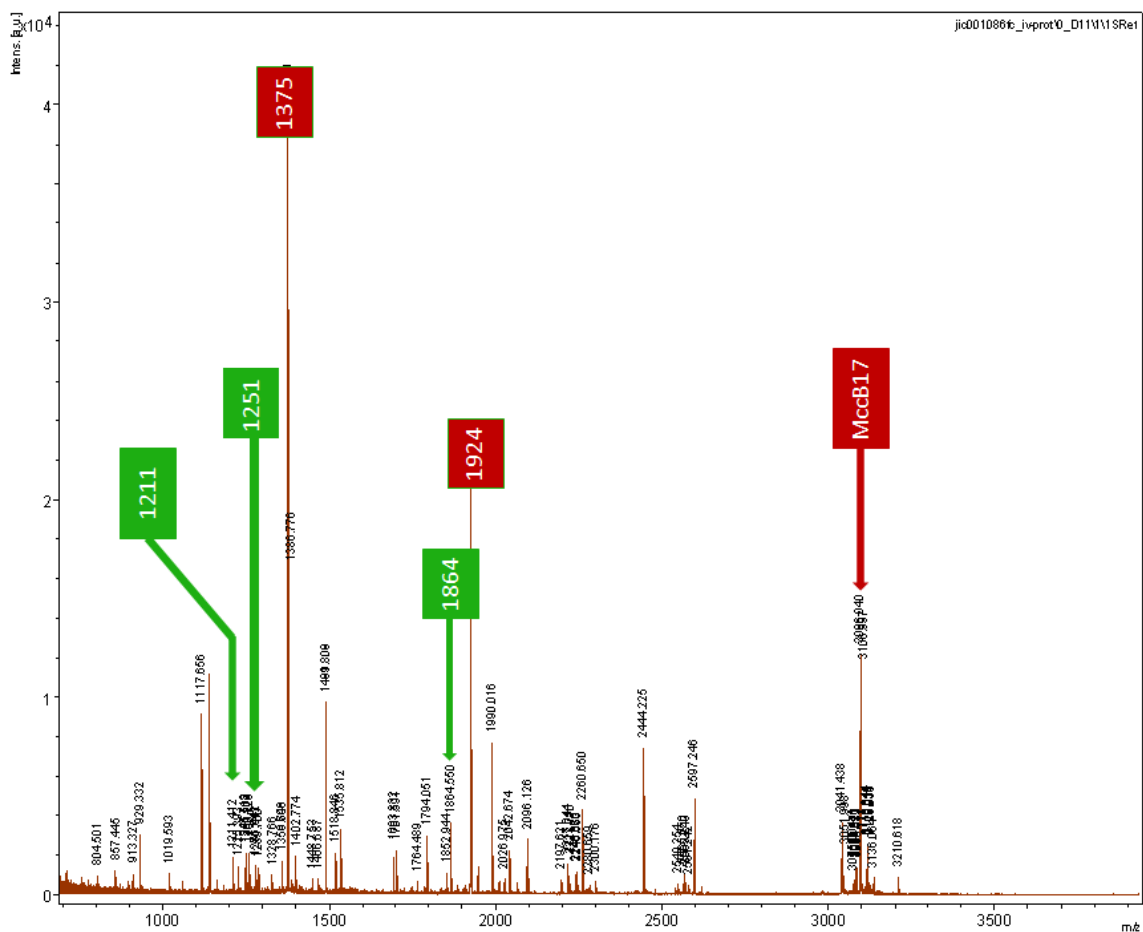
Figure 93 MALDI-ToF spectra of the endoprotease Glu-C digest mixture: fragments resulting from endo Glu-C cleavage are shown in green, their intensity is very weak. Major fragments not resulting from endo Glu-C cleavage are shown in red.

120

Fragments in endoprotease Glu C digest																												
Sequence																												
V	G	I	G	7xG	G	oztz	G	G	E	G	G	tz	G	tz	S	D	tzoz	G	G	D	G	oz	G	oz	G	S	H	I
3095.013																												
2338.715																		774.309										
1902.633																1210.391												
1249.498								1863.527																				
				1107.228																								

Figure 94 Fragments present in the endo Glu-C digest: the MccB17 sequence is shown in orange with the cleavage sites in red. All the potential fragments are shown in the figure as boxes with the corresponding MW written inside, the fragments present in the digest are shown in green, whereas the fragments in grey are not present. Only small amount of the expected fragments were present in the digest.

2.2.2 Subtilisin

The MALDI-ToF analysis of the purified fraction reveals that the reaction is complete, as the signal from initial MccB17 is negligible. Five of the expected fragments can be identified on the spectra: MW = 981; 1106; 1210.5 ; 1632.5; and 1863; however the most intense signal observed comes from the MccB17 degradation product Mw = 1393 (Figure 95). The peak at 923 can result from a loss of a glycine residue by the fragment of Mw = 980. The fragment corresponding to these molecular weights are summarized in Figure 96.
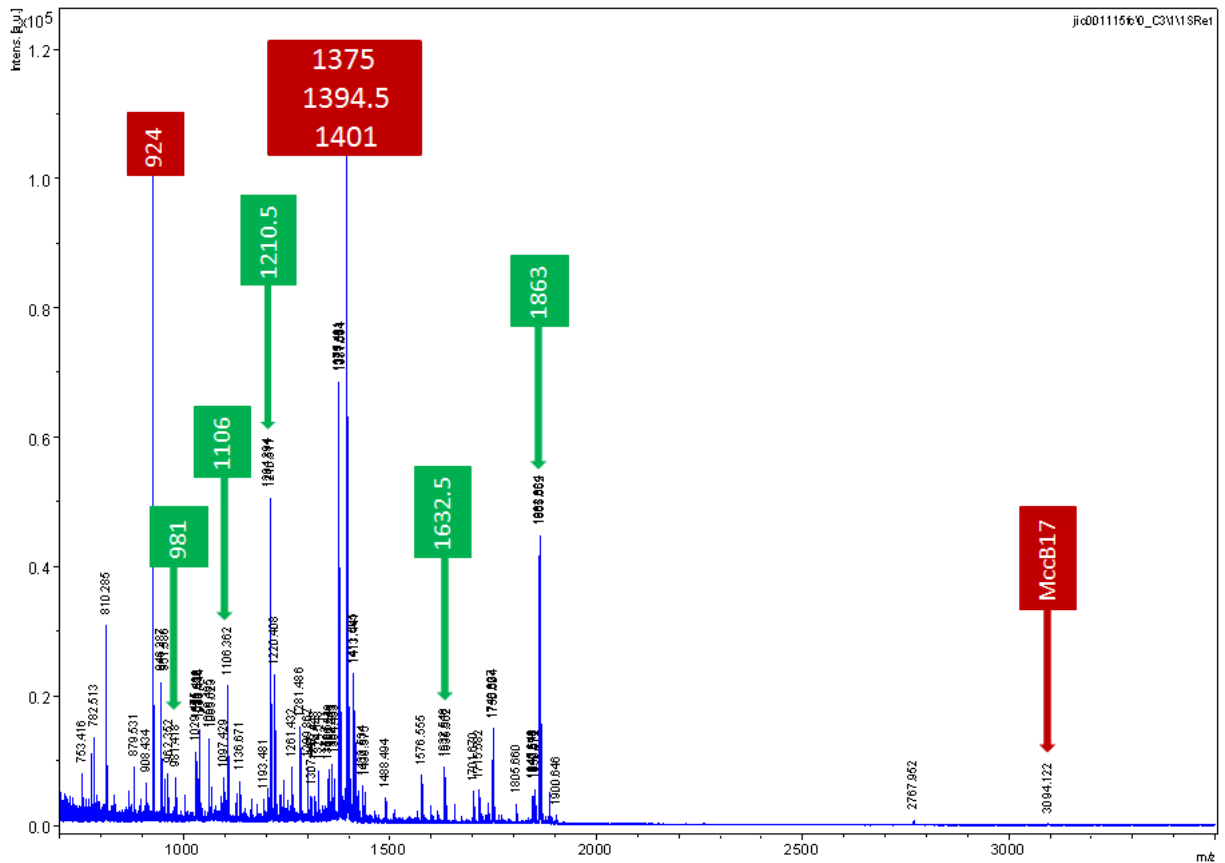
Figure 95 MALDI-ToF spectra of the subtilisin digest mixture: fragments resulting from subtilisin cleavage are shown in green. Major fragments not resulting from subtilisin cleavage are shown in red.

121

Fragments in subtilisin digest

Sequence

V G I G 7xG G oztz G G Q G G tz G tz S N tzoz G G N G oz G oz G S H I

Mw=3093.045633

Fragment	MS spectra % intensity
2336.747 / 774.309	
1901.649 / 1209.407	1% / 45%
1249.498 / 1861.559	39%
1105.260	17%
670.162 / 453.109	
2993.976	
2237.678	
1802.580	
1150.428	
287.187 / 2823.869	
2067.570	
1632.472	7%
188.118 / 980.321	5%
923.395 / 1410.595	85%
? / 1393.571	100%

V G I G 7xG G oztz G G Q G G tz G tz S N tzoz G G N G oz G oz G S H I

Figure 96 Fragments present in the subtilisin digest: the MccB17 sequence is shown in orange with the cleavage sites in red. All the potential fragments are shown in the figure as boxes with the corresponding MW written inside, the fragments present in the digest are shown in green, with the brightness of the colour corresponding to the intensity of the peak in the MS spectra. In grey, are the expected fragments that are absent. In yellow are fragments of MccB17 present in the digest but not resulting from subtilisin cleavage.

2.2.3 Evaluation of digests activity on gyrase

Solutions of the two proteolysis mixtures in DMSO were used to assay the activity on gyrase. The mixture obtained from proteolysis with subtilisin showed inhibitory activity on supercoiling at a minimal concentration of 33 µM.
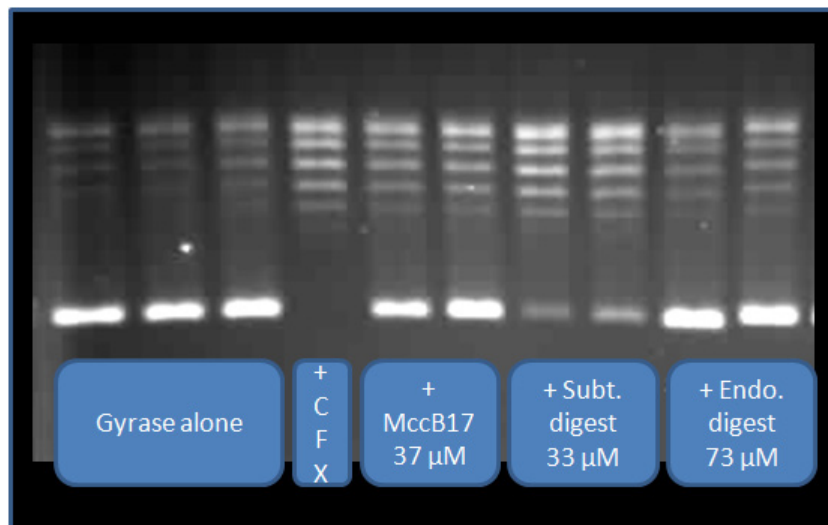
Figure 97 Supercoiling assays of the proteolytic digests of MccB17: the mixtures obtained by digesting MccB17 with subtilisin (Subt. digest) and endo Glu-C (endo digest) were evaluated for their inhibitory activity on gyrase supercoiling. Only the subtilisin digest inhibits the supercoiling reaction.

2.2.4 HPLC analysis of the mixture

The proteolysate was analysed on a Primesphere 5μ/300 Å/4.8 mm X 250 mm analytical HPLC column. 0.86 mg of the proteolysis residue was diluted in 200 μl of 10% CH$_3$CN/H$_2$O and used as a stock solution. The conditions were optimised to separate the components of the mixture using a 1/300 dilution of the stock solution in 5% CH$_3$CN/H$_2$O/0.1% TFA. A gradient of 0.66 % acetonitrile/min gave a good resolution of the peaks. A dilution of 1/30 the stock solution in 5% CH$_3$CN/H$_2$O/0.1% TFA was used for the purification, fractions were collected every minute from 10 to 60 min, and concentrated under vacuum. Fractions that were evaluated for inhibitory activity on gyrase supercoiling were named A to Q and are shown on Figure 98. Unfortunately not enough material was available to assess the activity on gyrase. The experiment was repeated on a bigger scale.

Fraction	Mw observed	Fraction	Mw observed
A	662.33; 1178.53; 612.94	J	1394.47; 1393.47; 1410.48;1392.48
B	923.32; 566.95	K	1861.55; 1700.57; 1393.46; 1747.51
C	809.20; 923.32; 663.32	L	907.43; 1393.47; 763.38; 1209.62; 1151.59; 795.44; 1861.56; 2766.8
D	781.43; 752.37; 694.25; 857.43	M	950.52; 879.48; (1376.46)
E	878.45; 662.32; (1576; 1364; 1307)	N	950.51; 922.42; (1376.43)
F	1374.37; (662.30; 774.31; 1219.30; 1059.41; 1105.26; 1631.43)	O	893.5;
G	662.31; (1028.39; 1374.38)	P	710.38; 893.52; 891.50
H	(662.32; 1209.41; 1249.50)	Q	751
I	662.32; 1209.41; 1410.49; (1249.50)		

Figure 98 Purification of the subtilisin digest of MccB17: the top figure is the trace from the HPLC purification, letters A to Q have been associated to each fraction collected. The bottom table shows the MW observed with MALDI-ToF MS for each fraction. The MW in red represents fragments expected from subtilisin cleavage. In green are fragments related to MccB17 which have been identified, but which are not resulting from cleavage by subtilisin.

123

2.3 Identification of the active component of Subtilisin digest

2.3.1 Scaling up the digest

As the first results were encouraging, the same reaction was planned on a bigger scale in order to separate and evaluates the components from the mixture. Unfortunately the experimental conditions at this stage led to a large amount of precipitate that hindered the reaction and reduced dramatically the yield. Subtilisin is used as a catalyst in organic solvents, it can retain some its activity in such conditions, a certain tolerance to DMSO has been reported: at 50%

Table 5 HPLC program for the purification of the subtilisin digest.

Program	t	% A
flow: 0.5 ml/min	0	5
Eluent A: CH_3CN, 0.1% TFA	5	5
Eluent B: water, 0.1% TFA	65	45
	70	90
	75	90
	76	5

DMSO concentration, the enzyme retains half of its protease activity (Flynne 2008). Therefore, the DMSO concentration was increased to 50% in order to circumvent this solubility problem.

2.3.2 Proteolysis in 50% DMSO: MccSub50%

2.3.2.1 Proteolysis reaction

MccB17 at 180 µM in a buffer containing 42 mM potassium phosphate, 1.7 mM sodium acetate, 0.8 mM calcium acetate and 50% DMSO at pH=7.5. 1.1 mg of subtilisin in the same buffer without DMSO was added to the mixture. The reaction mixture was incubated for 48 h at 37°C. The sample was diluted 1/5 in water before being loaded on a 20 ml Oasis® HLB reverse-phase column equilibrated with 50 ml water and 50 ml acetonitrile. The column was eluted with 60 ml water and 75 ml 50% CH_3CN/H_2O and this last fraction was collected, concentrated under vacuum and freeze dried. The residue was diluted in DMSO. The activity of the solution was validated using a gyrase supercoiling assay, its composition was checked with MALDI-ToF MS.

2.3.2.2 Characterisation of MccSub50%

The activity of the MccSub50% on gyrase supercoiling was assayed using the standard assay method, strong inhibitory activity was observed at 100 µM (equivalent MccB17).

The MALDI-ToF analysis of the MccSub50% shows that the mixtures generated in 10% and 50% DMSO are significantly different; Figure 100 show a comparison of both spectra with the expected fragments highlighted. In the 10% DMSO reaction, the most intense peak was the expected fragment Mw = 1861.5 and nothing was present at a higher molecular weight. At 50% DMSO, new fragments corresponding
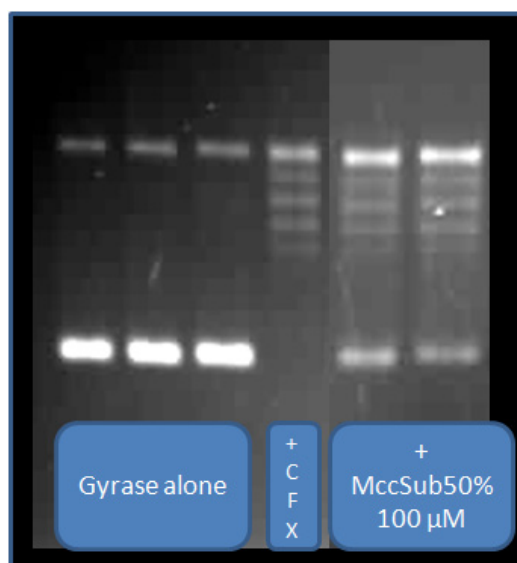
Figure 99 Activity of the MccSub50% mixture: the inhibitory activity of the mixture resulting from the subtilisin digest of MccB17 in a 50% DSMSO environment is shown on the gel. Ciprofloxacin control (CFX) is at 8 µM concentration.

124

to Mw = 2767.81 and Mw = 2258.61 appeared as the main fragments, Mw = 1862.5 and MccB17 (Mw = 3093.03) were also observed as before, but with a lower intensity. An improvement brought by the new conditions is that the level of MccB17 degradation by products around 1400 Da had significantly decreased compared to the first experiment where they were the strongest peaks. The compounds with Mw = 2767.81; Mw = 2258.61 seems to be MccB17 degradation products as they are not resulting from any expected specific cleavage by the protease. As the mixture contained MccB17 fragments of interest and displayed inhibitory activity on gyrase, we proceeded to the HPLC purification.
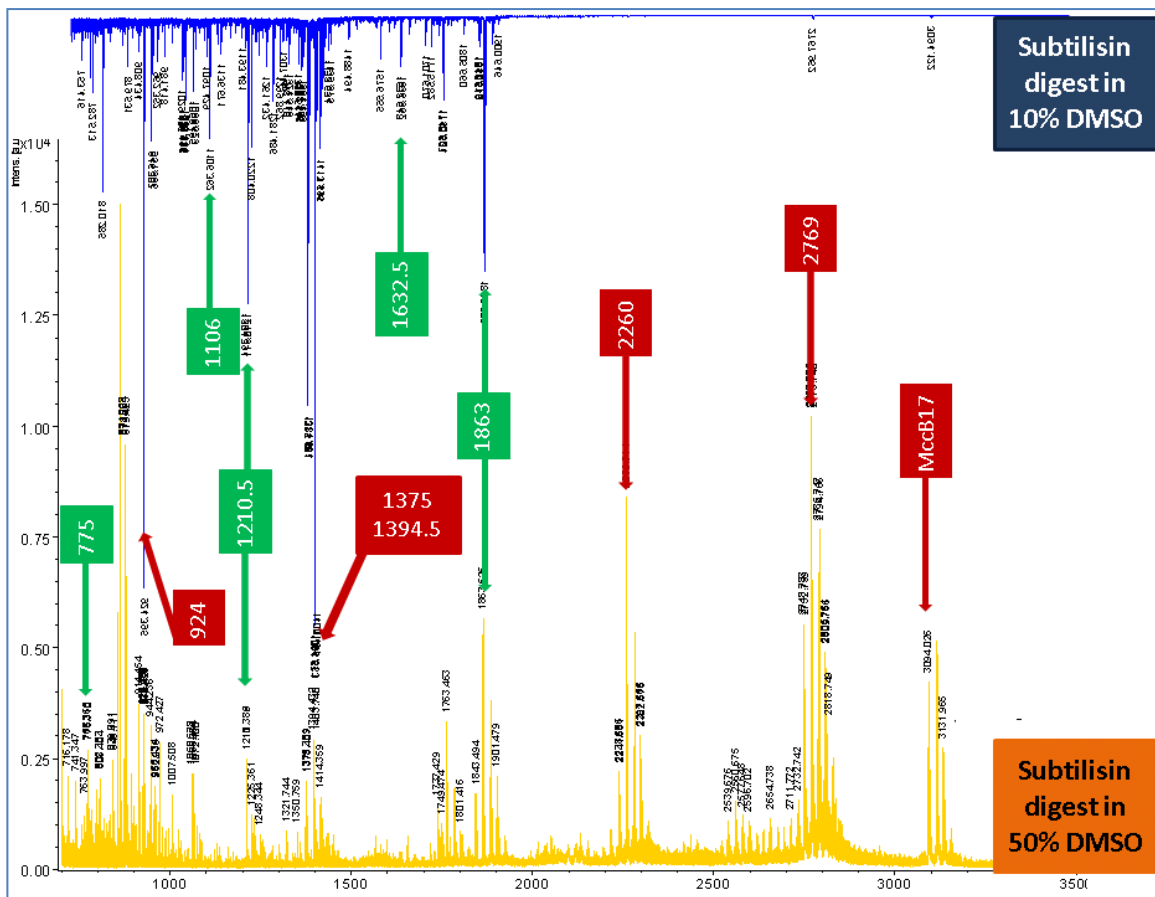
Figure 100 Comparison of MccB17 subtilisin digest in presence of 10% and 50% DMSO: Maldi-Tof spectra of MccB17 subtilisin digest in 10% DMSO (top) and 50% DMSO (bottom) are aligned for comparison. The increase of DMSO percentage leads to a decrease of the enzyme activity (reaction not complete, MccB17 present) and the appearance of new species unrelated to subtilisin cleavage. However the production of MW=1375, and 1394.5, which do not result from subtilisin cleavage is diminished.

Fragments in 50% subtilisin digest

Sequence

| V | G | I | G | 7xG | G | oztz | G | G | Q | G | G | tz | G | tz | S | N | tzoz | G | G | N | G | oz | G | oz | G | S | H | I |

Mw=3093.045633

2336.747 | 774.309

1901.649 | 1209.407

1249.498 | 1861.559

1105.260

670.162 | 453.109

2993.976

2237.678

1802.580

1150.428

287.187 | 2823.869

2067.570

1632.472

188.118 | 980.321

2766.847

6XG | 2258.604

| V | G | I | G | 7xG | G | oztz | G | G | Q | G | G | tz | G | tz | S | N | tzoz | G | G | N | G | oz | G | oz | G | S | H | I |
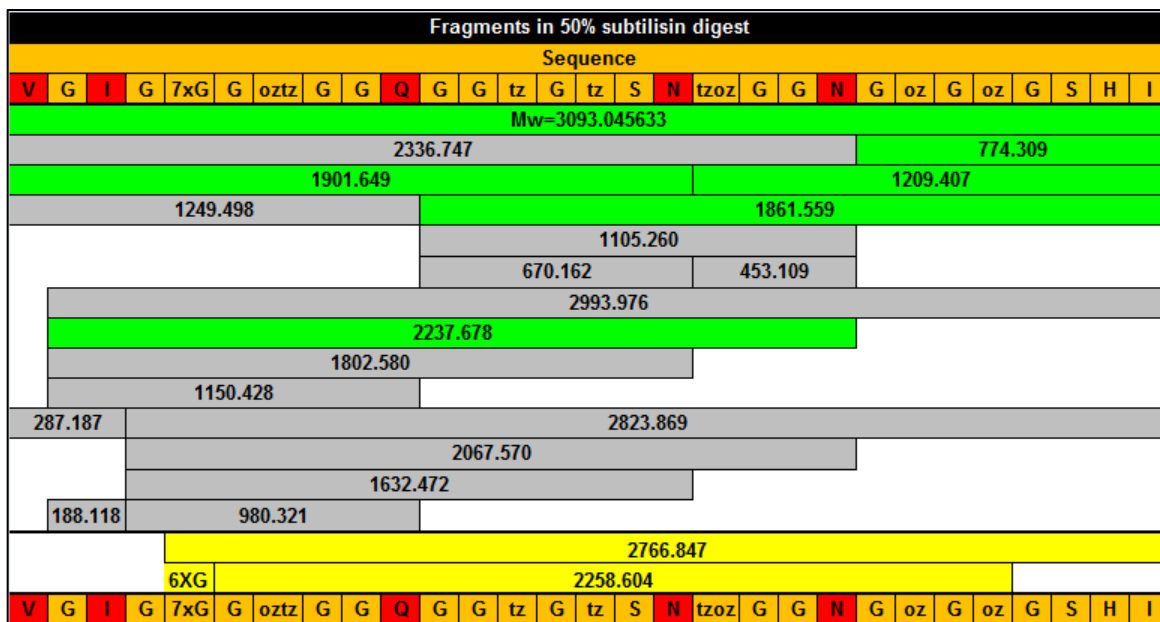
Figure 101 Fragments present in the digest of MccB17 by subtilisin in 50% DMSO (MccSub50%): in orange at the top and bottom, the sequence of MccB17 with the cleavage site in red. The fragments present in the proteolysate resulting from subtilisin cleavage are shown in green boxes with the related MW inside. In grey the expected fragments that are absent in the proteolysate. In yellow the fragment unrelated to subtilisin cleavage but present in the mixture.

2.3.2.3   HPLC separation:

Mass spectrometry analysis shows that the mixture generated in higher DMSO concentration was slightly different from the first experiment and, as a consequence, displayed a different HPLC profile. The same HPLC column was used with the conditions described in 2.2.4 modified to improve the profile of the new subtilisin digest. A gradient of 0.5% CH$_3$CN/min yielded a better resolution and thus was selected for the purification; the conditions are detailed in Table 6 on the right. As some MccB17 was present the sample, a MccB17 control was run beforehand to evaluate in which fraction it should be expected; Figure 102 shows the HPLC profile of the proteolysis mixture as well as MccB17's for comparison.

Table 6 HPLC program for subtilisin digest separation

Program	t	% A
flow:0.5 ml/min	0	5
Eluent A: CH$_3$CN, 0.1 % TFA	5	5
Eluent B: water, 0.1% TFA	16	16
	36	26
	50	40
	55	90
	60	90
	61	5
	80	5
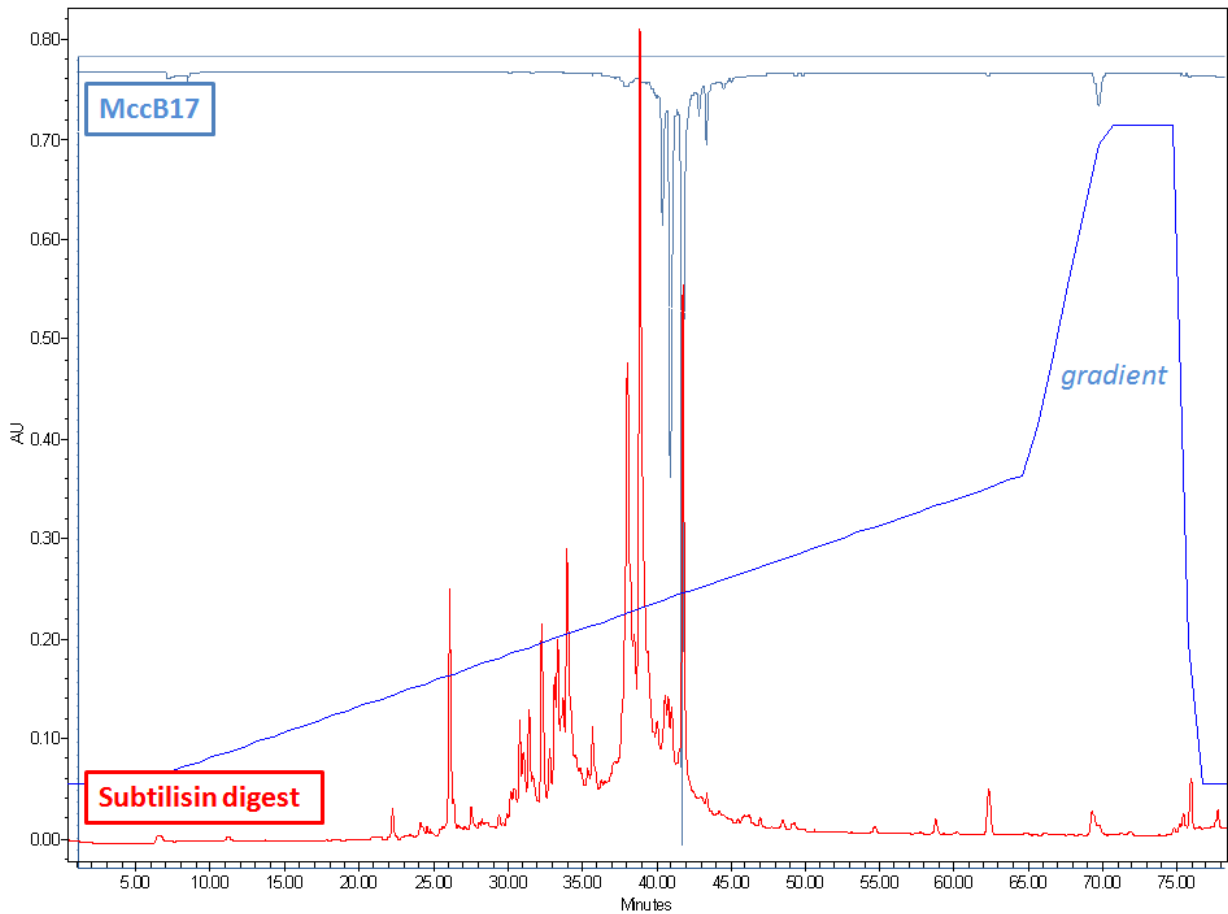
Figure 102 Separation of the MccB17 digest by subtilisin in 50% DMSO: the HPLC trace at 254 nm is shown at the bottom in red. For comparison, the HPLC trace of MccB17 in the same HPLC conditions is shown in blue at the top.

Fractions were collected every minute from t = 18 to 48 min, and concentrated under vacuum. Figure 103 below shows a zoom of the HPLC trace with the fraction numbers and the amount of material isolated.

127
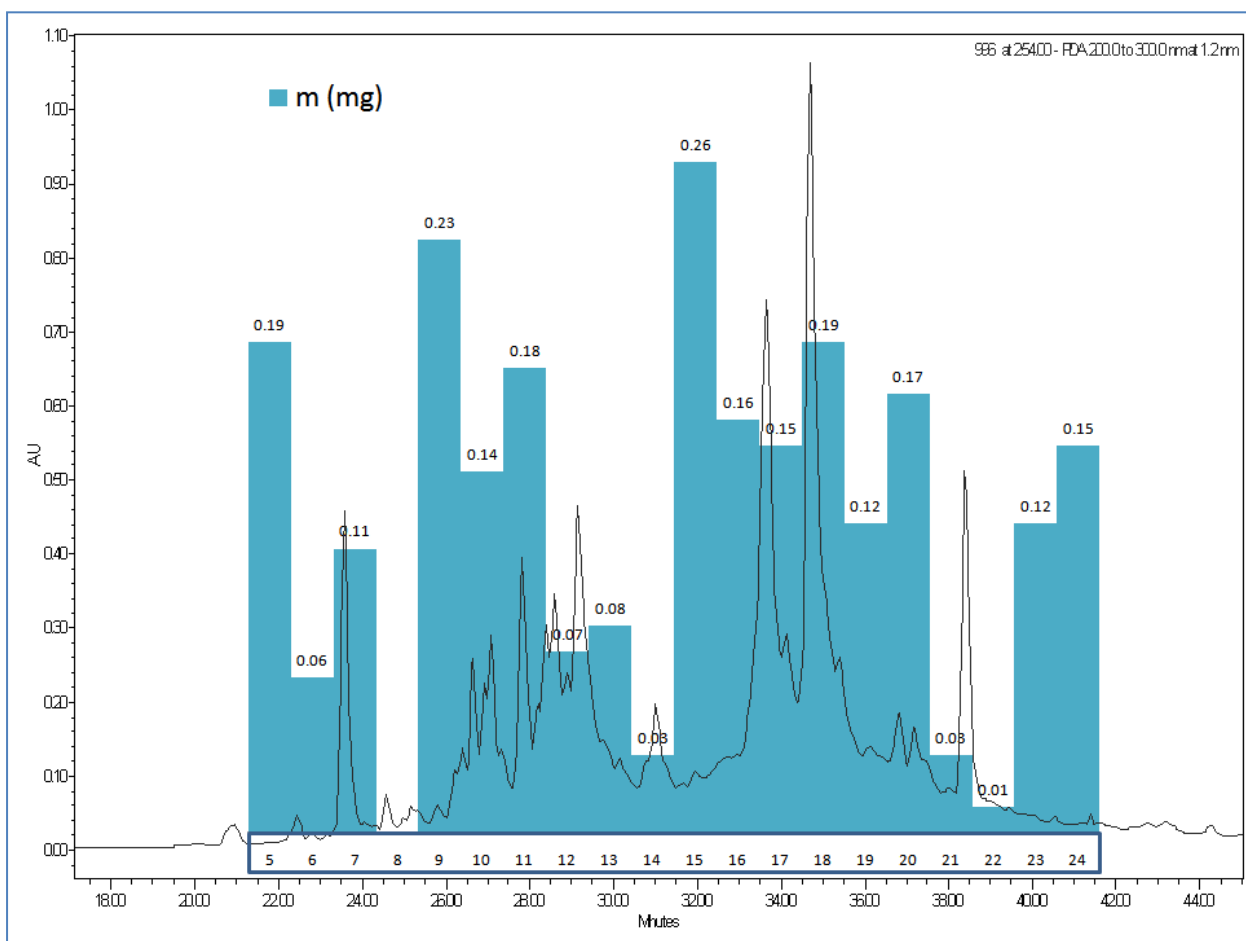
Figure 103 Quantification of the MccSub50% fraction isolated: the HPLC trace of MccB17 proteolysis by subtilisin in 50% DMSO is shown with the amount of material isolated from each fraction overlaid as blue bars. The weight of the fraction is shown at the top of the blue bar in mg.

As the quantity of the different fractions collected was very low, the residues were redissolved in 10 µl DMSO, the minimum volume allowing the recovery of the residues. The activity on gyrase was therefore assayed on solutions with concentrations ranging from 0.3 to 6 mM.

2.3.2.4 Analysis and evaluation of MccSub_50% HPLC fraction

The HPLC fractions were assayed using both *E. coli* gyrase supercoiling and cleavage assays. The assays were conducted as described in Materials & Methods with the following changes: 2 µl of the tested HPLC fraction solution was added instead of 1 µl leading to a final DMSO concentration of 6.6 %, and the reaction time was extended to 2.5 h to compensate the slowing down effect of increased DMSO concentration in the reaction. The gels assays are detailed in Figure 104 and the quantification of the gel is shown in Figure 105. Inhibitory activity on gyrase supercoiling over 30% was observed for fractions 17, 18, 19, 21, 22, 24, among them only 18, 21 and 22 were stabilizing the DNA-gyrase cleavage complex.
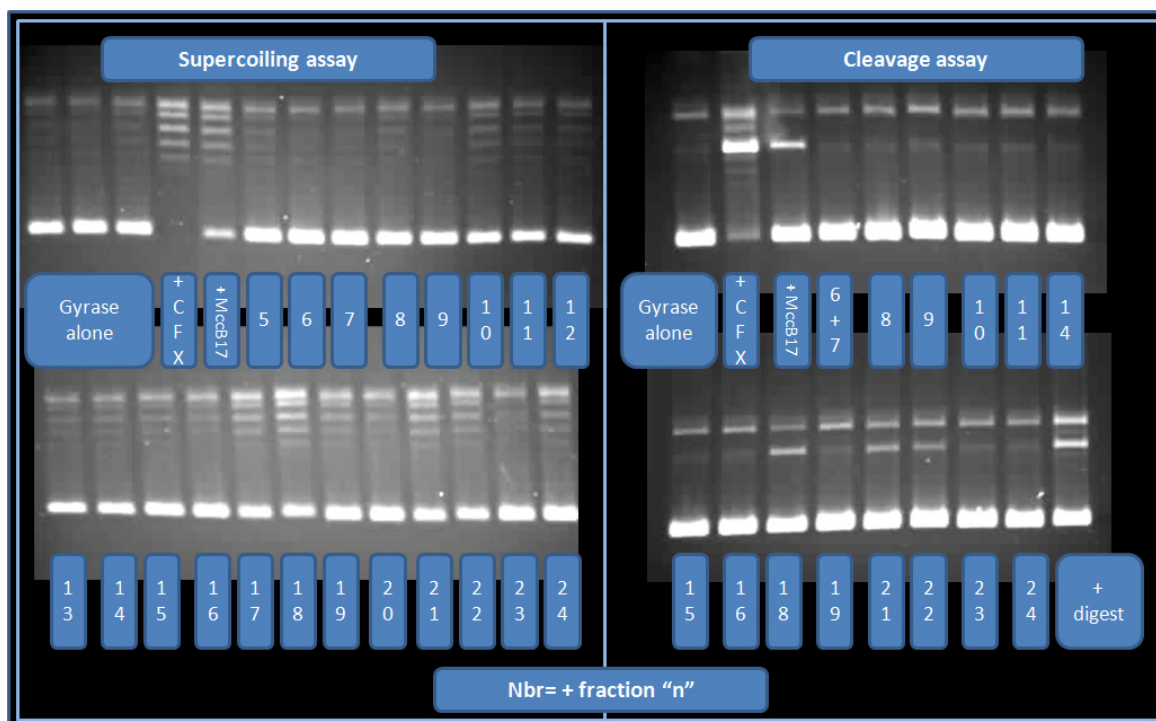
Figure 104 Evaluation of HPLC fractions from MccSub50%: supercoiling and cleavage assays. The numbers displayed on the gel correspond to the fraction as shown on Figure 15. The effect on supercoiling by gyrase, is shown on the left side, and the stabilization of the gyrase-DNA cleavage complex on the right side. Fraction 18 is of particular interest due to its activity on both supercoiling and cleavage. It is also important to note that fraction 21 and 22 contains MccB17.

Fraction 5 to 24 were submitted to MALDI-ToF MS analysis, the fragments observed in each fraction linked to the activity on supercoiling displayed by the fraction are detailed in Table 7, the fragments expected from the proteolysis are in bold, and the intensity of the corresponding peak compared to the main peak of the fraction are in blue.
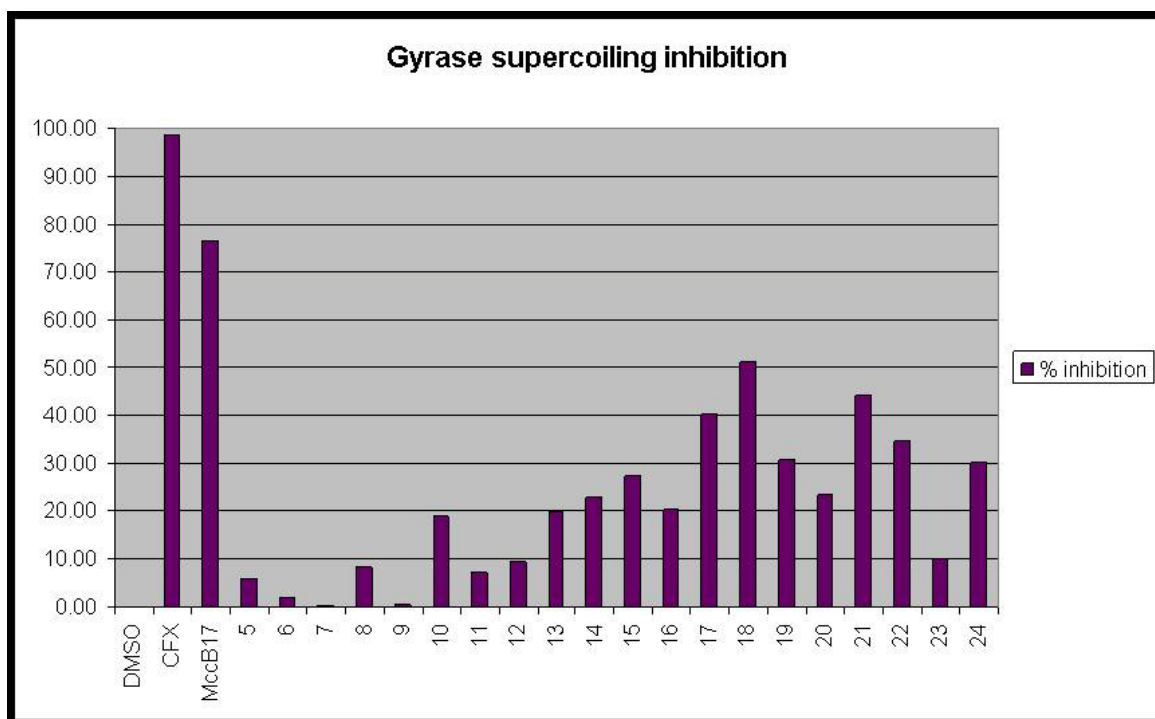
Figure 105 Quantification of the inhibitory activity of the HPLC fraction of MccB17 subtilisin digest in 50% DMSO: this is a bar chart showing the percentage of inhibition of gyrase supercoiling by the various fractions isolated by HPLC from the MccB17 subtilisin digest. The quantification was done using Genetools from Syngene. "DMSO" point correspond to the gyrase alone control, CFX is the ciprofloxacin control, and the numbers correspond to the associated HPLC fraction.

We can see from Table 7 that fractions 21 and 22 contained mainly MccB17 which is a good blind internal control for our method. Fraction 18 contains mainly two species MW = 950 and 2768; 950 is found as well as the main component of fraction 19 which display a lower inhibitory activity and no cleavage stabilization, so this suggest MW = 2768 as the active species. This fragment corresponds to MccB17 lacking the first four amino acids: MccB17\VGIG, the MS fragmentation of the structure was in agreement with this hypothesis. In the context of isolating a new antibacterial structure this result was disappointing as the fragment isolated is very close to MccB17 and thus will probably display physical properties very similar to MccB17 and so be unsuitable for therapeutical purpose. On the other hand the fact that the lost of these N-terminal amino acids still leads to a compound displaying inhibitory activity on gyrase supercoiling and stabilisation is significant information about MccB17 itself, indeed most of the modifications carried out on MccB17 in the literature tend to diminish significantly its activity on gyrase, the stabilisation of cleavage complex being the most sensitive property. This discovery inspired the mutagenesis work on MccB17 N- and C-termini that is described in Chapter II.

Table 7 Content of HPLC fractions isolated from MccSub50%: for each fraction, are shown the main species observed by MALDI-ToF MS (in black). The fragments expected from subtilisin cleavage are shown in bold. The intensity of the corresponding species is shown in blue, the main peak is use as a reference (value = 1), others are shown as a fraction of the main peak (i.e. 0.4 is 40% of the main peak intensity).

Fraction	Mw (% intensity)	% inhibition SC
5	979.29 (1); 1217.40 (0.4)	6
6	923.28 (1)	2
7	923.28 (1)	0
8	1233.38 (1); 1176.36 (1); 809.19 (0.9); 905.29 (0.8); 923.30 (0.8)	8
9	1575.45 (1); 1217.43(0.4); 1652.45 (0.3)	1
10	1631.43 (1); 1374.36 (0.8); 1575.43 (0.6); **1105.25** (0.5); 1219.29 (0.3)	19
11	**774.3** (1); 1374.35 (0.9); 1396.33 (0.5); 1714.44 (0.4)	7
12	2537.65 (1); 1028.36 (0.3)	10
13	784.47 (1); **1209.39**(0.6); 2538.64 (0.4)	20
14	1410.45 (1); **1209.38** (0.6); 1210.36 (0.5); 1394.45 (0.4); 1694.40 (0.3)	23
15	1393.44 (1); 699.20 (0.7); 1165.65 (0.6); 1990.47 (0.5); 2517.60 (0.5)	27
16	**1861.53** (1); 1375.43 (0.4); 1747.48 (0.3); 1393.44 (0.3)	20
17	1862.50 (1); 1393.43 (0.9); 2767.71 (0.8); 1415.40 (0.6); **1861.51** (0.5)	40
18	2767.72 (1); 949.45 (0.7); 987.40 (0.3)	51
19	949.45 (1); 971.43 (0.7); 2258.59 (0.2)	31
20	2747.75 (1); 2758.68 (1)	23
21	3092.96 (1); 2747.72 (0.2)	44
22	3092.96 (1); 2240.56 (0.5)	35
23	1649.79 (1); 1003.58 (0.6); 902.48 (0.4); 984.53 (0.3)	10
24	984.53 (1); 1379.80 (0.6); 1649.78 (0.6); 1022.48 (0.6); 1349.75 (0.5)	30

In the first subtilisin digest experiment this MccB17\VGIG fragment was not present and so could not account for the activity observed, this means that there was in the initial mixture a different active compound. The assays on MccSub50% fraction have shown some weak inhibitory activity that could not be validated and some of the fractions isolated contained a really small amount of material. So we considered repeating the experiment under conditions closer to what has been used initially; the purification process developed for MccSub50% will be used on the new proteolytic digest as it has proved successful. Carrying out the HPLC purification on two different mixtures had improved our understanding of the elution properties of the different fragments. Figure 106 shows the comparison of MccSub1 and MccSub50% HPLC purification traces with the species identified that will be useful markers for future purification.
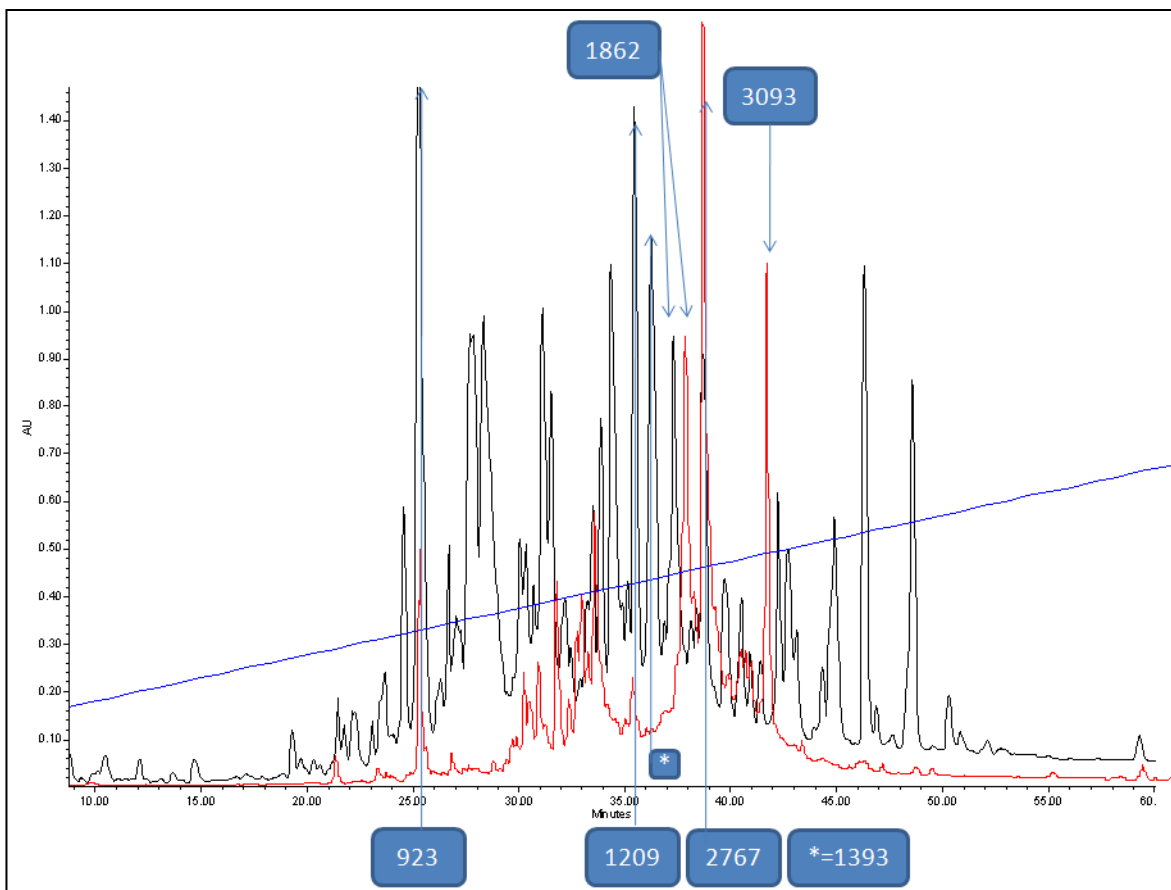
Figure 106 Comparison of HPLC purification of MccB17 proteolysis by subtilisin in 10% and 50% DMSO: traces from the HPLC purification of the digest of MccB17 by subtilisin, in black is the trace of the first digest in 10% DMSO (MccSub1); in red is the trace of the digest in 50% DMSO (MccSub50%).

2.3.3 Proteolysis in 20% DMSO: MccSub20%

2.3.3.1 *Proteolysis reaction*

The reaction was carried out by incubating at 37°C for 48 h 2 mg/ml MccB17 and 0.1 mg/ml subtilisin in a buffer pH = 7.5 containing 40 mM sodium phosphate, 1.7 mM sodium acetate, 0.8 mM calcium acetate and 20% DMSO. The solution was loaded on a Sep-Pak ® reverse phase column eluted with acetonitrile and water, first with H_2O to remove salts and enzyme, the proteolysis fragments were collected by elution with 50% CH_3CN/H_2O. The collected fraction was concentrated under vacuum and freeze dried. The inhibitory activity of the mixture on gyrase supercoiling was validated as described before.

132

2.3.3.2 HPLC separation

The HPLC purification was scaled up to accommodate the increased amount of material used in this experiment. A Jupiter 5aC18 300 Å 10x250 mm HPLC column was chosen, the dimensions of the new column corresponded to a 4.3-fold volume increase. A new method was extrapolated from the previous conditions on this basis: basically the same gradient was used but with a flow of 2 ml/min instead of 0.5 ml/min. The column was fed with a 5 mg/ml solution of the proteolysis residue in 50% DMSO/ H_2O, 0.1% TFA. Figure 107 shows the elution profile.
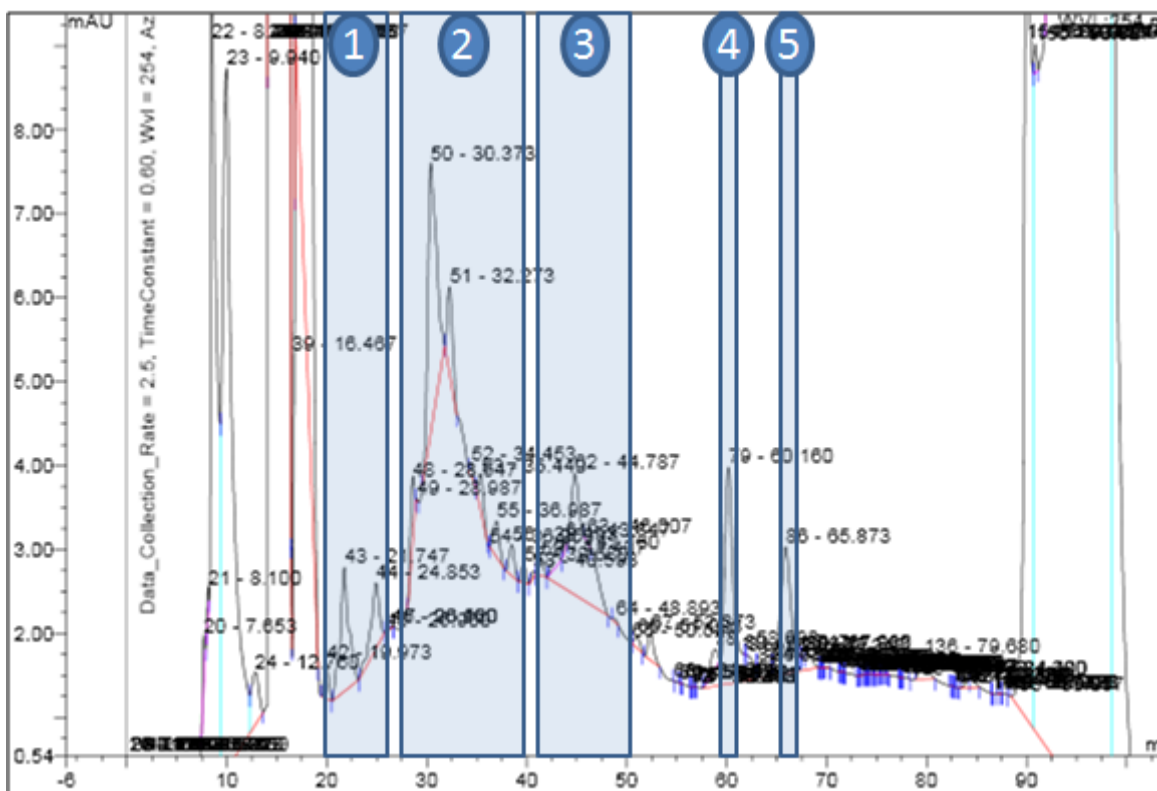
Figure 107 Collected fractions from the HPLC separation of MccSub20%: The blue boxes are showing the time window of each collected fraction with its numbering.

As before a lot of different peaks can be observed from the gradient; we decided to use a first rough separation, evaluate the mixtures and then run again the active fraction with conditions optimised for the gradient window where the compounds elute. Five fractions were isolated as shown in Figure 107 and assayed for inhibition of gyrase supercoiling using the standard method. The results are shown in Figure 108.

Fraction	Mw (intensity)
1	923.37 (1); 809.27 (0.3)
2	1085.36 (1); 1374.50 (0.8); **1105.38** (0.5); 809.30 (0.5); 1227.37 (0.4); 971.3 (0.3); 1611.55 (0.3); 1219.42 (0.3)
3	**1861.61** (1); 1393.49 (0.8); 1747.54 (0.5); 1700.60 (0.3)
4	1402.86 (1); 789.49 (0.3)
5	916.60 (1); 1524.83 (0.8); 1323.74 (0.7); 1490.88 (0.7); 1862.07 (0.7); 1402.84 (0.5)
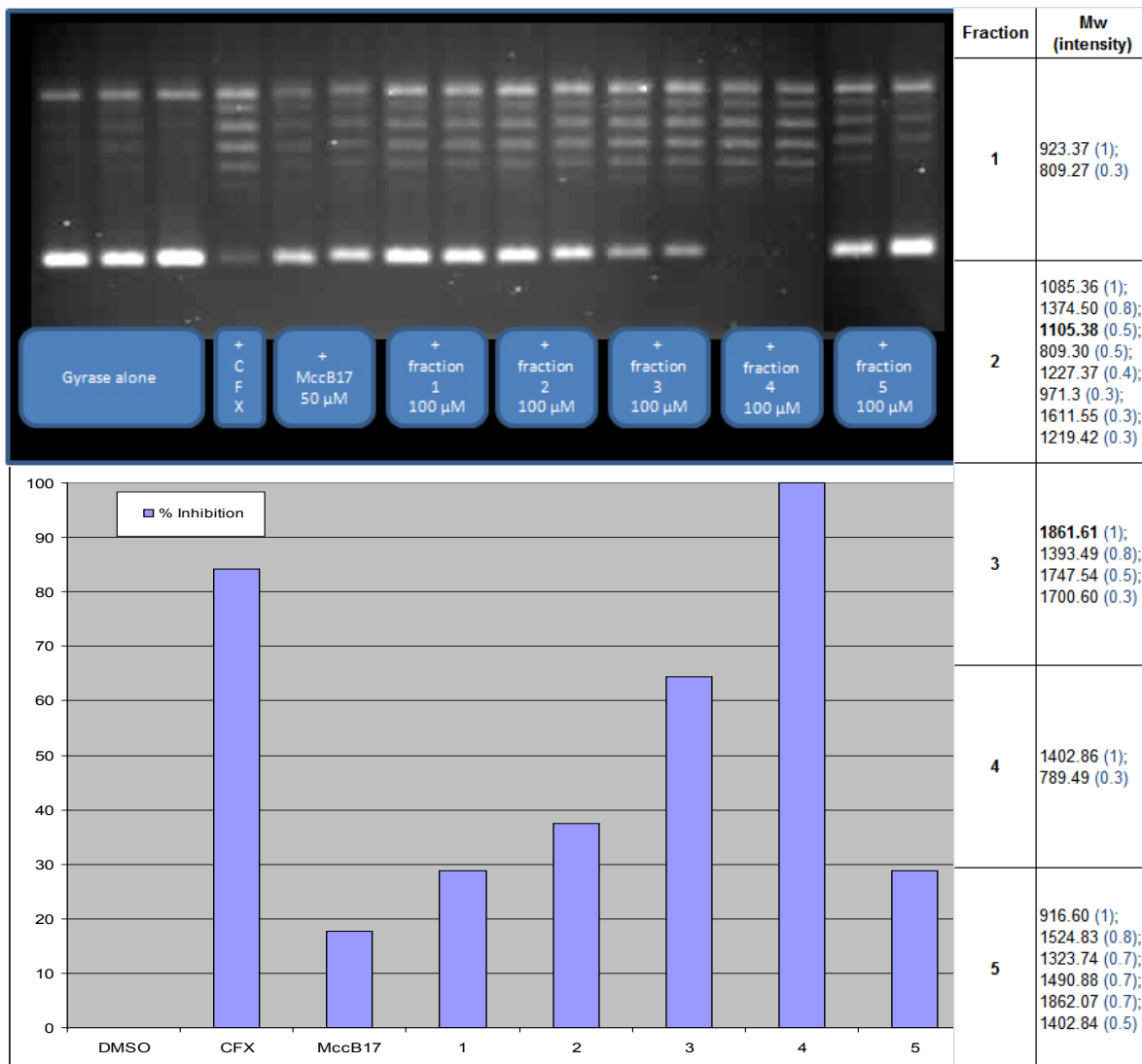
Figure 108 Evaluation and identification of MccSub20% collected HPLC fractions: top left, supercoiling assays of the different fractions; all fractions show a background inhibitory activity, but fraction 3 and 4 are the most active. Bottom left, bar-chart of the quantification of the inhibition observed in the supercoiling assay gel (Genetools from Syngene).The column on the right shows the MW of the species observed in each fraction by MALDI-ToF MS (in black), and the intensity of the related species in blue, the main peak is use as a reference (value = 1), others are shown as a fraction of the main peak (i.e 0.3 is 30% of the main peak intensity).

All the fractions display some background activity, but 3 and 4 are the most active; all were analysed by MALDI-ToF MS and the results are summarized in Figure 108. Fraction 4, the most active, contains only one main species with a Mw = 1402.86, but MS fragmentation did not link it to any MccB17 substructure. Fraction 3 however contains four main components some being expected proteolysis fragments. The next step was to separate the components of Fraction 4. Unfortunately this fraction consists of only 0.5 mg of material which would probably not yield enough material from a second purification to perform the assays. The solution was to produce new material and proceed the HPLC purification with conditions improving the separation in the elution window of fraction 3.

2.3.3.3 Second Proteolysis reaction MccSub20%_2

The proteolysis experimental conditions were modified to address two different concerns: first we wondered if the presence of calcium ions could promote the production of MccB17 degradation product during our experiment, as we realised that the sodium and calcium acetate were not required in the subtilisin reaction buffer we decided to use a phosphate buffer. The second modification involved the purification on a sep-pak® column, we noticed that a fair amount of material seemed to be lost during this step, so we decided to omit it for this experiment. The reaction was carried out using 2 mg/ml MccB17 and 0.1 mg/ml subtilisin in a 40 mM sodium phosphate buffer pH = 7.5 containing 20% DMSO. The reaction mixture was incubated at 37°C for 48h. Some precipitate had appeared during the reaction, the mixture was centrifuged 10 min at 13000 rpm and the supernatant stored at -20°C. The solid residue was resuspended in 50% DMSO/water, vortexed and centrifuged again, the second supernatant stored as well to be tested on HPLC.

2.3.3.4 Mass spectrometry analysis of the proteolysis reaction product
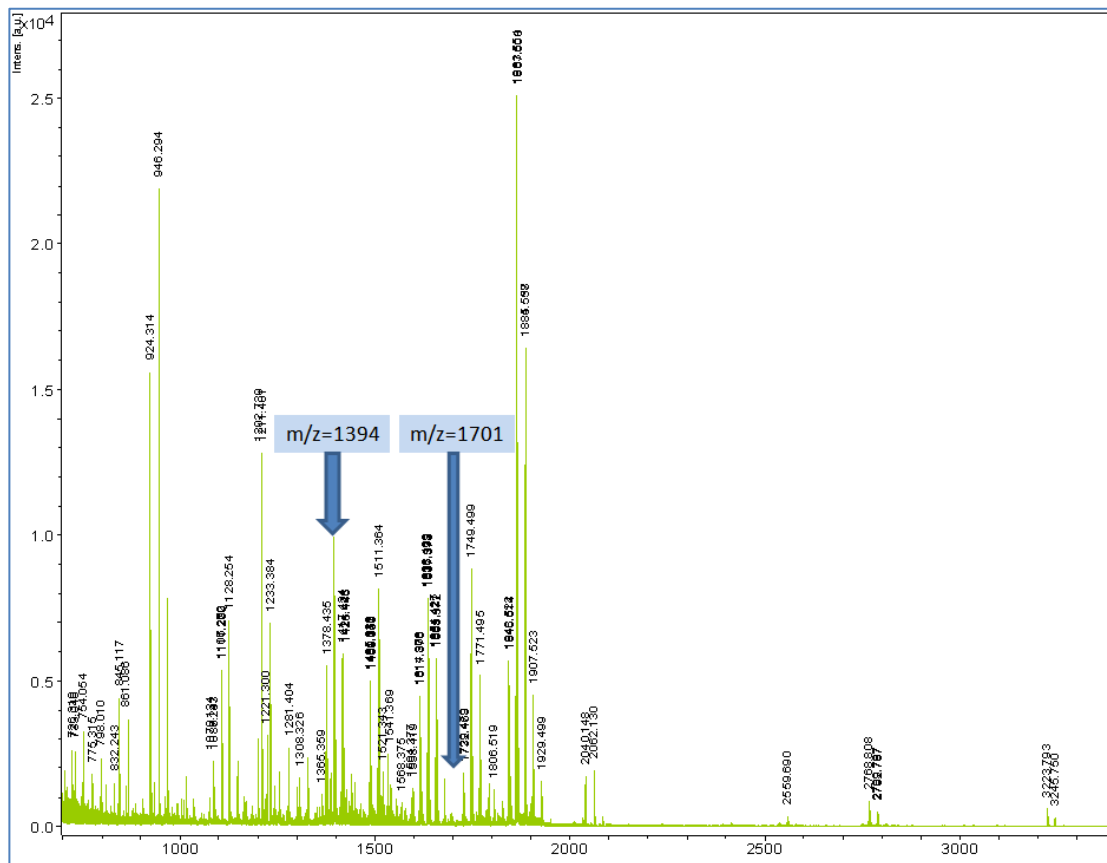
Figure 109 MALDI-ToF spectra of MccSub20%_2: MALDI-ToF spectra from the MccB17 digest by subtilisin in a phosphate buffer with 20% DMSO mixture. The side products that have been reduced by the new experimental conditions are shown by the blue arrows with their MW on the top.

Carrying out the proteolysis in just a phosphate buffer seemed to have reduced the amount of MccB17 degradation products MW = 1393 and 1700 generated (blue arrows in Figure 109). The various expected fragments are present, so we proceeded to the HPLC purification.

2.3.3.5   HPLC Purification

In the previous HPLC purification fraction 3 was collected between RT = 40 and 49 min, considering that the void volume correspond to 8 min and that the following formula gives the percentage of acetonitrile as a function of time for the window [5; 80] min in the previous program: %CH$_3$CN = 5 + (RT - 8 - 5) X 0.33. Applying the retention time in that formula led to the following acetonitrile gradient window for the elution of fraction 3: 13.9 < %CH$_3$CN Fraction 3 < 16.8%. A gradient of 0.24 % CH$_3$CN/min was used between t = 5 min and 80 min in order to improve the separation in this range. Figure 110 below shows the HPLC trace of the new method.
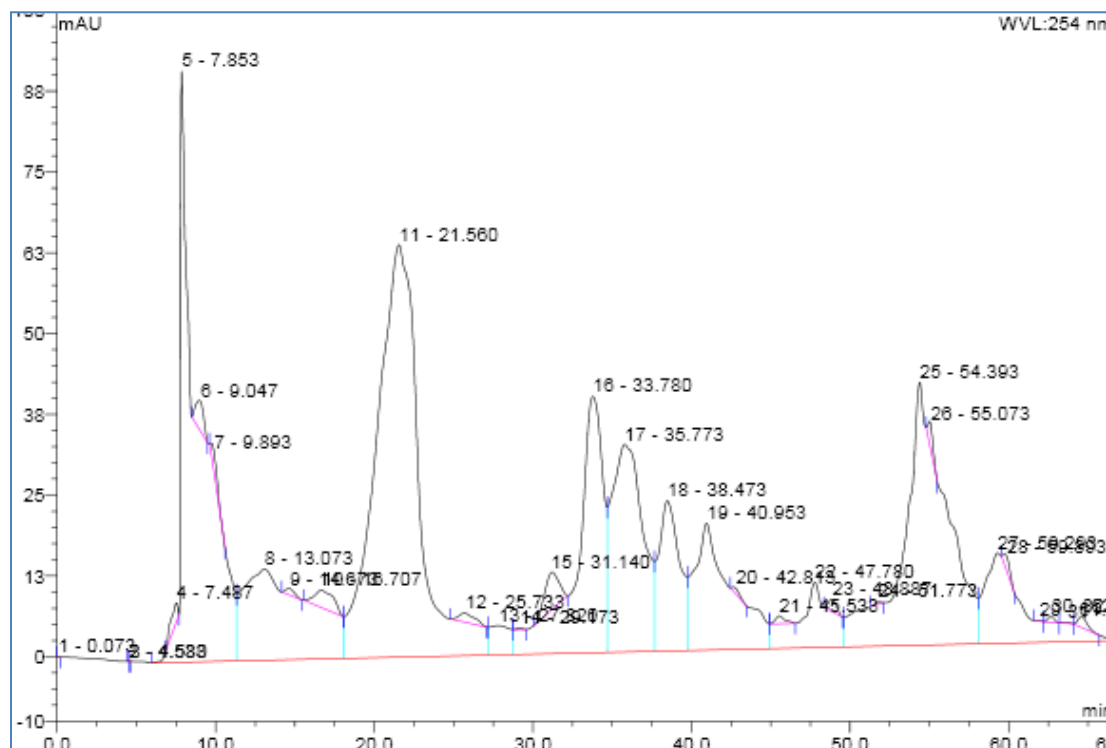
Figure 110 Separation of MccSub20%_2 components by HPLC.

The change in the gradient improved the separation, unfortunately it seems not to have particularly improved the resolution in the fraction 2 elution window and the separation between fraction 2 and 3, we decided nonetheless to isolate the peaks generated by this method, as displayed below on the zoomed trace.

136
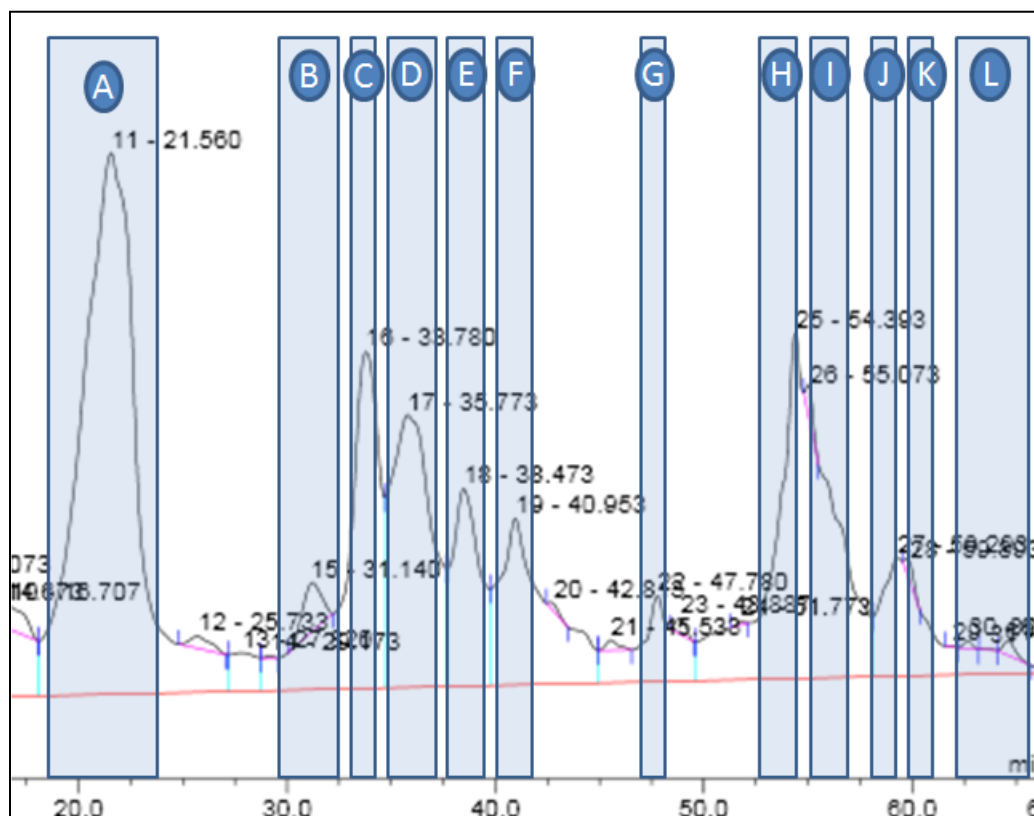
Figure 111 Collected fractions of the HPLC separation of MccSub20%_2: The blue boxes are showing the time window of each collected fraction with its reference letter.

2.3.3.6 Evaluation of the activity for the different fractions

In the previous digest, inhibitory activity has been observed for fractions at the end of the gradient, so in this experiment factions G to K, that correspond to the window where activity has been observed previously, were assayed in priority with supercoiling and cleavage assays. Fraction J and K were pooled together as they contains the same species (MALDI-ToF analysis not shown). Fraction I and (J+K) shows strong inhibitory activity on gyrase supercoiling at 200 μM. Fraction I was not assayed on the cleavage reaction because it contains MW=2767, and we had shown (in paragraph 2.3.2) that it stabilises the cleavage complex. No strong stabilisation of cleavage complex had been observed for the others fractions, however a faint band is visible for fraction H that will require further investigation.

Fraction	Mw (intensity)
G	1210.36 (1); **1209.50** (0.6); 1232.42 (0.5); 1411.52 (0.4)
H	**1861.53** (1); 1748.52 (0.8); 1376.43 (0.5)
I	1862.61 (1); 1884.55 (0.5); 1749.46 (0.3); 2766.82 (0.3)
J	1395.45 (1); 1843.56 (0.7); 1728.50 (0.5); 1394.46 (0.5); 1842.60 (0.4)
K	1395.46 (1); 1842.61 (0.9); 1394.47 (0.3)
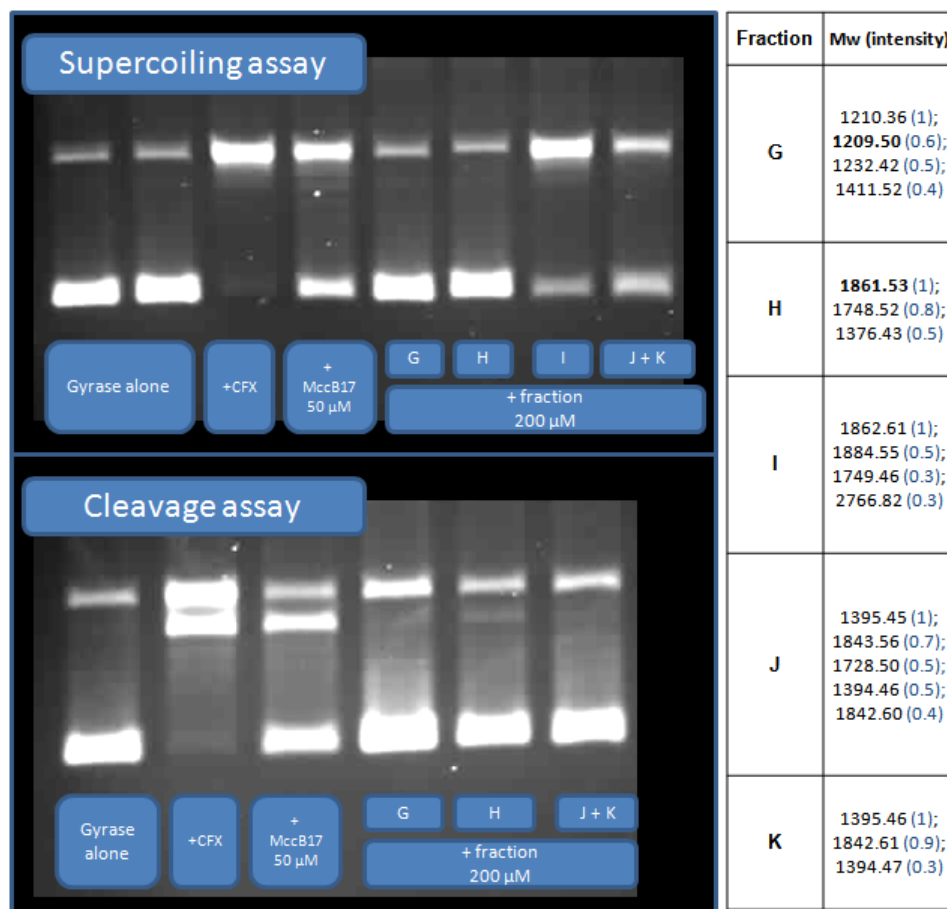
Figure 112 Evaluation and identification of MccSub20%_2 collected HPLC fraction: top left, supercoiling assays of the different fractions; fraction I and J+K are the most active. Bottom left, gyrase cleavage assays, no strong stabilization of cleavage complex is shown, however a weak cleavage band might be present for G and H. The column on the right shows the MW of the species observed in each fraction by MALDI-ToF MS (in black), and the intensity of the related species in blue, the main peak is use as a reference (value = 1), others are shown as a fraction of the main peak (i.e 0.6 is 60% of the main peak intensity).

2.4   Summary of proteolysis experiments and conclusion

An initial experiment had shown that the complete digestion of MccB17 by subtilisin generates a mixture containing products resulting from MccB17 specific cleavage and degradation. This mixture was able to inhibit DNA supercoiling by gyrase at a concentration of 33 µM. Following this encouraging result we decided to isolate the active species from the mixture. Precipitation issues arose as we scaled up the reaction, so we increased the DMSO concentration to 50% (MccSub50%), and still observed the same results concerning the activity on gyrase. The reaction mixture was separated with an HPLC apparatus building up on our experience with the hydrolysate. Among the different fractions isolated one was able to inhibit gyrase supercoiling as well as stabilize the cleavage complex. The fragment with MW=2767 was identified as the active compound of this fraction. Unfortunately this compound was corresponding to MccB17 lacking the four N-terminal amino acids. Interestingly this fragment

138

was not present in the initial reaction mixture, and appeared to be a side product favoured by the reaction with 50% DMSO. We repeated the same strategy with a lower concentration of 20% DMSO, and two fractions, having strong inhibitory activity on gyrase supercoiling at 100 µM, were isolated. The first one contained a mixture of compounds: MW = 1862; 1393; 1747; and 1700. The second, the most active, contained mainly one species MW = 1403, but this compound seemed not to be related to MccB17. Not enough material was available to try to separate further the components of first fraction. The proteolysis experiment was repeated to produce more material. It was carried out with 20% DMSO as before but without sodium acetate and calcium acetate in the buffer. In these conditions we observed a reduction of MccB17 degradation products. The HPLC conditions were modified to improve the separation in the window of elution where active compounds in the previous proteolysis were observed. Unfortunately only mixtures were still isolated. Two fractions active against gyrase supercoiling, the first contained fragments of MW = 1863; 1884; 1749; 2767; and the second contained MW: 1395.5; 1843.5; 1728. Annoyingly there is not a strong enough correlation between the two experiments to draw sound conclusion about the active compound, we had isolated similar structures over the two experiments but not exactly the same. Another concern is that some of the compounds present in the active fractions are related to the MccB17 degradation compound; this suggests that they may be responsible for the inhibitory properties observed. The activity of MccB17 degradation product will be discussed in the next section.

3   Isolation and evaluation of MccB17 by products

We have described in Chapter II how some compounds related to MccB17 were eluting ahead of MccB17 species during its purification. The determination of their structure by MS is described in Chapter II. Figure 113 and Figure 114 show the collected fraction from MccB17 purification containing this species and their structure. The compounds identified described in Figure 114, although unlikely to be active species, were included in our supercoiling assays trials. Our attention was further brought to these fragments as similar compounds were generated as by-products during the proteolysis experiments, and were also observed in the fraction showing inhibitory activity on gyrase.
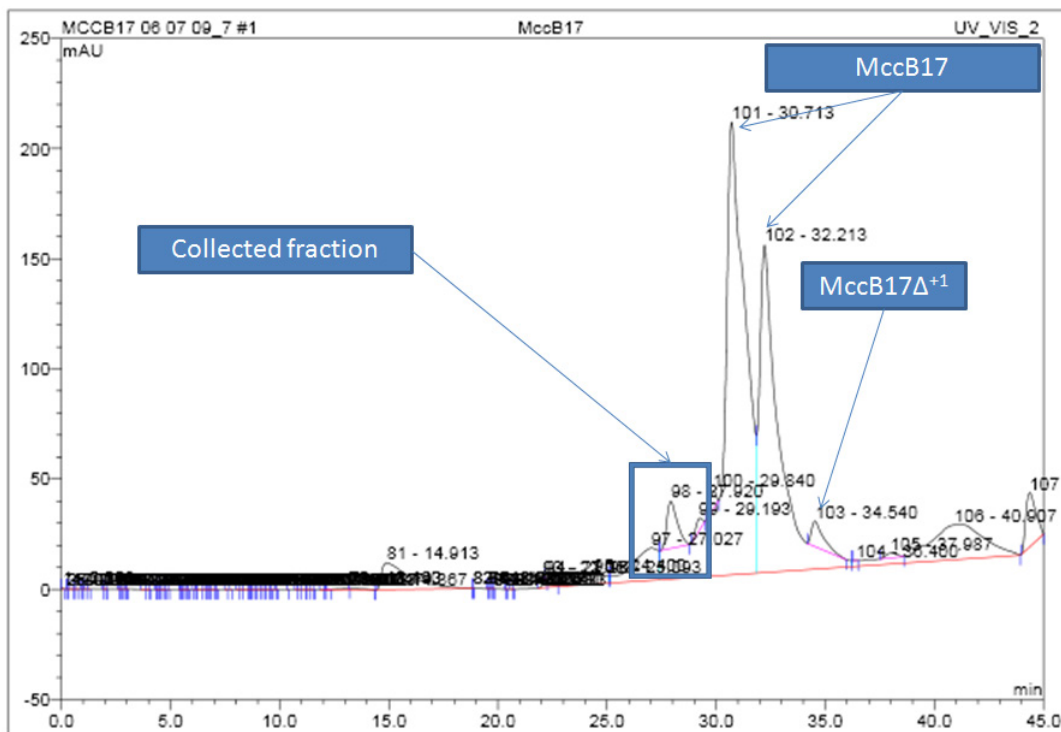
Figure 113 MccB17 HPLC purification trace.

Fragments from mccB17 preparation																												
Sequence																												
V	G	I	G	7xG	G	oztz	G	G	Q	G	G	tz	G	tz	S	N	tzoz	G	G	N	G	oz	G	oz	G	S	H	I
1700.57															1410.48													
857.41					G										?		1393.46											
																	1323.370											

Figure 114 Fragments of MccB17 isolated from MccB17 preparation: the sequence of MccB17 is shown in orange, the coloured boxes correspond to MccB17 fragments with their corresponding MW, in bold are the fragments isolated, in italic are related fragment for information.

3.1 Evaluation of activity of the mixture isolated from MccB17 prep

The standard supercoiling and cleavage assay were performed as described in Materials & Methods to evaluate the activity of the mixture. During the various preparation of MccB17 and others experiments fractions containing the fragments of interest as their main component have been isolated. The compound with MW = 857 Da has been found as the main component of several inactive fractions during the work on alkaline hydrolysis of MccB17, so we focused on the two others compounds observed: MW = 1393.4 Da, and MW = 1700.6 Da.

140

3.1.1 Initial validation of activity:

A fraction isolated from the purification of MccB17 by HPLC during its production, and eluting ahead of the expected MccB17 peaks appeared to have inhibitory activity on gyrase supercoiling as shown in Figure 115. MALDI-ToF analysis of this fraction revealed that it did not contain any MccB17 species, but smaller molecules related MccB17, as described in Chapter II-4.
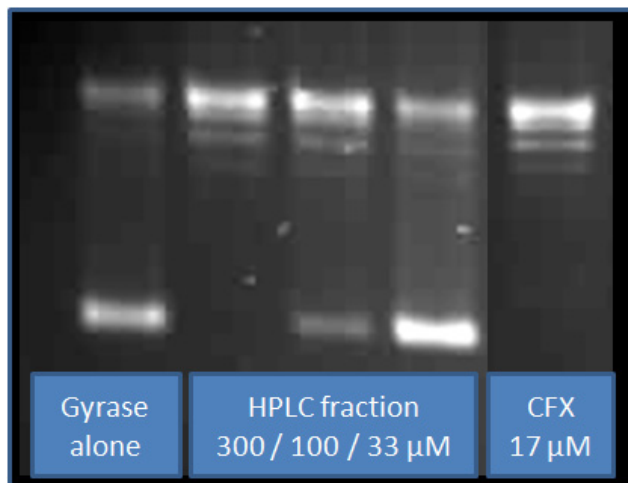
Figure 115 Evaluation of the fraction preceding MccB17 in HPLC: gyrase supercoiling assay of the fraction eluting before MccB17 species during its HPLC purification

The analysis of the sample using MALDI-ToF MS spectrometry shows that it contains MW = 1700.6 and MW = 1393.4. In later experiments special attention was paid to fractions that contain this species alone.

3.1.2 MW = 1700.6 Da

In later purification of MccB17 we managed to isolate the compound with MW = 1700.6 alone. It was assayed both on *E. coli* gyrase supercoiling and human topo II relaxation.
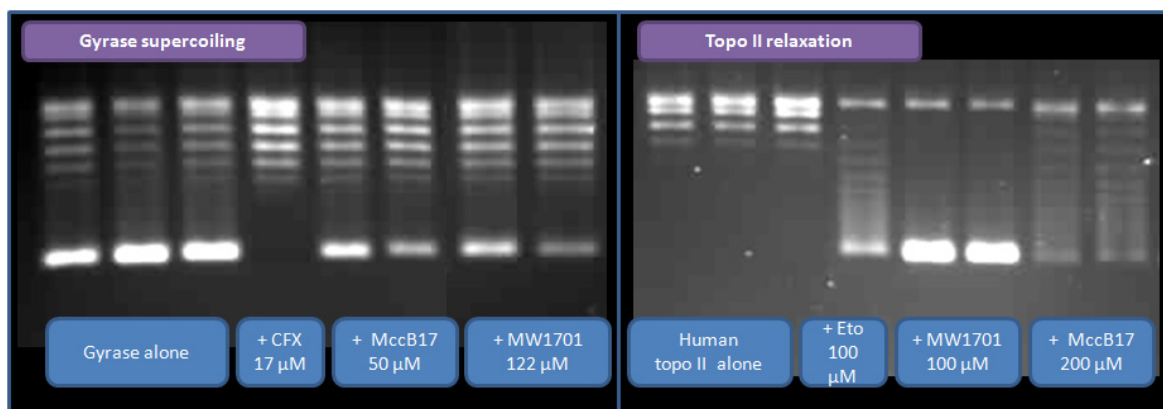
Figure 116 Evaluation of the inhibitory activity of MW = 1700.6 Da on gyrase supercoiling and topo II relaxation.

Inhibition of gyrase supercoiling had been observed at a concentration of 122 µM. The compound shows a complete inhibition of human topo II at a concentration of 100 µM. Interestingly, MW = 1700.6Da was more active on topo II than the native MccB17. This is encouraging in considering MccB17 substructures as inhibitors for topoisomerases other than gyrase.

3.1.3   MW= 1393.4 Da

Isolating this compound had proved more challenging, and we were not able to obtain it singular. The initial characterisation of the mixture containing MW = 1700.6 Da and MW = 1393.4 Da, exhibited a strong inhibition of the supercoiling reaction at 100 µM, by comparison, MW=1700.6 Da alone exhibited a weak inhibition at 122 µM (Figure 115 and 116), suggesting that MW = 1393.4 Da increases the inhibition in this reaction. Fractions containing MW = 1393.4 were pooled together and submitted to HPLC purification using the same method as for the proteolysis mixtures in 2.3.3.5. Unfortunately the compound co-eluted with another compound, MW = 2937 Da corresponding to Mcc\VG, known to be active. The intensities observed for the two peaks on the MALDI-ToF MS spectra, are 1 for MW=1393.4 and 0.3 for Mcc\VG, a rough estimation of the concentrations of each component in the mixture from these proportion, led to a Mcc\VG having a concentration close to our MccB17 control. In the supercoiling assays the fraction containing MW = 1393.4 and Mcc\VG display a stronger inhibitory activity than the MccB17 control Figure 117.
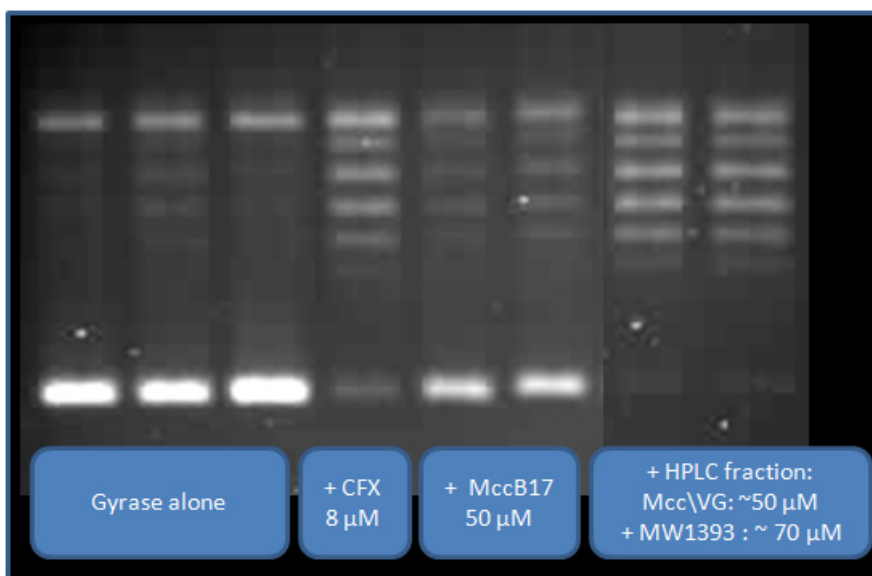
Figure 117 gyrase supercoiling assays of the HPLC fraction containing MW = 1393.4.

Finally a fraction containing MW = 1393.4 (50%), 1374.5 (25%), and 1410.5 (25%) has been isolated from the subtilisin digest experiments. This fraction was shown to inhibit gyrase supercoiling (Figure 118).
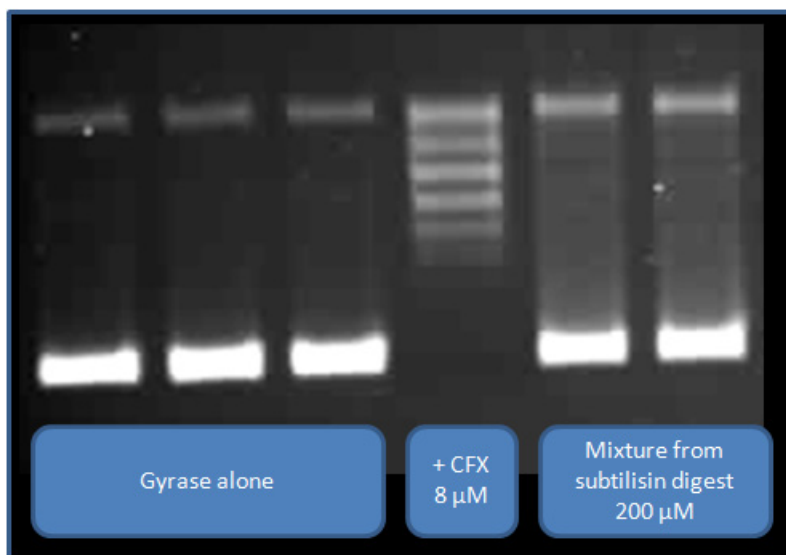
Figure 118 Gyrase supercoiling assay of a mixture containing MW = 1393.4: the inhibitory activity on gyrase supercoiling of a mixture containing (MW (relative MS intensity)): 1393.4 (1), 1374.5 (0.5) and 1410.5 (0.5) is shown. A weak ladder of relaxed species is visible (top), the control without drug is completely supercoiled which is not ideal to characterize MccB17-type inhibitors.

We were not able to have direct evidence for the MW = 1393.4 inhibitory activity on gyrase. However, we gathered a body of information that suggests that this compound is active in the 100 µM range. Isolation of the pure compound and evaluation of its activity will be necessary to consolidate this hypothesis.

3.2 Summary of MccB17 fragments from MccB17 degradation and proteolytic cleavage

We have shown in the last paragraph that fragments of MccB17 spontaneously produced during MccB17 preparation possessed inhibitory activity on gyrase supercoiling. As they were also present in some active fractions isolated from proteolysis mixture they could be responsible for the inhibitory activity observed. Fortunately, we have reduced the amount of these compound produced in our last proteolysis experiment, and it was still active, suggesting that other species are involved in the inhibitory effect, probably compounds derived from MW = 1861.5. Our final list of active candidates contains MW = 1393.5; 1700.6; 1862.5.

MccB17 fragment found in active fractions																												
Sequence																												
V	G	I	G	7xG	G	oztz	G	G	Q	G	G	tz	G	tz	S	N	tzoz	G	G	N	G	oz	G	oz	G	S	H	I
1700.57																	1410.48											
857.41					G											?	1393.46											
																		1209.41										
															1861.5													

Figure 119 Fragments of MccB17 found in active fractions.

It will be required to isolate each of them as single compounds to ascertain that there are indeed active species and quantify their activity. This will require an improvement of the separation technique by using different type of columns, with aromatic selectivity for example. The interesting preliminary results obtained on topo II with the MccB17 "natural" fragments suggest that extension of the investigation of the proteolytic cleavage species to human topo II might yield good results as well.

4 Conclusion

This chapter had described the various approaches we had used to generate fragments of MccB17. An alkaline hydrolysis strategy initially produced complex mixtures which did not permit us to identify any active component, followed by a more moderate method involving enzymatic proteolysis which was more fruitful. The inhibition of gyrase that was consistently observed independently of the cleavage method used, probably caused by different structures, highlights the fact that fragments of MccB17 have the potential for being topoisomerase inhibitors. Two major difficulties were inherent to this approach: first the physical properties of the starting material MccB17 made it particularly hard to work with as it tended to precipitate with its by-products after some time in a very stable form. Secondly MccB17 is not a very diverse molecule apart from the presence of heterocyclic residues and possesses some sort of symmetry which causes the fragments generated to have very similar physicochemical properties and makes their separation very difficult. We have isolated and identified fragments of half the size of MccB17 with inhibitory activity on gyrase in the same range as their parent molecule, but unfortunately not with a strong ability to stabilize the DNA-gyrase cleavage complex. These structures where isolated as the main component of mixtures with other MccB17 fragments, to evaluate accurately their inhibitory activity and validate these results it will be necessary to isolate them as pure compounds. This can be achieved by improving the HPLC condition with a different solvent system, and a column with different selectivity. An alternative method will be to use site-directed mutagenesis to introduce specific cleavage sites, this method will ensure that only one compound is produced but the yields and post translational modifications might be altered. If we consider the coverage of the native MccB17 structure by our active candidates, and other fragments that are not active we can start to draw a picture of the structural requirement. The fact that MW = 1209.4 is the main product of

the inactive fraction G of the second proteolysis, and MW = 1393.5 had been shown to be active, suggest that either MW = 1393.5 is close to a minimal required structure or that the Ser-Asn residues that differentiate the two compounds are vital for the activity. This finding gave additional information on MccB17 mechanism and these structures can be the starting point to define what is really required in MccB17 to stabilize the cleavage complex. Even if they are not stabilizing the cleavage complex, these compounds are *E. coli* gyrase inhibitors, and in some case human topo II inhibitors, this would make the systematic investigation of their potency against gyrase and topo IV from pathogenic bacteria, or human topo II the next logical step in a drug discovery approach.

CHAPTER IV
Small molecules related to microcin B17

CHAPTER IV Small molecules related to microcin B17

The previous chapters covered initially MccB17 as a whole molecule, its activity on various topoisomerases and some key elements required for its activity. It was followed by the investigation of fragmentation of MccB17 to diverse degrees that revealed that some parts of the molecule alone have inherent inhibitory activity. The most significant feature of MccB17 and its fragments, is the presence of heterocyclic amino acids that result from post-translation modification, some of these residues have been reported to be essential for MccB17 activity on gyrase (Sinha Roy, Kelleher et al. 1999). The alkaline hydrolysis of MccB17, outlined in Chapter III and described in a previous study (Coquin 2005), showed that heterocyclic amino acids specific to MccB17, as well as these same amino acids associated with a glycine or an aspartic acid residue were present in the resulting mixture, which was able to inhibit gyrase. It is legitimate to wonder what the activity of these heterocyclic amino acids molecule on gyrase is. Preliminary studies of these compounds have shown an inhibitory effect under 100 µM on gyrase supercoiling and no stabilization of the cleavage complex for the tzoz, and tz amino acids. As these heterocyclic residues were the necessary building blocks to synthesize the MccB17 fragments we planned to study, we decided to generate these compounds and validate these preliminary results. In the first part will be described how these compounds have been synthesised and their activity on topoisomerases evaluated. A second part will deal with the evaluation of small molecules that are not present in MccB17 but possessed similarities with MccB17's heterocyclic amino acids. A general overview of the results obtained with these small molecules will conclude this chapter.

1   Heterocyclic amino acids from microcin B17

The full synthesis of MccB17 has been reported by Videnov *et al* (Videnov, Kaiser et al. 1996) and has been described in chapter I. The part involving the synthesis of MccB17 heterocyclic moieties (Videnov, Kaiser et al. 1996), H-oz-OH: 2-aminomethyl oxazole-4-carboxylic acid, H-tz-OH: 2-aminomethyl thiazole-4-carboxylic, H-oztz-OH: 2-(2'-aminomethyloxazole-4'-yl)thiazole-4-carboxylic acid, and H-tzoz-OH: 2-(2'-aminomethylthiazole-4'-yl)oxazole-4-carboxylic acid, is of particular interest here, as it was our reference method to generate these residues. Recent innovation in the synthetic chemistry of oxazole rings has been included in our synthetic strategy as it provides some improvements to our method. The Hantzsch method described by Videnov was used to generate the thiazole rings, whereas oxazole rings were synthesized by using a one-pot method involving a Gly-Ser motif (Phillips, Uto et al. 2000).

1.1 A novel method to generate oxazole rings for MccB17 heterocyclic amino acids

An efficient method to convert β-hydroxy amides to oxazoline, which can be further oxidized into an oxazole in a one-pot reaction, has been developed by Phillips *et al* (Phillips, Uto et al. 2000)*,* it is shown in the top part of figure 120 below. We decided to use this method to generate our oxazole species because it possesses two advantages: first, the cyclisation reaction and further oxidation of the oxazoline can be performed via a one-pot method which makes it a simpler route compared to the modified Hantzsch method employed by Videnov *et al* (Figure 120). Second, the fact that this method involves β-hydroxy amides means that it is a more flexible method potentially applicable to a variety of peptide templates containing a serine residue. This is particularly interesting in the context of this study as this route involves a mechanism closer to MccB17 biosynthesis where a X-Gly-Ser-X, or X-Gly-Ser-Cys-X and X-Gly-Cys-Ser-X motifs are converted respectively into oz, oztz, and tzoz. Once this method is validated on generating MccB17 oxazole-containing building blocks, it open the possibility of synthesizing peptides derived from MccB17 containing oxazole rings from the corresponding Gly-Ser- or tz-Ser-containing peptide.
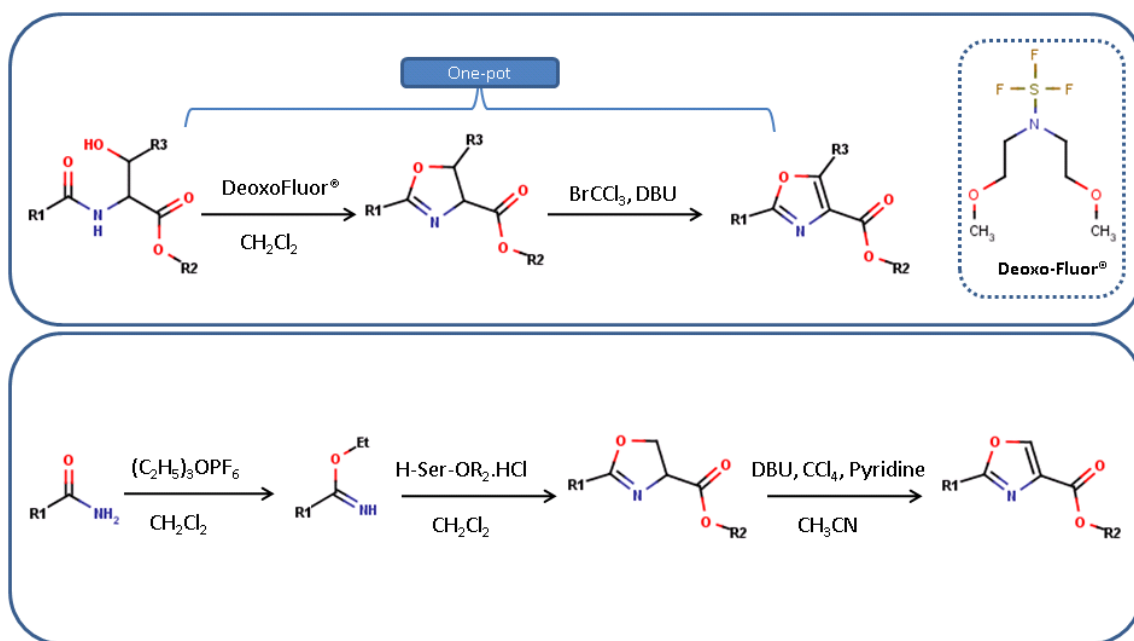
Figure 120 Comparison of oxazole synthetic routes: the top part of the figure describes the one-pot method involving deoxofluor. The lower part concerns the more classic approach with the modified Hantzsch method.

148

1.2 Synthesis of oxazole amino acid (H-oz-OH): 2-aminomethyl oxazole-4-carboxylic acid
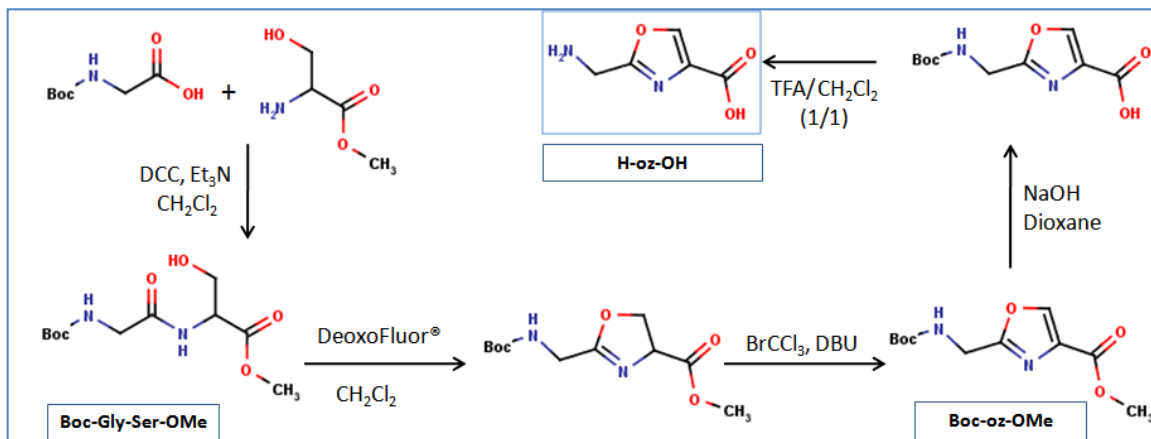
Figure 121 synthetic route of 2-aminomethyl oxazole-4-carboxylic acid (H-oz-OH)

1.2.1 Boc-Gly-Ser-OMe:
Methyl 2-(2-(N-tert-butoxycarbonyl)aminoacetamido)-3-hydroxypropanoate

The reaction was carried out at 0°C and under anhydrous conditions. Boc-Gly-Ser was mixed with equimolar amount of N-(tert-butoxycarbonyl)glycine), O-methyl serine chlorhydrate, N,N'-dicyclohexylcarbodiimide (DCC), and triethylamine (Et$_3$N,) in dichloromethane. The reaction proceeded overnight at 0°C. After removal of the solvent *in vacuo*; trituration with ethyl acetate, and removal of the solid residue, the filtrate was concentrated under vacuum. The isolated residue was triturated with a small amount of tetrahydrofuran and filtered, the filtrate was concentrated *in vacuo*. The isolated residue was purified by silica gel column chromatography with AcOEt, 5% MeOH as eluent.

1.2.2 Boc-oz-OMe: Methyl 2-(N-tert-butoxycarbonyl)aminomethyloxazole-4-carboxylate

The reaction was carried out at -20°C under anhydrous conditions. To a solution of N-Boc-Gly-Ser-OMe in anhydrous dichloromethane, 1.15 equivalent (eq) of bis(2-methoxyethyl)aminosulfur trifluoride (Deoxo-Fluor®) was added. After 30 min stirring, 3.75 eq of bromotrichloromethane were added to the mixture, followed by 3.75 eq of DBU. The reaction mixture was stirred at T= 2-3°C for 8 h before being quenched with a saturated solution of sodium bicarbonate. The mixture was extracted with ethyl acetate, the organic phase dried and concentrated under vacuum. The residue was purified on silica gel column chromatography with n-hexane/AcOEt (1/1) as eluent.

1.2.3 Boc-oz-OH: 2-(N-tert-butoxycarbonyl)aminomethyloxazole-4-carboxylic acid

The Boc-oz-OMe residue was resuspended in a solution of dioxane/water (3/1) containing 1 eq NaOH, and the mixture was stirred for 1 h at RT. The solution was neutralized

and extracted with dichloromethane. The organic phase was dried; the removal of the solvent *in vacuo* led to Boc-oz-OH.

1.2.4   H-oz-OH: 2- aminomethyloxazole-4-carboxylic acid

Boc-oz-OH was dissolved in TFA/CH$_2$Cl$_2$ (1/1) and stirred for 2 h. The mixture was concentrated *in vacuo* to lead to the final product.

1.3   Synthesis of thiazole amino acid (H-tz-OH): 2-aminomethyl thiazole-4-carboxylic acid

The method used to generate this compound is directly inspired from the synthesis described by Videnov *et al*.
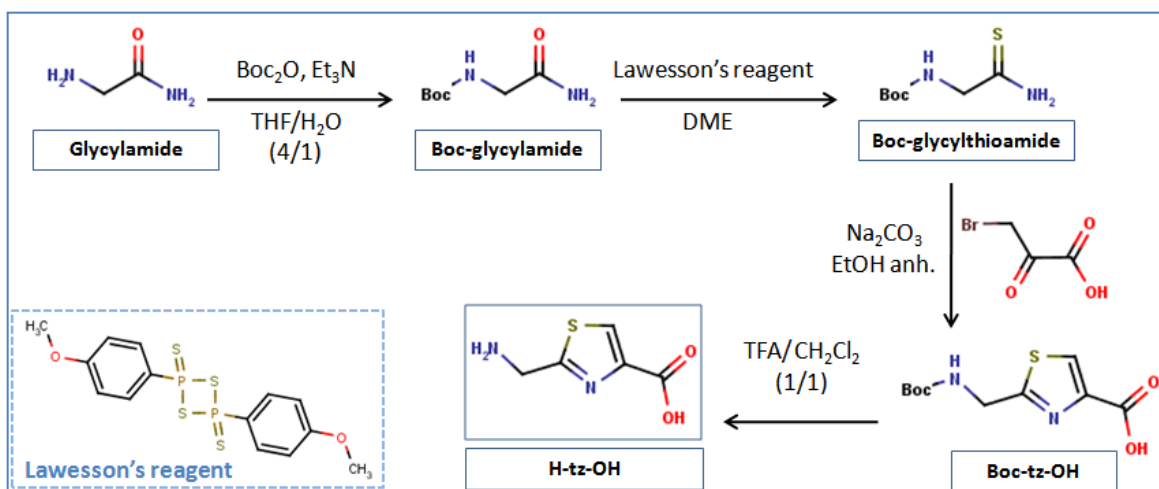
Figure 122 Synthetic route of 2-aminomethyl thiazole-4-carboxylic acid (H-tz-OH)

1.3.1   Boc-glycine amide: N-tert-butoxycarbonylglycine amide

Di-tert-butylcarbonate was added to a solution of 0.9 eq of glycylamide and TEA in THF/H$_2$O (4/1). The mixture was stirred for 5 h at RT. The mixture was extracted with ethyl acetate. The organic phase was washed respectively with 1 M sodium hydrogencarbonate solution and brine before being dried and concentrated *in vacuo* to yield to the Boc-protected glycylamide.

1.3.2   Boc-glycylthioamide: N-tert-butoxycarbonylglycine thioamide

Lawesson's reagent (0.75 eq) was added to a solution of Boc-protected glycylamide in dimethoxyethane (DME), the solution was stirred overnight at RT. The solvent was removed under vacuum. Ethyl acetate and 1 M sodium hydrogencarbonate were added to the residues and stirred for 10 min. The organic phase was recovered and the aqueous phase was washed

with ethyl acetate. The combined organic phases were washed with brine, dried, and concentrated *in vacuo*. The solid residue was recrystallised in EtOAc/n-hexane.

1.3.3 Boc-tz-OH: 2-(N-tert-butoxycarbonyl)aminomethylthiazole-4-carboxylic acid

Under anhydrous conditions, N-Boc-2-glycylethioamide, and 4 eq of potassium carbonate were introduced in ethanol. 1.5 eq of 3-bromo-2-oxopropanoic acid in anhydrous ethanol was added dropwise. The reaction mixture was stirred for 4 h at RT, before being filtered, the filtrate was concentrated under vacuum. The residue isolated was recrystallised in AcOEt/n-hexane and led to the pure expected product.

1.3.4 H-tz-OH

N-Boc-tz-OH was dissolved in TFA/CH_2Cl_2 (1/1) and stirred for 2 h at RT. The mixture was concentrated *in vacuo* to lead to the TFA salt of H-tz-OH.

1.4 Synthesis of H-oztz-OH: 2-(2'-aminomethyloxazole-4'-yl)-thiazole-4-carboxylic acid

The synthesis of this bis-heterocyclic compound use the Boc-oz-OMe described in 1.2.2 as the starting material using the same method described to produce H-tz-OH.
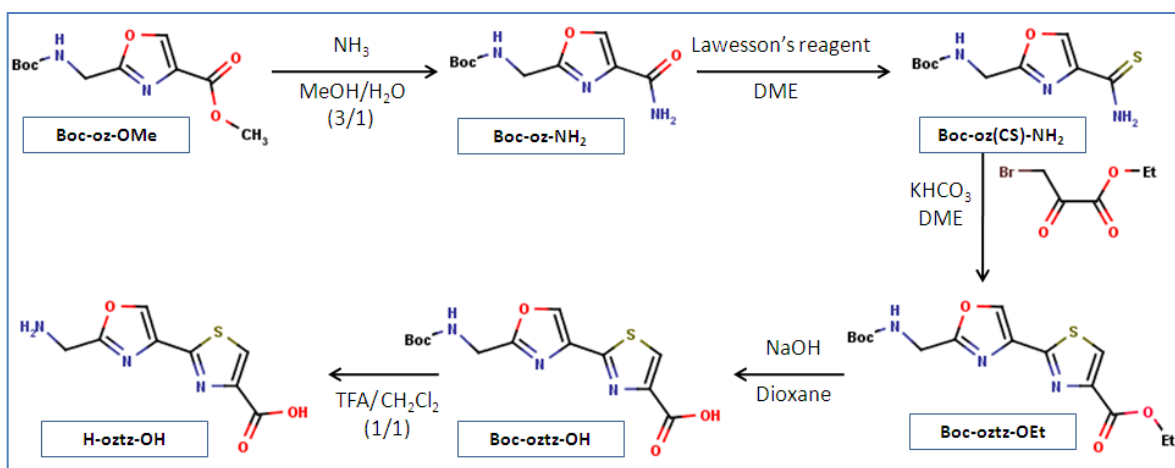
Figure 123 Synthetic route of 2-(2'-aminomethyloxazole-4'-yl)-thiazole-4-carboxylic acid (H-oztz-OH)

1.4.1 Boc-oz-NH₂: 2-(N-tert-butoxycarbonyl)aminomethyloxazole-4-amide

35% aqueous ammonia were added to a solution of Boc-oz-OMe in methanol, the mixture was stirred overnight at RT. After concentration *in vacuo*, a solution of $NaHCO_3$ was added. The solid residue was filtered and washed with water.

1.4.2 Boc-oz(CS)-NH₂: 2-(N-tert-butoxycarbonyl)aminomethyloxazole-4-thioamide

0.75 eq of Lawesson's reagent was added to a solution of Boc-oz-NH₂ in DME, the solution was stirred overnight at RT. The solvent was removed and ethyl acetate and 1 M

sodium hydrogencarbonate were added to the residues and stirred for 10 min. The organic phase was recovered and washed with brine, dried, and concentrated *in vacuo*. The solid residue was recrystalized in EtOAc/n-hexane.

1.4.3 Boc-oztz-OEt:
Ethyl-2-((N-tert-butoxycarbonyl)-2'-aminomethyloxazole-4'-yl)-thiazole-4-carboxylate

Under anhydrous conditions, Boc-oz(CS)-NH$_2$ and 6 eq potassium hydrogencarbonate suspended in anhydrous DME were stirred for 10 min before the addition of 3.5 eq of ethylbromopyruvate. The reaction mixture was left stirring overnight at RT. The mixture was filtered, washed with brine, dried, and concentrated. The residue was purified by silica gel column chromatography with EtOAc/n-hexane (2/1) as eluent.

1.4.4 Boc-oztz-OH:
2-((N-tert-butoxycarbonyl)-2'-aminomethyloxazole-4'-yl)-thiazole-4-carboxylic acid

A mixture of Boc-oztz-OEt dissolved in dioxane/water (3/1) with 2 eq of sodium hydroxide (0.52 mmol) was stirred for 1 h at RT. The solution was set to pH = 6. The dioxane was removed under vacuum, the pH of the solution further set to pH = 3 before being extracted with ethyl acetate. The organic phase was dried and the solvent removed *in vacuo* to lead to Boc-oztz-OH.

1.4.5 H-oztz-OH

Boc-oztz-OH was dissolved in TFA/CH$_2$Cl$_2$ (1/1) and stirred for 1 h at RT. The mixture was concentrated *in vacuo* to lead to the TFA salt of H-oztz-OH.

1.5 Synthesis of H-tzoz-OH:
2-(2'-aminomethylthiazole-4'-yl)-oxazole-4-carboxylic acid

The synthesis of this bis-heterocyclic compound use the Boc-tz-OH described in 1.3.3 as starting material with a method similar to the synthesis of H-oz-OH (Figure 124).

1.5.1 Boc-tz-Ser-OMe:
N-(2-(N'-tert-butoxycarbonyl)aminomethylthiazole-4-carbonyl)-Serine methyl ester

Under anhydrous conditions at 0°C, Boc-tz-OH was dissolved in dichloromethane, 2 eq of TEA, 2 eq serine hydrochloride and 2 eq of DCC were added to the mixture. The reaction mixture was stirred overnight at 0°C. The solvent was removed *in vacuo* and the residue resuspended in ethyl acetate. The dicyclohexylurea (DCU) was removed by filtration, and the filtrate concentrated under vacuum. A small amount of THF was added and the ammonium chloride precipitate was removed The filtrate was concentrated before being purified by silica gel column chromatography with AcOEt/ 5% MeOH as eluent.
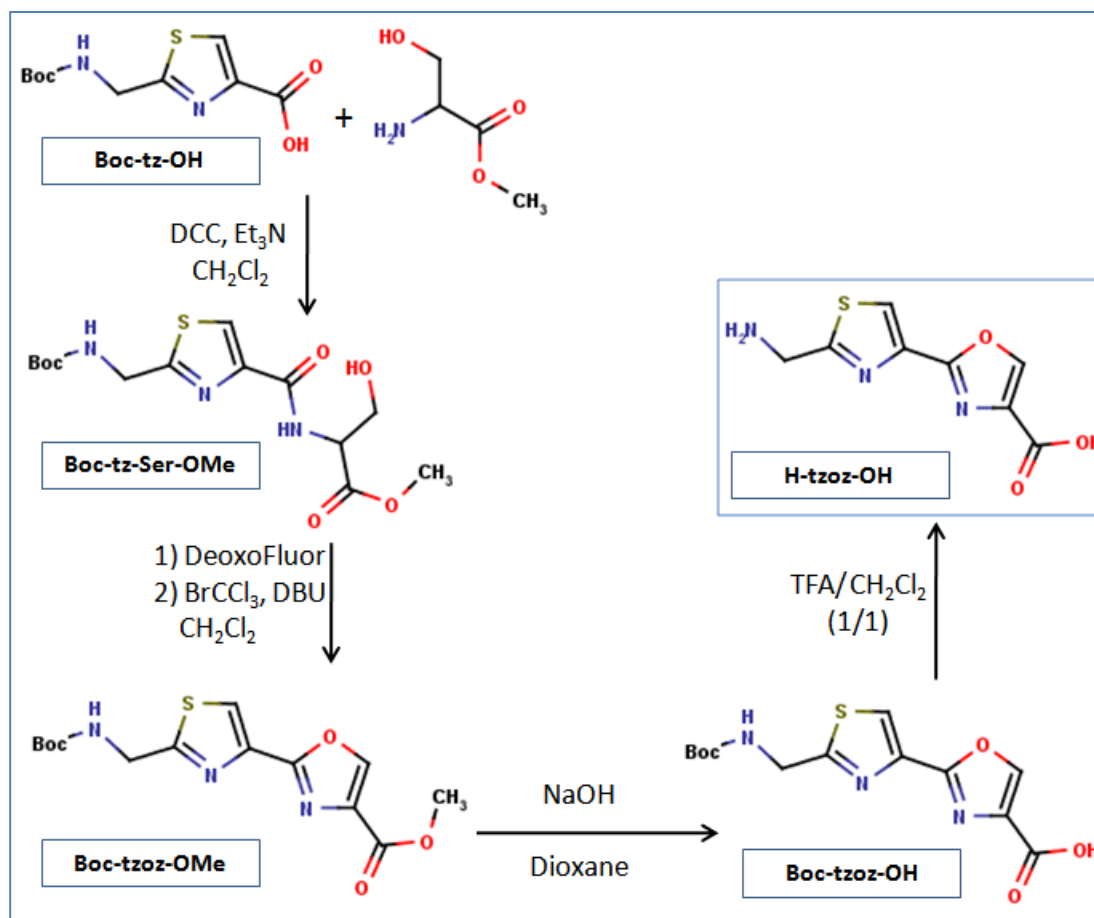
Figure 124 Synthetic route of 2-(2'-aminomethylthiazole-4'-yl)-oxazole-4-carboxylic acid (H-tzoz-OH).

1.5.2 Boc-tzoz-OMe:
Methyl-2-((N-tert-butoxycarbonyl)-2'-aminomethylthiazole-4'-yl)-oxazole-4-carboxylate

At -20°C, under anhydrous conditions, 1.1 eq of DeoxoFluor® was added to Boc-tz-Ser-OMe in dichloromethane. After 30 min, 3.6 eq of bromotrichloromethane DBU were added, the reaction mixture was stirred for 8 h at 0°C. The mixture was quenched with a saturated solution of sodium hydrogencarbonate, the dichloromethane was removed under vacuum and the remaining aqueous phase was extracted with ethyl acetate. The organic extract was dried and concentrated *in vacuo*. The residue was purified by silica gel column chromatography with ethyl acetate as solvent.

1.5.3 Boc-tzoz-OH:
2-((N-tert-butoxycarbonyl)-2'-aminomethylthiazole-4'-yl)-oxazole-4-carboxylic acid

Boc-tzoz-OMe was dissolved in a dioxane/water (3/1) containing 1 eq of sodium hydroxide. After being stirred at RT for 1 h, the dioxane was removed from the mixture and the

pH was adjusted to 3. The solution was extracted with ethyl acetate, and the organic phase was dried and concentrated *in vacuo*.

1.5.4 H-tzoz-OH

Boc-tzoz-OH was dissolved TFA/CH$_2$Cl$_2$ (1/1) and stirred for 1 h at RT. The mixture was concentrated under vacuum and led to the TFA salt of H-tzoz-OH.

1.6 *In vitro* assays of synthesized compounds

1.6.1 *E. coli* gyrase

The heterocyclic amino acids found in MccB17 as well as synthetic intermediates were assayed for activity on gyrase supercoiling using the standard method described in Chapter II. Initial results show inhibitory activity for some of the compounds at the millimolar range. The determination of precise IC$_{50}$ was not successful due to the low level of activity of the studied compounds and the variability of the assays. Examples of supercoiling assays are available in Figure 125. The results obtained with the various heterocyclic amino acids are summarized in Table 8.
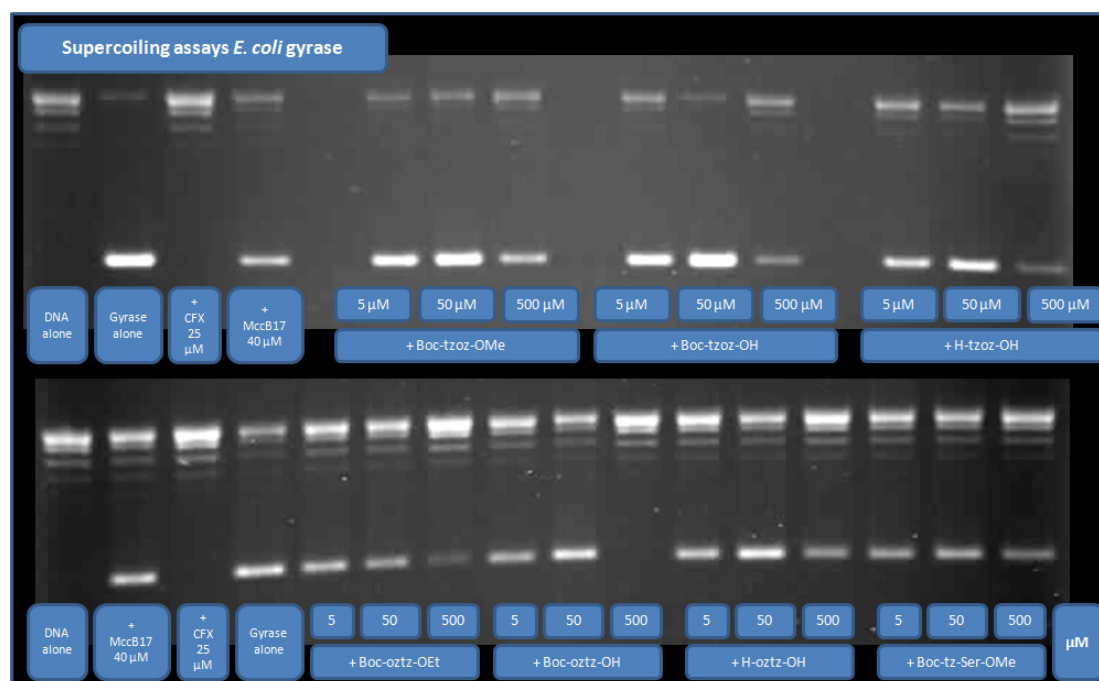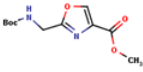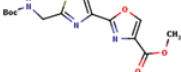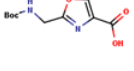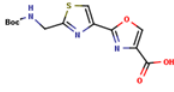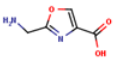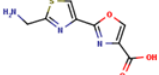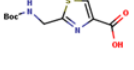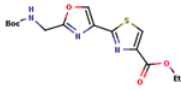
Figure 125 Evaluation of the inhibitory concentration of Mcc17 heterocyclic compounds on gyrase supercoiling (example): Gel electrophoresis of the product of standard supercoiling assays in the presence of no drug, 25 μM ciprofloxacin, 40 μM MccB17, or 5/50/500 μM of tested heterocyclic compound. The upper bands represent the starting relaxed DNA, the lower band represents the produced supercoiled DNA. In the presence of inhibitor, the lower band loses in intensity in favour of the upper band.

Table 8 Summary of inhibitory concentration of MccB17's natural and chemically protected heterocyclic compounds on the *E. coli* gyrase supercoiling reaction

N°	Compound	[Het]~ inh MccB17	N°	Compound	[Het]~ inh MccB17
Boc-oz-OMe		no inh at 1 mM	Boc-tzoz-OMe		1 mM > inh > 0.5 mM
Boc-oz-OH		no inh at 1 mM	Boc-tzoz-OH		500 µM > inh > 200 µM
H-oz-OH		no inh at 1 mM	H-tzoz-OH		500 µM > inh > 50 µM
Boc-tz-OMe		> 1 mM	Boc-oztz-OEt		500 µM >
H-tz-OH		> 1 mM	Boc-oztz-OH		500 µM >
Boc-tz-Ser-OMe		> 1 mM	H-oztz-OH		500 µM

Further characterization of this series was performed by submitting Boc-tz-OH and Boc-tzoz-OMe to relaxation assays: a difference of inhibitory activity toward relaxation and supercoiling would suggest an involvement of the inhibitors with the ATPase activity of the enzyme. Additionally, difference of susceptibility to these compounds between gyrase wild type and gyrase carrying the MccB17 resistance mutation Y751R was evaluated. Finally stabilization of gyrase-DNA cleavage complex was assayed on Boc-tz-OH, H-tz-OH, H-tzoz-OH, Boc-oztz-OEt. Examples of the extra experiments carried out on this series are provided in Figures 126 and 127.

The compounds displayed the same activity on gyrase supercoiling and relaxation. The compounds had approximately the same level of inhibitory activity on supercoiling by WT gyrase and MccB17-resistant gyrase, suggesting that their mechanism of action differs from MccB17's. It should be noted that MccB17 control for the relaxation reaction failed, however the two compounds assayed showed clearly inhibition of relaxation. The compounds tested were not able to stabilize the cleavage complex at 1 mM concentration.

Figure 126 Relaxation and cleavage assays of MccB17's heterocyclic compounds (example):
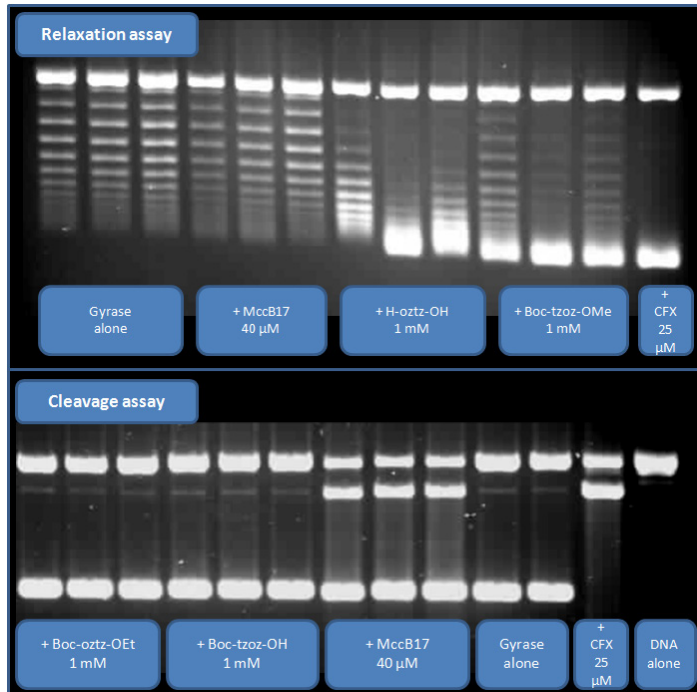
<u>Relaxation:</u> gel electrophoresis of standard relaxation assays performed in presence of 25 µM ciprofloxacin, 40 µM MccB17, or 1 mM of tested MccB17 heterocyclic compounds. The lower band represent the starting supercoiled DNA, the upper bands represent the produced relaxed DNA. In the presence of an inhibitor, the upper bands lose in intensity in favor of the lower band. The ladder observed in between corresponds to various topoisomer intermediates.

<u>Cleavage:</u> gel electrophoresis of standard cleavage assays performed in presence of 25 µM ciprofloxacin, 40 µM MccB17, or 1 mM of MccB17 heterocyclic compounds. The upper band represents the starting relaxed DNA, the lower band represents the produced supercoiled DNA. In presence of a cleavage complex stabilizing agent a new band corresponding to linear DNA appears between the two others. None of the compounds tested stabilized the cleavage complex.
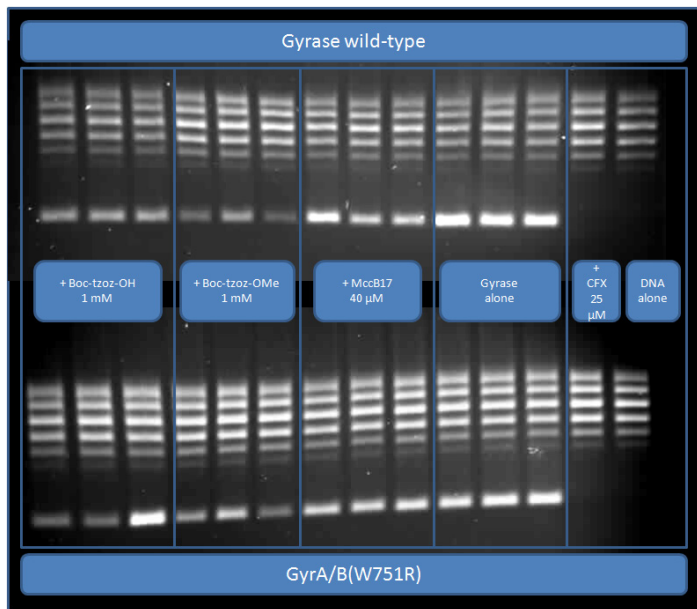
Figure 127 comparison of inhibition by MccB17's heterocyclic compounds of wild type and MccB17-resistant gyrase (example): gel electrophoresis of standard supercoiling assays using either wild type gyrase or gyrA+gyrB(W751R), in the presence of 25 µM ciprofloxacin, 40 µM MccB17, or 1 mM of tested MccB17's heterocyclic compound. The upper bands represent the starting relaxed DNA, the lower band represents the produced supercoiled DNA. In the presence of an inhibitor, the lower bands loses in intensity in favor of the upper bands. The upper part of the figure shows the inhibition of wild-type gyrase by various agents, and the lower part of the figure shows the same experiment with MccB17-resistant gyrase. In this last part, MccB17 displays no inhibitory activity whereas the heterocyclic compounds tested show the same inhibitory activity in both experiments.

These results were disappointing considering the level of inhibition observed. The results were similar to what had been previously reported: no effect of protecting groups on activity, the oxazole amino acid had no activity, the thiazole and the bis-heterocycle amino acids displayed inhibitory activity, with the bis-heterocycles being the best (tz < oztz < tzoz). However the activity we observed was ten-fold lower than what was expected from the

preliminary study (Coquin 2005). Interestingly the compounds retain their activity on the MccB17-resistant mutant, and as no stabilization of cleavage complex was observed, it suggests that the mode of action of these small molecules is different from MccB17's.

1.6.2 Human topo II

Four representative compounds from the series were tested with topo II: H-oz-OH, Boc-tz-OH, H-tzoz-OH, H-oztz-OH using the standard procedure.
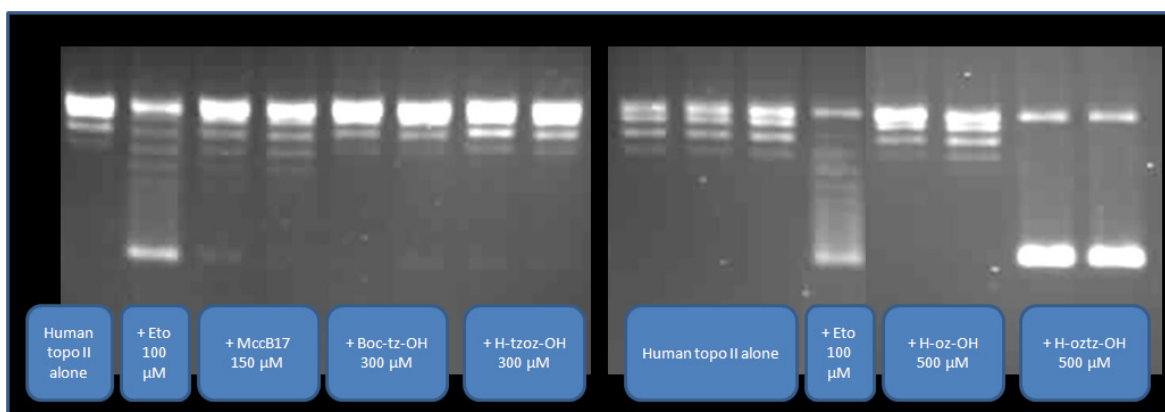
Figure 128 Inhibition of human topo II by MccB17 heterocyclic compounds: the inhibitory activity was evaluated using standard topo II relaxation assays in the presence of either no drug, 100 μM etoposide, 150 μM MccB17, 300 μM of Boc-tz-OH or H-tzoz-OH   or 500 μM of H-oz-OH or H-oztz-OH. The lower band represents the starting supercoiled DNA, in the presence of topo II the lower band is converted to the ladder of upper bands that represent the relaxed DNA species. . In the presence of an inhibitor, the upper bands lose intensity in favor of the lower bands. A very faint lower band is visible in the presence of some of our inhibitors: MccB17, Boc-tz-OH, and H-tz-OH. H-oztz-OH on the other hand did fully inhibit the reaction at 500 μM.

Very weak inhibition of relaxation was observed at 300 μM for Boc-tz-OH and H-tzoz-OH, at 500 μM H-oz-OH had no activity whereas H-oztz-OH showed complete inhibition.

1.7   Conclusion

All the compounds we desired to obtain have been successfully synthesized; the method described by Phillips *et al* (Phillips, Uto et al. 2000) to generate oxazole has been successfully integrated into our synthetic pathway and yielded the expected heterocycles. In the context of this synthesis, the use of a one-pot cyclization/oxidation step simplifies the production of oxazole-containing compounds, but more importantly the glycylserine substrate used in this reaction introduces more flexibility into the method: for example, peptides bearing multiple glycylserine sites can be generated and multiple cyclization can be achieved in a single step; another possibility is to use already existing natural peptides containing the Gly-Ser motif as a substrate to introduce new oxazole ring in the structure. We have considered this last possibility to efficiently generate the MccB17 derivatives carrying an extra oxazole ring observed as a side-product during MccB17 preparation; this is a compound of interest as it had been reported to have superior inhibitory activity compared to MccB17. Inhibitory activity has been observed on gyrase supercoiling and relaxation and on topo II relaxation at concentrations around 500 μM for the thiazole and the bis-heterocycles. The few inhibitors that were tested did not produce any stabilization of gyrase-DNA cleavage complex.

157

2 Compounds related to microcin B17

2.1 Pyrrole

The first class of compounds related to MccB17 heterocyclic amino acids we have considered were pyrrole amino acids, that as pentaheterocyclic amino acids can be considered as bioisosters of our thiazole and oxazole compounds. These compounds were available through the courtesy of our collaborator Christian Greeff (Chris Pickett lab, CAP department, UEA, Norwich).
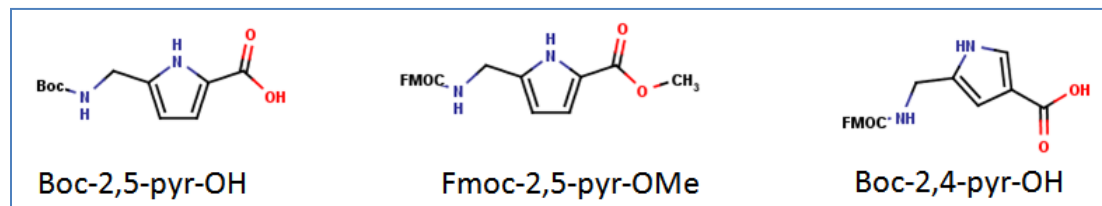
Figure 129 Pyrrole compounds

Three different compounds have been tested:

- Boc-2,5pyr-OH: 5-((tert-butoxycarbonyl)aminomethyl)-1H-pyrrole-2-carboxylic acid.
- Fmoc-2,5pyr-OMe: methyl 5-(fluorenylmethoxy)carbonyl)aminomethyl)-1H-pyrrole-2-carboxylate.
- Fmoc-2,4pyr-OH: 4-(fluorenylmethoxy)carbonyl)aminomethyl)-1H-pyrrole-2-carboxylic acid.

This set was interesting as the effect of two different protecting groups Boc and Fmoc can be compared as well as two different substitutions of the pyrrole ring. The compounds were analysed using standard gyrase supercoiling assays.
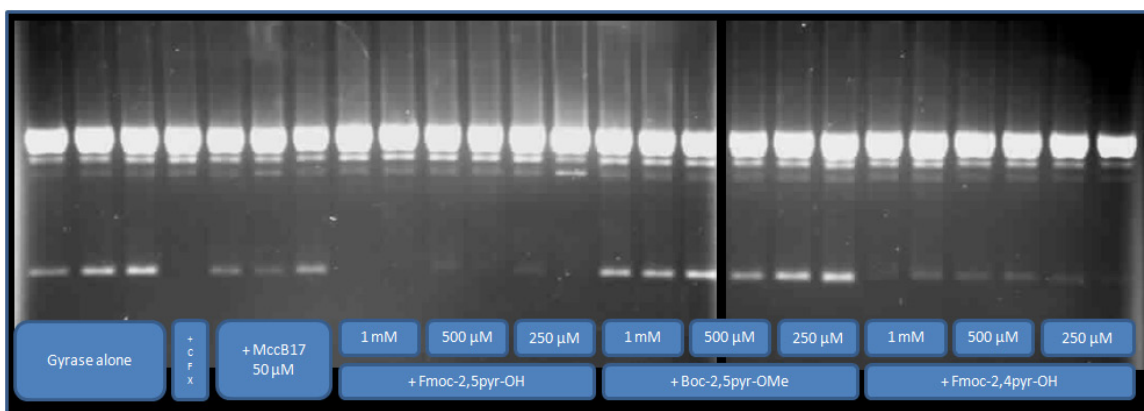
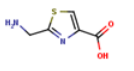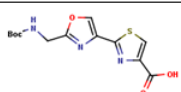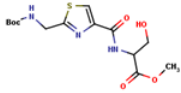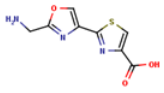**Figure 130 Evaluation of the inhibitory concentration of pyrrole compounds on gyrase supercoiling: Gel electrophoresis of the product of standard supercoiling assays in the presence of no drug, 25 μM ciprofloxacin, 50 μM MccB17, or 1000/500/250 μM of the tested pyrrole compound. The upper bands represent the starting relaxed DNA, the lower band represents the produced supercoiled DNA species. In the presence of inhibitor the lower band loses intensity in favor of the upper bands. Fmoc-2,5pyr-OH and Fmoc-2,4pyr-OH show inhibition for all concentrations tested whereas Boc-2,5pyr-OMe did not show any inhibition.**

158

It appears from the assays that Fmoc-2,5pyr-OH and Fmoc-2,4pyr-OH can completely inhibit supercoiling down to 250 µM, while Boc-2,5pyr-OMe shows no activity. We wondered if this difference came from the difference in protecting group or from the esterification of the acid group. To address this question we used two different experiments. First we removed the Fmoc protecting group from Fmoc-pyr-OH in order to evaluate the activity of the non protected pyrrole amino acid. And second, we decided to introduce a Fmoc protecting group on one of the McB17 heterocyclic amino acids. We chose to use H-tzoz-OH for this experiment as it was one of the most active heterocycles. Using this compound has both the advantage of evaluating the influence of the Fmoc group and of isolating a potentially potent compound.

2.1.1 H-2, 5pyr-OH

Fmoc-2,5pyr-OH (0.07 mmol) was dissolved in 2 ml DMF, 1 ml of 0.1 sodium hydroxide solution was added and the mixture was stirred for 10 min. The reaction mixture was set to pH = 7 by addition of 1 M hydrochloric acid solution, 10 ml water were added and the solution was extracted with ethyl acetate. The organic phase was dried and concentrated under vacuum.

2.1.2 Fmoc-tzoz-OH:

H-tz-OH (0.09 mmol) and sodium carbonate (0.18) were added to 0.265 ml water. A solution of 0.11 mmol Fmoc-OSu (N-(9-Fluorenylmethoxycarbonyloxy) succinimide) in 0.53 ml THF was added to the mixture. The reaction mixture was stirred overnight at RT. Water was added to quench the mixture, and it was acidified to pH = 3. The precipitate was filtered, washed with water and dried.

2.1.3 Evaluation of H-2,5pyr-OH and Fmoc -tzoz-OH effect on gyrase

The two compounds isolated H-2,5pyr-OH and Fmoc -tzoz-OH were assayed on gyrase supercoiling, and compared with the respective starting material Fmoc-2,5pyr-OH and H -tzoz-OH. In the assay displayed in Figure 131 a lower activity than what was observed initially for the reference compounds was observed, this was probably due to greater supercoiling activity by gyrase. Nonetheless we can notice that the removal of the Fmoc group from the pyrrole compounds disrupts its activity, whereas its addition to the tzoz compound increases the inhibitory effect.

The study of these compounds was not pushed forward as even if addition of a Fmoc group increases the activity of our heterocyclic compounds, it is still in the range of 100 µM and without any stabilization of gyrase-DNA cleavage complex (data not shown). Another issue was that the introduction of the Fluorenyl group is significantly increasing the lipophilicity of the compound, which is something we want to avoid in a drug design approach.
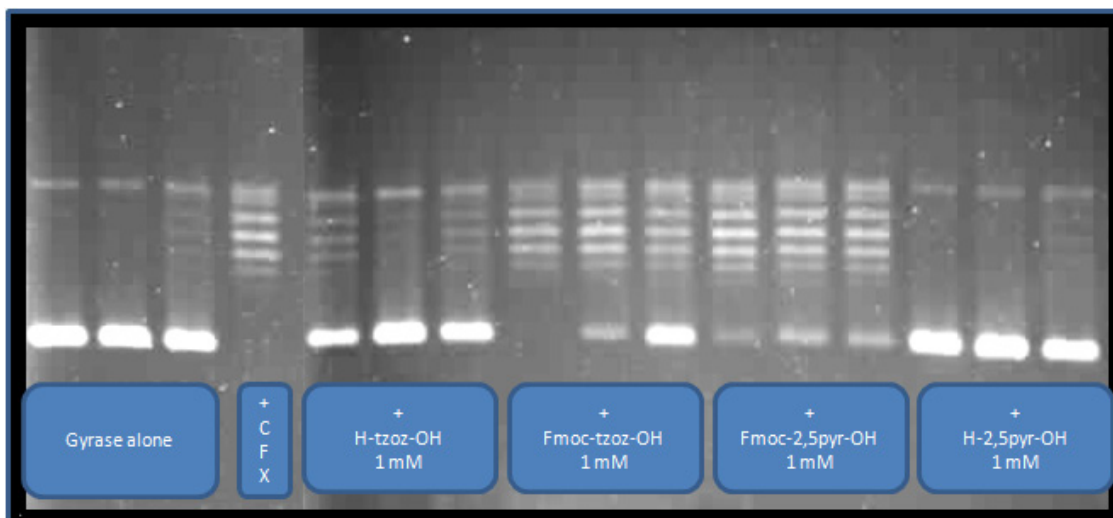
Figure 131 Evaluation of the effect of protecting groups variation on pyrrole and tzoz compounds on gyrase supercoiling: gel electrophoresis of the reaction mixture of standard supercoiling assays in presence of no drug, 17 μM ciprofloxacin, or 1 mM of the tested compound. The results for Fmoc-tzoz-OH are not very clear but there is definitely an improvement of inhibition compared to the related unprotected amino acid. Additionally removal of the protecting group from Fmoc-2,5-pyr-OH led to a compound without any inhibitory activity at 1 mM concentration.

2.2 Peptides related to MccB17

Two series of peptides were studied here, the first were two heptapeptides described previously that we considered as potential starting templates for variation of amino acids to establish structure-activity relationship and potentially generate new lead compounds. This series will be referred as HeptX. The second series was inspired by the MccB17 alkaline hydrolysis experiment. In several fractions with inhibitory activity on gyrase, a compound with MW = 857 was observed, this compound could be related to the MccB17 fragment $G_{43}toN_{53}$ (MW = 856). This fragment contain two tz residues, and two amide residues, which are important MccB17 features and make this compound a plausible candidate for a gyrase inhibitor. The fragment corresponding exactly to this MW would be MccB17($G_{43}toN_{53}$) where only one of the amide groups has been converted to an acidic residue in the alkaline conditions. The possibility that one of the amide residues, likely the glutamine, could have been unaffected by the hydrolysis seems a possibility as we have observed in Chapter I that the glutamine residue remained untouched during the conversion of MccB17 amide residue to acid in mild alkaline condition. We extended our field of investigation to all the possible variations of this fragment that are described in Figure 132 in order to identify the optimal inhibitor. All these peptides were ordered from EMC-microcollections (Tübingen). This series of compounds will be referred as PeptXX.
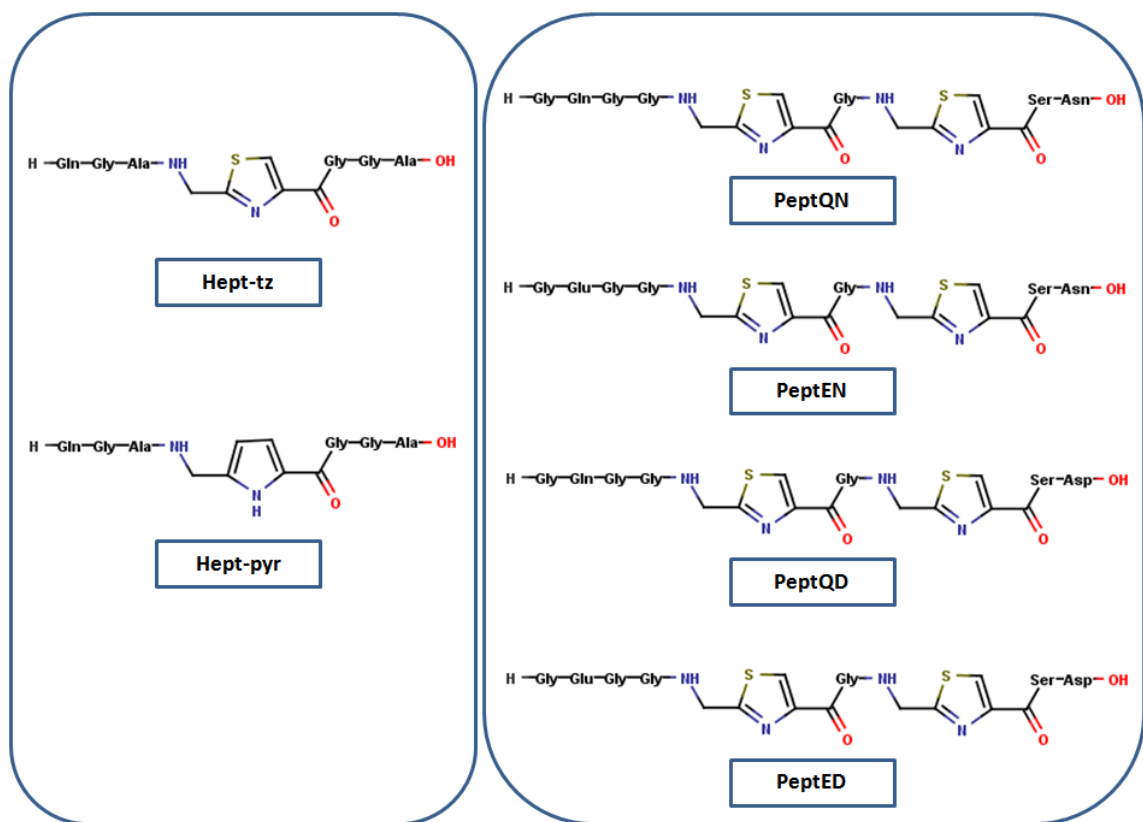
Figure 132 Structures and references of the Heptapetides and PeptXX compounds series

2.2.1 Evaluation of the peptides:

2.2.1.1 Heptapeptides

2.2.1.1.1 E. coli gyrase

Preliminary studies have shown that these peptides have inhibitory activity on supercoiling at 20 µM for Hept-tz, and 70 µM for Hept-pyr (Coquin 2005). The two peptides were evaluated using standard supercoiling assays. As the activity observed was below what we expected, we decided to follow the inhibitory activity over a time course, as described for MccB17 in Chapter II. The supercoiling time courses are shown below in Figure 133. The time courses show a weak activity at 1 mM, and Hept-pyr appear to be more active than Hept-tz.

161
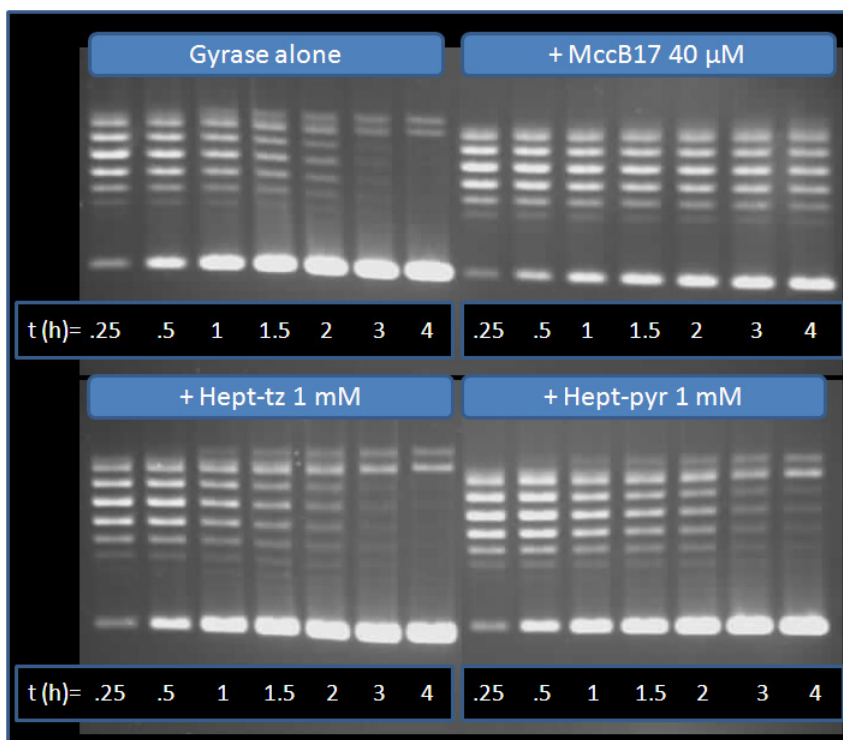
Figure 133 Inhibition of gyrase supercoiling by Hept-tz and Hept-pyr over time: gel electrophoresis from samples of a standard supercoiling assay in the presence of no drug, MccB17 40 µM, or Heptapeptide at 1 mM, taken at 15 min, 30 min, 1 h, 1 h 30, 2 h, 3 h, and 4 h. The upper ladder corresponds to the starting relaxed DNA species, the lower band corresponds to the supercoiled DNA products. Inhibition of supercoiling reaction by MccB17 shows an increase of relaxed species, i.e. brighter top bands. Only Hept-pyr displays a weak inhibitory activity at 1 mM.
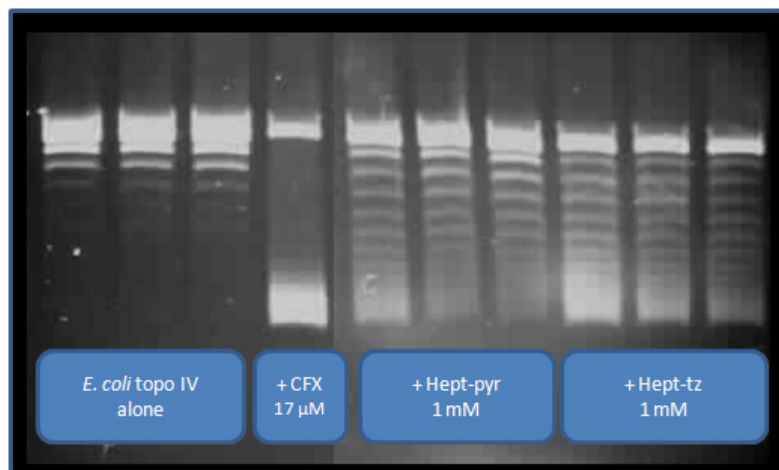
Figure 134 Evaluation of Hept-pyr and Hept-tz on *E. coli* topo IV: gel electrophoresis of standard topo IV relaxation assay in presence of 17 µM of ciprofloxacin, or 1 mM of heptapetide. The lower bands represent the starting supercoiled DNA, the upper band represents the produced relaxed DNA. In the presence of an inhibitor (ciprofloxacin) the upper bands loses in intensity in favor of the lower band. Some activity is observed for both tested compounds.

162

2.2.1.1.2 *E. coli* topo IV

The compounds were reported to be active on topo IV as well so assays on *E. coli* topo IV were performed to complement our observations. As with gyrase, weak inhibitory activity on topo IV was observed for both peptides at 1 mM concentration (Figure 134).

2.2.1.2 PeptXX

2.2.1.2.1 *E. coli* gyrase

PeptXX compounds were assayed for activity on gyrase supercoiling and cleavage using the standard method. The results are shown in Figures 135 and 136. Inhibition of gyrase supercoiling activity was observed at 500 µM concentration for all compounds.
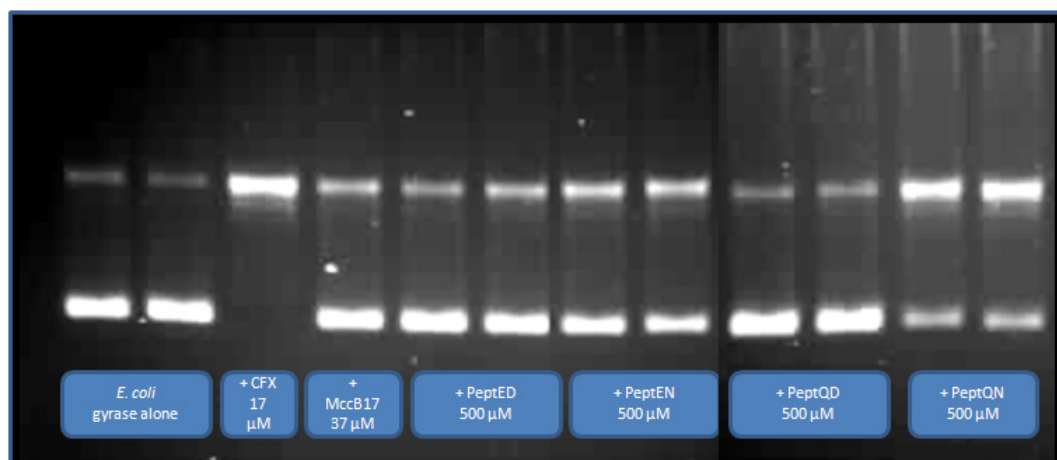
Figure 135 Activity of the PeptXX compounds on *E. coli* gyrase supercoiling: gel electrophoresis from samples of a standard supercoiling assay in the presence of no drug, MccB17 40 µM, or peptXX at 500 µM. The upper band corresponds to the starting relaxed DNA species, the lower band corresponds to the supercoiled DNA products. In the presence of an inhibitor (ciprofloxacin) the lower band loses intensity in favor of the upper band. PeptED, PeptEN and PeptQN inhibit the reaction at 500 µM, PeptQN being the most potent.
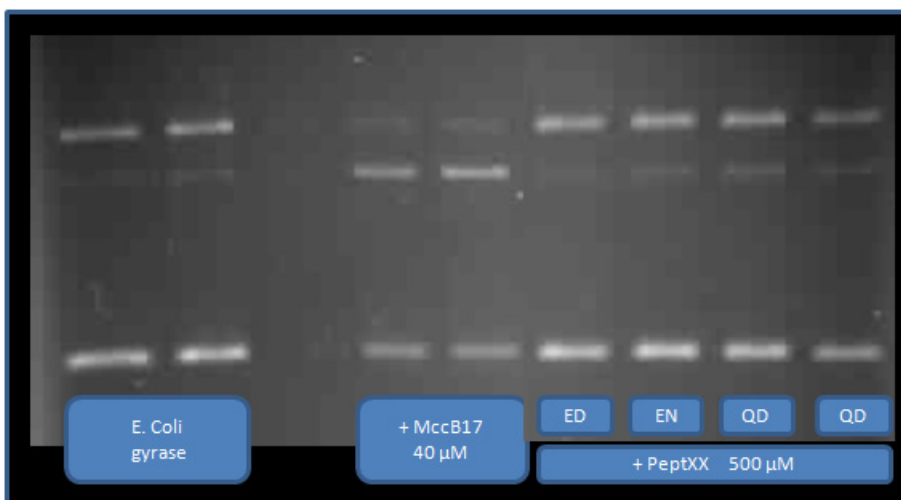
Figure 136 Evaluation of the stabilisation of cleavage complex by PeptXX: gel electrophoresis of standard cleavage assays performed in presence of 40 µM MccB17 or 500 µM of PeptXX. The upper band represents the starting relaxed DNA, the lower band represent the produced supercoiled DNA. In the presence of a cleavage complex stabilizer (MccB17) a new band corresponding to linear DNA appears between the two others. None of the compounds tested stabilised the cleavage complex.

163

2.2.2 Heptapetides and PeptXX on human Topo II

The inhibitory activity displayed by the Heptapeptides and PeptXX series encouraged us to evaluate them on other topoisomerases, even if their activity was weak on gyrase they might have a increased potency on another target. Inhibitory activity on human topo II relaxation was assayed using standard method. The compounds were initially tested at 333 µM for the heptapepides and 250 µM for PeptXX series. As no inhibitory activity was observed, no further studies were performed on these compounds.

2.2.3 Conclusion

The low level of activity that we observed for both heptapeptides discouraged us from using them as models to develop peptide topoisomerase inhibitors as was planned initially. The PeptXX series was not much more successful, the level of activity displayed could not account for the activity of the alkaline hydrolysis mixture observed in Chapter III-1. In the light of our present knowledge this is not surprising: the initial observation of a species with a MW = 857 in the hydrolysate was very likely to be related to the inactive MccB17 by-product described in Chapter II-3. Interestingly the most active of our PeptXX compounds was the MccB17 "natural" fragment, the one containing two amide residues, the inhibitory activity seems to weaken with the replacement of amide residues by acid residues. None of the compounds were able to stabilise the gyrase-DNA cleavage complex. This was an additional clue showing the importance of these residues for MccB17 interaction with gyrase and the fact that the toxin is an "optimised" structure. Even if these results were disappointing, we had achieved inhibition of gyrase supercoiling with a small fragment of MccB17 at ten times the MccB17 inhibitory concentration, this is encouraging evidence that sub structures of MccB17 have the potential to produce good topoisomerase inhibitors.

2.3 Benzothiazole

This series of compounds derived from benzothiazole were reported as *Staphylococcus aureus (S. aureus)* inhibitors with an unknown target. All the benzothiazole series displayed in Figure 137 was kindly provided by our collaborator Marco Antonio Florio (Dipartimento Farmaco-Chimico, Università degli Studi di Bari).
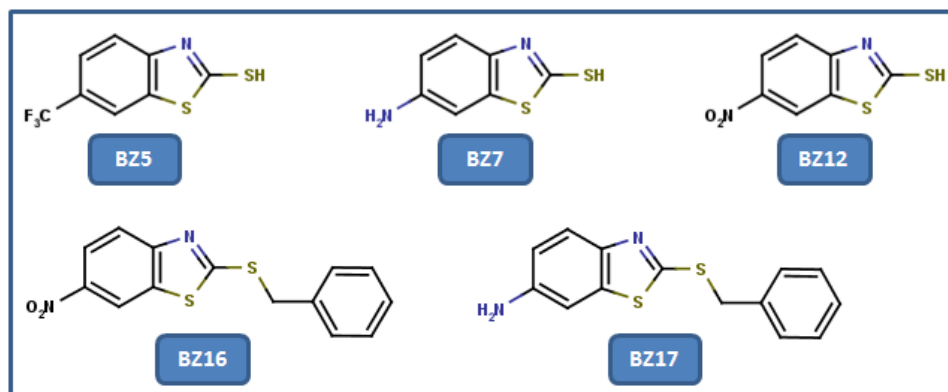
Figure 137 Structures and references of the benzothiazole series compounds

164

2.3.1 Evaluation of activity on *E. coli* gyrase

The activity of BZ compounds was first evaluated on *E. coli* gyrase using standard supercoiling assays. Preliminary results displayed strong inhibitory activity so concentrations ranging from 1 mM to 1 µM were used to obtain an approximate IC_{50}. The values were extrapolated by a linear regression of the percentage of inhibition observed on the gel as a function of the concentration for the point corresponding to 50% inhibition. The IC_{50}s values obtained, structure, and the *in vivo* activity on *S. aureus* (personal communication M. A. Florio (Dipartimento Farmaco-Chimico, Università degli Studi di Bari)) of the BZ compounds are summarized in Figure 138

Name	R_1	R_2	MIC *S.a.*	IC50 gyrase
BZ5	H	CF₃	4 µM	Not active
BZ7	H	NH₂	16 µM	Not active
BZ12	H	NO₂	128 µM	1 mM
BZ16	Ph	NO₂	not active	150 µM
BZ17	Ph	NH₂	not active	30 µM
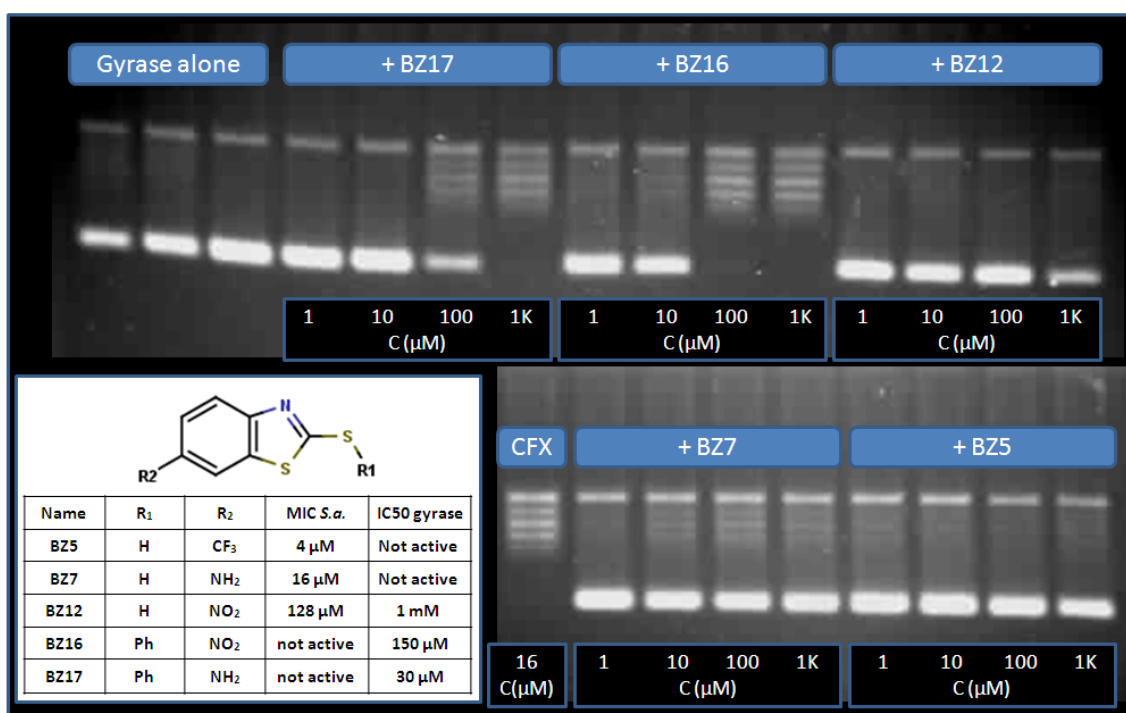
Figure 138 Supercoiling assays of the benzothiazole compounds and summary of evaluated IC$_{50}$ and MIC values reported for *S. aureus*: In this table can be seen the gel electrophoresis results of standard supercoiling assay reaction in the presence of 16 µM ciprofloxacin, or 1/10/100/1000 µM of the benzothiazole compound tested. The upper bands correspond to the starting relaxed DNA species, the lower band corresponds to the supercoiled DNA products. In the presence of an inhibitor (ciprofloxacin) the lower band loses in intensity in favor of the upper band. In the bottom left corner are summarised the IC$_{50}$s extrapolated from this gel by linear regression of percentage of the inhibition observed for the two points surrounding 50% inhibition; the reported MIC on *S. aureus* is present for information as well.

The BZ series had shown some interesting inhibitory activity on *E. coli* gyrase, surprisingly the most active compounds on *E. coli* gyrase are different from those that are active on *S. aureus*. This suggests that gyrase is unlikely to be the main target of the

benzothiazole series, but until these compounds are evaluated on the *S. aureus* gyrase this cannot be certain. To further characterize these active species, BZ16 and BZ17 were assessed in cleavage assays, but no stabilization of the gyrase-DNA cleavage complex was observed (data not shown).

2.3.2   Evaluation of activity on *Staphylococcus aureus* gyrase

Supercoiling assays were carried out with the BZ compounds on *S. aureus* gyrase as described in Chapter II. These assays were performed with the collaboration of Terence Chung (Dept Biological Chemistry, John Innes Centre).

Figure 139 Evaluation of Inhibitory activity of benzothiazole on *S. aureus* gyrase supercoiling: gel electrophoresis from samples of *S. aureus* supercoiling assay as described in Chap II in the presence of no drug, ciprofloxacin 17 µM, novobiocin 1 µM, or benzothiazole compound at 500 µM. The upper bands correspond to the starting relaxed DNA species, the lower band corresponds to the supercoiled DNA products. In presence of an inhibitor (ciprofloxacin) the lower band loses intensity in favor of the upper band. BZ5, BZ12 and BZ17 inhibit weakly the reaction at 500 µM.

Some inhibition of *S. aureus* gyrse supercoiling has been observed at 500 µM for the following compounds BZ17, BZ12, BZ5 in order of increasing inhibitory activity.

2.3.3   Evaluation of activity on human topo II

As the BZ compounds appeared to have a topoisomerase inhibitor profile, we decided to extend our study to human topo II. Relaxation assays were performed as described in Chapter I. Three compounds show inhibitory properties on topo II at 200 µM: BZ 12, BZ 16 and BZ17, the last being the most active and further assays placing its IC_{50} between 100 and 200 µM (Figure 140).
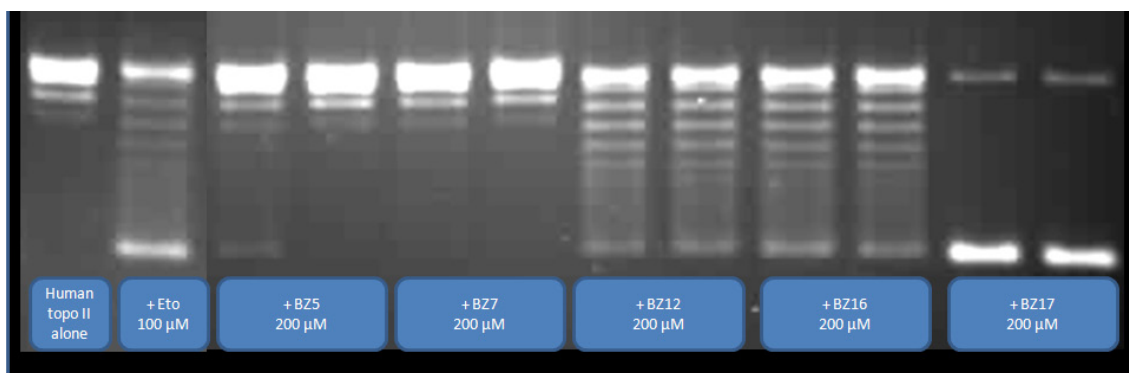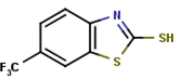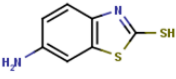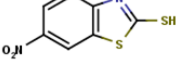
Figure 140 Evaluation of Inhibitory activity of benzothiazole on human topo II relaxation: gel electrophoresis from samples of standard topo II supercoiling assay as described in Chap II) in the presence of no drug, etoposide at 100 μM, or benzothiazole compound at 200 μM. The lower band corresponds to the starting supercoiled DNA species, the upper band correspond to the relaxed DNA products. In presence of an inhibitor (etoposide) the upper band lose in intensity in favor of the lower band. BZ12 and BZ16 inhibit the reaction at 200 μM at a lower level than the etoposide control.

2.3.4   Conclusion

The benzothiazole compounds have proved to be successful inhibitors on human topo II (BZ17 particularly) and *E. coli* gyrase (BZ16), but were not cleavage gyrase-DNA complex stabilizer for *E. coli*. The assays on *S. aureus* gyrase did not show a sufficient level of inhibitory activity to explain the antibacterial properties of the BZ series on *S. aureus*. It would be interesting to evaluate these compounds on *S. aureus* topo IV as weak inhibition was displayed on gyrase. This family of compounds might worth further investigation on human topo II as the inhibitory concentration of BZ17 not far from what we use for the etoposide control.

Table 9 Summary of benzothiazole compound activity on topoisomerases.

Ref. \ Conc. In μM		*E. coli* gyrase		human topo II	*S. aureus* gyrase
		supercoiling	cleavage	relaxation	supercoiling
BZ5		no inh at 1K	no	no inh at 200	~ 500
BZ7		no inh at 1K	no	no inh at 200	
BZ12		1 K	no	> 200	> 500
BZ16		30	no	> 200	
BZ17		150	no	100 < inh < 200	500

167

2.4 Prodiginines (SWH)

Prodiginines are pigmented tripyrrolic antibacterial compounds produced by actinomycetes and eubacteria. They have been shown to have a wide range of other therapeutic potential, immunosuppressant and antitumour agent for example. A series of compounds produced by the modification of the undecylprodiginine biosynthetic pathway have been provided by our collaborator Stuart Haynes (Greg Challis lab, Department of Chemistry, University of Warwick). As some of these compounds share some similarities with MccB17 heterocyclic residues we included them in this study and evaluated their inhibitory activity on a set of topoisomerases. The compounds are described in Figure 141 with the references allocated.
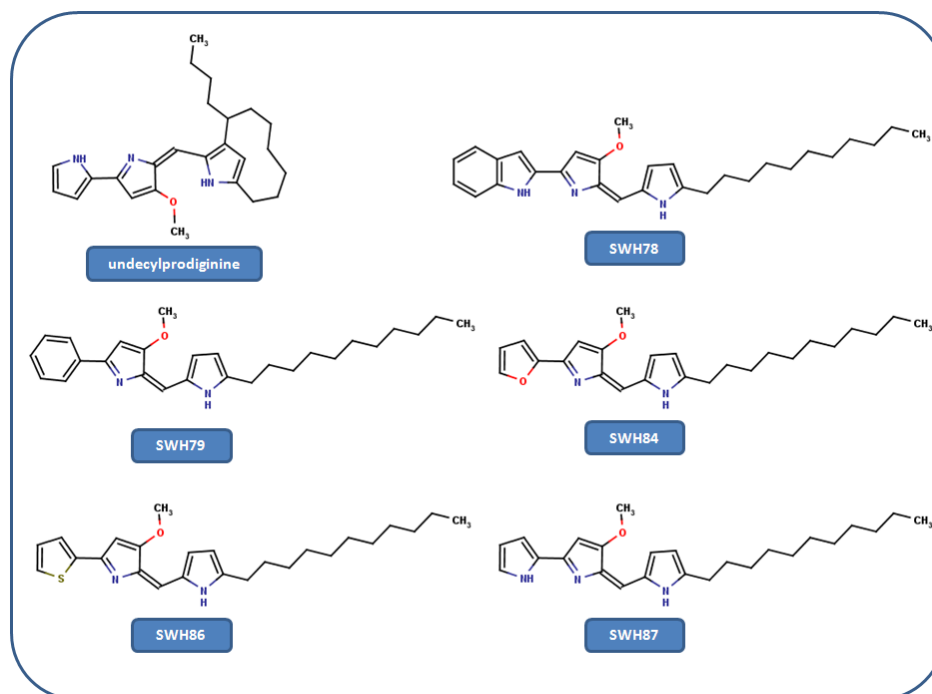
Figure 141 Structures and references of the prodiginines series compounds (SWH)

2.4.1 Evaluation on *E. coli* gyrase

The activity of prodiginines was evaluated in the gyrase supercoiling reaction. The inhibitory activity observed at 200, 66, 22 and 7 µM concentrations, were used to obtain approximate IC_{50} values as shown on Figure 142. Following this observation of a good inhibitory activity, the compounds were evaluated for their ability to stabilise the gyrase-DNA cleavage complex using standard cleavage assays (Figure 143).
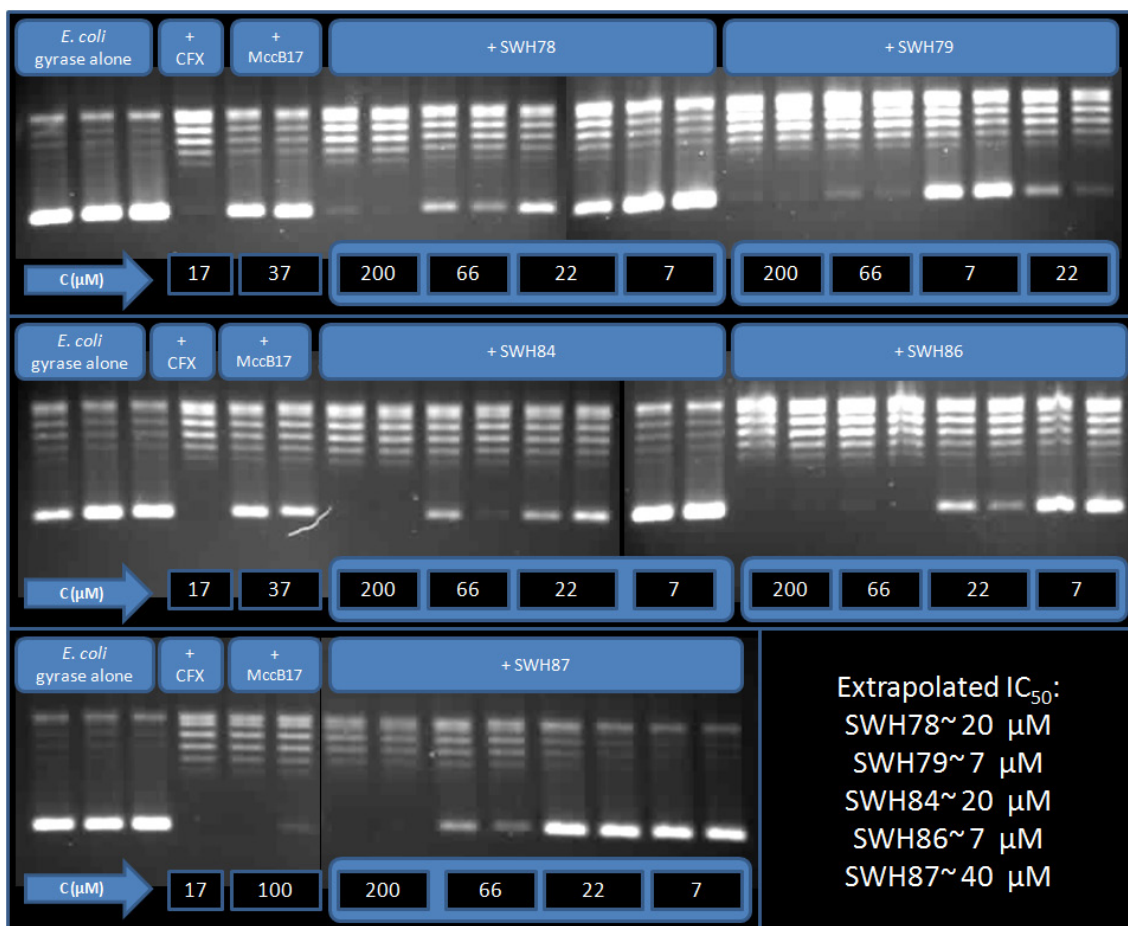
Figure 142 Supercoiling assays of the prodiginine series and summary of evaluated IC$_{50}$s : In this table can be seen the gel electrophoresis results of standard supercoiling assays in the presence of 17 µM ciprofloxacin, or 200/66/22/7 µM of the SWH compound tested. The upper bands correspond to the starting relaxed DNA species, the lower band corresponds to the supercoiled DNA products. In the presence of an inhibitor, the lower band loses intensity in favor of the upper bands (MccB17) or disappears if the inhibition is total (ciprofloxacin). In the lower right corner are summarized the IC$_{50}$ approximated from the plotted the percentage of inhibition observed on this gel versus the concentration of inhibitor.
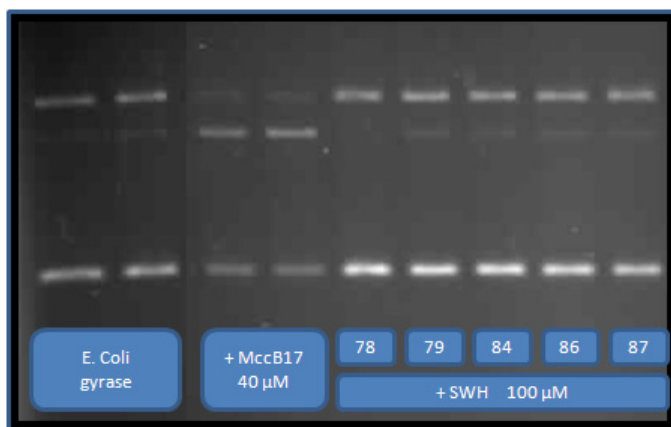
Figure 143 Evaluation of the stabilisation of the gyrase-DNA cleavage complex by prodiginines: gel electrophoresis of standard cleavage assays performed in presence of 40 µM MccB17 or 500 µM of SWH compound. The upper band represents the starting relaxed DNA, the lower band represents the produced supercoiled DNA. In presence of a cleavage complex stabilizer (MccB17) a new band corresponding to linear DNA appears between the two others. None of the compounds tested shows an increased level of linear DNA compared to the gyrase alone control.

2.4.2 Evaluation on human topo II

Following the success on *E. coli* gyrase, the prodiginine trial was extended to human topo II, all the compounds were tested at 200, and 100 µM. The results obtained at 100 µM are shown in Figure 144 (left). Compounds showing activity at 100 µM were subsequently assayed at 50 µM where only SWH84 was still active Figure 144 (right).
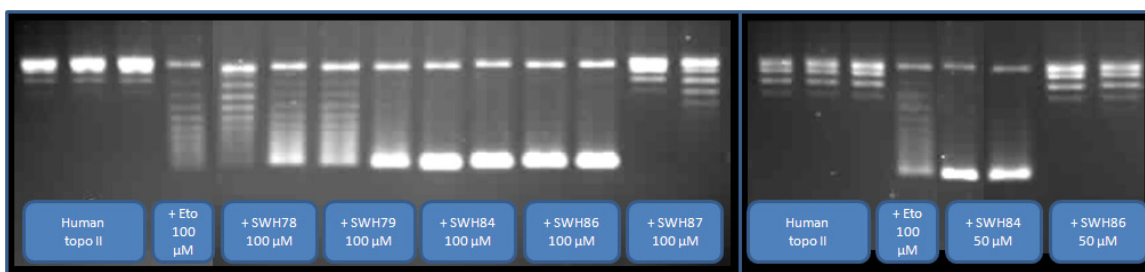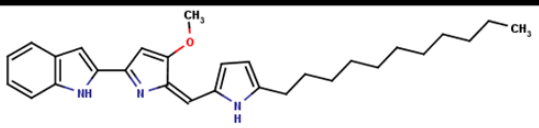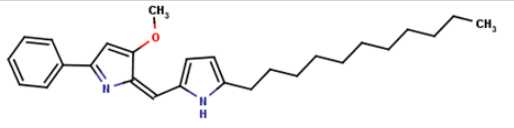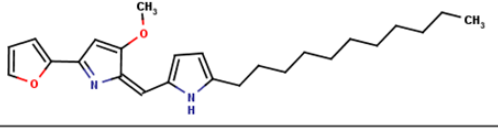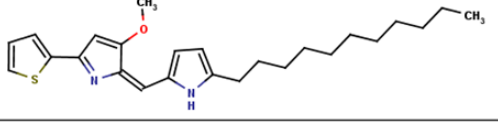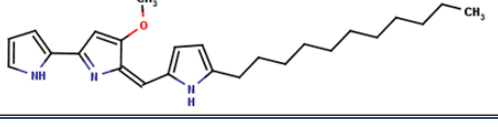
Figure 144 Evaluation of the Inhibitory activity of prodiginines on human topo II relaxation: gel electrophoresis from samples of standard topo II supercoiling assay in presence of no drug, etoposide at 100 µM, or SWH compound at 100 µM and 50 µM for SWH84 and SWH86. The lower band corresponds to the starting supercoiled DNA species, the upper bands correspond to the relaxed DNA products. In presence of an inhibitor (etoposide) the upper band lose in intensity in favor of the lower band. All prodiginines inhibit the reaction at 100 µM some of them at a higher level than the etoposide control. SWH84 displayed complete inhibition of relaxation at 50 µM.

2.4.3 Conclusion

The prodiginine derivatives displayed some promising properties as topoisomerase inhibitors both with *E. coli* gyrase and human topo II; these results are summarised in Table 10. SWH79 and SWH86 where the best inhibitors of *E. coli* gyrase with $IC_{50}s$ = 7 µM; this is comparable to the level of activity shown by ciprofloxacin in our assays. SWH84 was the best inhibitor of human topo II, with 100% inhibition at 50 µM, whereas etoposide had an IC_{50} of 100 µM in our assays. Interestingly the higher level of inhibition of *E. coli* gyrase and human topo II was achieved by different compounds in the series. This suggests that different features of the prodiginines are involved in the interaction with *E. coli* gyrase or human topo II, therefore prodiginine-inhibitors specific to *E. coli* gyrase or human topo II could be designed. Unfortunately in spite of these promising results, due to lack of time, no additional experiments were conducted on these compounds, although further investigation of this series will be planned in concert with our collaborators.

Table 10 Summary of the prodiginines activity on topoisomerases.

Ref. \ Conc. In µM	E. coli gyrase		human topo II
	supercoiling	cleavage	relaxation
SWH78	20	no	> 100
SWH79	7	no	~ 100
SWH84	20	no	< 50
SWH86	7	no	50 < inh < 100
SWH87	40	no	100 < inh < 200

2.5 Methylenomycin

Methylenomycins are antibacterial compounds produced by *Streptomyces coelicolor*. Two of these cyclopentanoid compounds have been studied here: methylenomycin A (MetA), methylenomycin C (MetC), their structures are described below in Figure 145. These compounds were kindly provided by our collaborator Christophe Corre (Greg Challis lab, Department of Chemistry, University of Warwick, Coventry).
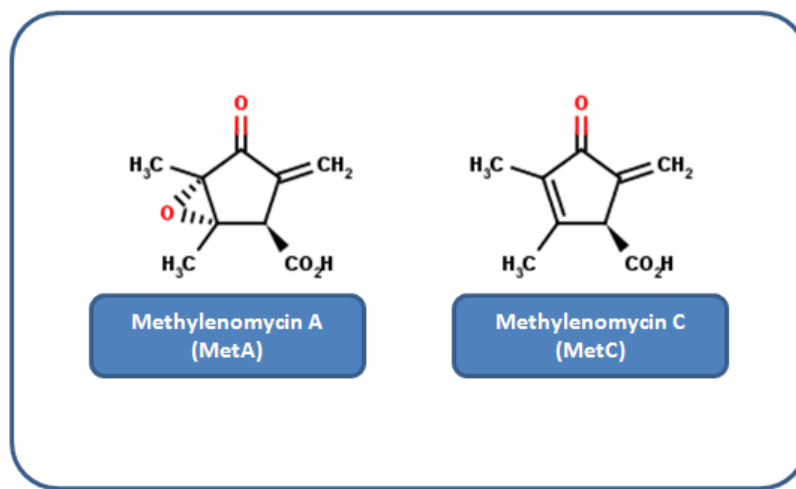
Figure 145 Methylenomycin A and C structures and references.

171

2.5.1 Evaluation of inhibitory activity on *E. coli* gyrase

The activity of the two compounds was assayed using standard supercoiling, relaxation and cleavage protocols. The various assays are shown in Figure 146. Gyrase supercoiling was inhibited by concentrations as low as 90 μM for MetA and 20 μM for MetC. The relaxation experiment was not so conclusive, very weak inhibition was observed. None of the compounds was able to stabilize the gyrase-DNA cleavage complex.
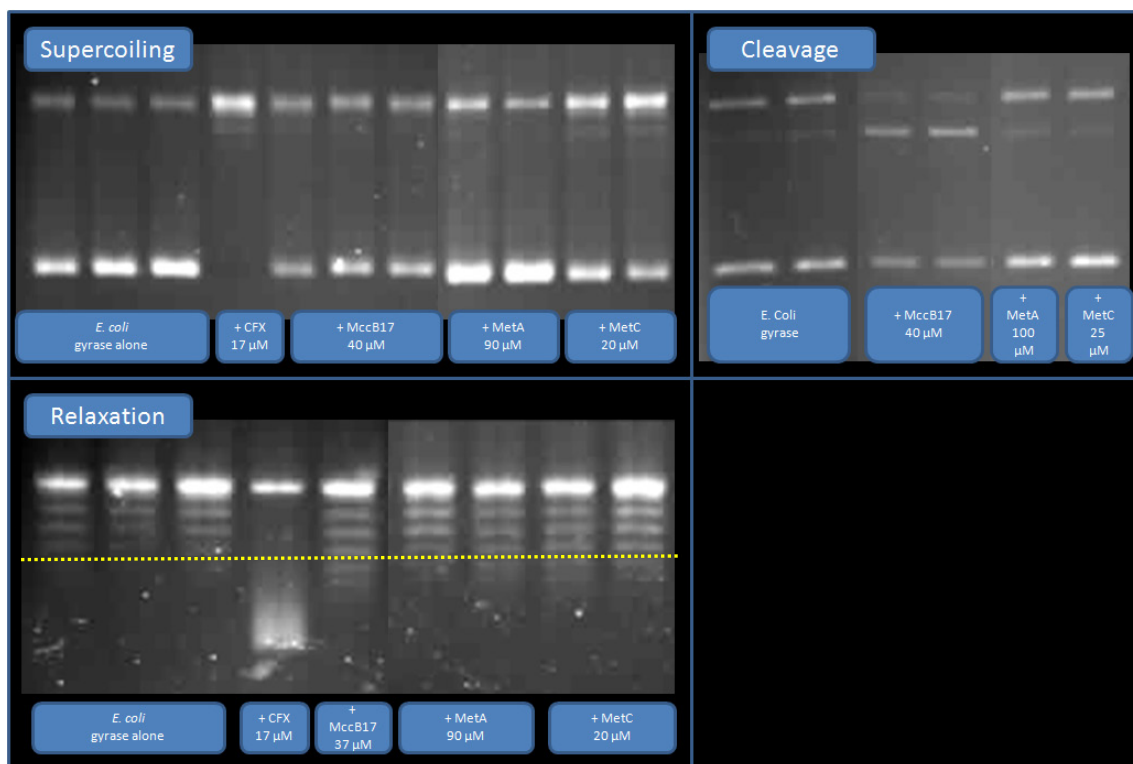
Figure 146 Supercoiling, relaxation and cleavage assays of methylenomycin A and C on gyrase:

Supercoiling: gel electrophoresis results of standard supercoiling assay reaction in presence of 17 μM ciprofloxacin, 40 μM MccB17 or 90 μM MetA or 20 μM MetC. The upper bands correspond to the starting relaxed DNA species, the lower band corresponds to the supercoiled DNA products. In the presence of an inhibitor the lower band loses intensity in favor of the upper band (MccB17) or disappears if the inhibition is total (ciprofloxacin). MetA shows a weak inhibition at 90 μM, MetC seems to give 50% inhibition of supercoiling at 20 μM.

Relaxation: gel electrophoresis results of standard relaxation assay reaction in presence of 17 μM ciprofloxacin, 40 μM MccB17 or 90 μM MetA or 20 μM MetC. The lower band corresponds to the starting supercoiled DNA, the upper band correspond to the relaxed DNA products. In the presence of an inhibitor the lower band loses intensity in favor of the upper band (ciprofloxacin). A very weak inhibitory effect is observed for the two compounds at their respective concentration, similarly to the MccB17 control in this experiment (the ladder of relaxed species is larger for MccB17, MetA and MetC compared to gyrase alone).

Cleavage: gel electrophoresis of standard cleavage assays performed in presence of 40 μM MccB17, 100 μM MetA or 25 μM MetC. The upper band represent the starting relaxed DNA, the lower band represent the produced supercoiled DNA. In presence of a cleavage complex stabilizer (MccB17) a new band corresponding to linear DNA appears between the two others. None of the compounds tested increased the level of linear DNA compared to the gyrase alone control.

2.5.2 Evaluation of inhibitory activity on human topo II

As the two methylenomycins show activity on *E. coli* gyrase their evaluation was extended to human topo II. Their inhibitory activity was evaluated using standard topo II relaxation assays with concentration of compounds of 100 μM and 200 μM. MetA did not show any inhibitory activity at 200 μM. MetC displayed complete inhibition of relaxation at 100 μM, which is a stronger effect than the etoposide control (Figure 147).
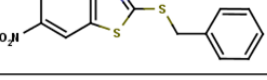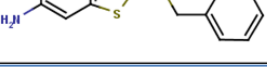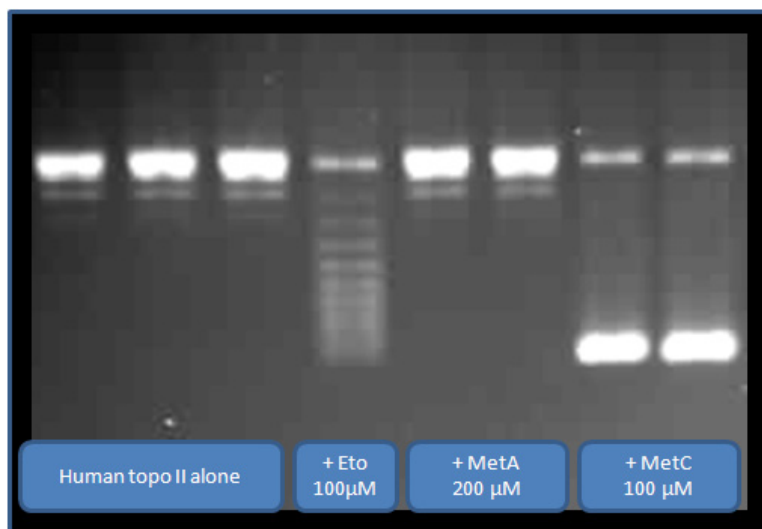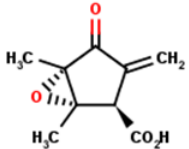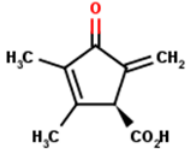

Figure 147 Evaluation of Inhibitory activity of Methylenomycin A and C on human topo II relaxation: gel electrophoresis from samples of standard topo II supercoiling assay in the presence of no drug, etoposide at 100 μM, or methylenomycin at 200 μM or 100 μM. The lower band corresponds to the starting supercoiled DNA species, the upper band corresponds to the relaxed DNA products. In the presence of an inhibitor (etoposide) the upper bands lose intensity in favor of the lower band. MetC inhibit the reaction at 100 μM at a higher level than the etoposide control.

2.5.3 Conclusion

From the two methylenomycin compounds MetC was the most active on both *E. coli* gyrase (20 μM) and on human topo II (<100 μM), MetA was fifty times less active on gyrase and not active on topo II. The significant difference of activity between the two compounds is quite surprising as they only differ by the presence of an epoxide function in MetA where MetC has a double bond. This difference of activity might indicate that the "flatness" of MetC in this region of the molecule is important for its activity, and thus should be conserved if derivatives are generated. Although these results are promising, they were preliminary and will require validation before the series can be further investigated.

Table 11 Summary of methylenomycins activity on topoisomerases.

Ref. \ Conc. In µM	E. coli gyrase		human topo II
	supercoiling	cleavage	relaxation
MetA	1K	no	no inh at 200
MetC	20	no	< 100

3 Activity of compounds related to MccB17 on *E. coli* cells

The heterocycles from MccB17, the pyrroles compounds and the heptapeptides described above were submitted to *in vitro* test on *E. coli* colonies. Two different strains were used for the halo assays: MG1655 a standard *E. coli* strain and NR698, an *E. coli* drug-permeable strain that has been described in chapter II. The halo assays were performed using the following method: 200 µl of overnight culture of either MG1655 or NR698 were added to 3 ml of molten LSS agar, after gentle mixing the mixture was poured onto a LB agar plate to form a homogeneous layer. Drops of 2 µl of DMSO containing the drug tested were laid down on the surface of the agar plate. The plate was incubated overnight at 37°C before being read. The table below summarizes the level of inhibitory activity observed for the various compounds on the two strains, a custom reference system that was created to classify the level of inhibition observed is detailed as well. The inhibitory activity on *in vivo* growth of MG1655 and NR698 observed with the different compounds were in no case comparable to the MccB17 control, inhibition was lower than MccB17's with concentrations at least fifty times higher. The best inhibitors were the two Fmoc-pyrrole compounds. The overall low inhibitory activity displayed can be explained by a low uptake of the compounds used: MccB17 benefit from an active transport system, OmpF in the outer membrane and SbmA in the inner membrane to reach its target; probably no transport system is available to bring the compounds assayed to their target. The increased inhibition of growth observed on NR698 compared to MG1655 supports this hypothesis, as the outer membrane is permeable to the compounds it removes one of the barriers on the way to their potential target, but the inner membrane still remains to be crossed.

Compound	Conc.	Halo on MG1155 Size (mm)	Potency	Halo on NR698 Size (mm)	Potency
DMSO alone		No effect		No effect	
MccB17	55 µM	10 (5)	Medium (strong)	10	Strong
Boc-tz-OH	30 mM	2	V. weak	3	V. weak
Boc-tz-Ser-OMe	30 mM			3	V. weak
Boc-tzoz-OMe	30 mM	2	Weak	3	Weak
Boc-tzoz-OMe	3 mM			3	Weak
Boc-tzoz-OH	30 mM	3	V. weak	4	Weak
H-tzoz-OH	30 mM	3	V. weak	4	V. weak
Boc-oztz-OEt	30 mM			4	V. weak
Boc-oztz-OH	30 mM			3	V. weak
Fmoc-2,5pyr-OH	30 mM	4.5	Medium	5	Strong
Fmoc-2,5pyr-OH	3 mM	4	Medium	5	Medium
Boc-2,5pyr-OEt	30 mM	3	Weak	4	Weak
Boc-2,5pyr-OEt	3 mM			4	Weak
Fmoc-2,4pyr-OH	30 mM	4	Medium	5	Strong
Fmoc-2,4pyr-OH	3 mM			4	Weak
Hept-pyr	30 mM	2	V. weak	4	Weak
Hept-tz	30 mM	3	Weak	4	Weak

Strong: visible on a black background, nearly 100% cells killed.

Medium: visible on a black background, not all cells killed.

Weak: can only be seen with a white lighting from behind.

V. weak: can only be seen with raking light illumination.

Table 12 Summary of *in vivo* activity of the MccB17's heterocyclic compounds, pyrroles, and heptapeptides series on wild type and permeable *E. coli* strains: the table details the size of the halo created by a 2 µl drop of DMSO containing the concentration described in the table under Conc. on an agar plate layered either with the wild type strain MG1655 or the drug-permeable strain NR698. Only the Fmoc-pyr compounds displayed inhibitory activity equivalent to MccB17 but at higher concentration. On the right side is defined the reference system used to characterize the level of inhibition.

4 Summary

The *in vitro* assays results obtained in this chapter are summarized in Table 13. The various compounds are colour-coded by family, written in red are the reference compounds used in the assays.

Table 13 Summary of the inhibitory activity observed on various topoisomerases with the series of compounds described in this chapter

Ref. \ Conc. In µM	*E. coli* gyrase			gyr W751R	*E. coli* topo IV	human topo II	*S. aureus* gyrase
	supercoiling	relaxation	cleavage	supercoiling	relaxation	relaxation	supercoiling
Boc-oz-OMe	no inh at 1K						
Boc-oz-OH	no inh at 1K						
H-oz-OH	no inh at 1K					no inh at 500	
Boc-tz-OH	> 1K	1 K				weak inh at 300	
H-tz-OH	> 1K						
Boc-tz-Ser-OMe	> 1K						
Boc-tzoz-OMe	1 K > inh > 500		no	1 K			
Boc-tzoz-OH	500 > inh > 200			1 K			
H-tzoz-OH	500 > inh > 50	1 K	no	1 K		weak inh at 300	
Boc-oztz-OEt	< 500		no	1 K			
Boc-oztz-OH	< 500						
H-oztz-OH	500					< 500	
Fmoc-2,5pyr-OH	250	< 1 K	no				
Fmoc-2,4pyr-OH	250						
Boc-2,5pyr-OMe	no inh at 1K						
H-2,5pyr-OH	no inh at 1K						
Fmoc-tzoz-OH	500 > inh > 50						
Hept-tz	>1K		no		1 K	no inh at 333	
Hept-pyr	>1K		no		1 K	no inh at 333	
PeptQN	< 500		no			no inh at 250	
PeptEN	500		no			no inh at 250	
PeptQD	no inh at 500		no			no inh at 250	
PeptED	>500		no			no inh at 250	
BZ5	no inh at 1K		no			no inh at 200	~ 500
BZ7	no inh at 1K		no			no inh at 200	
BZ12	1 K		no			>200	>500
BZ16	30		no			>200	
BZ17	150		no			100 < inh < 200	500
SWH78	20		no			>100	
SWH79	7		no			~ 100	
SWH84	20		no			< 50	
SWH86	7		no			50 < inh < 100	
SWH87	40		no			100 < inh < 200	
MetA	1K		no			no inh at 200	
MetC	20		no			< 100	
MccB17	40	40	yes	no inh	no inh at 40		
CFX	7	7	yes	7	<17		17
Etoposide						100	

176

5 Conclusion

The Investigation of the activity of small molecules containing heterocyclic moieties on various topoisomerases was described in this chapter. We started with the heterocyclic amino acids found in MccB17 both in their natural or chemically protected form. Although inhibitory activity displayed by these compounds was observed around 500 µM at best, it implies that some of these structures are interacting with gyrase with a low affinity and might prove a good starting point to build up series of topoisomerase inhibitors. This is supported by the results obtained with the alkaline hydrolysate described in Chapter III, where even if no precise compound has been identified, there are strong hints that the mixture contains such heterocyclic derivatives. The evaluation of compounds directly related to MccB17 was followed by the study of compounds more remotely related to these structures. In the three series of molecules provided by our collaborators we have found promising hits that inhibits *E. coli* gyrase in the same range as MccB17 or ciprofloxacin, and topo II at the same range as etoposide. Although the results gathered were preliminary and will require further validation, they will be pushed forward with our collaborators in the near future. The results obtained with benzothiazoles, prodiginines, and methylenomycins compounds once validated will open these chemical families for the design of potential new topoisomerase inhibitors. Unfortunately, none of the compounds studied in this chapter was able to stabilize the gyrase-DNA cleavage complex which would be the real breakthrough in antibacterial drug discovery we were aiming at. Although it is still possible that such property can be attained by building more complex structures based on MccB17's heterocycles.

CHAPTER V
Discussion

CHAPTER V Discussion

Over the previous chapters we have described the various approaches carried out on MccB17 to understand its mechanism and use it as a template to generate topoisomerase inhibitors. After describing the various antibacterial agents and their mechanism, we had put a special focus on topoisomerases. We mentioned the successful exploitation by the fluoroquinolone drugs of two topoisomerases, gyrase and topo IV, through a mechanism called topoisomerase poisoning. Placing MccB17 in the context of the present antibacterial agent crisis, we highlighted its importance as one of the rare non-quinolone structures able to poison gyrase. We had described how we planned to explore MccB17 activity and its structure as a potential source for small molecule topoisomerase inhibitors over three aspects: the first focusing on the mechanistic aspect of MccB17 action, the second involving the fragmentation of the toxin and evaluation of the resulting species, and finally the evaluation of the heterocyclic moieties that characterise MccB17 and some related species. We will cover this last part first as it stand aside from the other results.

Previous studies suggested that some of the heterocyclic amino acids found in MccB17 had some inhibitory activity on gyrase by themselves. As we were planning to build on such structures to generate new topoisomerase inhibitors, we evaluated the activity of the various heterocyclic residues found in MccB17, and incorporated as well various protected intermediates in the study. The level of activity we observed was weaker than what we expected, thiazole, bis-heterocyclic amino acids and their protected counterparts showed inhibition of gyrase at ~ 500 µM at best. The compounds were not able to poison gyrase, and were affecting MccB17-resistant gyrase at the same concentration as the wild type. This evidence suggested that their mechanism of inhibition was unrelated to MccB17's; this, added to their weak activity observed, discouraged us from performing further investigation. However, three families of related compounds were investigated as well: benzothiazoles, prodiginines and methylenomycins. Interestingly in each family were found compounds able to inhibit gyrase to some degree, the best were: BZ16 at 30 µM for the benzothiazole, SWH79 and SWH86 at 7 µM for the prodiginines, and methylenomycin C at 20 µM for the methylenomycins; none of them were able to stabilize the gyrase-DNA cleavage complex. These preliminary data are encouraging to investigate further these chemical families. It will be important first to clarify the compound's mechanism of action, knowing if it involves the ATPase activity of the enzyme for example; this can be done by using relaxation assays or ATPase assays. Another possibility is the generation of spontaneous mutations of gyrase *in vivo* that confer resistance to the best compound identified; the location of these mutations will give insight into the mode of action of these different compounds. Finally the structure-activity relationship for each group can be built by assaying a set of compounds covering a range of chemical variations for each family. The prodiginine family seems the most promising, as all its members have their inhibitory activity below 40 µM, with the best at 7 µM, which is close to the ciprofloxacin IC_{50} in our assays. The only downside of the prodiginines is their high

lipophilicity (calculated LogP $_{SWH86}$ = 5.3 and LogP$_{SWH79}$ = 5.5, Lipinski rule advise LogP < 5), which limits their solubility and will probably hinder their uptake.

One aspect we wanted to tackle here was the molecular basis of MccB17 interaction with gyrase. To address this we relied on isolating spontaneous mutations mapping to gyrase and conferring resistance to MccB17 *in vivo*. As previous studies reported that most resistance to MccB17 were due to uptake impairment, we considered using a strain with an increased permeability to chemicals. Unfortunately none of the MccB17-resistant mutants isolated carried mutations on gyrase. It appeared that the resistance observed were caused by mutation of the MccB17 transporter SbmA in the inner membrane; this was confirmed by the fact that strain resistant to MccB17 were also resistant to bleomycin, which uses the same transporter. The only spontaneous mutation leading to resistance to MccB17 reported so far in the literature is GyrB W751R (Vizan, Hernandez-Chico et al. 1991; del Castillo, del Castillo et al. 2001). The mutant was isolated from strains modified to overexpress SbmA, after discarding colonies where resistances were caused by outer membrane mutations, which were representing the majority of resistant colonies. By modifying our permeable strain NR698 to overexpress SbmA, we will avoid all possible resistance linked with the uptake of the toxin, thus increasing the possibility that resistance will arise by mutation of the MccB17's target, gyrase. Even if this part of the work did not yield the information we were expecting, we found a way to address this problem in the future, with confidence about a positive outcome. Dealing with the *in vivo* resistance mechanism to MccB17, we became aware of the critical role of the uptake system for MccB17 action, and how easily bacteria can acquire a way to protect themselves against the toxin. Taking that into account, we should aim at new antibacterials derived from MccB17 that are not dependent on this uptake system. In future work, early tracking of the emergence of resistant colonies to a given MccB17 derivative should be kept in mind.

The central question in this study was: which features of MccB17 are responsible for its activity, and can they be copied to produce new antibacterial agents? Elements from both the study of the whole MccB17 molecule in Chapter II and the generation and evaluation of MccB17 fragments in Chapter III led to convergent evidence regarding these aspects. The first major discovery was the fact that removal of terminal amino acids affects differently the activity of the toxin depending if they belong to N- or C-terminus of the peptide. This was first hinted by a MccB17 species, present as the main component of a fraction isolated from the digest of MccB17 by subtilisin: the MccB17 derivative, even if it was lacking the four N-terminal amino acids, seems to have its activity unaltered. To complement this information, the effect of shortening the C-terminus on MccB17 activity was studied by digesting the peptide with the exoprotease Carboxypeptidase A. The resulting mixture contained mainly a species corresponding to MccB17 lacking the last C-terminal residue, an isoleucine. Other species observed in lower amounts were corresponding to species lacking two and three C-terminal amino acids. The mixture did not show any inhibitory activity on gyrase supercoiling at twice the usual MccB17 concentration. These two experiments suggested that modification of the N-

terminus of MccB17 did not alter its activity whereas alteration of the C-terminus was highly detrimental to its activity. To validate this hypothesis we produced the species observed in the two experiments as pure compounds, by site-directed mutagenesis of the *mcbA* gene coding for MccB17 sequence in the *pmcb17* plasmid, and transformation of *E. coli* DH5α. A stop codon was used to remove up to 4 C-terminal amino acids, whereas the substitution of a glycine by a lysine followed by a tryptic digest removed the substituted and upstream amino acids from the N-terminus. Evaluation of the MccB17 species lacking C-terminal amino acids shows a significant decrease of activity directly linked with the number of amino acids removed. An even more drastic loss of the ability to stabilize the cleavage complex was observed with the removal of the amino acid. The species lacking four N-terminal amino acids retain, as observed before, its full inhibitory activity on gyrase and its ability to stabilize the cleavage complex. The tolerance of the N-terminus of MccB17 to modification confirms what was earlier hypothesised in the literature about MccB17 synthetase: the N-terminus residues are mainly involved in the maturation of the peptide as a spacer necessary for synthetase activity. The sensitivity of the C-terminus on the other hand suggests a more critical role in MccB17 antibacterial activity. This finding opens some interesting perspectives to produce a "minimal MccB17" as a working template, which will be a MccB17 where all the N-terminal residues unnecessary for the stabilisation of the cleavage complex have been removed. We had demonstrated that a derivative with eight glycine residue upstream of the A site is as active as MccB17, but how many glycines are really required to maintain the gyrase-poisoning activity. If this area of MccB17 is only a spacer required for processing the toxin, as we think it is, it is possible that a MccB17 derivative starting at the A site or with only a few glycines upstream will still be active. Let us imagine that a compound corresponding to MccB17 where the first 10 N-terminal residues have been removed leaving only two glycines upstream of the A site is active. This compound would have a MW =2425 which is a ~20% decrease in MW compared to MccB17, and two less lipophilic residues, Val and Ile; these modifications represent a significant improvement toward drugability.
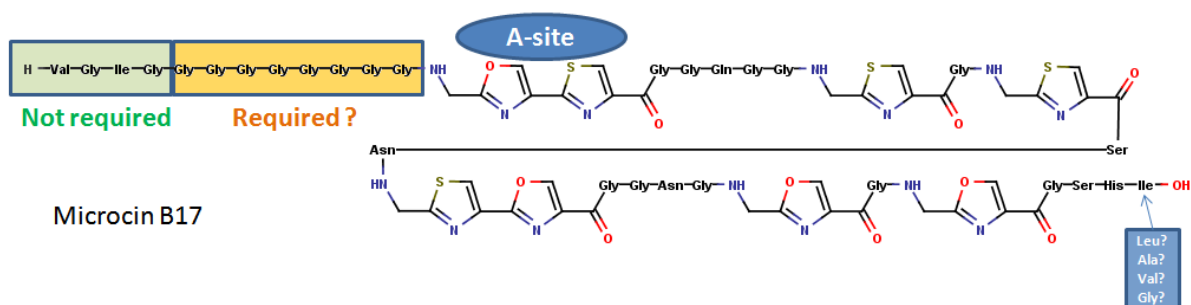
Figure 148 MccB17 modification area: the green box shows the amino acids that have been successfully removed without altering the peptide activity. The yellow box shows residues that can be removed by proteolytic or chemical methods to evaluate their importance. The blue box shows the variation we consider to characterise the essential C-terminal Ile.

Once the "minimal MccB17" template is identified, the next step will be to evaluate if the remaining glycines upstream of the A-site can be substituted by other residues to increase the affinity of the peptide for the cleavage complex. Concerning the C-terminus, we revealed that removing the terminal isoleucine is detrimental to the toxin activity, and further removal of residues kills completely the activity. But what is the cause of the loss of activity observed when the Ile is removed, is it due to the loss of specific interaction of this residue with a lipophilic pocket? In that case replacement of the Ile by another lipophilic residue of similar size should not be too detrimental for the activity of the resulting compound. Another possible reason for the loss of activity is that removing the Ile residue causes the shift of the negatively charged carboxylate group from the Ile end to the His end, this can have a destabilizing effect on the DNA-gyrase-peptide complex if repulsive electrostatic interactions take place at the new position of the carboxylate group. In this case, the substitution of the C-terminal Ile by a Gly should restore the position of the carboxylate and lead to an active compound. Answering these questions will be a real breakthrough in the understanding of MccB17 structure-activity relationships. To investigate further the modification of the N-terminus of MccB17, the application of site directed mutagenesis techniques seems the obvious choice to address this issue. The only limitation is that the introduction of a Lys residue in the vicinity of the A site may prevent its processing, and generally hinder the toxin production. An alternative will be to consider again the exopeptidase digest strategy; it will probably worth optimising the conditions we have used with the Leu-aminopeptidase, as only one unsuccessful attempt was made and was not studied further as we obtained what we wanted from a different method. It might be sensible to consider different aminopeptidases as well. These two methods have their advantage and drawbacks: if similar results to what we obtained with the Carboxypeptidase A can be achieved with an aminopeptidase, then the aminopeptidase digest of MccB17 can be set up to remove the required N-terminal amino acid from MccB17. The exoprotease digest reactions are straightforward once the optimisation is done, and usually give very good yield, the downside of the method being that we had only a relative control over the species produced, and the final product is likely to be the expected compound as the main component in mixture with other species with one more or one less amino-acid. The site-directed mutagenesis on the other hand produces a single compound with good purity, but there is no certainty that it will be processed, and the yield is unpredictable. Site-directed mutagenesis is the method of choice to generate MccB17 C-terminal mutants as there is no problem with the processing due to the position of the change. An alternative method for the N-terminal modification we have considered lately, but had not tried, is Edman degradation. This method is usually applied for peptide sequencing, but it is applicable in our case to remove the N-terminal residues of MccB17. By reacting an amino group with phenylisothiocyanate, this method transforms the N-terminal residue of a peptide into a phenylthiocarbamyl in moderate alkaline conditions (pH = 8). The shift to acidic conditions causes the phenylcarbamyl-N-terminal residue to cyclise into a thiazolinone, thus releasing the peptide minus one residue. The thiazolinone is recovered to be analysed; heating it in acidic conditions converts it into a phenylthiohydantoin, which is a better analyte for electrophoresis or chromatography. In our case, by only using the two first steps, and removing the thiazolinone with an organic extraction with solvent where MccB17 is not soluble, we should be able to remove one N-terminal amino acid from MccB17. Repeating this process over a defined number of cycles will produce MccB17 lacking the desired number of residues on its N-terminus. Such a method will require some experimental set up, but it is routinely applied to peptides for sequencing and

the solvent system is compatible with MccB17, we are confident that it will yield the expected results.

More drastic alteration of MccB17 has been explored by cutting it into fragments. The initial means used to fragment MccB17 was the non-selective hydrolysis of its peptide bonds by sodium hydroxide. It had been reported in previous work that such treatment led to a mixture of small fragments that can inhibit gyrase activity. We followed the same approach with the intent of using purification methods to isolate the different components of the mixture and identify the inhibitor(s). We observed as well the effect of the hydrolysate mixture on gyrase supercoiling, but no stabilization of cleavage complex. Our efforts to isolate the active component(s) were unfruitful. We decided to use a more selective method involving the proteolytic cleavage of MccB17 to generate large fragment as potential gyrase inhibitors or poisons. During the production of MccB17 we observed that some by-products turned out to be fragments of MccB17; these "spontaneous" fragments were integrated into our set of evaluated MccB17 fragments. Initially we were wondering if these fragments were resulting from the degradation of MccB17 in the conditions used to extract the toxin from the producing cells, or if they were by products from the biosynthesis in the cell. Interestingly these "spontaneous" fragments were observed repeatedly in the proteolysis experiments as well, suggesting that they are likely to be spontaneous products from MccB17 degradation in the experimental conditions. Lately we realized that some of these "spontaneous" fragments were, to our surprise, active. This was both good and bad news, on one hand we had substructures of MccB17 that can be easily generated and that possess interesting inhibitory properties. On the other hand, in the meantime, the digest of MccB17 by subtilisin had successfully yielded mixtures active on gyrase, but they were containing as well some of these "spontaneous" fragments, making us worried that the observed inhibition was only due to these compounds, and not from any specific subtilisin cleavage. Fortunately, as we have used different conditions in the course of our proteolysis experiments, these "spontaneous" fragments were produced in various amounts depending on the experiment, whereas the level of activity observed was nearly constant. This was confirmed by some of the fractions isolated from the HPLC purification from MccB17 digest by subtilisin were active and did not contain any "spontaneous" fragment.

Fragments in active fractions																												
Sequence																												
V	G	I	G	7xG	G	oztz	G	G	Q	G	G	tz	G	tz	S	N	tzoz	G	G	N	G	oz	G	oz	G	S	H	I
									1861.559																			
											1747.515																	
1700.573:													1410.595															
1374.374										?			1393.571															
Inactive fragments																												
923.395												1209.407																
													774.309															

Figure 149 Summary of MccB17 fragmentation results: the top part of the table shows fragments that are present in the active fractions as the main components. The lower part shows identified inactive proteolytic fragments.

In spite of our effort to separate the components of the various active mixtures, we were not able to isolate and identify the active entities. The species observed in the active fraction over our different experiments narrowed the possibilities to a list of a few candidate compounds. Interestingly, these compounds are related to two main area of MccB17 as shown

in Figure 149, this list is completed with a few other compounds that were present as the main component in fractions with no inhibitory activity on gyrase. By comparing the active and inactive fragments we can start to formulate a hypothesis about the requirements to have a gyrase inhibitor.

The most significant information we can get from Figure 149 is the comparison of Mw = 1393.4 and 1410.6 which are active at ~100 μM, with MW = 1209.4 which is not. MW = 1410.6 and 1209.4 differ only by two amino acids on the N-terminus, Ser-Asn, whereas MW = 1393.6 is a derivative from MW= 1410.6 by loss of ammonia. This suggests that these two amino acids are of some importance in the interaction with the gyrase-DNA complex. Furthermore supporting the importance of this Asn residue, is the fact that when Asn residues in MccB17 were converted to Asps, we observed a loss of the ability to stabilize the cleavage complex, and at least a two-fold decrease in the inhibition of gyrase supercoiling. This evidence implies that the MW=1410.6 fragment might be one of the minimal structures necessary to duplicate MccB17 inhibition of gyrase. Unfortunately we have only preliminary data, but they suggest that these compounds are not able to stabilize the cleavage complex. Slightly contradictory is the fact that MW = 1700.6, which is the complementary part of MccB17 to MW = 1410.6, has some inhibitory activity on gyrase supercoiling between 100 and 300 μM (and no cleavage complex stabilisation), and MW = 1374.4 is among our active candidates. On the other hand if we compare the structure it appears that they share a common pattern of residues distribution: bisheterocycle, amide, heterocycle, heterocycle, each feature separated by a glycine spacer. This arrangement of residues can be interpreted as a scaffold that can bind to the gyrase-DNA complex. In the case of MW=1410.6 there is the Ser-Asn that is missing in the inactive MW = 1209.4 at one end, and the Ser-His-Ile that is critical to the whole MccB17 on the other end, these two fragments adding favourable interaction with gyrase whereas they are absent in MW=1700.6, explaining the difference of activity. The long glycine tail in MW=1700.6 can be an additional source of destabilisation.
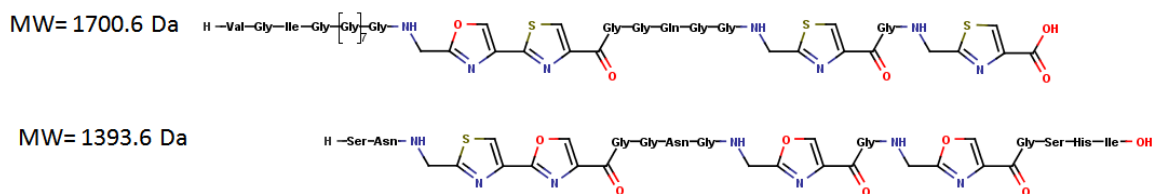
Figure 150 Comparison of the two halves of MccB17: alignment of fragment 1700.6 and 1393.6 display their similarities in the distribution of their heterocyclic and amide residues.

The question arising is what these structures are lacking to be able to stabilize the cleavage complex? It may be that they need an extra interaction with the gyrase cleavage complex to have the proper fit, and that can be achieved by the addition of a hydrogen bond donor/acceptor or a lipophilic/aromatic residue in the right place. The other possibility is that the whole two sequences are required to stabilize the gyrase-DNA complex. A partial answer can be given by testing if an equimolar mixture of MW = 1700.6 plus MW = 1393.6 is able to stabilize the cleavage complex, unfortunately that experiment would require us to isolate each compound alone, and separation of MccB17 fragments was one of the major issues in this

work. If the whole sequence of heterocycles is required, it seems difficult to reproduce the effect of such a large molecule, but this not certain until we know exactly what the mechanism of MccB17 action is.

As a summary, we can say that the heterocyclic amino acids found in MccB17 do not have a strong activity by themselves, and the weak effect observed was probably not related to the MccB17 mode of action. Substructures of MccB17, about half the size of the toxin, have inhibitory activity on gyrase between one to five times the MccB17 concentration; we did not get precise inhibitory concentration because the different species couldn't be isolated as pure products. Preliminary experiments suggest that these fragments are not able to stabilise the cleavage complex, but further study should validate this fact. Considering the variation observed during the assays over various mixtures it is possible that different fragments can act synergistically mimicking the effect of the whole MccB17, but this will require better purification techniques to be addressed. The two main fragments of MccB17 that have shown activity have a common arrangement of heterocyclic and amide residues, this pattern (Figure 151), and can be viewed as a potential template to design a synthetic chemical library of potential gyrase inhibitors.
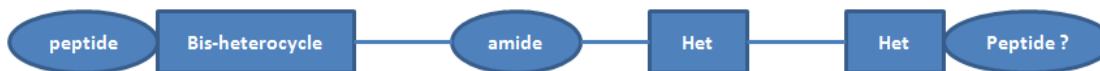
Figure 151 Schematic of the template inspired by MccB17 fragments for new synthetic topoisomerase inhibitors.

Considering the whole MccB17, we demonstrated that the removal of residues from the N- and C- terminus of the native MccB17 had different effects on its activity: the modification of the C-terminus is very detrimental to the toxin activity whereas the N-terminus can tolerate the loss of at least four amino acids without any alteration of activity. Based on these data, we suggest that N-terminal amino acids can be removed further to identify at which point a loss of activity can be monitored and thus define a "minimal" MccB17 structure able to poison gyrase. Such a structure would not only be useful to define the structural requirements for the activity, but would be a formidable tool for further structural studies. Peptide toxins have proved that they can adopt unusual structures and modes of action. CcdB and MccJ25, that have been mentioned before, illustrate perfectly how structural information can be critical with such compounds: CcdB's mode of action was only really understood when the crystal structure of a fragment of GyrA and CcdB was solved, and shows how the CcdB dimer was filling a space created by gyrase conformational change during its cycle in the GyrA dimer and creating a dead end in the cycle, preventing gyrase from closing back its DNA gate, and thus stabilising the cleavage complex. Before these structural data were released, biochemical evidence was not able to give a coherent picture of the mechanism of CcdB.
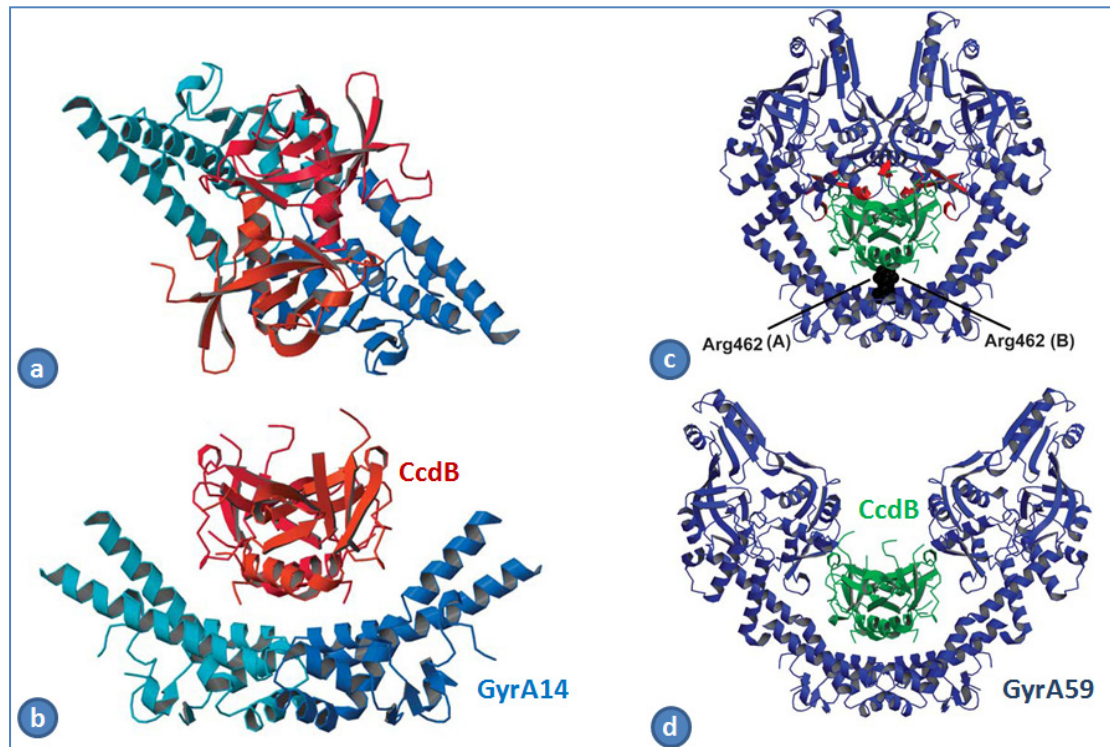
Figure 152 Complex of CcdB and GyrA14 and models: (a) Gyr-A14: CcdB complex viewed along its 2-fold axis. The two CcdB monomers are drawn in orange and red and the two GyrA14 monomers in two shades of blue. (b) Same as (a), but rotated 90°. (c) Model of closed GyrA59 (blue) with CcdB (green) docked onto it by superposition of the GyrA14:CcdB complex on the crystal structure of GyrA59 (Reece and Maxwell 1989). Residues Arg462 of both monomers of GyrA59 are highlighted. Strong steric overlaps (red) with the CAP domains are observed. (d) Model of the GyrA59: CcdB complex with GyrA59 in its open conformation. The open conformation of GyrA59 was modelled according to the corresponding yeast topoisomerase II structure (PDB entry 1BGW (Berger, Gamblin et al. 1996)). In this model, there is no steric overlap between CcdB and GyrA59. Reproduced from Dhao Thi & Van Melderen (Dao-Thi, Van Melderen et al. 2005).

As for MccJ25, this 21 amino acids peptide was thought to be a head to tail cyclic peptide, as there was an 18 Da difference compared to the translation product. The biochemical evidence was understood when the 3-dimensional structure of MccJ25 was solved by extensive NMR and MS studies, and appears to adopt an unusual lassoed tail fold (Figure 153). Its is not unlikely for MccB17 to have such an unusual structural twist, we already know that there is two different MccB17 species observed during the HPLC purification, and that their population varies depending on the pH. The problem encountered with MccB17 solubility in our experiments, suggest that it can agglomerate in a very stable form.

Direct evidence about MccB17 interaction with gyrase is scarce: only one mutation conferring resistance to MccB17 have been identified on gyrase (B subunit) and no structural data are available. Finding news mutations conferring resistance to MccB17 will help define its binding site, but this work had shown the inherent difficulties of this approach, even if we had defined a strategy likely to be successful in the future. But the major progress will be to have information about the 3-dimensional structure of MccB17, this can be achieved by crystallography using the toxin alone, or better with gyrase and DNA; or by using protein NMR techniques on MccB17 in the presence and absence of gyrase and DNA. One of the features of

MccB17, which was detrimental to such approaches, is the presence of the polyglycine tail, this disordered area is unfavourable for crystallography experiments, and creates unassignable signals in NMR analysis. The "minimal" MccB17 we mentioned above, once identified, may improve the output of these techniques, as a significant amount of the problematic residues might be removed. Until spectroscopic techniques generate such a structural breakthrough, the mode of action of MccB17 will probably remain a black box. We have the conviction that this is where future work on this subject should primarily focus.
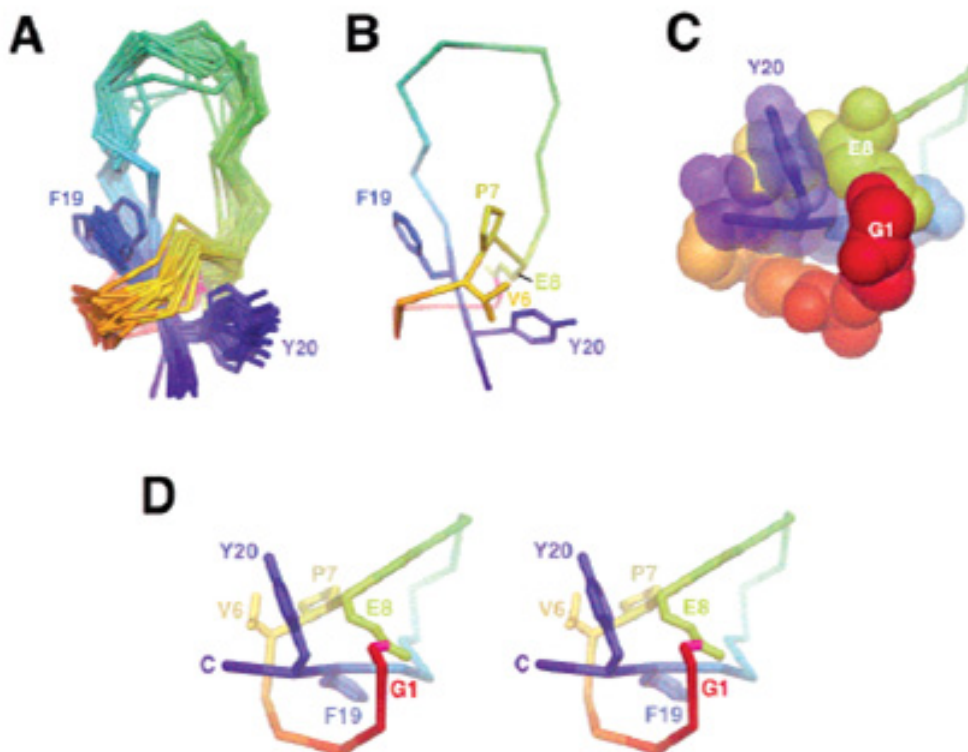
Figure 153 NMR-based structural model of MccJ25. In each view, the peptide chain is colored in a ramp (red-orange-yellow-green-blue) from the N-terminal Gly1 (red) to the C-terminal Gly21 (blue), with the isopeptide bond linking the R-amino group of Gly1 with the γ-carboxyl of Glu8 coloured magenta. *(a)* Ensemble of 20 models resulting from distance geometry simulated annealing calculations. The side chains of E8, F19, and Y20 are shown and labeled. (b) Representative structure, shown in the same view as part a. The side-chains of V6, P7, E8, F19, and Y20 are shown. (c) The lariat ring (G1-E8) and the C-terminal tail (S18-G21) are shown as CPK atoms, with the C-terminal tail rendered transparent so the backbone is visible. Selected side-chains are labeled. (d) Stereoview with selected side-chains shown and labeled. Reproduced from Wilson *et al* (Wilson, Kalkum et al. 2003).

The reader may have the feeling from this summary that the stabilisation of the cleavage complex, which is the key feature of MccB17, requires most of the peptide structure. Even if all the residues upstream of the site A can be removed, the resulting compound might seem of limited interest as it still will be a large 31-residue peptide with properties close to MccB17's. Two arguments can be propounded in favour of MccB17 derivatives: first, until the mode of action is precisely defined, the possibility of reproducing it by different means can not be dismissed. Second, once the smallest MccB17 fragment able to poison gyrase is isolated, the areas of the peptide that can tolerate modifications can be investigated and modified in order

187

to improve the drugability of the molecule. The stabilisation of the cleavage complex has proved to be such an efficient way of killing cells that it will be a shame to miss the opportunity of identifying a new mechanism favouring it. Simple inhibition of gyrase, is not as lethal as poisoning, but is valuable if the inhibitors have a high affinity for the enzyme and can block efficiently its activity, as demonstrated by the aminocoumarins. We have focused here on MccB17 for its mode of action, and the potential of compounds duplicating it, as new antibacterial drugs. But other natural products, able to stabilize the gyrase-DNA cleavage complex have the same potential. Three other compounds seem to share that potential with MccB17: we had already mentioned CcdB, and albicidin as well as the toxin ParE are two other compounds that arouse our interest. We have described the mode of action of CcdB, and it seems hard to reproduce it with small molecule for therapeutic application, however some synthetic peptide (Figure 154) copying some feature of CcdB were shown to have inhibitory activity on gyrase and topo IV, but no stabilization of cleavage complex (Trovatti, Cotrim et al. 2008).

^{84}SHRENDIKNAINLMFWGI^{101} (*CcdBET1*)

^{1}MQFKVYTYK^{9}-Z-^{40}RLLSDKVSREL^{50}-Z-^{84}SHRENDIKNAINLMFWGI^{101} (*CcdBET2*)

^{1}MQFKVYTYK^{9}-Z-^{84}SHRENDIKNAINLMFWGI^{101} (*CcdBET3*)

^{68}MASVPVSVIGEEVADLSHRENDIKNAINLMFWGI^{101} (*CcdBET4*)
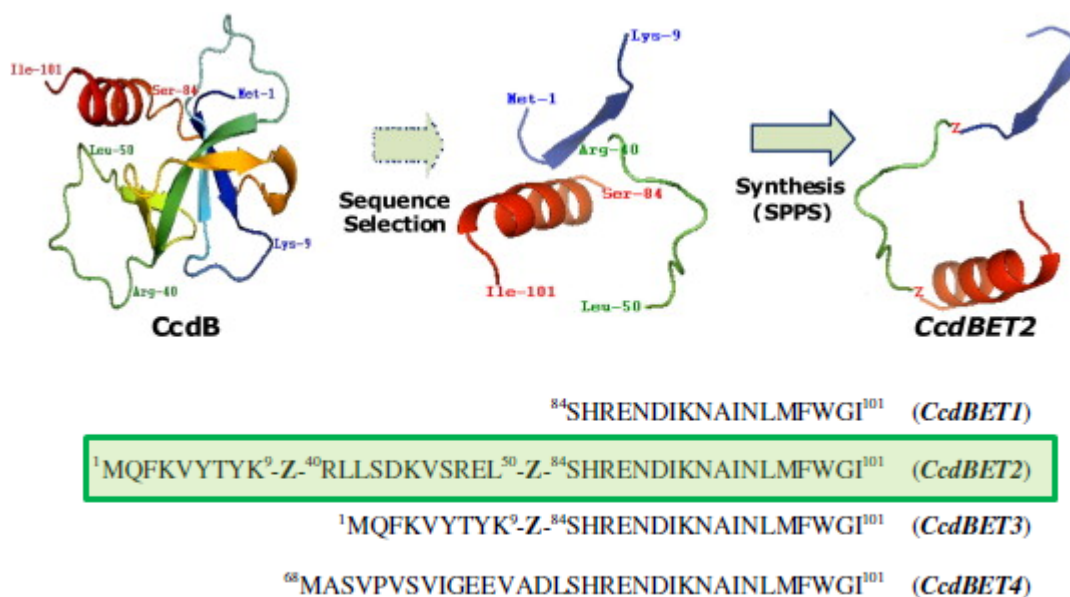
The primary structures of the synthesized CcdB analogues (Z = ε-amino hexanoic acid).

Figure 154 CcdB and derived peptides: the various peptides evaluated by Trovatti *et al*, the green box highlight the peptide that shows a complete inhibition of on gyrase at 10 µM and of topo IV at 5 µM (Trovatti, Cotrim et al. 2008).

Albicidin is a toxin produce by *Xanthomonas albilineans*, the agent that causes the sugarcane leaf scald. The toxin had been shown to have attractive antibacterial properties (Birch and Patil 1985) as an ATP-dependent gyrase cleavage complex stabilizer (Hashimi, Wall et al. 2007). Albicidin's primary structure is still under investigation: a gene required for it synthesis have been identified, and is encoding for a hybrid polyketide-peptide synthetase, this added to the NMR data reporting several aromatic ring and around 38 carbon atoms and, and the MS data giving an approximate MW = 842, give some indication about its chemical structure (Royer, Costet et al. 2004). The study of the toxin have been made difficult by the slow growth of the producing bacterium, fortunately heterologous production of albicidin has been reported recently and open perspectives for the identification of its chemical structure

and application in drug discovery (Vivien, Pitorre et al. 2007). If we consider its activity, and reasonable molecular weight, it is a promising compound. The ParE toxin is very similar to CcdB. ParE is a part of a toxin-antitoxin system with ParD that are included in the addiction plasmid RK2, whereas CcdB and the antitoxin CcdA are included in the F plasmid. ParE is a 12 kDa protein that has been shown, like CcdB to stabilise the cleavage complex. The crystallographic structure of the ParE-ParD complex has been solved recently (Dalton and Crosson 2010).
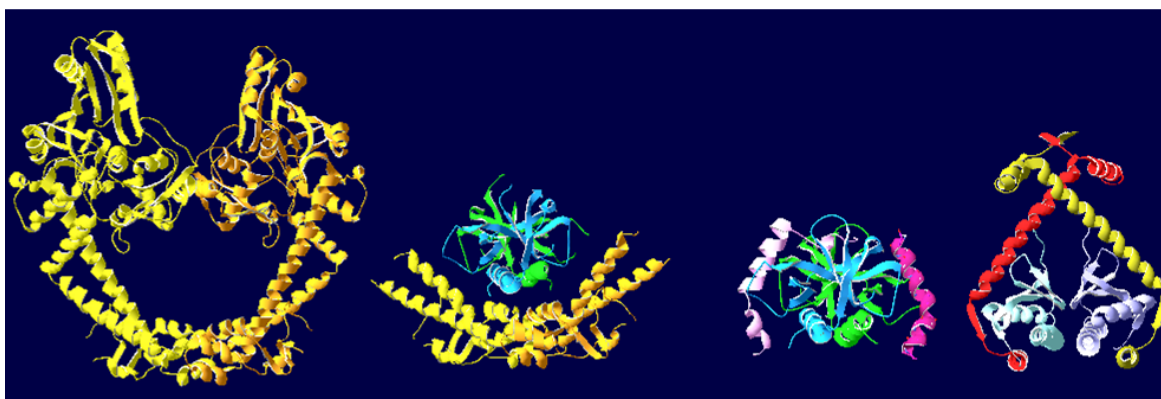
Figure 155 Illustration of CcdB, ParE, their antitoxin and GyrA crystal structures: from left to right, GyrA59 dimer (yellow and orange) from Edwards *et al* (Edwards, Flatman et al. 2009); CcdB dimer (blue and green) and gyrA14 dimer (yellow and orange) from Dao-Thi *et al* (Dao-Thi, Van Melderen et al. 2005), CcdB dimer (blue and green) and two CcdA (C-terminal domain; pink and magenta) from De Jonge *et al*; ParE dimer (turquoise and violet) and two ParD (red and yellow) from Dalton and Crosson (Dalton and Crosson 2010).

Looking at the toxin anti-toxin complex in comparison with the gyrA dimer, it is easy to imagine a mode of action similar to CcdB, even if the structures are quite different. It is very likely that the successful generation of peptide inhibitors from CcdB, can be applied with the toxin ParE. And if CcdB and ParE have similarities in their interaction with gyrase, features of both structures can be combined to design new gyrase inhibitors. A more remote approach to identify new compounds is related to MccB17 biosynthesis. MccB17 synthetase is an unusual enzyme that is converting specific sequence of, Gly, Ser, Cys into heterocycles. There are a multitude of bio-active molecules carrying oxazole and thiazole heterocycle that have been reported, some close to MccB17 are referred as TOMM (thiazole/oxazole-modified microcin) like the recently discovered plantazolicin (Scholz, Molohon et al.), others have a more remote structure like bleomycin, microcyclamides (Raveh, Moshe et al.), thiocillin (Wieland Brown, Acker et al. 2009), nostocyclamides, telomestatine, micrococcin P1 (Hughes and Moody 2007), tioseptron or pathelamides (Nolan and Walsh 2009). Tracking genes coding for protein similar to MccB17 synthetase, is a potential way of using the MccB17 biosynthetic pathway to discover new heterocyclic bioactive compounds. This approach is supported by the recent study of the streptolysin S biosynthesis from *Streptococcus pyogenes*. This toxin is produced by the *sag* gene cluster, *sagA* encodes the protoxin, and following *sagB*, *sagC*, *sagD* gene, have around 20% identity with respectively *mcbC*, *mcbB*, and *mcbD*, and convert SagA to a cytolysin by heterocyclisation of peptide sequences (Lee, Mitchell et al. 2008). There is a close relation between these two pathways, and the fact that the biosynthetic operon, responsible for the

production of oxazole- and thiazole-containing toxins, is widely distributed is very encouraging to adopt such approach. Similarly, tracking proteins related to the immunity peptide McbG can be a way of finding in the related toxin, a compound with biological relevance.

Our principal interest in this study was to isolate new topoisomerase inhibitor antibacterials, and we had principally being involved with gyrase. But occasionally we had widened our target scope to topo IV, a logical choice, as it is the sister target of gyrase for quinolones, and topo II for its relevance in cancer therapy. This digression had proved valuable as we have identified that MccB17 and some of its fragments were able to inhibit human topo II at ~100 μM, this opens a completely new prospect for MccB17 derivatives applications. This is as well an encouraging example of the relevance of evaluating families of topoisomerase inhibitors on various other topoisomerases. This can be further illustrated by the successful example of the transfer of quinolone structures from application in antibacterial therapy to anti-cancer therapy (Hawtin, Stockett et al. ; Sissi and Palumbo 2003). It makes perfect sense in the context of topoisomerase poisons if we consider them globally. Topoisomerase poisons are structures that interact with the cleavage complex, and generally, apart from CcdB, by stabilizing it through direct interaction with DNA and the protein at or close to, the cleavage site. This means that if we have compounds with the features to interact both with DNA and a topoisomerase, and possibly with the architecture of a cleavage site, its derivatives are likely to still have a topoisomerase inhibitor profile, but maybe fitting better with a different topoisomerase cleavage complex. We think it is worth keeping that in mind: not restricting studies on only one topoisomerase, and evaluating the potential on other topoisomerases of both successful and failed inhibitors.

We hope we had convinced the reader of the great potential of natural products and their application on validated drug targets through new mechanisms. We chose to study the gyrase poison MccB17, and we have opened perspectives in using MccB17 derivatives to create new topoisomerase inhibitors. We had discussed the possible limitations of future work on this subject, as well as the potential for a significant breakthrough. Regardless of the outcome of MccB17 uses for new topoisomerase inhibitors, we have mentioned the vast pool of related compounds available from natural sources. Microorganisms have, through their evolution, explored multiple possibilities to kill the competition, we have just to observe, understand, and duplicate or improve the means they have developed and make them ours. Synthesis by Nature has a set of limitations, it works in aqueous environment and at a limited range of temperature, but it has evolved a gigantic range of catalytic tools to widen its synthetic capacity. A few of these tools are at our disposition as well, and we have an extra advantage with the chemistry we have developed that allows us to work in various solvents, with anhydrous condition, and very reactive species that cannot exist in aqueous environments. A wide range of temperature and pressure are available as well to us. However Nature inside its limitation is able to construct far more complex structure and more efficiently that we are, it has tested and refined its tools over millions of years. We have developed wonderful methods, but they are in a limited number and what we produce is biased most of the time by what is available from our suppliers. This means that we have through pure synthesis a restricted chemical space to explore, and that fact can account for the plateau we reached in drug discovery. We should benefit from the two sources, identifying unusual structures and mechanisms present in nature, which are not available through chemical synthesis, and improve them so they would not be sensitive to defence mechanism like proteolysis of peptides. Other improvement can be gained through exploration of chemistry unusual in

nature like halogenation and particularly fluorination, or the use of retropeptide and bioisostere to optimise activity and stability. We hope that this work and its future perspective illustrate fully this approach, and have given hope in our ability to restore the antibacterial Era.

CHAPTER VI
Materials & Methods

CHAPTER VI Materials and Methods

1 Materials

1.1 Softwares

Chemical structure drawing: **MarvinSketch** (ChemAxon).

DNA sequence analysis: **Sequencher** (Gene Codes).

Gel picture analysis: **Genetools** (SynGene).

1.2 Chemicals

All chemicals were purchased from Sigma-Aldrich.

1.3 Buffers and gels

TAE: 40 mM Tris.acetate, 2 mM Na_2EDTA, pH = 8.5.

TE: 10 ml Tris.HCl pH = 8.0, 1 mM EDTA.

LB (amp): 10 g/l bacto-tryptone, 5 g/l yeast extract, 10 g/l NaCl, pH = 7.5.

M63 glucose media (amp): 3 g/l KH_2PO_4, 7 g/l K_2HPO_4, 2 g/l $(NH_4)SO_4$, 1 mM $MgSO_4$, 1 µg/ml thiamine, 0.2% glucose (0.1 mg/ml ampicillin added just before use).

Mac Conkey Agar: peptone 17.0 g/l, proteose peptone 3.0 g/l, lactose 10.0 g/l, bile salts nº3 1.5 g/l, sodium chloride 5.0 g/l, agar 13.5 g/l, neutral red 0.03 g, crystal violet, 0.001 g/l.

1.4 Enzymes

DpnI: was purchased from Biolab (RO176S).

Subtilisin: was purchased from Sigma-Aldrich (P5380).

Endoprotease Glu-C: was purchased from Sigma-Aldrich (P2922).

Carboxypeptidase A: was purchase from Sigma-Aldrich (C9268).

Taq DNA polymerase: was purchased from Invitrogen.

Pfu-turbo DNA polymerase: was purchased from Stratagen (600250).

Trypsin: was purchased from Promega (V5111).

1.5 Primers

Table 14 List of primers

Gyrase sequencing primers	
GyrA_F	ATGAGCGACCTTGCTCGAGAAATTACACCG
GyrA_R	TTATTCTTCTTCTGGCTCGTCGTCAACGTC
GyrA_308R	CCAGCATATAACGCAGCGAG
GyrA_246F	CTCGGCGGTCTATGACACG
GyrA_812F	GCGCGCCTGATCGAGAAGA
GyrA_1210F	GCAGAAGCGAAAACTGCGC
GyrA_1692F	GAAAGGTAAATCTGCCGC
GyrA_2041F	GAGCTGATCGGCGTTGAC
GyrA_2401F	GCCGGTACGCTGGTACG
GyrB_F	ATGTCGAATTCTTATGACTCCTCCAGTATC
GyrB_R	TTAAATATCGATATTCGCCGCTTTCAGGGC
GyrB_318R	TGCTGGAAGAAGATGCGTTT
GyrB_661F	TTCTGCGTCGCGTTGTACTC
GyrB_1231F	TTTACGGCGGGTCATTTCAC
GyrB_1863F	CAGACGTTTCGCCAGAATTT

MccB17 site-directed-mutagenesis primers			
Serie i		Serie ii	
G30toKF	TGTTGGCATTAAAGGTGGTGG	G30toKF2	TTGTTGGCATTAAAGGTGGTGGCG
G30toKR	CCACCACCTTTAATGCCAACA	G30toKR2	CGCCACCACCTTTAATGCCAACA
G32toKF	ATTGGTGGTAAAGGCGGCG	G32toKF2	CATTGGTGGTAAAGGCGGCGGCG
G32toKR	CGCCGCCTTTACCACCAAT	G32toKR2	CGCCGCCGCCTTTACCACCAATG
G34toKF	ATTGGTGGTGGTGGCAAAGGC	G34toKF2	TGGTGGTGGCAAAGGCGGCGGCG
G34toKR	GCCTTTGCCACCACCACCAAT	G34toKR2	CGCCGCCGCCTTTGCCACCACCA
G36toKF	GGCAAAGGCGGCGGTAG	G36toKF2	TGGCGGCGGCAAAGGCGGCGGTA
G36toKR	CTACCGCCGCCTTTGCC	G36toKR2	TACCGCCGCCTTTGCCGCCGCCA
GtoStopF	CGGAAGTTAATCACATATCTGATA	GtoStopF2	CGGCGGAAGTTAATCACATATCT
GtoStopR	TATCAGATATGTGATTAACTTCCG	GtoStopR2	AGATATGTGATTAACTTCCGCCG
StoStopF	AAGTGGTTAACATATCTGATACGTT	StoStopF2	CGGAAGTGGTTAACATATCTGATA
StoStopR	AACGTATCAGATATGTTAACCACTT	StoStopR2	TATCAGATATGTTAACCACTTCCG
HtoStopF	AAGTGGTTCATAAATCTGATA	HtoStopF2	AAGTGGTTCATAAATCTGATACG
HtoStopR	TATCAGATTTATGAACCACTT	HtoStopR2	CGTATCAGATTTATGAACCACTT
ItoStopF	TTCACATTAATGATACGTTGAATTAA	ItoStopF2	TGGTTCACATTAATGATACGTTG
ItoStopR	TTAATTCAACGTATCATTAATGTGAA	ItoStopR2	CAACGTATCATTAATGTGAACCA

1.6 Apparatus

1.6.1 High pressure liquid chromatography

A Dionex Ultimate 3000 HPLC system was used for most of the purifications. Two different columns were used in conjunction with this system. The first was a preparative reverse phase column ACE 5 C18-300 250 X 21.2mm (ACE-221-2520). The second, was a semi-preparative column Phenomenex Jupiter 300 5μ C18, 10 mm X 250 mm. The initial separation of the subtilisin digest of MccB17 was performed with an analytical column Phenomenex primesphere 5μ C18MC 300 Å, 4.6 mm X 250 mm adapted on a Waters™ system: a Waters 626 pump was associated with a Waters 600S controller, the detection was performed with a photodiode array detector 996, and the collection was done using a 717plus Autosampler.

1.6.2 Nuclear magnetic resonance

NMR data was recorded at 300 K, on a Bruker Avance II 600 MHz NMR spectrometer with Bruker TCI cryoprobe (1H and 13C). 1H and 13C NMR chemical shifts (δ) are referenced with respect to the DMSO-d6 solvent: (DMSO: delta 1H 2.49 ppm and delta 13C 39.5 ppm).

1.6.3 Mass spectrometry

Mass spectrometry analysis were performed on either on a Bruker Ultraflex™ MALDI-ToF/ToF (referred as MALDI-ToF), or a Thermo-Fisher LCQ DecaXP[plus] (EI).

2 Methods

2.1 Production and purification of Microcin B17 (MccB17)

2.1.1 Expression in *E. coli*

The toxin was produced using a protocol similar to the one describe by Roy *et al* (Sinha Roy, Kelleher et al. 1999). The *E. coli* strain used had been designed and reported by Milne *et al* (Milne, Eliot et al. 1998) is a DH5α carrying a pUC-19-plasmid containing the MccB17 operon mcbABCDEFG. DH5α-pmccB17 from the glycerol stock was grown overnight at 37°C in 12x5 ml of LB-amp media (10 g/l bacto-tryptone, 5 g/l yeast extract, 10 g/l NaCl, 0.1 mg/ml ampicillin). The culture were used to inoculate 12 X 1l of M63 glucose Ap media (3 g/l KH_2PO_4, 7g/l K_2HPO_4, 2 g/l $(NH4)_2SO_4$, 1 mM $MgSO_4$, 1 mg/ml thiamine, 0.2% glucose and 0.1 mg/ml ampicillin) in 2 l baffled flasks, which were incubated overnight at 37°C with stirring at 220 rpm. The cells where centrifuged for 15 min at 4250 g and the pellets collected. The pellets where resuspended in 500 ml of a boiling solution containing 1 mM EDTA and 100 mM acetic acid solution and stirred for 10 min. The solution was allowed to cool to ~40°C before centrifugation at 4500 rpm for 10 min. The warm supernatant was then divided in four fractions and loaded separately on a 35cc (10 g) Sep-Pak® column (Waters WAT043345) equilibrated beforehand with 300 ml of acetonitrile and 300 ml water. Elution with 250 ml water followed by 250 ml 12.5% acetonitrile in water removed contaminants, then the MccB17-containing fraction was collected by elution with 250 ml of 50% acetonitrile in water. Acetonitrile was removed from the collected fraction under vacuum, and the remaining solution was freeze dried to lead to solid raw MccB17. The solid was dissolved in DMSO at a mM concentration and stored at -20ºC.

2.1.2 Purification of raw microcin by HPLC:

The raw microcin solution was purified on a Dionex Ultimate 3000 HPLC system with a preparative reverse phase column ACE 5 C18-300 250 X 21.2mm (ACE-221-2520). The solution of raw MccB17 in DMSO (mM concentration) was loaded onto the HPLC via a 5 ml loop. The elution program was a linear gradient from 13% to 23% CH_3CN in water, with 0.1% TFA, over 40 min. The peaks highlighted on Figure 156 were collected manually. The difference fractions collected were concentrated under vacuum before being freeze-dried. The solid residues were dissolved in DMSO and stored at -20°C. The various fractions collected were concentrated under vacuum before being freeze dried.

2.1.3 Methanol-water alternative system

Due to the global shortage of acetonitrile in 2008-2009 the HPLC purification of microcin was shifted from a water-acetonitrile system to a water-methanol (relative polarities $H_2O = 1$; MeOH = 0.762; $CH_3CN = 0.460$) (Reichardt 2003).
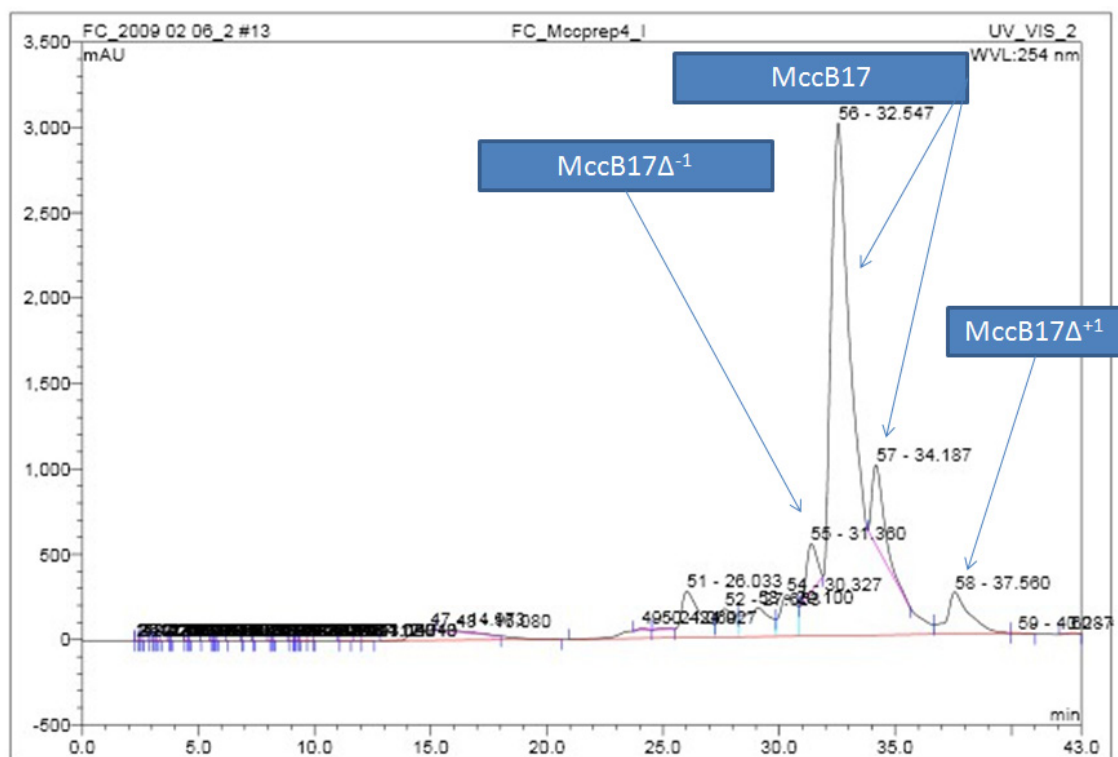
Figure 156 Trace at 254 nm of the HPLC purification of raw MccB17
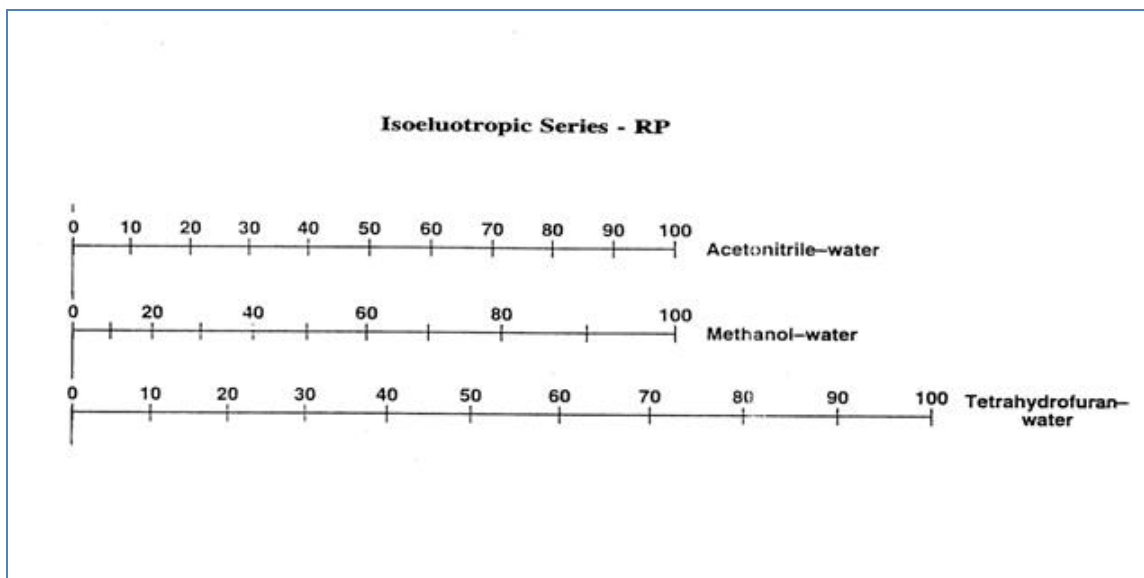
Figure 157 HPLC system solvent equivalence (http://www.discoverysciences.com/product.aspx?id=6306)

As before, the purification was performed on a Dionex Ultimate 3000 HPLC system with a preparative reverse phase column ACE 5 C18-300 250x21.2mm (ACE-221-2520). The solution of raw MccB17 in DMSO (mM concentration) was loaded onto the HPLC via a 5 ml loop. The elution program was a linear gradient from 20% to 35% over 40 min.

2.1.4 Isolation of microcin B17 by-products

The chromatogram of MccB17 purification shows a few peaks coming out of the column before MccB17. The fraction with 25 min<RT< 31 min was collected for further analysis. In later purifications individual peaks were collected. The fractions collected were concentrated under vacuum, freeze-dried and redissolved in DMSO.

2.2 *In vitro* assays on topoisomerases:

2.2.1 *E. coli* Gyrase

In the cell, gyrase is an enzyme that introduces negative supercoils in DNA at the expense of ATP in order to remove topological stress. This property can be reproduced *in vitro* and the influence of inhibitors recorded. It is possible as well *in vitro* for the enzyme to relax supercoiled DNA in the absence of ATP; this is not a reaction the enzyme is designed for and so its activity is a lot lower than a relaxing enzyme like topo IV. By comparing supercoiling and relaxation reactions for a given inhibitor it is possible to trace its involvement in the ATPase activity of the enzyme; an ATPase inhibitor will hinder the supercoiling reaction but will have little effect on relaxation. The last *in vitro* assay used to characterise inhibitor of gyrase is the cleavage assay that relies on the formation of the DNA-gyrase cleavage complex. This complex is a transient intermediate of the supercoiling and relaxation reactions, by using an increased amount of enzyme the equilibrium is pushed toward its formation. Cleavage assays are used to characterize inhibitors like fluoroquinolones, drugs that are cleavage-complex stabilizers and so increase its formation in this assay.

197

2.2.1.1 Supercoiling

The supercoiling reaction was carried out in the following conditions: for a 30 µl reaction, 6 µl of reaction buffer 5X (175 mM Tris.HCl pH = 7.5, 120 mM KCl, 20 mM MgCl$_2$, 10 mM DTT, 9 mM spermidine, 1 mM ATP, 32.5% v/w glycerol, 0.5 g/l BSA), 16.5 µl MQ water, and 0.5 µl of 1 mg/ml relaxed pBR322 were mixed on ice. Solutions of GyrA, GyrB, and the gyrase dilution buffer (50 mM Tris.HCl pH = 7.5, 100 mM KCl, 2 mM DTT, 1 mM EDTA, 10% w/v glycerol) were mixed to lead to 27 nM GyrA and 27 nM GyrB solution and left for 5 min on ice. 6 µl of the gyrase mixture was added to the reaction mixture. Finally 1 µl of DMSO or drug in DMSO were added. Special attention was paid to make sure the DMSO solutions didn't freeze in the pipette tips during the addition. To avoid such trouble, when

Gyrase supercoiling assay mixture		
Compound	Conc.	
Gyrase	2.7	nM
Relaxed pBR322	5.4	nM
DMSO	3.3	% V/V
compound (in DMSO)	variable	
ATP	1	mM
MgCl$_2$	4	mM
Tris.HCl pH = 7.5	45	mM
KCl	44	mM
DTT	2.4	mM
spermidine	1.8	mM
glycerol	8.5	% w/V
BSA	0.1	mg/ml

possible, to a reaction mixture containing only 12.5 µl of MQ water were added to 5 µl of the drug in 20% DMSO solution in the last step. The table on the right shows the final concentrations in the reaction mixture. The mixture was incubated for 2 h at 25°C. Then 30 µl of chloroform/isoamyl alcohol (24:1) and 30 µl of STEB were added to stop the reaction. The mixture was vortexed for 10 s and centrifuged 2 min at 13000 rpm. The aqueous layer was loaded on a 1% w/v agarose gel and run either overnight at 17 V or 3 h at 70 V.

2.2.1.2 Relaxation

The relaxation reaction was carried out in the following conditions: for a 30 µl reaction, 6 µl of reaction buffer 5X (175 mM Tris.HCl pH = 7.5, 120 mM KCl, 20 mM MgCl$_2$, 10 mM DTT, 32.5% v/w glycerol, 0.5 g/l BSA), 16.5 µl MQ water, and 0.5 µl of 1 mg/ml supercoiled pBR322 were mixed on ice. Solutions of GyrA, GyrB, and the gyrase dilution buffer (50 mM Tris.HCl pH = 7.5, 100 mM KCl, 2 mM DTT, 1 mM EDTA, 10% w/v glycerol) were mixed to lead to 200 nM GyrA and 200 nM GyrB solution and left for 5 min on ice. 6 µl of the gyrase mixture was added to the reaction mixture. Finally 1 µl of DMSO or drug in DMSO were added. The same method described for supercoiling assays was used to make sure the DMSO solutions

Gyrase relaxation assay mixture		
Compound	Conc.	
Gyrase	20	nM
supercoiled pBR322	5.4	nM
DMSO	3.3	% V/V
compound (in DMSO)	variable	
MgCl$_2$	4	mM
Tris.HCl pH = 7.5	45	mM
KCl	44	mM
DTT	2.4	mM
glycerol	8.5	% w/V
BSA	0.1	mg/ml

didn't freeze: to a reaction mixture containing only 12.5 µl of MQ water was added 5 µl of the drug in 20% DMSO solution in the last step. The final concentrations in the reaction mixture are shown in the table on the right. The mixture was incubated for 2 h at 37°C. Then 30 µl of chloroform/isoamyl alcohol (24:1) and 30 µl of STEB were added to stop the reaction. The

mixture was vortexed for 10 s and centrifuged 2 min at 13000 rpm The aqueous layer was loaded on a 1% w/v agarose gel and run either overnight at 17 V or 3 h at 70 V.

2.2.1.3 Cleavage

The cleavage reaction was carried out as described above but with a 79.5 nM gyrase final concentration, using supercoiling conditions, if the reaction was studied in presence of ATP or relaxation condition if the reaction was studied in its absence. The mixture was incubated for 1 h at 37°C. 6 μl of 1% w/v SDS and 3 μl of proteinase K (20 mg/ml) were added and the reaction was incubated for 30 min at 37°C. 30 μl of chloroform/isoamyl alcohol (24:1) and 30 μl of STEB were added, the mixture was vortexed for 10 s and centrifuged 2 min at 13000 rpm. The aqueous layer was loaded on a 1% w/v agarose gel and run either overnight at 17 V or 3 h at 70 V. The gel may contain 1 μg/ml ethidium bromide in order to discriminate linear DNA, relaxed species and nicked DNA Figure 158.
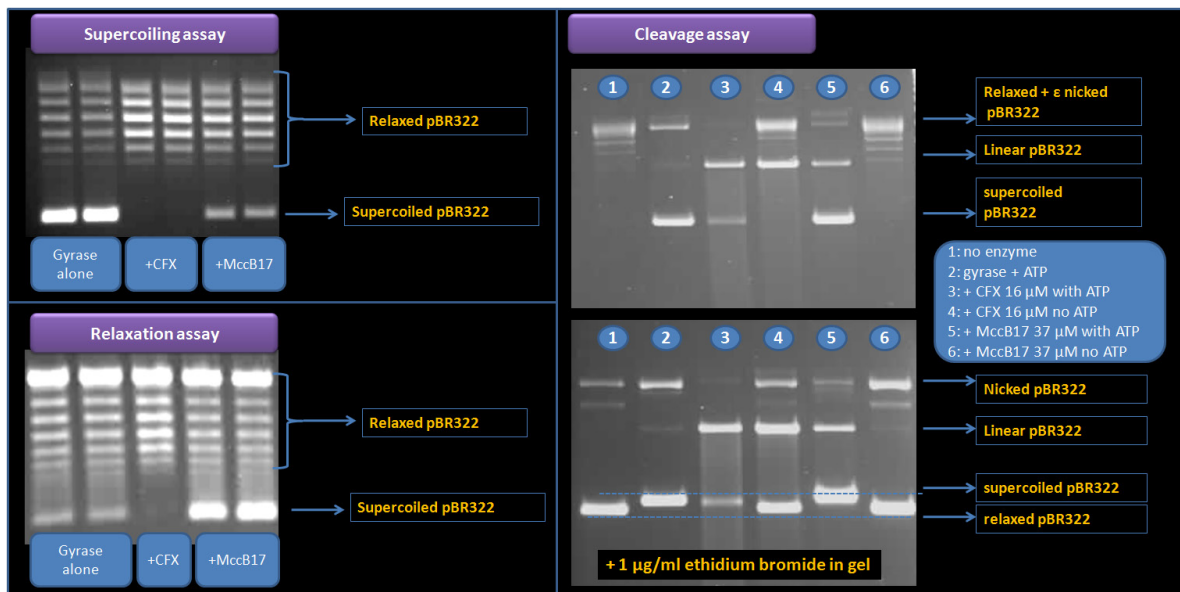
Figure 158 Examples of supercoiling, relaxation and cleavage assays: Top left, supercoiling assay, relaxed DNA (upper ladder) is converted into supercoiled DNA by gyrase (bottom band). In the presence of an inhibitor the bottom band intensity is reduced in favour of the top bands. Bottom left, relaxation assay, supercoiled DNA (lower band) is converted into relaxed DNA (upper ladder) by gyrase; the presence of an inhibitor induces a decrease of the upper bands in favour of the lower band. Right side, cleavage assays, during a supercoiling or relaxation reaction with increased amount of enzyme, linear DNA is produced. Unfavourable in normal conditions, this reaction is favoured by the presence of a cleavage complex stabilizer like ciprofloxacin or MccB17 (with ATP) and leads to the appearance of a band in the middle.

2.2.2 *E. coli* topo IV relaxation

Topo IV is a topoisomerase specialized in relaxation and decatenation. Both activities can be reproduced *in vitro*, but only relaxation has been carried out in this study. The reaction was carried out in the following conditions: for a 30 µl reaction, 6 µl of reaction buffer 5X (200 mM HEPES.KOH pH = 7.6, 500 mM KCl, 50 mM MgCl$_2$, 50 mM DTT, 0.25 g/l BSA), 16.5 µl MQ water, and 0.5 µl of 1 mg/ml supercoiled pBR322 were mixed on ice. 6 µl of 0.11 µM topo IV in dilution buffer (40 mM HEPES.KOH, pH = 7.6, 100 mM KCl, 1 mM DTT, 1 mM EDTA, 40% w/v glycerol) and 1 µl of 30 mM ATP were added. Finally 1 µl of DMSO or drug in DMSO were added to the mixture. Ciprofloxacin at 17 µM was used as a positive control. The table on the right shows the

Topo IV	22 nM
supercoiled pBR322	5.4 nM
ATP	1 mM
HEPES.KOH (pH = 7.6)	48 mM
KCl	120 mM
MgCl$_2$	10 mM
DTT	10.2 mM
EDTA	0.2 mM
Glycerol	8%
BSA	50 µg/ml

final concentrations in the reaction mixture. The mixture was incubated for 30 min at 37°C. Then 30 µl of chloroform/isoamyl alcohol (24:1) and 30 µl of STEB were added to stop the reaction. The mixture was vortexed for 10 s and centrifuged 2 min at 13000 rpm. The aqueous layer was loaded on a 1% w/v agarose gel and run either overnight at 17 V or 3 h at 70 V.

2.2.3 Human topoisomerase II relaxation

The reaction was carried out in the following conditions: for a 30 µl reaction, 3 µl of reaction buffer 10X (500 mM Tris.HCl pH = 7.5, 1.25 M NaCl, 100 mM MgCl$_2$, 50 mM DTT, 1 g/l BSA), 24.5 µl MQ water, and 0.5 µl of 1 mg/ml supercoiled pBR322 were mixed on ice. 0.1 µl of topo II (1 Unit) in (50 mM Tris.HCl, pH = 7.5, 100 mM NaCl, 1 mM DTT, 0.5 mM EDTA, 50% w/v glycerol, 50 µg/ml BSA) and 1 µl of 30 mM ATP were added. Finally 1 µl of DMSO or drug in DMSO were added to the mixture. Etoposide at 100 µM was used as a positive control. The table on the right shows the final concentrations in the reaction mixture. The mixture was

Topo II	22 nM
supercoiled pBR322	5.4 nM
ATP	1 mM
Tris.HCl (pH = 7.5)	50 mM
NaCl	125 mM
MgCl$_2$	10 mM
DTT	5 mM
BSA	100 µg/ml

incubated for 30 min at 37°C. 30 µl of chloroform/isoamyl alcohol (24:1) and 30 µl of STEB were added to stop the reaction. The mixture was vortexed for 10 s and centrifuged 2 min at 13000rpm. The aqueous layer was loaded on a 1% w/v agarose gel and run either overnight at 17 V or 3 h at 70 V.

2.2.4 *Staphylococcus aureus* gyrase supercoiling

The reaction was carried out in the following conditions: for a 30 µl reaction, 6 µl of reaction buffer 5X (200 mM HEPES.KOH pH = 7.6, 50 mM Mg(OAc)$_2$, 50 mM DTT, 0.25 g/l BSA, 10 mM ATP), 17.5 µl MQ water, 0.5 µl of 1 mg/ml of relaxed pBR322, and 5 µl of 6X KGlu (3 M) were mixed on ice. 6 µl of 72 nM SaGyrA and 720 nM SaGyrB in dilution buffer (50 mM Tris.HCl, pH = 8.0, 1 mM DTT, 1 mM EDTA, 10% w/v glycerol). Finally 1 µl of DMSO or drug in DMSO were added to the mixture. Ciprofloxacin at 17 µM was used as a positive control. The table on the right shows the final concentrations in the reaction mixture. The mixture was incubated for 1 h 45 at 25°C. 30 µl of chloroform/isoamyl alcohol (24:1) and 30 µl of STEB were added to stop the reaction. The mixture was vortexed for 10 s and centrifuged 2 min at 13000 rpm. The aqueous layer was loaded on a 1% w/v agarose gel and run either overnight at 17 V or 3 h at 70 V.

SaGyrA	2.4 nM
SaGyrB	23 nM
relaxed pBR322	5.4 nM
ATP	2 mM
HEPES.KOH (pH = 7.6)	40 mM
Tris.HCl (pH = 8)	10 mM
Mg(OAc)$_2$	10 mM
DTT	11 mM
EDTA	0.2 mM
Glycerol	2%
BSA	50 µg/ml

2.2.5 Agarose gel electrophoresis

1% w/v of agarose was added to TAE buffer (40 mM Tris acetate, 1 mM EDTA). The mixture was boiled until complete dissolution of the agarose. The gel was allowed to cool down for 5 min. If the gel was run in presence of ethidium bromide, 1 µg/ml was added at this stage. The gel was poured into the rack with a comb. The gel was allowed to solidify at least for 30 min. The comb was removed, and the gel with the rack was put in the tank. The gel was covered with TAE buffer (containing 1 µg/ml ethidium bromide if needed). The gel was run run either overnight at 17 V or 3 h at 70 V, which brings the bromophenol blue front to the end of the gel. If the gel was ethidium bromide free, it was then soaked in TAE containing 1 µg/ml ethidium bromide for 20 min. The gel was visualized under UV light after being destained in TAE buffer for 20 min.

2.3 In vivo assays

2.3.1 Slope plates

Slope plates are designed to create a concentration gradient of a compound from one side of a square plate to the other. This gradient is generated by pouring 50 ml liquid LB-agar containing the compound at the higher concentration desired for the gradient on an angled square Petri dish. The plate is angled so the agar covers the whole surface but has a negligible height on one side. The agar is allowed to solidify, then 50 ml liquid LB-agar are poured on the Petri dish lying flat. The plate was streaked in the direction of the gradient with the different strains. Plates are incubated at 37°C overnight.

2.3.2   Resistant colonies plates

E. coli NR698 was grown overnight in 10 ml LB, the cells were centrifuged for 3 min. at 3000 g, the volume was adjusted to give an inoculating solution with a concentration of 4 X 10^9 cells/ml. An LB-agar plate containing 2.5 µM MccB17 was inoculated with 2 X 10^9 cells (500 µl), and incubated overnight at 37°C.

2.3.3   Glycerol stock

Produced strains were stored at -80°C as glycerol stocks: 750 µl of overnight grown culture were added to a mixture of 107 µl DMSO and 214 µl glycerol, the mixture was briefly vortexed and flash frozen in liquid nitrogen before storage.

2.4   MccB17 mutants production

2.4.1   Template for MccB17 production

The plasmid coding for MccB17 was extracted from the strain DH5α-pmccB17 as follows: 2 X 5 ml of LB 0.1 mg/ml Amp were inoculated with colonies grown overnight on LB-agar containing 0.1 mg/ml Amp. The plasmid was extracted from the 2 X 5 ml using QIAprep® Miniprep kit from Qiagen. The miniprep yielded 2 X 50 µl containing 500-600 µg/µl of pUC19-*mcbABCDEF*. The plasmid's size was checked by digestion with EcoRI.

2.4.2   Production of mutated mcb gene

The template coding for MccB17 was amplified by PCR using primers carrying the desired mutation or stop codon as described in the table below. In a PCR tube, 5 µl of Pfu Turbo buffer (10X), 1 µl dNTP (10 mM), 1 µl of F-primer 200 nM, 1 µl of R-primer 200 nM, 1 µl of Pfu turbo (2.5 U), 1 µl of pmccB17 50 µg/µl and 40 µl MQ water were mixed and submitted to the sequence described in the table bellow. 25 µl of the amplification mixture were added to 5 µl of NEB-buffer n°4, 2 µl of DPNI (40 units), and 18 µl of MQ water and incubated overnight at 37°C in order to remove the pUC19-*mcbABCDEF* template.

2.4.3   Transformation

DH5α high efficiency *E. coli* cells were transformed as follow. In an eppendorf microcentrifuge tube on ice, 2.3 µl of the DPNI digest was added to 50 µl of DH5α cells and left for 20 min. The mixture was heat-shocked 2 min at 42°C, and 500 µl LB were added. The culture was incubated 1 h at 37°C before being centrifuged at 3000 rpm for 1 min. The supernatant was discarded by inverting the tube, the cells were resuspended in the remaining supernatant before being plated on LB-amp agar and incubated overnight at 37°C. Up to three surviving colonies were picked up from the plate and used to inoculate 10 ml of LB-amp that was incubated overnight at 37°C. Glycerol stocks were prepared using the overnight cultures, and the plasmid containing the modified *mccb17* gene was extracted from 5 ml using a QIAprep® Miniprep kit from Qiagen before being submitted to sequencing.

2.5 Alkaline hydrolysis of microcin B17

Example: A 2.5 ml (2.3 µmol) of a 0.9 mM solution of MccB17 in DMSO, 2.5 ml MQ water, and 0.16 ml of aqueous 5M NaOH (345 µmol), were introduced in a 10 ml round bottom flask equipped with a stirred, and a condenser. The mixture was stirred at 120°C for 7 days, water was added to complement evaporation. The solution was cooled, and the pH adjusted to 7. The mixture was diluted in water to reach 1/40 DMSO in water, and freeze dried.

Variation: other experiments have been carried out in 20% DMSO with 0.9 mM MccB17.

Raw MccB17 treatment: depending on the purification methods, the raw MccB17 was treated as described in Chapter III-1.2.

2.6 Proteolysis experiments

2.6.1 Endoprotease Glu-C

The digestion of the Mcc (N53D, N59D) by endoprotease Glu-C was conducted as follows: On ice, 0.1 mg of endo Glu-C in 500 µl of 100 mM ammonium bicarbonate pH = 7 were introduced in an eppendorf, 10.8 µl of a 3 mM solution of Mcc(N53D, N59D) in DMSO were added. The mixture was incubated for 48 h at 37°C. A strata C18_EC QSPE reverse phase column was equilibrated with 30 ml acetonitrile and 30 ml MQ water. The reaction mixture was loaded onto the column, and the column was eluted with 30 ml MQ water and 30 ml 50% acetonitrile/MQ water, this last fraction was collected and freeze dried after being flushed with air.

2.6.2 Subtilisin digest

The digestion of MccB17 by subtilisin was conducted as follow: in an universal, 200 µl of 5 mM solution of MccB17 in DMSO were added to 0.8 ml of reaction buffer (10 mM NaAcO, 5 mM Ca(AcO)$_2$). To the mixture placed on ice, was added 1 ml of 0.15 mg/ml subtilisin solution in the same ice-cooled buffer. The mixture was stirred and incubated at 37°C for 48 h. A strata C18_EC QSPE reverse phase column was equilibrated with 30 ml acetonitrile and 30 ml MQ water. The reaction mixture was loaded on the column, and the column was eluted with 30 ml MQ water and 30 ml 50% acetonitrile/MQ water, this last fraction was collected and freeze dried after being flushed with air.

2.6.3 Aminopeptidase digest

110 µl of 3 mM MccB17 solution in DMSO were added to 1 ml of reaction buffer (50 mM NaHPO$_3$, pH = 7.2). On ice, 1 µl (~0.1 units) of leucine aminopeptidase commercial solution (Sigma-Aldrich L5006) was added to the mixture. The reaction mixture was incubated 6 h 30 min at 37°C. The mixture was directly loaded on a 3 ml Oasis™ (Waters) column equilibrated with 6 ml CH$_3$CN and 6 ml MQ water. The column was eluated with 9 ml MQ water, and 9 ml 50% CH$_3$CN/water, this last fraction was collected and freeze dried.

2.6.4 Carboxypeptidase digest

110 µl of 3 mM MccB17 solution in DMSO were added to 1 ml of reaction buffer (25 mM TrisHCl, 500 mM NaCl, pH = 7.5). On ice, 2 µl (~3.5 units) of carboxypeptidase A commercial solution (Sigma-Aldrich C9268) was added to the mixture. The reaction mixture was incubated 6 h 30 at room temperature (25°C). The mixture was directly loaded on a 3 ml Oasis™ (Waters) column equilibrated with 6 ml CH_3CN and 6 ml MQ water. The column was eluated with 9 ml MQ water, and 9 ml 50% CH_3CN/water, this last fraction was collected and freeze dried.

2.7 Synthesis

2.7.1 Synthesis of oxazole amino acid (H-oz-OH): 2-aminomethyl oxazole-4-carboxylic acid

2.7.1.1 Boc-oz-OMe: Methyl 2-(N-tert-butoxycarbonyl)aminomethyloxazole-4-carboxylate

On a ice-cooled bath, 5 g of N-(tert-butoxycarbonyl)glycine (28 mmol), 4.2 g of O-methyl serine chlorhydrate (27 mmol), 5.5 g of N,N'-dicyclohexylcarbodiimide (27 mmol) were mixed in a round bottom flask under N_2, equipped with a stirrer. 150 ml of anhydrous dichloromethane and 3.9 ml triethylamine (Et_3N, 27 mmol) were added to the solids. The reaction mixture was stirred overnight at 0°C under N_2. The solvent was removed *in vacuo*; the solid residue obtained was triturated with ethyl acetate, filtered, and the filtrate was concentrated under vacuum. The isolated residue was triturated with a small amount of tetrahydrofuran and filtered, the residual ammonium chloride discarded, and the filtrate concentrated *in vacuo*. The isolated residue was purified by silica gel column chromatography with AcOEt/MeOH (19/1) as eluent, the fractions were controlled by TLC in the same conditions, $RF_{BocGlySerOMe}$ = 0.5. 2.3 g (8 mmol) of N-Boc-Gly-Ser-OMe were isolated, and introduced in a round-bottom flask, equipped with a stirrer and under N_2. 4 ml of bis(2-methoxyethyl)aminosulfur trifluoride (Deoxo-Fluor®, 9.2 mmol) in 64 ml anhydrous dichloromethane were added dropwise at -20°C. After stirring for 30 min at -20°C, 3 ml of bromotrichloromethane (30 mmol) were added dropwise to the mixture, followed by 4.6 ml of DBU (30 mmol). The reaction mixture was stirred for 8 h on an ice bath (T = 2-3°C) before being quenched with 100 ml of a saturated solution of $NaHCO_3$. The mixture was extracted 3 X with AcOEt, the decantation was very slow and the last extraction was left overnight to separate. The organic phase was dried on anhydrous Na_2SO_4 and concentrated under vacuum. The residue was purified on silica gel column chromatography with n-hexane/AcOEt (1/1) as eluent. The fractions were controlled by TLC with the same eluent, $RF_{BocozOMe}$ = 0.34. 1.22 g of the expected product were isolated, yield = 17%. The structure was confirmed by ^{1}H NMR (400Hz) DMSO-d6: 1.4 (s, 9H, Boc); 3.8 (s, 3H, OMe); 4.3 (s, 2H, CH_2); 8.8 (s, 1H, CH (oxazole)). And MS-ESI (+): *m/z* = 279.0 (M+Na^{+}); *m/z* = 257.0 (M+H^{+}); 201.0 (M-[t]Bu) in source fragment, in agreement with MS2 data from *m/z* = 257.0: ->201.0->159.0. The spectroscopic data were in agreement with those previously reported (Videnov, Kaiser et al. 1996).

2.7.1.2 Boc-oz-OH: 2-(N-tert-butoxycarbonyl)aminomethyloxazole-4-carboxylic acid

In a beaker, 40 mg of Boc-oz-OMe (0.15 mmol) was resuspended in 10 ml dioxan, and 5 ml of 1 M NaOH was added. The mixture was stirred for 1 h at RT, then the solution was neutralized by addition of 1 M H_2SO_4 and extracted with 3 X 15 ml dichloromethane. The organic phase was dried on anhydrous Na_2SO_4 before removing the solvent *in vacuo*. The structure was confirmed by MS-ESI (+): m/z = 265.1 (M+Na$^+$); m/z = 187.1 (M-^{t}Bu+Na$^+$) in source fragment. MS-ESI(-): m/z = 286.7 (M+HCO$_2^-$); m/z = 241.1 (M-H$^+$). The spectroscopic data were in agreement with those previously reported (Videnov, Kaiser et al. 1996).

2.7.1.3 H-oz-OH: 2- aminomethyloxazole-4-carboxylic acid

The previous Boc-oz-OH (0.15 mmol) was redissolved in 2 ml TFA/CH$_2$Cl$_2$ (1/1) and stirred for 2 h at RT. The mixture was concentrated *in vacuo* and led to the final product: 38 mg, yield 100%. The structure was confirmed by ^{1}H NMR (400Hz) DMSO-d6: 4.33 (s, 2H); 8.9 (s, 1H); MS-ESI (+): m/z = 143.0 (M+H$^+$). The spectroscopic data were in agreement with those previously reported (Coquin 2005).

2.7.2 Synthesis of thiazole amino acid (H-tz-OH): 2-aminomethyl thiazole-4-carboxylic acid

2.7.2.1 Boc-glycine amide: N-tert-butoxycarbonylglycine amide

In a round-bottom flask equipped with a stirrer, 4.8 g of Di-tert-butylcarbonate (0.22 mol) were added to a solution of 2.2 g of glycylamide (0.2 mol) and 3 ml TEA (0.2 mol) in 30 ml of THF/H$_2$O (4/1). The mixture was stirred for 5 h at RT. The mixture was extracted with 3 X 40 ml of AcOEt. The organic phase was washed respectively with 100 ml of 1 M sodium hydrogencarbonate solution and 100 ml brine before being dried on anhydrous Na$_2$SO and concentrated *in vacu.* 3.5 g of Boc-glycylamide were isolated, yield = 79 %. The structure was confirmed by ^{1}H NMR (400Hz) DMSO-d6: 1.42 (s, 9H, Boc); 3.8 (s, 2H, CH$_2$); 5.1 (s, 1H, NH); 5.45 (s, 1H, NH$_2$); 6.0 (s, 1H, NH$_2$). The spectroscopic data were in agreement with those previously reported (Videnov, Kaiser et al. 1996).

2.7.2.2 Boc-tz-OH: 2-(N-tert-butoxycarbonyl)aminomethylthiazole-4-carboxylic acid

In a round-bottom flask, 62 g of Lawesson's reagent (0.15 mol) were added to a solution of 34.7 g of Boc-glycinamide (0.2 mol) in 500 ml dimethoxyethane (DME), the reaction mixture was stirred overnight at RT. The solvent was removed under vacuum. 500 ml AcOEt and 500 ml 1M NaHCO$_3$ were added to the residues and stirred for 10 min. The organic phase was recovered and the aqueous phase was washed with 2 X 250 ml AcOEt. The combined organic phases were washed with 300 ml brine, dried on anhydrous Na$_2$SO4, and concentrated *in vacuo*. The solid residue was recrystalised in EtOAc/n-hexane and led to 29.3 g of Boc-glycylthioamide. 19 g of N-Boc-2-glycylethioamide (0.15 mol), and 61 g of potassium carbonate (0.6 mol) were introduced in a round bottom flask under N$_2$. 300 ml of anhydrous ethanol were added to the solids. A solution of 25 g of 3-bromo-2-oxopropanoic acid (0.23 mol) in 200 ml anhydrous ethanol was added dropwise. The reaction mixture was stirred for 4 h at RT. The

reaction completion is controlled by TLC (CHCl$_3$/MeOH/H$_2$O; 8/3/0.5). The reaction mixture is filtered, and the filtrate concentrated under vacuum. The residue isolated was recrystallized in AcOEt/n-hexane and led to m = 9.8 g of the expected product, yield = 25%. The structure was confirmed by ^{1}H NMR (400Hz) DMSO-d6: 1.4 (s, 9H, Boc); 4.35 (d, 2H, CH$_2$); 7.8 (t, 1H, NH); 8.3 (s, 1H, CH, tz). And MS-ESI (+): m/z = 281.1 (M+Na$^+$); m/z = 259.1 (M+Na$^+$); m/z = 203.0 (M-^{t}Bu+H$^+$). MS-ESI (-): m/z = 302.9 (M+HCO$_2$$^-$); m/z = 257.0 (M-H$^+$). The spectroscopic data were in agreement with those previously reported (Videnov, Kaiser et al. 1996).

2.7.2.3   H-tz-OH

70 mg of N-Boc-tz-OH (0.27 mmol) was dissolved in 4 ml TFA/CH$_2$Cl$_2$ (1/1) and stirred for 2 h at RT. The mixture was concentrated *in vacuo* to lead to the TFA salt of H-tz-OH m = 73 mg, yield = 100%. The structure was confirmed by ^{1}H NMR (400Hz) DMSO-d6: 4.5(s,2H); 8.5 (s, 1H). And MS-ESI (+): m/z = 159.0 (M+H$^+$). The spectroscopic data were in agreement with those previously reported (Coquin 2005).

2.7.3   Synthesis of H-oztz-OH

2.7.3.1   Boc-oztz-OH:
2-((N-tert-butoxycarbonyl)-2'-aminomethyloxazole-4'-yl)-thiazole-4-carboxylic acid

In a round-bottom flask equipped with a stirrer, 0.50 g of Boc-oz-OMe (2 mmol) were dissolved in 30 ml methanol. 10 ml of 35% aqueous ammonia were added at once and the mixture was stirred at RT overnight. The reaction mixture was concentrated in *vacuo*, and 50 ml of 1 M NaHCO$_3$ were added. The solid residue was filtered and washed with water, and led to m = 0.37 g of Boc-glycinamide. In a round-bottom flask, 0.20 g of Lawesson's reagent (0.8 mmol) were added to a solution of 0.24 g of Boc-glycinamide (0.6 mmol) in 4 ml DME, the reaction mixture was stirred overnight at RT. The solvent was removed under vacuum. 10 ml AcOEt and 10 ml 1 M NaHCO$_3$ were added to the residues and stirred for 10 min. The organic phase was recovered and the aqueous phase was washed with 2X 10 ml AcOEt. The combined organic phases were washed with 20 ml brine, dried on anhydrous Na$_2$SO4, and concentrated *in vacuo*. The solid residue was recrystallized in EtOAc/n-hexane and led to 0.17 g of Boc-oz(CS)-NH$_2$. In a round-bottom flask under N$_2$ equipped with a stirrer, 0.17 g Boc-oz(CS)-NH$_2$ (0.6 mmol) and 0.38 g of anhydrous potassium hydrogencarbonate (3.7 mmol) were added. 15 ml of anhydrous DME were added. The mixture was stirred for 10 min before adding dropwise 0.3 ml of ethylbromopyruvate (2.2 mmol). The reaction mixture was stirred overnight at RT. The mixture was filtered, washed with 3 X 15 ml brine, dried on anhydrous Na$_2$SO$_4$, and concentrated under vacuum. The residue was purified by silica gel column chromatography with EtOAc/n-hexane (2/1) as eluent, the fractions containing the expected product were identified by TLC in the same eluent, RF$_{BocoztzOEt}$ = 0.49. 0.9 g of Boc-oztz-OEt was obtained. In a beaker, 0.9 g of Boc-oztz-OEt (0.26 mmol) was dissolved in 3 ml dioxane, and 21 mg NaOH (0.52 mmol) in 1 ml water were added. The mixture was stirred 1 h at RT. The solution was set to pH = 6 by addition of 1M H$_2$SO$_4$. The dioxane was removed under vacuum, and the pH of the

solution was set to pH = 3. The mixture was extracted with 3 X 5 ml AcOEt. The organic phase was dried on anhydrous Na_2SO_4 and concentrated *in vacuo*. 0.6 g of the expected acid was isolated, yield = 19%. The structure was validated by MS-ESI (+): *m/z* = 348.0 (M+Na^{+}); *m/z* = 343.0 (M+NH$_4$[+]). *m/z* = 256 in source fragment-> 200 ->157 ->124 loss of Boc.

2.7.3.2   H-oztz-OH

In a beaker, 0.6 g of Boc-oztz-OH (0.19 mmol) were dissolved in 2 ml TFA/CH_2Cl_2 (1/1) and stirred 1h at RT. The mixture was concentrated *in vacuo* to lead to the TFA salt of H-oztz-OH, m = 64 mg. Structure confirmed by ^{1}H NMR (400Hz) DMSO-d6: 4.5 (s, 2H); 8.6 (s, 1H, tz); 8.9 (s, 1H, oz); MS-ESI (+): *m/z* = 226. The spectroscopic data were in agreement with those previously reported (Coquin 2005).

2.7.4   Synthesis of H-tzoz-OH:
2-(2'-aminomethylthiazole-4'-yl)-oxazole-4-carboxylic acid

2.7.4.1   Boc-tz-Ser-OMe:
N-(2-(N'-tert-butoxycarbonyl)aminomethylthiazole-4-carbonyl)-Serine methyl ester

In a round-bottom flask in an ice-cooled bath, under N_2, 4 g Boc-tz-OH (15.5 mmol) were dissolved in 75 ml anhydrous dichloromethane. TEA (30 mmol), serine hydrochloride (30 mmol) and DCC were added to the mixture. The reaction mixture was stirred overnight at 0°C. The solvent was removed *in vacuo* and the residue triturated with 100 ml AcOEt. The DCU was removed by filtration, and the filtrate concentrated under vacuum. A small amount of THF was added, the NH_4Cl was allowed to precipitate before being removed by filtration. The filtrate was concentrated, and the residue purified by silica gel column chromatography with AcOEt/MeOH 19/1 as eluent. The structure was confirmed by ^{1}H NMR (400Hz) DMSO-d6: 1.4 (s, 9H, Boc); 3.6 (s, 3H, OCH_3); 3.5-4 (m, 3H, CH & CH_2, Ser); 4.4(s, 2H, CH_2-tz); 5.2 (s, 1H, NH, amide); 7.8 (s, 1H, NH, Boc); 8.18 (1H, CH, tz). And MS-ESI (+): *m/z* = 382.1 (M+Na^{+}); *m/z* = 360.0 (M+H^{+}).

2.7.4.2   Boc-tzoz-OMe:
Methyl-2-((N-tert-butoxycarbonyl)-2'-aminomethylthiazole-4'-yl)-oxazole-4-carboxylate

In a round-bottom flask, at -20°C, under N_2, 0.256 g of Boc-tz-Ser-OMe (0.7 mmol) in 8 ml of anhydrous CH_2Cl_2. DeoxoFluor® (0.77 mmol) was added dropwise to the reaction mixture. After stirring the mixture for 30 min at -20°C, 250 µl bromotrichloromethane (2.5 mmol) and 383 µl DBU (2.5 mmol) were added. The reaction mixture was stirred on an ice bath for 8 h. The mixture was quenched with 10 ml of a saturated solution of $NaHCO_3$, the CH_2Cl_2 was removed under vacuum and the remaining aqueous phase was extracted with 3 X 10 ml of AcOEt. The organic extract was dried and concentrated *in vacuo*. The residue was purified by silica gel column chromatography with AcOEt as eluent. 150 mg of the compound were

isolated, yield = 63%. The structure was confirmed by MS-ESI (+): m/z = 284.1 (M-^{t}Bu+H^{+}); m/z = 357.0 (M+Na^{+}); m/z = 362.1 (M +NH$_4^{+}$).

2.7.4.3   Boc-tzoz-OH:
2-((N-tert-butoxycarbonyl)-2'-aminomethylthiazole-4'-yl)-oxazole-4-carboxylic acid

In a beaker, 140 mg of Boc-tzoz-OMe (0.4 mmol) were dissolved in 3 ml dioxane. 16 mg of sodium hydroxide (0.4 mmol) in 1 ml water were added to the solution. The mixture was stirred at RT for 1 h. The dioxane was removed under vacuum, and the pH of the solution was adjusted to 3 before extraction with 3x 5 ml AcOEt. The organic phases were collected, dried with anhydrous Na_2SO_4, and concentrated *in vacuo*. 128 mg of the acid were isolated, yield = 94%. The structure was confirmed by MS-ESI (+): m/z = 348.1 (M+K^{+}); m/z = 343.0 (M+NH$_4^{+}$). MS-ESI (-): m/z = 370.0 (M+HCO$_2^{-}$); m/z = 324.1 (M-H^{+}).

2.7.4.4   H-tzoz-OH

64 mg Boc-tzoz-OH (0.2 mmol) was dissolved in 2 ml TFA/CH$_2$Cl$_2$ (1/1), the mixture was stirred for 1 h at RT. The mixture was concentrated under vacuum and lead to the TFA salt of H-tzoz-OH. 68 mg were isolated, yield = 100%. The structure was confirmed by ^{1}H NMR (400Hz) DMSO-d6: 4.4 (s, 2H); 8.5 (s, 1H, tz); 9.0 (s, 1H, oz). MS-ESI (+): m/z = 226.1 (M+H^{+}). The spectroscopic data were in agreement with those previously reported (Coquin 2005).

Abbreviations

A. baumannii: *Acinetobacter baumannii*

AcOEt: ethyl acetate

ATP: Adenosine triphosphate

Boc: tert-butyloxycarbonyl

CFX: ciprofloxacin

CTD: C-terminal domain

DBU: 1,8-Diazabicyclo[5.4.0]undec-7-ene.

DCC: N,N'-dicyclohexylcarbodiimide

Deoxo-Fluor®: bis(2-methoxyethyl)aminosulfur trifluoride

DIEA: diisopropylethylamine

DME: dimethoxyethane

DMF: dimethylformamide

DMSO: dimethyl sulfoxide

DNA: Deoxyribonucleic acid

E. coli: *Escherichia coli*

EDTA: ethylenediaminetetraacetic acid

eq: equivalent

Et: ethyl

Et$_3$N : triethylamine

GlcNAc: N-acetylglucosamine

G-segment: gate segment

GTP: guanosine triphosphate

GyrA: gyrase A

GyrB: gyrase B

HEPES: (4-(2-hydroxyethyl)-1-piperazineethanesulfonic acid)

HOBt: N-Hydroxybenzotriazole

HOBt: N-hydroxybenzotriazole

H-oz-OH: 2-aminomethyloxazole-4-carboxylic acid

H-oztz-OH: 2-[2'-aminomethyloxazole-4'-yl]thiazole-4-carboxylic acid

HPLC: high-performance liquid chromatography

H-tz-OH: 2-aminomethylthiazole carboxylic acid

H-tzoz-OH: 2-[2'-aminomethylthiazole-4'-yl]oxazole-4-carboxylic acid

IC$_{50}$: inhibitory concentation for 50% inhibition

kb: kilobases

M. tuberculosis: *Mycobacterium tuberculosis*

MALDI-ToF (MS): Matrix-assisted laser desorption/ionization coupled-time-of-flight (mass spectrometry)

Mcc: microcin

MccB17: microcin B17

MDR-TB: multidrug-resistant tuberculosis

Me: methyl

MeOH: methanol

MetA: methylenomycin A

MetC: methylenomycin C

MIC: minimal inhibitory concentration

MQ water: milli-q water, high purity ion-exchanged water.

mRNA: messenger ribonucleic acid

MRSA: meticillin-resistant *Staphylococcus aureus*

MS: mass spectrometry

MurNAc: N-acetylmuramic acid

MW: molecular weight

NTD: N-terminal domain

PBP: penicillin binding protein

PEG: polyethylene glycol

PolyG: polyglycine

QRDR: quinolone-resistance-determining region

rRNA: ribosomal ribonucleic acid

RT: room temperature

S. aureus: *Staphylococcus aureus*

S. cerevisiae: *Saccharomyces cerevisiae*

SaGyrA: *Staphylococcus aureus* gyrase A

SaGyrB: *Staphylococcus aureus* gyrase A

SimD8: simocyclinone D8

TBTU: 2-(1 H-benzotriazol-1-yl)-1,1,3,3-tetramethyluronium tetrafluoroborate

TBTU: O-(Benzotriazol-1-yl)-N,N,N',N'-tetramethyluronium tetrafluoroborate

TFA: trifluoroacetic acid

THF: tetrahydrofuran

TLC: thin layer chromatography

Topo : topoisomerase

Topo II: topoisomerase II

Topo IV: topoisomerase IV

tRNA: transfer ribonucleic acid

T-segment: transported segment

UDP: Uridine diphosphate

VRE: vancomycin-resistant *Enterococcus*

WHD: winged helix domain

XDR-TB: extensively drug-resistant tuberculosis

Bibliography

Alekshun, M. N. and S. B. Levy (2007). "Molecular Mechanisms of Antibacterial Multidrug Resistance." Cell **128**(6): 1037-1050.

Andersen, N. R. and P. R. Rasmussen (1984). "The constitution of clerocidin a new antibiotic isolated from." Tetrahedron Lett. **25**(4): 465-468.

Andoh, T. and R. Ishida (1998). "Catalytic inhibitors of DNA topoisomerase II." Biochim. Biophys. Acta **1400**(1-3): 155-171.

Angehrn, P., S. Buchmann, et al. (2004). "New Antibacterial Agents Derived from the DNA Gyrase Inhibitor Cyclothialidine." J. Med. Chem. **47**(6): 1487-1513.

Aravind, L., L. M. Iyer, et al. (2003). "Plasmodium biology: genomic gleanings." Cell **115**(7): 771-785.

Asensio, C. and J. C. Perez-Diaz (1976). "A new family of low molecular weight antibiotics from enterobacteria." Biochem. Biophys. Res. Commun. **69**(1): 7-14.

Bahassi, E. M., M. H. O'Dea, et al. (1999). "Interactions of CcdB with DNA gyrase. Inactivation of Gyra, poisoning of the gyrase-DNA complex, and the antidote action of CcdA." J. Biol. Chem. **274**(16): 10936-10944.

Baird, C. L., M. S. Gordon, et al. (2001). "The ATPase reaction cycle of yeast DNA topoisomerase II. Slow rates of ATP resynthesis and P(i) release." J.Biol. Chem. **276**(30): 27893-27898.

Baird, C. L., T. T. Harkins, et al. (1999). "Topoisomerase II drives DNA transport by hydrolyzing one ATP." Proc. Natl. Acad. Sci. U. S. A. **96**(24): 13685-13690.

Baker, N. M., S. Weigand, et al. (2010). "Solution structures of DNA-bound gyrase." Nucleic Acids Res..

Baltz, R. H. (2009). "Daptomycin: mechanisms of action and resistance, and biosynthetic engineering." Curr. Opin. Chem. Biol. **13**(2): 144-151.

Baquero, F., D. Bouanchaud, et al. (1978). "Microcin plasmids: a group of extrachromosomal elements coding for low-molecular-weight antibiotics in Escherichia coli." J. Bacteriol. **135**(2): 342-347.

Baquero, F. and F. Moreno (1984). "The Microcins." FEMS Microbiol. Lett. **23**(2-3): 117-124.

Bateman, A., A. G. Murzin, et al. (1998). "Structure and distribution of pentapeptide repeats in bacteria." Protein Sci. **7**(6): 1477-1480.

Bates, A. D. (2001). Topoisomerases, John Wiley & Sons, Ltd.

Bauernfeind, A. and C. Petermuller (1983). "In vitro activity of ciprofloxacin, norfloxacin and nalidixic acid." Eur. J. Clin. Microbiol. **2**(2): 111-115.

Bax, B. D., P. F. Chan, et al. "Type IIA topoisomerase inhibition by a new class of antibacterial agents." Nature **466**(7309): 935-940.

Bax, B. D., P. F. Chan, et al. (2010). "Type IIA topoisomerase inhibition by a new class of antibacterial agents." Nature **466**(7309): 935-940.

Bayer, A., S. Freund, et al. (1995). "Post-translational heterocyclic backbone modifications in the 43-peptide antibiotic microcin B17. Structure elucidation and NMR study of a 13C,15N-labelled gyrase inhibitor." Eur. J. Biochem. **234**(2): 414-426.

Bayer, A., S. Freund, et al. (1993). "Posttranslational Backbone Modifications in the Ribosomal Biosynthesis of the Glycine-Rich Antibiotic Microcin-B17." Angew. Chem. Int. Ed. **32**(9): 1336-1339.

Bellon, S., J. D. Parsons, et al. (2004). "Crystal structures of Escherichia coli topoisomerase IV ParE subunit (24 and 43 kilodaltons): a single residue dictates differences in novobiocin potency against topoisomerase IV and DNA gyrase." <u>Antimicrob. Agents Chemother.</u> **48**(5): 1856-1864.

Belshaw, P. J., R. S. Roy, et al. (1998). "Kinetics and regioselectivity of peptide-to-heterocycle conversions by microcin B17 synthetase." <u>Chem. Biol.</u> **5**(7): 373-384.

Berger, J. M., S. J. Gamblin, et al. (1996). "Structure and mechanism of DNA topoisomerase II." <u>Nature</u> **379**(6562): 225-232.

Bergerat, A., B. de Massy, et al. (1997). "An atypical topoisomerase II from Archaea with implications for meiotic recombination." <u>Nature</u> **386**(6623): 414-417.

Bergerat, A., D. Gadelle, et al. (1994). "Purification of a DNA topoisomerase II from the hyperthermophilic archaeon Sulfolobus shibatae. A thermostable enzyme with both bacterial and eucaryal features." <u>J. Biol. Chem.</u> **269**(44): 27663-27669.

Bernard, P. and M. Couturier (1992). "Cell killing by the F plasmid CcdB protein involves poisoning of DNA-topoisomerase II complexes." <u>J. Mol. Biol.</u> **226**(3): 735-745.

Bernard, P., K. E. Kezdy, et al. (1993). "The F plasmid CcdB protein induces efficient ATP-dependent DNA cleavage by gyrase." <u>J. Mol. Biol.</u> **234**(3): 534-541.

Binaschi, M., G. Zagotto, et al. (1997). "Irreversible and reversible topoisomerase II DNA cleavage stimulated by clerocidin: sequence specificity and structural drug determinants." <u>Cancer Res.</u> **57**(9): 1710-1716.

Birch, R. G. and S. S. Patil (1985). "Preliminary Characterization of an Antibiotic Produced by Xanthomonas albilineans Which Inhibits DNA Synthesis in Escherichia coli." <u>J. Gen. Microbiol.</u> **131**(5): 1069-1075.

Biron, E., J. Chatterjee, et al. (2006). "Solid-phase synthesis of 1,3-azole-based peptides and peptidomimetics." <u>Org. Lett.</u> **8**(11): 2417-2420.

Boger, D. L. (2001). "Vancomycin, teicoplanin, and ramoplanin: synthetic and mechanistic studies." <u>Med. Res. Rev.</u> **21**(5): 356-381.

Boucher, H. W., G. H. Talbot, et al. (2009). "Bad bugs, no drugs: no ESKAPE! An update from the Infectious Diseases Society of America." <u>Clin. Infect. Dis.</u> **48**(1): 1-12.

Bouhss, A., A. E. Trunkfield, et al. (2008). "The biosynthesis of peptidoglycan lipid-linked intermediates." <u>FEMS Microbiol. Rev.</u> **32**(2): 208-233.

Bozdogan, B., D. Esel, et al. (2003). "Antibacterial susceptibility of a vancomycin-resistant Staphylococcus aureus strain isolated at the Hershey Medical Center." <u>J. Antimicrob. Chemother.</u> **52**(5): 864-868.

Braun, M. and T. J. Silhavy (2002). "Imp/OstA is required for cell envelope biogenesis in Escherichia coli." <u>Mol. Microbiol.</u> **45**(5): 1289-1302.

Brino, L., A. Urzhumtsev, et al. (2000). "Dimerization of Escherichia coli DNA-gyrase B provides a structural mechanism for activating the ATPase catalytic center." <u>J. Biol. Chem.</u> **275**(13): 9468-9475.

Bromberg, K. D., A. B. Burgin, et al. (2003). "Quinolone action against human topoisomerase IIalpha: stimulation of enzyme-mediated double-stranded DNA cleavage." <u>Biochemistry</u> **42**(12): 3393-3398.

Brotzu, G. (1948). "Research on a new antibiotic." <u>Publication of the Cagliari Institute of Hygiene</u>: 1-11.

Brown, P. O., C. L. Peebles, et al. (1979). "A topoisomerase from Escherichia coli related to DNA gyrase." <u>Proc. Natl. Acad. Sci. U. S. A.</u> **76**(12): 6110-6114.

Brvar, M., A. Perdih, et al. (2010). "In silico discovery of 2-amino-4-(2,4-dihydroxyphenyl)thiazoles as novel inhibitors of DNA gyrase B." Bioorg. Med. Chem. Lett. **20**(3): 958-962.

Bush, K. (2010). "Alarming [beta]-lactamase-mediated resistance in multidrug-resistant Enterobacteriaceae." Curr. Opin. Microbiol. **13**(5): 558-564.

Champoux, J. J. (2001). "DNA topoisomerases: structure, function, and mechanism." Annu. Rev. Biochem. **70**: 369-413.

Champoux, J. J. and R. Dulbecco (1972). "An activity from mammalian cells that untwists superhelical DNA--a possible swivel for DNA replication (polyoma-ethidium bromide-mouse-embryo cells-dye binding assay)." Proc. Natl. Acad. Sci. U. S. A. **69**(1): 143-146.

Chatterji, M., S. Unniraman, et al. (2000). "The additional 165 amino acids in the B protein of Escherichia coli DNA gyrase have an important role in DNA binding." J. Biol. Chem. **275**(30): 22888-22894.

Chen, C. R., M. Malik, et al. (1996). "DNA gyrase and topoisomerase IV on the bacterial chromosome: quinolone-induced DNA cleavage." J. Mol. Biol. **258**(4): 627-637.

Chen, G. L., L. Yang, et al. (1984). "Nonintercalative antitumor drugs interfere with the breakage-reunion reaction of mammalian DNA topoisomerase II." J. Biol. Chem. **259**(21): 13560-13566.

Chiang, C.-Y., R. Centis, et al. "Drug-resistant tuberculosis: Past, present, future." Respirology **15**(3): 413-432.

Chopra, I. and M. Roberts (2001). "Tetracycline antibiotics: mode of action, applications, molecular biology, and epidemiology of bacterial resistance." Microbiol. Mol. Biol. Rev. **65**(2): 232-260 ; second page, table of contents.

Cline, S. D., T. L. Macdonald, et al. (1997). "Azatoxin is a mechanistic hybrid of the topoisomerase II-targeted anticancer drugs etoposide and ellipticine." Biochemistry **36**(42): 13095-13101.

Collins, L. A., G. M. Eliopoulos, et al. (1993). "In vitro activity of ramoplanin against vancomycin-resistant gram-positive organisms." Antimicrob. Agents Chemother. **37**(6): 1364-1366.

Coquin, L. (2005). Synthesis and biological activity of heterocycles and heptapeptide derivatives related to microcin B17 : potential leads for new herbicides and antibiotics School of Chemical Science. Norwich, UK., University of East Anglia. Thesis.

Corbett, K. D., A. J. Schoeffler, et al. (2005). "The structural basis for substrate specificity in DNA topoisomerase IV." J. Mol. Biol. **351**(3): 545-561.

Corbett, K. D., R. K. Shultzaberger, et al. (2004). "The C-terminal domain of DNA gyrase A adopts a DNA-bending beta-pinwheel fold." Proc. Natl. Acad. Sci. USA **101**(19): 7293-7298.

Cornforth, J. W. and R. H. Cornforth (1947). "A New Synthesis of Oxazoles and Iminazoles Including Its Application to the Preparation of Oxazole." J. Chem. Soc.(Jan): 96-102.

Costenaro, L., J. G. Grossmann, et al. (2005). "Small-angle X-ray scattering reveals the solution structure of the full-length DNA gyrase a subunit." Structure **13**(2): 287-296.

Costenaro, L., J. G. Grossmann, et al. (2007). "Modular structure of the full-length DNA gyrase B subunit revealed by small-angle X-ray scattering." Structure **15**(3): 329-339.

Crisona, N. J., T. R. Strick, et al. (2000). "Preferential relaxation of positively supercoiled DNA by E. coli topoisomerase IV in single-molecule and ensemble measurements." Genes Dev. **14**(22): 2881-2892.

Critchlow, S. E., M. H. O'Dea, et al. (1997). "The interaction of the F plasmid killer protein, CcdB, with DNA gyrase: induction of DNA cleavage and blocking of transcription." J. Mol. Biol. **273**(4): 826-839.

Dalhoff, A., N. Janjic, et al. (2006). "Redefining penems." Biochem. Pharmacol. **71**(7): 1085-1095.

Dalton, K. M. and S. Crosson (2010). "A Conserved Mode of Protein Recognition and Binding in a ParDˆ'ParE Toxinˆ'Antitoxin Complex." Biochemistry **49**(10): 2205-2215.

Dao-Thi, M.-H., L. Van Melderen, et al. (2005). "Molecular Basis of Gyrase Poisoning by the Addiction Toxin CcdB." J. Mol. Biol. **348**(5): 1091-1102.

Dao-Thi, M. H., L. Van Melderen, et al. (2005). "Molecular basis of gyrase poisoning by the addiction toxin CcdB." J. Mol. Biol. **348**(5): 1091-1102.

Dao-Thi, M. H., L. Van Melderen, et al. (2004). "Crystallization of CcdB in complex with a GyrA fragment." Acta Crystallogr., Sect. D. Biol. Crystallogr. **60**(Pt 6): 1132-1134.

Davagnino, J., M. Herrero, et al. (1986). "The DNA replication inhibitor microcin B17 is a forty-three-amino-acid protein containing sixty percent glycine." Proteins **1**(3): 230-238.

De Jonge, N., L. Buts, et al. (2007). "Purification and crystallization of Vibrio fischeri CcdB and its complexes with fragments of gyrase and CcdA." Acta Crystallogr., Sect. F Struct. Biol .Cryst. Commun. **63**(Pt 4): 356-360.

De Jonge, N., A. Garcia-Pino, et al. (2009). "Rejuvenation of CcdB-poisoned gyrase by an intrinsically disordered protein domain." Mol. Cell **35**(2): 154-163.

Decroix, M. O., J. C. Chaumeil, et al. (1984). "Binding of cefalotin to human serum albumin." Eur. J. Drug Metab. Pharmacokinet. **9**(3): 191-194.

Deibler, R. W., S. Rahmati, et al. (2001). "Topoisomerase IV, alone, unknots DNA in E. coli." Genes Dev. **15**(6): 748-761.

del Castillo, F. J., I. del Castillo, et al. (2001). "Construction and Characterization of Mutations at Codon 751 of the Escherichia coli gyrB Gene That Confer Resistance to the Antimicrobial Peptide Microcin B17 and Alter the Activity of DNA Gyrase." J. Bacteriol. **183**(6): 2137-2140.

Dong, K. C. and J. M. Berger (2007). "Structural basis for gate-DNA recognition and bending by type IIA topoisomerases." Nature **450**(7173): 1201-1205.

Drlica, K. and X. Zhao (1997). "DNA gyrase, topoisomerase IV, and the 4-quinolones." Microbiol. Mol. Biol. Rev. **61**(3): 377-392.

Duquesne, S., D. Destoumieux-Garzon, et al. (2007). "Microcins, gene-encoded antibacterial peptides from enterobacteria." Nat. Prod. Rep. **24**(4): 708-734.

Edson, R. S. and C. L. Terrell (1999). "The aminoglycosides." Mayo. Clin. Proc. **74**(5): 519-528.

Edwards, D. I. (1993). "Nitroimidazole drugs--action and resistance mechanisms. I. Mechanisms of action." J. Antimicrob. Chemother. **31**(1): 9-20.

Edwards, D. I. (1993). "Nitroimidazole drugs--action and resistance mechanisms. II. Mechanisms of resistance." J. Antimicrob. Chemother. **31**(2): 201-210.

Edwards, M. J., R. H. Flatman, et al. (2009). "A Crystal Structure of the Bifunctional Antibiotic Simocyclinone D8, Bound to DNA Gyrase." Science **326**(5958): 1415-1418.

El-Shaboury, S. R., G. A. Saleh, et al. (2007). "Analysis of cephalosporin antibiotics." J. Pharm. Biomed. Anal. **45**(1): 1-19.

Emmerson, A. M. and A. M. Jones (2003). "The quinolones: decades of development and use." J. Antimicrob. Chemother. **51 Suppl 1**: 13-20.

Falagas, M. E., A. C. Kastoris, et al. (2009). "Fosfomycin for the treatment of infections caused by multidrug-resistant non-fermenting Gram-negative bacilli: a systematic review of microbiological, animal and clinical studies." Int. J. Antimicrob. Agents **34**(2): 111-120.

Feder, H. M., Jr. (1986). "Chloramphenicol: what we have learned in the last decade." South Med. J. **79**(9): 1129-1134.

Flynne, W. G. (2008). Biotechnology and bioengineering. Hauppauge, N.Y., Nova Biomedical ; Lancaster : Gazelle [distributor].

Forterre, P., S. Gribaldo, et al. (2007). "Origin and evolution of DNA topoisomerases." Biochimie **89**(4): 427-446.

Fortune, J. M. and N. Osheroff (1998). "Merbarone inhibits the catalytic activity of human topoisomerase IIalpha by blocking DNA cleavage." J. Biol. Chem. **273**(28): 17643-17650.

Fortune, J. M., L. Velea, et al. (1999). "DNA topoisomerases as targets for the anticancer drug TAS-103: DNA interactions and topoisomerase catalytic inhibition." Biochemistry **38**(47): 15580-15586.

Fowler, V. G., H. W. Boucher, et al. (2006). "Daptomycin versus Standard Therapy for Bacteremia and Endocarditis Caused by Staphylococcus aureus." N. Engl. J. Med.**355**(7): 653-665.

Fritsche, T. R., H. S. Sader, et al. (2008). "Antimicrobial activity of ceftobiprole, a novel anti-methicillin-resistant *Staphylococcus aureus* cephalosporin, tested against contemporary pathogens: results from the SENTRY Antimicrobial Surveillance Program (2005-2006)." Diagn. Micr. Infec. Dis. **61**(1): 86-95.

Fu, G., J. Wu, et al. (2009). "Crystal structure of DNA gyrase B' domain sheds lights on the mechanism for T-segment navigation." Nucleic Acids Res. **37**(17): 5908-5916.

Garrido, M. C., M. Herrero, et al. (1988). "The export of the DNA replication inhibitor Microcin B17 provides immunity for the host cell." EMBO J. **7**(6): 1853-1862.

Garrido, M. C., M. Herrero, et al. (1988). "The export of the DNA replication inhibitor Microcin B 17 provides immunity for the host cell." EMBO J. **7**(6): 1853-1862.

Gatto, B., S. Richter, et al. (2001). "The topoisomerase II poison clerocidin alkylates non-paired guanines of DNA: implications for irreversible stimulation of DNA cleavage." Nucleic Acids Res. **29**(20): 4224-4230.

Gellert, M. (1981). "DNA Topoisomerases." Annu. Rev. Biochem. **50**(1): 879-910.

Gellert, M., K. Mizuuchi, et al. (1977). "Nalidixic acid resistance: a second genetic character involved in DNA gyrase activity." Proc. Natl. Acad. Sci. U. S. A. **74**(11): 4772-4776.

Gellert, M., K. Mizuuchi, et al. (1976). "DNA gyrase: an enzyme that introduces superhelical turns into DNA." Proc. Natl. Acad. Sci. U. S. A. **73**(11): 3872-3876.

Gellert, M., M. H. O'Dea, et al. (1976). "Novobiocin and coumermycin inhibit DNA supercoiling catalyzed by DNA gyrase." Proc. Natl. Acad. Sci. U. S. A. **73**(12): 4474-4478.

Genilloud, O., F. Moreno, et al. (1989). "DNA sequence, products, and transcriptional pattern of the genes involved in production of the DNA replication inhibitor microcin B17." J Bacteriol **171**(2): 1126-1135.

Goetschi, E., P. Angehrn, et al. (1993). "Cyclothialidine and its congeners: A new class of DNA gyrase inhibitors." Pharmacol. Ther. **60**(2): 367-380.

Gomez, L., M. D. Hack, et al. (2007). "Novel pyrazole derivatives as potent inhibitors of type II topoisomerases. Part 1: Synthesis and preliminary SAR analysis." Bioorg. Med. Chem. Lett. **17**(10): 2723-2727.

Goss, W. A., W. H. Deitz, et al. (1965). "Mechanism of Action of Nalidixic Acid on Escherichia Coli.Ii. Inhibition of Deoxyribonucleic Acid Synthesis." J. Bacteriol. **89**: 1068-1074.

Greenstein, M., J. L. Speth, et al. (1981). "Mechanism of action of cinodine, a glycocinnamoylspermidine antibiotic." Antimicrob. Agents Chemother. **20**(4): 425-432.

Griffith, R. S. and H. R. Black (1964). "Cephalothin--a New Antibiotic. Preliminary Clinical and Laboratory Studies." JAMA **189**: 823-828.

Gross, C. H., J. D. Parsons, et al. (2003). "Active-site residues of Escherichia coli DNA gyrase required in coupling ATP hydrolysis to DNA supercoiling and amino acid substitutions leading to novobiocin resistance." Antimicrob. Agents Chemother. **47**(3): 1037-1046.

Hamad, B. (2010). "The antibiotics market." Nat. Rev. Drug. Discov. **9**(9): 675-676.

Hartung, F. and H. Puchta (2001). "Molecular characterization of homologues of both subunits A (SPO11) and B of the archaebacterial topoisomerase 6 in plants." Gene **271**(1): 81-86.

Hashimi, S. M., M. K. Wall, et al. (2007). "The Phytotoxin Albicidin is a Novel Inhibitor of DNA Gyrase." Antimicrob. Agents Chemother. **51**(1): 181-187.

Hawtin, R. E., D. E. Stockett, et al. (2010). "Voreloxin is an anticancer quinolone derivative that intercalates DNA and poisons topoisomerase II." PLoS One **5**(4): e10186.

Hawtin, R. E., D. E. Stockett, et al. "Voreloxin Is an Anticancer Quinolone Derivative that Intercalates DNA and Poisons Topoisomerase II." PLoS ONE **5**(4): e10186.

Heddle, J. G., S. J. Blance, et al. (2001). "The antibiotic microcin B17 is a DNA gyrase poison: characterisation of the mode of inhibition." J. Mol. Biol. **307**(5): 1223-1234.

Heddle, J. G., S. Mitelheiser, et al. (2004). "Nucleotide binding to DNA gyrase causes loss of DNA wrap." J. Mol. Biol. **337**(3): 597-610.

Hegde, S. S., M. W. Vetting, et al. (2005). "A fluoroquinolone resistance protein from Mycobacterium tuberculosis that mimics DNA." Science **308**(5727): 1480-1483.

Herrero, M. and F. Moreno (1986). "Microcin B17 blocks DNA replication and induces the SOS system in Escherichia coli." J. Gen. Microbiol. **132**(2): 393-402.

Ho, M. X., B. P. Hudson, et al. (2009). "Structures of RNA polymerase-antibiotic complexes." Curr. Opin.Struct. Biol. **19**(6): 715-723.

Holden, J. A. (2001). "DNA topoisomerases as anticancer drug targets: from the laboratory to the clinic." Curr. Med. Chem. Anticancer Agents **1**(1): 1-25.

Hooper, D. C. (1998). "Bacterial topoisomerases, anti-topoisomerases, and anti-topoisomerase resistance." Clin. Infect. Dis. **27 Suppl 1**: S54-63.

Hopkins, K. L., R. H. Davies, et al. (2005). "Mechanisms of quinolone resistance in Escherichia coli and Salmonella: recent developments." Int. J. Antimicrob. Agents **25**(5): 358-373.

Horowitz, D. S. and J. C. Wang (1987). "Mapping the active site tyrosine of Escherichia coli DNA gyrase." J. Biol. Chem. **262**(11): 5339-5344.

Huband, M. D., M. A. Cohen, et al. (2007). "In Vitro and In Vivo Activities of PD 0305970 and PD 0326448, New Bacterial Gyrase/Topoisomerase Inhibitors with Potent Antibacterial Activities versus Multidrug-Resistant Gram-Positive and Fastidious Organism Groups." Antimicrob. Agents Chemother. **51**(4): 1191-1201.

Hughes, R. A. and C. J. Moody (2007). "From Amino Acids to Heteroaromatics—Thiopeptide Antibiotics, Nature's Heterocyclic Peptides." Angew. Chem. Int. Ed. **46**(42): 7930-7954.

Jamora, C., M. A. Theodoraki, et al. (2001). "Investigation of the biological mode of action of clerocidin using whole cell assays." Bioorg. Med. Chem. **9**(6): 1365-1370.

Jana, S. and J. K. Deb (2006). "Molecular understanding of aminoglycoside action and resistance." Appl. Microbiol. Biotechnol. **70**(2): 140-150.

Jiang, Y., J. Pogliano, et al. (2002). "ParE toxin encoded by the broad-host-range plasmid RK2 is an inhibitor of Escherichia coli gyrase". Mol. Microbiol. **44**(4): 971-979.

Johnson, E. P., A. R. Strom, et al. (1996). "Plasmid RK2 toxin protein ParE: purification and interaction with the ParD antitoxin protein." J. Bacteriol. **178**(5): 1420-1429.

Johnston, N. J., T. A. Mukhtar, et al. (2002). "Streptogramin antibiotics: mode of action and resistance." Curr. Drug Targets **3**(4): 335-344.

Jung, H.-M., M. Jeya, et al. (2009). "Biosynthesis, biotechnological production, and application of teicoplanin: current state and perspectives." Appl. Microbiol. Biotechnol. **84**(3): 417-428.

Kampranis, S. C., N. A. Gormley, et al. (1999). "Probing the binding of coumarins and cyclothialidines to DNA gyrase." Biochemistry **38**(7): 1967-1976.

Kampranis, S. C., A. J. Howells, et al. (1999). "The interaction of DNA gyrase with the bacterial toxin CcdB: evidence for the existence of two gyrase-CcdB complexes." J. Mol. Biol. **293**(3): 733-744.

Kampranis, S. C. and A. Maxwell (1996). "Conversion of DNA gyrase into a conventional type II topoisomerase." Proc. Natl. Acad. Sci. U. S. A. **93**(25): 14416-14421.

Kampranis, S. C. and A. Maxwell (1998). "Conformational changes in DNA gyrase revealed by limited proteolysis." J. Biol. Chem. **273**(35): 22606-22614.

Kastoris, A., P. Rafailidis, et al. (2010). "Synergy of fosfomycin with other antibiotics for Gram-positive and Gram-negative bacteria." Eur. J. Clin. Pharmacol.**66**(4): 359-368.

Kato, J., Y. Nishimura, et al. (1990). "New topoisomerase essential for chromosome segregation in E. coli." Cell **63**(2): 393-404.

Kato, J., H. Suzuki, et al. (1992). "Purification and characterization of DNA topoisomerase IV in Escherichia coli." J. Biol. Chem. **267**(36): 25676-25684.

Kawada, S., Y. Yamashita, et al. (1991). "Induction of a heat-stable topoisomerase II-DNA cleavable complex by nonintercalative terpenoides, terpentecin and clerocidin." Cancer Res. **51**(11): 2922-2925.

Khapli, S., S. Dey, et al. (2003). "Burgess Reagent in Organic Synthesis." Chem. Inform. **34**(40): no-no.

Kikuchi, A. and K. Asai (1984). "Reverse gyrase a topoisomerase which introduces positive superhelical turns into DNA." Nature **309**(5970): 677-681.

Kloss, P., L. Xiong, et al. (1999). "Resistance mutations in 23 S rRNA identify the site of action of the protein synthesis inhibitor linezolid in the ribosomal peptidyl transferase center." J. Mol. Biol. **294**(1): 93-101.

Kramlinger, V. M. and H. Hiasa (2006). "The "GyrA-box" is required for the ability of DNA gyrase to wrap DNA and catalyze the supercoiling reaction." J. Biol. Chem. **281**(6): 3738-3742.

Laponogov, I., X.-S. Pan, et al. (2010). "Structural Basis of Gate-DNA Breakage and Resealing by Type II Topoisomerases." PLoS ONE **5**(6): e11338.

Laponogov, I., M. K. Sohi, et al. (2009). "Structural insight into the quinolone-DNA cleavage complex of type IIA topoisomerases." Nat. Struct. Mol. Biol. **16**(6): 667-669.

Larsen, A. K., A. E. Escargueil, et al. (2003). "Catalytic topoisomerase II inhibitors in cancer therapy." Pharmacol. Ther. **99**(2): 167-181.

Lavina, M., A. P. Pugsley, et al. (1986). "Identification, Mapping, Cloning and Characterization of a Gene (sbmA) Required for Microcin B17 Action on Escherichia coli K12." J. Gen. Microbiol. **132**(6): 1685-1693.

Leclercq, R. and P. Courvalin (1991). "Bacterial resistance to macrolide, lincosamide, and streptogramin antibiotics by target modification." Antimicrob. Agents Chemother. **35**(7): 1267-1272.

Lee, S. W., D. A. Mitchell, et al. (2008). "Discovery of a widely distributed toxin biosynthetic gene cluster." Proc. Natl. Acad. Sci. U. S. A. **105**(15): 5879-5884.

Lewis, R. J., O. M. Singh, et al. (1996). "The nature of inhibition of DNA gyrase by the coumarins and the cyclothialidines revealed by X-ray crystallography." EMBO J. **15**(6): 1412-1420.

Li, Y. M., J. C. Milne, et al. (1996). "From peptide precursors to oxazole and thiazole-containing peptide antibiotics: microcin B17 synthase." Science **274**(5290): 1188-1193.

Liu, Z., J. K. Mann, et al. (2006). "Topological information embodied in local juxtaposition geometry provides a statistical mechanical basis for unknotting by type-2 DNA topoisomerases." J. Mol. Biol. **361**(2): 268-285.

Livermore, D. M. (2005). "Tigecycline: what is it, and where should it be used?" J. Antimicrob. Chemother. **56**(4): 611-614.

Madison, L. L., E. I. Vivas, et al. (1997). "The leader peptide is essential for the post-translational modification of the DNA-gyrase inhibitor microcin B17." Mol. Microbiol. **23**(1): 161-168.

Maki, S., S. Takiguchi, et al. (1992). "Modulation of DNA supercoiling activity of Escherichia coli DNA gyrase by F plasmid proteins. Antagonistic actions of LetA (CcdA) and LetD (CcdB) proteins." J. Biol. Chem. **267**(17): 12244-12251.

Malik, S. B., M. A. Ramesh, et al. (2007). "Protist homologs of the meiotic Spo11 gene and topoisomerase VI reveal an evolutionary history of gene duplication and lineage-specific loss." Mol. Biol. Evol. **24**(12): 2827-2841.

Marquardt, J. L., E. D. Brown, et al. (1994). "Kinetics, stoichiometry, and identification of the reactive thiolate in the inactivation of UDP-GlcNAc enolpyruvoyl transferase by the antibiotic fosfomycin." Biochemistry **33**(35): 10646-10651.

Martin, J. H., M. P. Kunstmann, et al. (1978). "Glycocinnamoylspermidines, a new class of antibiotics. II. Isolation, physiocochemical and biological properties of LL-BM123beta, gamma1 and gamma2." J. Antibiot. **31**(5): 398-404.

Maxwell, A. (1999). "DNA gyrase as a drug target." Biochem. Soc. Trans. **27**(2): 48-53.

Maxwell, A., L. Costenaro, et al. (2005). "Coupling ATP hydrolysis to DNA strand passage in type IIA DNA topoisomerases." Biochem. Soc. Trans. **33**(Pt 6): 1460-1464.

Maxwell, A. and D. M. Lawson (2003). "The ATP-binding site of type II topoisomerases as a target for antibacterial drugs." Curr. Top. Med. Chem. **3**(3): 283-303.

McCullough, J. E., M. T. Muller, et al. (1993). "Clerocidin, a terpenoid antibiotic, inhibits bacterial DNA gyrase." J. Antibiot. **46**(3): 526-530.

Metzger, J. (1979). Thiazole and its derivatives. J. Wiley. New York, Interscience publication. **34:** 165-335.

Miki, T., J. A. Park, et al. (1992). "Control of segregation of chromosomal DNA by sex factor F in Escherichia coli. Mutants of DNA gyrase subunit A suppress letD (ccdB) product growth inhibition." J. Mol. Biol. **225**(1): 39-52.

Milne, J. C., A. C. Eliot, et al. (1998). "ATP/GTP hydrolysis is required for oxazole and thiazole biosynthesis in the peptide antibiotic microcin B17." Biochemistry **37**(38): 13250-13261.

Milne, J. C., R. S. Roy, et al. (1999). "Cofactor Requirements and Reconstitution Of Microcin B17 Synthetase: A Multienzyme Complex that Catalyzes the Formation of Oxazoles and Thiazoles in the Antibiotic Microcin B17â€ " Biochemistry **38**(15): 4768-4781.

Morais Cabral, J. H., A. P. Jackson, et al. (1997). "Crystal structure of the breakage-reunion domain of DNA gyrase." Nature **388**(6645): 903-906.

Morrissey, I., Y. Ge, et al. (2009). "Activity of the new cephalosporin ceftaroline against bacteraemia isolates from patients with community-acquired pneumonia." Int. J. Antimicrob. Agents **33**(6): 515-519.

Nakada, N., H. Gmunder, et al. (1994). "Mechanism of inhibition of DNA gyrase by cyclothialidine, a novel DNA gyrase inhibitor." Antimicrob. Agents Chemother. **38**(9): 1966-1973.

Nakada, N., H. Shimada, et al. (1993). "Biological characterization of cyclothialidine, a new DNA gyrase inhibitor." Antimicrob. Agents Chemother. **37**(12): 2656-2661.

Nelson, E. M., K. M. Tewey, et al. (1984). "Mechanism of antitumor drug action: poisoning of mammalian DNA topoisomerase II on DNA by 4'-(9-acridinylamino)-methanesulfon-m-anisidide." Proc. Natl. Acad. Sci. U. S. A. **81**(5): 1361-1365.

Nightingale, C. H., D. S. Greene, et al. (1975). "Pharmacokinetics and clinical use of cephalosporin antibiotics." J. Pharm. Sci. **64**(12): 1899-1926.

Noble, C. G. and A. Maxwell (2002). "The role of GyrB in the DNA cleavage-religation reaction of DNA gyrase: a proposed two metal-ion mechanism." J. Mol. Biol. **318**(2): 361-371.

Nolan, E. M. and C. T. Walsh (2009). "How Nature Morphs Peptide Scaffolds into Antibiotics." ChemBioChem **10**(1): 34-53.

Nollmann, M., N. J. Crisona, et al. (2007). "Thirty years of Escherichia coli DNA gyrase: from in vivo function to single-molecule mechanism." Biochimie **89**(4): 490-499.

Norrby, S. R., C. E. Nord, et al. (2005). "Lack of development of new antimicrobial drugs: a potential serious threat to public health." Lancet Infect. Dis. **5**(2): 115-119.

O'Neil, M. J. (2006). The Merck index : an encyclopedia of chemicals, drugs, and biologicals (14th ed) ,Whitehouse Station, NJ :, Merck.

Oblak, M., M. Kotnik, et al. (2007). "Discovery and development of ATPase inhibitors of DNA gyrase as antibacterial agents." Curr. Med. Chem. **14**(19): 2033-2047.

Osburne, M. S., W. M. Maiese, et al. (1990). "In vitro inhibition of bacterial DNA gyrase by cinodine, a glycocinnamoylspermidine antibiotic." Antimicrob. Agents Chemother. **34**(7): 1450-1452.

Pan, X. S., M. Dias, et al. (2008). "Clerocidin selectively modifies the gyrase-DNA gate to induce irreversible and reversible DNA damage." Nucleic Acids Res. **36**(17): 5516-5529.

Parks, W. M., A. R. Bottrill, et al. (2007). "The action of the bacterial toxin, microcin B17, on DNA gyrase." Biochimie **89**(4): 500-507.

Payne, D. J., R. Cramp, et al. (1994). "Comparative activities of clavulanic acid, sulbactam, and tazobactam against clinically important beta-lactamases." Antimicrob. Agents Chemother. **38**(4): 767-772.

Phillips, A. J., Y. Uto, et al. (2000). "Synthesis of functionalized oxazolines and oxazoles with DAST and Deoxo-Fluor." Org. Lett. **2**(8): 1165-1168.

Pierrat, O. A. and A. Maxwell (2003). "The action of the bacterial toxin microcin B17. Insight into the cleavage-religation reaction of DNA gyrase." J. Biol. Chem. **278**(37): 35016-35023.

Pierrat, O. A. and A. Maxwell (2005). "Evidence for the role of DNA strand passage in the mechanism of action of microcin B17 on DNA gyrase." Biochemistry **44**(11): 4204-4215.

Piton, J., S. Petrella, et al. "Structural insights into the quinolone resistance mechanism of Mycobacterium tuberculosis DNA gyrase." PLoS One **5**(8): e12245.

Poehlsgaard, J. and S. Douthwaite (2005). "The bacterial ribosome as a target for antibiotics." Nat. Rev. Microbiol. **3**(11): 870-881.

Pommier, Y. (2009). "DNA Topoisomerase I Inhibitors: Chemistry, Biology, and Interfacial Inhibition." Chem. Rev. **109**(7): 2894-2902.

Pommier, Y., E. Leo, et al. (2010). "DNA Topoisomerases and Their Poisoning by Anticancer and Antibacterial Drugs." Chem. Biol. **17**(5): 421-433.

Pons, A. M., I. Lanneluc, et al. (2002). "New developments in non-post translationally modified microcins." Biochimie **84**(5-6): 531-537.

Porter, S. E. and J. J. Champoux (1989). "The basis for camptothecin enhancement of DNA breakage by eukaryotic topoisomerase I." Nucleic Acids Res. **17**(21): 8521-8532.

Raveh, A., S. Moshe, et al. "Novel thiazole and oxazole containing cyclic hexapeptides from a waterbloom of the cyanobacterium Microcystis sp." Tetrahedron **66**(14): 2705-2712.

Reece, R. J. and A. Maxwell (1989). "Tryptic fragments of the Escherichia coli DNA gyrase A protein." J.Biol. Chem. **264**(33): 19648-19653.

Reece, R. J. and A. Maxwell (1991). "DNA gyrase: structure and function." Crit. Rev. Biochem. Mo .Biol. **26**(3-4): 335-375.

Reichardt, C. (2003). Solvents and solvent effects in organic chemistry. Weinheim ; Cambridge, Wiley-VCH.

Reynolds, P. E. (1989). "Structure, biochemistry and mechanism of action of glycopeptide antibiotics." Eur. J. Clin. Microbiol. Infect. Dis. **8**(11): 943-950.

Reynolds, P. E. and P. Courvalin (2005). "Vancomycin Resistance in Enterococci Due to Synthesis of Precursors Terminating in D-Alanyl-D-Serine." Antimicrob. Agents Chemother. **49**(1): 21-25.

Richter, S., B. Gatto, et al. (2003). "Clerocidin alkylates DNA through its epoxide function: evidence for a fine tuned mechanism of action." Nucleic Acids Res. **31**(17): 5149-5156.

Richter, S. N., E. Leo, et al. (2006). "Clerocidin interacts with the cleavage complex of Streptococcus pneumoniae topoisomerase IV to induce selective irreversible DNA damage." Nucleic Acids Res. **34**(7): 1982-1991.

Richter, S. N., I. Menegazzo, et al. (2004). "Concerted bis-alkylating reactivity of clerocidin towards unpaired cytosine residues in DNA." Nucleic Acids Res. **32**(18): 5658-5667.

Richter, S. N., I. Menegazzo, et al. (2009). "Reactivity of clerocidin towards adenine: implications for base-modulated DNA damage." Org Biomol Chem **7**(5): 976-985.

Robbel, L. and M. A. Marahiel "Daptomycin, a Bacterial Lipopeptide Synthesized by a Nonribosomal Machinery." Journal of Biological Chemistry **285**(36): 27501-27508.

Roberts, M. C. (2008). "Update on macrolide-lincosamide-streptogramin, ketolide, and oxazolidinone resistance genes." FEMS Microbiol. Lett. **282**(2): 147-159.

Ronkin, S. M., M. Badia, et al. "Discovery of pyrazolthiazoles as novel and potent inhibitors of bacterial gyrase." Bioorg. Med. Chem. Lett. **20**(9): 2828-2831.

Roy, R. S., P. J. Belshaw, et al. (1998). "Mutational analysis of posttranslational heterocycle biosynthesis in the gyrase inhibitor microcin B17: Distance dependence from propeptide and tolerance for substitution in a GSCG cyclizable sequence." Biochemistry **37**(12): 4125-4136.

Royer, M., L. Costet, et al. (2004). "Albicidin Pathotoxin Produced by Xanthomonas albilineans Is Encoded by Three Large PKS and NRPS Genes Present in a Gene Cluster Also Containing Several Putative Modifying, Regulatory, and Resistance Genes." Molecular Plant-Microbe Interactions **17**(4): 414-427.

Ruiz, N., B. Falcone, et al. (2005). "Chemical conditionality: a genetic strategy to probe organelle assembly." Cell **121**(2): 307-317.

Ruthenburg, A. J., D. M. Graybosch, et al. (2005). "A superhelical spiral in the Escherichia coli DNA gyrase A C-terminal domain imparts unidirectional supercoiling bias." J. Biol. Chem. **280**(28): 26177-26184.

Salomon, R. A. and R. N. Farias (1995). "The peptide antibiotic microcin 25 is imported through the TonB pathway and the SbmA protein." J. Bacteriol. **177**(11): 3323-3325.

Samonis, G., S. Maraki, et al. "Antimicrobial susceptibility of Gram-negative nonurinary bacteria to fosfomycin and other antimicrobials." Future Microbiology **5**(6): 961-970.

Sands, L. C. and W. V. Shaw (1973). "Mechanism of chloramphenicol resistance in staphylococci: characterization and hybridization of variants of chloramphenicol acetyltransferase." Antimicrob Agents Chemother **3**(2): 299-305.

Scheffers, D.-J. and M. G. Pinho (2005). "Bacterial Cell Wall Synthesis: New Insights from Localization Studies." Microbiol. Mol. Biol. Rev. **69**(4): 585-607.

Schoeffler, A. J. and J. M. Berger (2008). "DNA topoisomerases: harnessing and constraining energy to govern chromosome topology." Q. Rev. Biophys. **41**(1): 41-101.

Scholz, R., K. J. Molohon, et al. "Plantazolicin, a novel microcin B17/streptolysin S-like natural product from Bacillus amyloliquefaciens FZB42." J. Bacteriol.: JB.00784-00710.

Schvartzman, J. B. and A. Stasiak (2004). "A topological view of the replicon." EMBO Rep. **5**(3): 256-261.

Schwarz, S., C. Kehrenberg, et al. (2004). "Molecular basis of bacterial resistance to chloramphenicol and florfenicol." FEMS Microbiol. Rev. **28**(5): 519-542.

Seydel, J. K. (1968). "Sulfonamides, structure-activity relationship, and mode of action. Structural problems of the antibacterial action of 4-aminobenzoic acid (PABA) antagonists." J. Pharm. Sci. **57**(9): 1455-1478.

Shibata, T., S. Nakasu, et al. (1987). "Intrinsic DNA-dependent ATPase activity of reverse gyrase." J. Biol. Chem. **262**(22): 10419-10421.

Sinha Roy, R., P. J. Belshaw, et al. (1998). "Mutational Analysis of Posttranslational Heterocycle Biosynthesis in the Gyrase Inhibitor Microcin B17: Distance Dependence from Propeptide and Tolerance for Substitution in a GSCG Cyclizable Sequenceâ€ " Biochemistry **37**(12): 4125-4136.

Sinha Roy, R., N. L. Kelleher, et al. (1999). "In vivo processing and antibiotic activity of microcin B17 analogs with varying ring content and altered bisheterocyclic sites." Chem. Biol. **6**(5): 305-318.

Sissi, C., A. Chemello, et al. (2008). "DNA gyrase requires DNA for effective two-site coordination of divalent metal ions: further insight into the mechanism of enzyme action." Biochemistry **47**(33): 8538-8545.

Sissi, C. and M. Palumbo (2003). "The Quinolone Family: From Antibacterial to Anticancer Agents." Curr. Med. Chem.: Anti-Cancer Agents **3**: 439-450.

Skold, O. (2001). "Resistance to trimethoprim and sulfonamides." Vet. Res. **32**(3-4): 261-273.

Slama, T. (2008). "Gram-negative antibiotic resistance: there is a price to pay." Crit. Care **12**(Suppl 4): S4.

Smith, A. B. and A. Maxwell (2006). "A strand-passage conformation of DNA gyrase is required to allow the bacterial toxin, CcdB, to access its binding site." Nucleic Acids Res. **34**(17): 4667-4676.

Snyder, M. and K. Drlica (1979). "DNA gyrase on the bacterial chromosome: DNA cleavage induced by oxolinic acid." J. Mol. Biol. **131**(2): 287-302.

Somoskovi, A., L. Parsons, et al. (2001). "The molecular basis of resistance to isoniazid, rifampin, and pyrazinamide in Mycobacterium tuberculosis." Respir. Res. **2**(3): 164 - 168.

Souli, M., I. Galani, et al. (2008). "Emergence of extensively drug-resistant and pandrug-resistant Gram-negative bacilli in Europe." Euro. Surveill. **13**(47).

Spížek, J. and T. Řezanka (2004). "Lincomycin, clindamycin and their applications." Appl. Microbiol. Biotechnol. **64**(4): 455-464.

Staker, B. L., K. Hjerrild, et al. (2002). "The mechanism of topoisomerase I poisoning by a camptothecin analog." Proc. Natl. Acad. Sci. U. S. A. **99**(24): 15387-15392.

Stankova, I. G., G. I. Videnov, et al. (1999). "Synthesis of thiazole, imidazole and oxazole containing amino acids for peptide backbone modification." J. Pept. Sci. **5**(9): 392-398.

Staudenbauer, W. L. (1976). "Replication of Escherichia coli DNA in vitro: inhibition by oxolinic acid." Eur. J. Biochem. **62**(3): 491-497.

Stiborova, M., M. Rupertova, et al. (2010). "Cytochrome P450- and peroxidase-mediated oxidation of anticancer alkaloid ellipticine dictates its anti-tumor efficiency." Biochim. Biophys. Acta **1814** (1): 175-185.

Stone, M. D., Z. Bryant, et al. (2003). "Chirality sensing by Escherichia coli topoisomerase IV and the mechanism of type II topoisomerases." Proc. Natl. Acad. Sci. U. S. A. **100**(15): 8654-8659.

Sugino, A., N. P. Higgins, et al. (1978). "Energy coupling in DNA gyrase and the mechanism of action of novobiocin." Proc. Natl. Acad. Sci. U. S. A. **75**(10): 4838-4842.

Sugino, A., C. L. Peebles, et al. (1977). "Mechanism of action of nalidixic acid: purification of Escherichia coli nalA gene product and its relationship to DNA gyrase and a novel nicking-closing enzyme." Proc. Natl. Acad. Sci. U. S. A. **74**(11): 4767-4771.

Swanberg, S. L. and J. C. Wang (1987). "Cloning and sequencing of the Escherichia coli gyrA gene coding for the A subunit of DNA gyrase." J. Mol. Biol. **197**(4): 729-736.

Swaney, S. M., H. Aoki, et al. (1998). "The Oxazolidinone Linezolid Inhibits Initiation of Protein Synthesis in Bacteria." Antimicrob. Agents Chemother. **42**(12): 3251-3255.

Taneja, B., A. Patel, et al. (2006). "Structure of the N-terminal fragment of topoisomerase V reveals a new family of topoisomerases." EMBO J **25**(2): 398-408.

Timmins, G. S., S. Master, et al. (2004). "Nitric Oxide Generated from Isoniazid Activation by KatG: Source of Nitric Oxide and Activity against Mycobacterium tuberculosis." Antimicrob. Agents Chemother. **48**(8): 3006-3009.

Tingey, A. P. and A. Maxwell (1996). "Probing the role of the ATP-operated clamp in the strand-passage reaction of DNA gyrase." Nucleic Acids Res. **24**(24): 4868-4873.

Tran, J. H., G. A. Jacoby, et al. (2005). "Interaction of the plasmid-encoded quinolone resistance protein Qnr with Escherichia coli DNA gyrase." Antimicrob. Agents Chemother. **49**(1): 118-125.

Tresner, H. D., J. H. Korshalla, et al. (1978). "Glycocinnamoylspermidines, a new class of antibiotics. I. Description and fermentation of the organism producing the LL-BM123 antibiotics." J. Antibiot. **31**(5): 394-397.

Tretter, E. M., A. J. Schoeffler, et al. "Crystal structure of the DNA gyrase GyrA N-terminal domain from Mycobacterium tuberculosis." Proteins **78**(2): 492-495.

Trovatti, E., C. A. Cotrim, et al. (2008). "Peptides based on CcdB protein as novel inhibitors of bacterial topoisomerases." Bioorg. Med. Chem. Lett. **18**(23): 6161-6164.

Tse-Dinh, Y. C. (2009). "Bacterial topoisomerase I as a target for discovery of antibacterial compounds." Nucleic Acids Res. **37**(3): 731-737.

Ullsperger, C. and N. R. Cozzarelli (1996). "Contrasting enzymatic activities of topoisomerase IV and DNA gyrase from Escherichia coli." J. Biol. Chem. **271**(49): 31549-31555.

van den Boogaard, J., G. S. Kibiki, et al. (2009). "New drugs against tuberculosis: problems, progress, and evaluation of agents in clinical development." Antimicrob. Agents Chemother. **53**(3): 849-862.

Vazquez, D. (1966). "Antibiotics affecting chloramphenicol uptake by bacteria Their effect on amino acid incorporation in a cell-free system." Biochim. et Biophys. Acta, Nucleic Acids Protein Synth. **114**(2): 289-295.

Videnov, G., D. Kaiser, et al. (1996). "Synthesis of the DNA Gyrase Inhibitor Microcin B17, a 43-Peptide Antibiotic with Eight Aromatic Heterocycles in its Backbone." Angew. Chem. Int. Ed. **35**(13-14): 1506-1508.

Videnov, G., D. Kaiser, et al. (1996). "Synthesis of the DNA gyrase inhibitor microcin B17, a 43-peptide antibiotic with eight aromatic heterocycles in its backbone." Angew. Chem. Int. Ed. **35**(13-14): 1506-1508.

Videnov, G., D. Kaiser, et al. (1996). "Synthesis of Naturally Occurring, Conformationally Restricted Oxazole- and Thiazole-Containing Di- and Tripeptide Mimetics." Angew. Chem. Int. Ed. **35**(13-14): 1503-1506.

Videnov, G., D. Kaiser, et al. (1996). "Synthesis of naturally occurring, conformationally restricted oxazole- and Thiazole-containing di- and tripeptide mimetics." Angew. Chem. Int. Ed. **35**(13-14): 1503-1506.

Vivien, E., D. Pitorre, et al. (2007). "Heterologous Production of Albicidin: a Promising Approach to Overproducing and Characterizing This Potent Inhibitor of DNA Gyrase." Antimicrob. Agents Chemother. **51**(4): 1549-1552.

Vizan, J. L., C. Hernandez-Chico, et al. (1991). "The peptide antibiotic microcin B17 induces double-strand cleavage of DNA mediated by E. coli DNA gyrase." EMBO J **10**(2): 467-476.

Volles, D. F. and T. N. Branan (2008). "Antibiotics in the Intensive Care Unit: Focus on Agents for Resistant Pathogens." Emerg. Med. Clin. North Am. **26**(3): 813-834.

Vollmer, W., D. Blanot, et al. (2008). "Peptidoglycan structure and architecture." FEMS Microbiol. Rev. **32**(2): 149-167.

Walker, S., L. Chen, et al. (2005). "Chemistry and biology of ramoplanin: a lipoglycodepsipeptide with potent antibiotic activity." Chem. Rev **105**(2): 449-476.

Wall, M. E., M. C. Wani, et al. (1966). "Plant Antitumor Agents. I. The Isolation and Structure of Camptothecin, a Novel Alkaloidal Leukemia and Tumor Inhibitor from Camptotheca acuminata1,2." J. Am. Chem. Soc. **88**(16): 3888-3890.

Wang, J. C. (1971). "Interaction between DNA and an Escherichia coli protein omega." J. Mol. Biol. **55**(3): 523-533.

Wang, J. C. (2002). "Cellular roles of DNA topoisomerases: a molecular perspective." Nat. Rev. Mol. Cell Biol. **3**(6): 430-440.

Waxman, D. J. and J. L. Strominger (1983). "Penicillin-binding proteins and the mechanism of action of beta-lactam antibiotics." Annu. Rev. Biochem. **52**: 825-869.

Waxman, D. J., R. R. Yocum, et al. (1980). "Penicillins and Cephalosporins are Active Site-Directed Acylating Agents: Evidence in Support of the Substrate Analogue Hypothesis." Philos. Trans. R. Soc. London, B **289**(1036): 257-271.

Wieland Brown, L. C., M. G. Acker, et al. (2009). "Thirteen posttranslational modifications convert a 14-residue peptide into the antibiotic thiocillin." Proc. Natl. Acad. Sci. U. S. A. **106**(8): 2549-2553.

Wiener, J. J. M., L. Gomez, et al. (2007). "Tetrahydroindazole inhibitors of bacterial type II topoisomerases. Part 2: SAR development and potency against multidrug-resistant strains." Bioorg. Med. Chem. Lett. **17**(10): 2718-2722.

Wigley, D. B., G. J. Davies, et al. (1991). "Crystal structure of an N-terminal fragment of the DNA gyrase B protein." Nature **351**(6328): 624-629.

Wilson, K.-A., M. Kalkum, et al. (2003). "Structure of Microcin J25, a Peptide Inhibitor of Bacterial RNA Polymerase, is a Lassoed Tail." J. Am. Chem. Soc. **125**(41): 12475-12483.

Wilson, R. J. (2002). "Progress with parasite plastids." J. Mol. Biol. **319**(2): 257-274.

Wipf, P. and C. P. Miller (1993). "A new synthesis of highly functionalized oxazoles." J. Org. Chem. **58**(14): 3604-3606.

Wohlkonig, A., P. F. Chan, et al. (2010). "Structural basis of quinolone inhibition of type IIA topoisomerases and target-mediated resistance." Nat. Struct. Mol. Biol. **17**(99): 1152-1153.

Wolfson, J. S. and D. C. Hooper (1985). "The fluoroquinolones: structures, mechanisms of action and resistance, and spectra of activity in vitro." Antimicrob. Agents Chemother. **28**(4): 581-586.

Woodford, N. and D. M. Livermore (2009). "Infections caused by Gram-positive bacteria: a review of the global challenge." J. Infect. **59 Suppl 1**: S4-16.

Xaplanteri, M. A., A. Andreou, et al. (2003). "Effect of polyamines on the inhibition of peptidyltransferase by antibiotics: revisiting the mechanism of chloramphenicol action." Nucleic Acids Res. **31**(17): 5074-5083.

Yamagishi, J., H. Yoshida, et al. (1986). "Nalidixic acid-resistant mutations of the gyrB gene of Escherichia coli." Mol. Gen. Genet. **204**(3): 367-373.

Yamashita, Y., S. Kawada, et al. (1990). "Induction of mammalian topoisomerase II dependent DNA cleavage by nonintercalative flavonoids, genistein and orobol." Biochem. Pharmacol. **39**(4): 737-744.

Yang, W., I. F. Moore, et al. (2004). "TetX is a flavin-dependent monooxygenase conferring resistance to tetracycline antibiotics." J. Biol. Chem. **279**(50): 52346-52352.

Yorgey, P., J. Davagnino, et al. (1993). "The maturation pathway of microcin B17, a peptide inhibitor of DNA gyrase." Mol. Microbiol. **9**(4): 897-905.

Yorgey, P., J. Lee, et al. (1994). "Posttranslational modifications in microcin B17 define an additional class of DNA gyrase inhibitor." Proc. Natl. Acad. Sci. U. S. A. **91**(10): 4519-4523.

You, S. L., H. Razavi, et al. (2003). "A Biomimetic Synthesis of Thiazolines Using Hexaphenyloxodiphosphonium Trifluoromethanesulfonate." Angew. Chem. Int. Ed. **42**(1): 83-85.

Yusupov, M. M., G. Z. Yusupova, et al. (2001). "Crystal Structure of the Ribosome at 5.5 A Resolution." Science **292**(5518): 883-896.

Zamble, D. B., D. A. Miller, et al. (2001). "In vitro characterization of DNA gyrase inhibition by microcin B17 analogs with altered bisheterocyclic sites." Proc. Natl. Acad. Sci. U. S. A. **98**(14): 7712-7717.

Zavascki, A. P., L. Z. Goldani, et al. (2007). "Polymyxin B for the treatment of multidrug-resistant pathogens: a critical review." J. Antimicrob. Chemother. **60**(6): 1206-1215.

Zhanel, G. G. S., Grace; Schweizer, Frank; Zelenitsky, Sheryl; Lagacé-Wiens, Philippe R.S.; Rubinstein, Ethan; Gin, Alfred S.; Hoban, Daryl J.; Karlowsky, James A. (2009). "Ceftaroline: A Novel Broad-Spectrum Cephalosporin with Activity against Meticillin-Resistant Staphylococcus aureus." Drugs **69**: 809-831.

Zuckerman, J. M. (2004). "Macrolides and ketolides: azithromycin, clarithromycin, telithromycin." Infect. Dis. Clin. North. Am. **18**(3): 621-649, xi-.

Zuckerman, J. M., F. Qamar, et al. (2009). "Macrolides, ketolides, and glycylcyclines: azithromycin, clarithromycin, telithromycin, tigecycline." Infect. Dis. Clin. North. Am. **23**(4): 997-1026, ix-x.